

# Ensemble Kalman Methods: A Mean Field Perspective

Edoardo Calvello\*, Sebastian Reich†, and Andrew M. Stuart‡

**Abstract.** This paper provides a unifying mean field based framework for the derivation and analysis of ensemble Kalman methods. Both state estimation and parameter estimation problems are considered, and formulations in both discrete and continuous time are employed. For state estimation problems both the control and filtering approaches are studied; analogously, for parameter estimation (inverse) problems the optimization and Bayesian perspectives are both studied. The approach taken unifies a wide-ranging literature in the field, provides a framework for analysis of ensemble Kalman methods, and suggests open problems.

**1. Introduction.** The ensemble Kalman methodology is an innovative and flexible set of tools which can be used for both state estimation in dynamical systems and parameter estimation for generic inverse problems. It has primarily been developed by practitioners in the geophysical sciences, with notable impact on the fields of oceanography, oil reservoir simulation and weather forecasting. Despite its wide adoption in the geosciences, the methodology is hard to analyze and firm theoretical foundations are only now starting to emerge. The purpose of this article is twofold: a) to describe a mathematical framework for the analysis of ensemble Kalman methods, describing what is known and highlighting the many open mathematical challenges in the field; b) to provide a literature survey which bridges the domain-specific development of the methodology with emerging mathematical analyses. In so doing we will also highlight the flexibility of the methodology for use in widespread applications, beyond its historical development in the geosciences.

The material is organized around the two separate themes of state estimation and inverse problems; within each, both discrete time and continuous time approaches are explained. The novel perspective which underlies all of this material is the derivation of ensemble Kalman methods as particle approximations of carefully designed mean-field models. The relationship of these mean-field models to exact transport models, for Gaussian problems, serves to motivate their form.

In Subsection 1.1 we overview the history of ensemble Kalman methods. Subsection 1.2 describes the organization of the paper. In Subsection 1.3 we make brief remarks about the pseudo-code that we make available as a supplementary resource for this paper. The introduction concludes, in Subsection 1.4, with a summary of the notation that we adopt throughout the paper.

**1.1. Historical Context.** The Kalman filter (KF) is arguably the first setting in which the integration of observational data with a dynamical system was considered, leading to both discrete time (Kalman, 1960) and continuous time (Kalman & Bucy, 1961) formulations; see Welch *et al.* (1995) for an overview. The Kalman filter applies only in the setting of linear Gaussian dynamics and observation; it computes the distribution of the state of the dynamical

\*California Institute of Technology, Pasadena, CA 91125, USA (e.calvello@caltech.edu).

†Institut für Mathematik, Universität Potsdam, D-14476 Potsdam, Germany (sebastian.reich@uni-potsdam.de).

‡California Institute of Technology, Pasadena, CA 91125, USA (astuart@caltech.edu).

system, given observations, exactly. The extended Kalman filter (historically denoted EKF; however the acronym ExKF is also used and is useful) was introduced in order to extend Kalman’s ideas to nonlinear problems; see the texts Jazwinski (2007) and Anderson & Moore (2012) for overviews. The extended Kalman approach is based on a linearization approximation; it hence fails to exactly compute the distribution of the state of the dynamical system, given observations, in general. Furthermore it requires propagation of covariance matrices which can be very large for applications arising in the geosciences (Ghil *et al.*, 1981).

The ensemble Kalman filter (EnKF) was introduced in the celebrated paper Evensen (1994) which made the consequential observation that, if an *ensemble* of state estimators is employed then it can also be used to make an approximation of the covariance. In geosciences applications this circumvents the computation of large covariances, replacing them instead with low rank approximations, with rank determined by the number of ensemble members. The original paper developed the idea in the context of ocean models, but was rapidly and concurrently developed in a variety of geoscience application domains (Van Leeuwen & Evensen, 1996; Burgers *et al.*, 1998; Houtekamer & Mitchell, 1998); the paper van Leeuwen (2020) provide a historical overview. These methods are sometimes referred as the *stochastic EnKF*: they require simulation of random variables to implement. A different class of ensemble methods, known collectively as *ensemble square root filters*, was subsequently developed (Anderson, 2001; Whitaker & Hamill, 2002; Bishop *et al.*, 2001; Hunt *et al.*, 2007; Tippett *et al.*, 2003; Sakov & Oke, 2008); these methods are a form of *deterministic EnKF*: they do not require simulation of random variables to implement.

Central to our mathematical presentation of Kalman-based methods is the adoption of mean-field and transport perspectives on the subject. The incorporation of data within filtering constitutes (possibly approximate) application of Bayes’ theorem; the papers Daum *et al.* (2010), Reich (2011), El Moselhy & Marzouk (2012), and the book Cotter & Reich (2013) introduce novel approaches to Bayesian inversion, rooted in transport and mean-field models. While El Moselhy & Marzouk (2012), Spantini *et al.* (2019a) propose a direct numerical approximation of the underlying optimal transportation problem, Daum *et al.* (2010) and Reich (2011) pursue a homotopy approach. We note that the homotopy approach is closely related to iterative implementations of the EnKF, as first considered by Li & Reynolds (2009), Gu & Oliver (2007), and Sakov *et al.* (2012); these homotopy approaches lead to continuous time formulations of the EnKF in the limit of infinitely many iterations, as first considered by Bergemann & Reich (2010a) and Bergemann & Reich (2010b).

The key connection between mean-field models and ensemble methods is that the latter can be derived as particle approximations of the mean-field limit; this viewpoint will play a guiding role in our presentation of the subject of ensemble methods in these notes. In this context it is notable that the field of optimization, which is linked to Bayesian sampling through MAP estimation (Kaipio & Somersalo, 2006), has also seen recent development using mean-field models – see Carrillo *et al.* (2018) for an overview and unifying mathematical framework.

The methods covered in this survey provide only approximate solutions to the underlying filtering, inference and/or optimization problem. The approximations invoked are based on assuming linear Gaussian structure, but applying the resulting methodology outside this regime. On the other hand, alternative methods, such as sequential Monte Carlo (resp. Monte

Carlo Markov chain) can be designed to be consistent with the underlying nonlinear filtering problem (resp. Bayesian inverse problem). The books [Doucet \*et al.\* \(2001\)](#) and [Chopin & Papaspiliopoulos \(2020\)](#) overview use of the sequential Monte Carlo methods for general discrete time filtering and inference problems (resp. [Kaipio & Somersalo, 2006](#) for Bayesian inverse problems). However, sequential Monte Carlo methods suffer from the curse of dimensionality and are presently not directly applicable to high dimensional problems as arising, for example, from geophysical applications. This issue with the curse of dimensionality provides the main motivation for the type of methods covered in this survey. See [Snyder \*et al.\* \(2008\)](#), [Bickel \*et al.\* \(2008\)](#), [Rebeschini & Van Handel \(2015\)](#), and [Agapiou \*et al.\* \(2017\)](#) for details.

This concludes our chronological overview of the historical context for the development of ensemble Kalman methods, and the specific mathematical context which will be our focus. Each section of the paper concludes with a bibliographic subsection in which a deeper literature review is given.

**1.2. Overview.** Section 2 is devoted to the problem of state estimation for discrete time (possibly stochastic) dynamical systems subject to noisy observations. We formulate the problem from the perspectives of both control theory and probability and we provide a unifying approach to algorithms for these problems; the approach rests on transport of measures and mean field stochastic dynamical systems. Ensemble Kalman methods are then derived as particle approximations of the mean field models. Section 3 adopts a perspective that parallels the previous section, but works in a continuous time setting. Stochastic differential equations (SDEs) are used to describe the state and its observation process, and mean field SDEs, and related stochastic partial differential equations (SPDEs), are used to provide the underpinnings of algorithms; particle approximations of the mean field systems give interacting systems of SDEs which describe ensemble Kalman methods. The formulation in continuous time is useful both because in some applications state estimation problems are most naturally formulated this way, and because they provide insight into discrete time algorithms, giving rise to cleaner analysis of phenomena present in both discrete and continuous time. Section 4 is devoted to the use of ensemble Kalman methods for parameter estimation and inverse problems, demonstrating how a useful change of perspective opens up their use in this broader setting; both discrete and continuous time are considered in parallel. Sections 2, 3 and 4 are

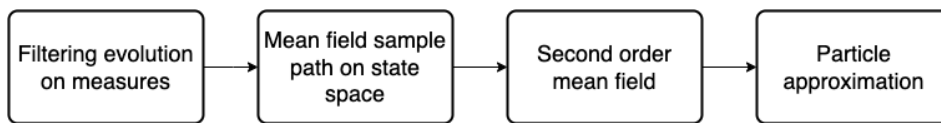


Figure 1.1: Organizational flow of sections 2, 3 and 4.

all organized according to the flow of ideas displayed in Figure 1.1. Indeed, starting from a probabilistic perspective, that describes the evolution of the filtering distribution, it is possible to formulate mean field maps whose sample paths on state space are equal in law to the filtering evolution. Since it is typically not tractable to identify these maps explicitly, it is of interest to determine mean field maps whose sample paths are only approximately equal in law to the filtering evolution. This leads to the idea of second order mean field

models whose sample paths have law with first and second order moments which match those of the filtering distribution, conditional on the prediction step in the filtering cycle. Particle approximations of these second order mean field maps are then used to derive implementable numerical algorithms which form the class of ensemble Kalman methods.

Section 5 concludes, and in particular highlights open problems in the area which might be of particular interest to the mathematical community. The appendices in Sections 6 and 7 are devoted to pseudo-code for the algorithms introduced and to background on the underlying example that we use throughout the paper. The appendices in Sections 8 and 9 provide underpinning material on mean-field maps and on stochastic integration.

**1.3. Pseudo-Code.** Pseudo-code describing several of the algorithms that we present and deploy in this paper are described in Appendix 6. The reader is encouraged to consult Algorithms 6.1 and 6.2, 3DVAR and the ensemble Kalman filter (EnKF) respectively, in the context of the problem of state estimation for discrete time dynamical systems presented in Section 2. The scheme 3DVAR is employed in Examples 2.1, 2.2, 2.3 and 2.10. The ensemble Kalman filter is applied in the context of Example 2.10. Ensemble Kalman methods for inversion, as shown in Algorithms 6.3, 6.4 and 6.5, are presented in Section 4 and applied in the context of Example 4.21.

**1.4. Notation.** Throughout we denote the positive integers and non-negative integers respectively by  $\mathbb{N} = \{1, 2, \dots\}$  and  $\mathbb{Z}^+ = \{0, 1, 2, \dots\}$ , and the notation  $\mathbb{R} = (-\infty, \infty)$  and  $\mathbb{R}^+ = [0, \infty)$  for the reals and the non-negative reals. We let  $\langle \cdot, \cdot \rangle, |\cdot|$  denote the Euclidean inner-product and norm, noting that  $|v|^2 = \langle v, v \rangle$ . We also use  $|\cdot|$  to denote the resulting induced norm on matrices. We use  $:$  to denote the Frobenius inner-product between matrices, and  $|\cdot|_F$  the induced norm on matrices. For any function  $g : \mathbb{R}^{d_1} \mapsto \mathbb{R}^{d_2}$  we denote by  $Dg(\cdot)$  the derivative.

We use  $\mathbb{E}$  and  $\mathbb{P}$  to denote expectation and probability under the prevailing probability measure; if we wish to make clear that measure  $\pi$  is the prevailing probability measure then we write  $\mathbb{E}^\pi$  and  $\mathbb{P}^\pi$ . We use  $Law(rv)$  to denote the law of random variable  $rv$ . We let  $\delta_u$  denote the Dirac mass on  $\mathbb{R}^d$ , centered at point  $u \in \mathbb{R}^d$ . We let  $\mathbf{N}(m, C)$  denote the distribution of a Gaussian random variable with mean  $m$  and covariance  $C$ .

We write  $A \succ B$  when  $A - B$  is positive definite and  $A \succeq B$  when  $A - B$  is positive semi-definite. We will also write  $A \prec B$  when  $B - A \succ 0$  and  $A \preceq B$  when  $B - A \succeq 0$ .

For  $C \succ 0$  (and therefore a covariance matrix) we define  $\langle \cdot, \cdot \rangle_C, |\cdot|_C$  the covariance-weighted Euclidean inner-product and norm, by  $\langle u, v \rangle_C = \langle u, C^{-1}v \rangle$  and  $|v|_C^2 = \langle v, v \rangle_C$ .

**2. Discrete Time.** In Subsection 2.1 we provide the set-up for the problem of state estimation in discrete time. Subsection 2.2 introduces an algorithm for this problem based on a control theoretic perspective. Subsection 2.3 describes the Bayesian probabilistic perspective; algorithms are not presented but foundations for the creation of algorithms are laid through the decomposition of the filtering cycle into an iteration which alternates prediction and the assimilation of data. In Subsection 2.4 we introduce the important idea of Gaussian projection, and the resulting Gaussian projected filter. Subsection 2.5 introduces various mean-field dynamical systems which approximate the filtering cycle; a unifying transport map perspective is adopted. This leads, in Subsection 2.6, to definitions of the ensemble Kalman filter, the

ensemble adjustment filter and the ensemble transform filter, all derived as particle approximations of specific mean-field models. We conclude with bibliographic notes in Subsection 2.7 in which we review relevant literature, and include discussion of a variety of other algorithms for state estimation, and relate them to the perspective we adopt here.

**2.1. Set-Up.** The objective of *sequential data assimilation* is to iteratively update the state of a (possibly stochastic) dynamical system based on observations and knowledge of the dynamical and observational processes; we refer to this as *state estimation*. The typical setting is one in which the initial condition is uncertain, but this uncertainty is compensated for by (typically noisy) observations of a (possibly nonlinear) function of the state. These observations often live in a space of lower dimension than the dimension of the state space meaning that the goal of state estimation goes beyond denoising, and into the realm of control theoretic considerations such as observability.

A useful starting point is to consider a stochastic dynamical system in which the evolution of the state, and the relationship between the observations (which we also refer to as data) and the state, are defined, respectively, by the equations

$$\begin{aligned} (2.1a) \quad & v_{n+1} = \Psi(v_n) + \xi_n, \\ (2.1b) \quad & y_{n+1} = h(v_{n+1}) + \eta_{n+1}, \end{aligned}$$

taken to hold for all  $n \in \mathbb{Z}^+$ . We assume that, for each fixed  $n \in \mathbb{Z}^+$ , the *state*  $v_n \in \mathbb{R}^{d_v}$  and the *observations*  $y_n \in \mathbb{R}^{d_y}$ . The maps  $\Psi(\cdot)$  and  $h(\cdot)$  describe the systematic, deterministic components of the dynamics and observation processes, and are assumed known. The initial condition for  $v_0$  is assumed random and the systematic components of the model are subjected to mean zero noise,  $\xi_n$  and  $\eta_{n+1}$ . To be concrete we assume  $v_0, \{\xi_n\}_{n \in \mathbb{Z}^+}$  and  $\{\eta_n\}_{n \in \mathbb{N}}$  are mutually independent Gaussians defined by

$$(2.2) \quad v_0 \sim \mathbf{N}(m_0, C_0), \quad \xi_n \sim \mathbf{N}(0, \Sigma) \text{ i.i.d.}, \quad \eta_n \sim \mathbf{N}(0, \Gamma) \text{ i.i.d.}.$$

In practice we will have available to us the observation coordinates of a specific true realization of the random dynamical system (2.1), from which we wish to recover the specific true realization of the state that gave rise to these observations. We denote the true realizations of the *state of the system* by sequence  $\{v_n^\dagger\}_{n \in \mathbb{Z}^+}$ , and the *observed data* by  $\{y_n^\dagger\}_{n \in \mathbb{N}}$ . These are generated by  $v_0^\dagger, \{\xi_n^\dagger\}_{n \in \mathbb{Z}^+}$  and  $\{\eta_n^\dagger\}_{n \in \mathbb{N}}$ , specific realizations of the initial condition and state and observational noise from the distribution defined by (2.2).

We let  $Y_n^\dagger = \{y_\ell^\dagger\}_{1 \leq \ell \leq n}$ . Our objective is to estimate the state  $v_n^\dagger$  at time  $n$  from data  $Y_n^\dagger$ . Specifically, it is natural to think about this design objective in two different ways:

- Objective 1: design an algorithm producing output  $v_n$  from  $Y_n^\dagger$  so that  $\{v_n\}_{n \in \mathbb{Z}^+}$  estimates  $\{v_n^\dagger\}_{n \in \mathbb{Z}^+}$ , the true state generated by (2.1a);
- Objective 2: design an algorithm which estimates the distribution of random variable  $v_n | Y_n^\dagger$ .

In both cases we are interested in Markovian formulations which update the estimate  $v_n$ , or the distribution  $v_n | Y_n^\dagger$ , sequentially as the data is acquired. In the next two subsections we describe control theoretic and probabilistic approaches to this problem which, respectively,

provide the basis for algorithms addressing Objectives 1 and 2. We note that fulfilling Objective 2 immediately implies resolution of Objective 1, for example by taking the mean of  $v_n|Y_n^\dagger$ ; but the reverse is not typically true. However, Objective 1 is easier to address, is especially relevant when noise levels are small, and more generally serves to motivate approaches which are used to address Objective 2.

**2.2. Control Theory Perspective.** A very natural idea from control theory underlies ensemble Kalman filtering and it is encapsulated in the following algorithmic approach. This way of attacking state estimation is most appropriate when  $|C_0|$ ,  $|\Gamma|$  and  $|\Sigma|$  are small so that the state and observations are close to deterministic. To understand this setting we will first study algorithms in which the covariances  $\Gamma$  and  $\Sigma$  are set to zero, and then return to the inclusion of noise.

The algorithmic idea works as follows: from current state estimate  $v_n$ , given  $Y_n^\dagger$ , *predict* the outcome of the model and data, denoted by  $(\hat{v}_{n+1}, \hat{h}_{n+1})$ , using the update equations (2.1), but ignoring the noise; then *correct* the state estimate by nudging the prediction using the mismatch between observed and predicted data  $(y_{n+1}^\dagger, \hat{h}_{n+1})$ . This results in a deterministic map  $v_n \mapsto v_{n+1}$ , assumed to hold for all  $n \in \mathbb{Z}^+$ , of the following form:

$$\begin{aligned} (2.3a) \quad & \hat{v}_{n+1} = \Psi(v_n), \\ (2.3b) \quad & \hat{h}_{n+1} = h(\hat{v}_{n+1}), \\ (2.3c) \quad & v_{n+1} = \hat{v}_{n+1} + K(y_{n+1}^\dagger - \hat{h}_{n+1}). \end{aligned}$$

Equations (2.3a, 2.3b) create predicted state and data. The difference between the predicted data and the true data  $\{y_{n+1}^\dagger\}_{n \in \mathbb{Z}^+}$ , the latter found from a fixed realization of (2.1), is then used to correct the predicted state resulting in (2.3c). We can write the algorithm compactly in the form

$$(2.4) \quad v_{n+1} = \Psi(v_n) + K(y_{n+1}^\dagger - h(\Psi(v_n))).$$

Choice of the *gain matrix*  $K$  will complete definition of an algorithm which we refer to as 3DVAR.<sup>1</sup> Pseudo-code for 3DVAR may be found as Algorithm 6.1 in Appendix 6. We note that the difference between the observed value  $y_{n+1}^\dagger$  and its estimator  $\hat{h}_{n+1} = h(\Psi(v_n))$  is often referred to as the *innovation*, and for this we introduce the notation

$$(2.5) \quad I_n = y_{n+1}^\dagger - \hat{h}_{n+1}.$$

In the following example we illustrate this algorithm. The example serves to demonstrate the viability of the proposed control theoretic way of thinking about state estimation, and

<sup>1</sup>The nomenclature “3DVAR” was coined in the geophysics community, and stands for three dimensional variational data assimilation. This is natural for algorithms which incorporate spatially distributed data sequentially in time, in the context where the state variable  $v$  varies across three spatial coordinates. In our setting the state variable  $v$  is not required to have any spatial structure, but the control formulation (2.4) reproduces the 3DVAR algorithm from the geophysics community when it does. Hence we still refer to it as 3DVAR.

addresses Objective 1. In subsequent subsections we will show how the ideas can be generalized to an adaptive gain matrix  $K_n$ , leading us to the ensemble Kalman methodology and to addressing both Objectives 1 and 2.

**Example 2.1.** To illustrate the problem of state estimation we consider the Lorenz '96 (singlescale) model for unknown  $v \in C(\mathbb{R}^+, \mathbb{R}^L)$  satisfying the equations

$$(2.6a) \quad \dot{v}_\ell = -v_{\ell-1}(v_{\ell-2} - v_{\ell+1}) - v_\ell + F + h_v m(v_\ell), \quad \ell = 1 \dots L,$$

$$(2.6b) \quad v_{\ell+L} = v_\ell, \quad \ell = 1 \dots L.$$

Here we set  $L = 9$ ,  $h_v = -0.8$  and  $F = 10$ . Function  $m$  is shown in Figure 2.1.<sup>2</sup>

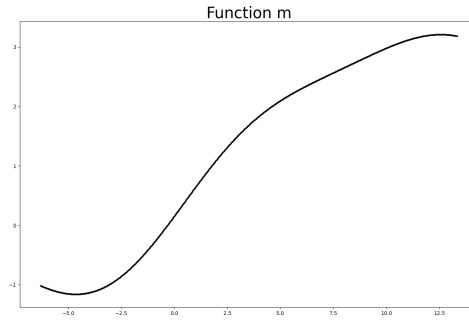


Figure 2.1: Plot of the approximation  $m$ .

Let  $\Psi$  denote the solution operator for (2.6) over the observation time interval  $\tau$ . We emphasize that, at the parameter values we have chosen, (2.6) is chaotic and exhibits sensitivity to perturbations. We consider observations  $\{y_n^\dagger\}_{n \in \mathbb{Z}^+}$  arising from the model

$$\begin{aligned} v_{n+1}^\dagger &= \Psi(v_n^\dagger) + \xi_n^\dagger, \\ y_{n+1}^\dagger &= h(v_{n+1}^\dagger) + \eta_{n+1}^\dagger, \end{aligned}$$

where  $\{\xi_n^\dagger\}_{n \in \mathbb{Z}^+}$ ,  $\{\eta_n^\dagger\}_{n \in \mathbb{N}}$  are mutually independent Gaussian sequences defined by

$$\xi_n^\dagger \sim \mathcal{N}(0, \sigma^2 I) \text{ i.i.d.}, \quad \eta_n^\dagger \sim \mathcal{N}(0, \gamma^2 I) \text{ i.i.d.}.$$

Because of the chaotic nature of the dynamical system defined by iteration of  $\Psi$ , a key question concerning the problem of determining the state  $v_n^\dagger$  from  $Y_n^\dagger$  is whether the observations compensate for the sensitive dependence of the state evolution, enabling accurate recovery of the state.

---

<sup>2</sup>This specific choice of  $m$  does not make any material difference to what is presented in this example; any  $m$  for which the equation is well-posed will lead to similar conclusions. However the specific choice of  $m$  shown in Figure 2.1 is relevant within Example 2.2. We note that setting  $h_v = 0$  in (2.6) leads to the standard singlescale Lorenz'96 model.



We assume that the observation function is linear:  $h(v) = Hv$  for matrix  $H : \mathbb{R}^9 \rightarrow \mathbb{R}^6$  defined by

$$(2.7) \quad Hv = (v_1, v_2, v_4, v_5, v_7, v_8)^\top.$$

The 3DVAR algorithm (2.3) reduces, in the setting of this example, to the mapping

$$(2.8) \quad v_{n+1} = (I - KH)\Psi(v_n) + Ky_{n+1}^\dagger.$$

We define the filter by choosing gain  $K : \mathbb{R}^6 \rightarrow \mathbb{R}^9$  to be

$$(2.9) \quad Kw = (w_1, w_2, 0, w_3, w_4, 0, w_5, w_6, 0)^\top.$$

To interpret the algorithm, and motivate the choice of  $K$ , given  $H$ , notice that

$$(2.10a) \quad KHv = (v_1, v_2, 0, v_4, v_5, 0, v_7, v_8, 0)^\top,$$

$$(2.10b) \quad (I - KH)v = (0, 0, v_3, 0, 0, v_6, 0, 0, v_9)^\top,$$

$$(2.10c) \quad HK = I.$$

Note that, applying the observation map  $H$  to the recursion (2.8) and using (2.10c) we find that

$$Hv_{n+1} = y_{n+1}^\dagger = H(\Psi(v_n^\dagger) + \xi_n^\dagger) + \eta_{n+1}^\dagger.$$

Assuming that  $\sigma^2$  and  $\gamma^2$  are small and neglecting the noise contributions shows that

$$y_{n+1}^\dagger \approx H\Psi(v_n^\dagger) \approx Hv_{n+1}^\dagger.$$

Thus, ignoring small noise perturbations,  $y_{n+1}^\dagger \approx Hv_{n+1}^\dagger$ . Then, using (2.10a) and (2.10b) we see that the algorithm (2.8) has the very natural approximate interpretation of iterating using the model and then overwriting using the observed true state in the observed components. This explains why the specific choice of  $K$  is reasonable.

Because of this interpretation it is natural to study the 3DVAR algorithm, for this example, by displaying the output of 3DVAR on one of the unobserved components, and comparing with the truth; the key question is whether the observed components induce synchronization of 3DVAR with the truth in the unobserved components. Thus, in the following numerical experiments, we display component  $v_3$ .

Figure 2.2 illustrates the foregoing intuition about the behavior of 3DVAR in experiments conducted with the choice  $\tau = 10^{-3}$ . For small noise with variances of size  $10^{-3}$  we observe in Figure 2.2a the phenomenon of near perfect synchronization of the 3DVAR output with the truth. Although not shown here, this synchronization occurs in all components of the solution, observed and unobserved, and thus the entire state of 3DVAR synchronizes with the truth, up to a small error on the scale of the noise. The algorithm thus produces an accurate estimate of the true state. In the scenario of larger state and observational noise, of variance  $10^{-1}$ , displayed in Figure 2.2b, 3DVAR still captures the correct trend of the true dynamics,



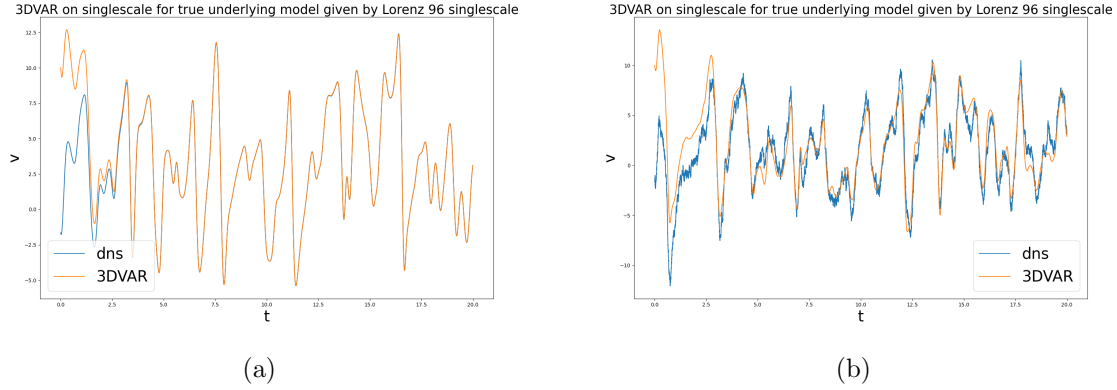


Figure 2.2: In both (a) and (b) the estimates of  $v_3$  in time produced by 3DVAR using  $\tau = 10^{-3}$  are displayed. In (a)  $\sigma^2$  and  $\gamma^2$  are set to  $10^{-3}$ , while in (b) to  $10^{-1}$ . The acronym “dns” refers to direct numerical simulation and, in both cases, it is noteworthy that 3DVAR is able to synchronize with the true trajectory of the chaotic dynamical system, even though it is initialized differently from the direct numerical simulation.

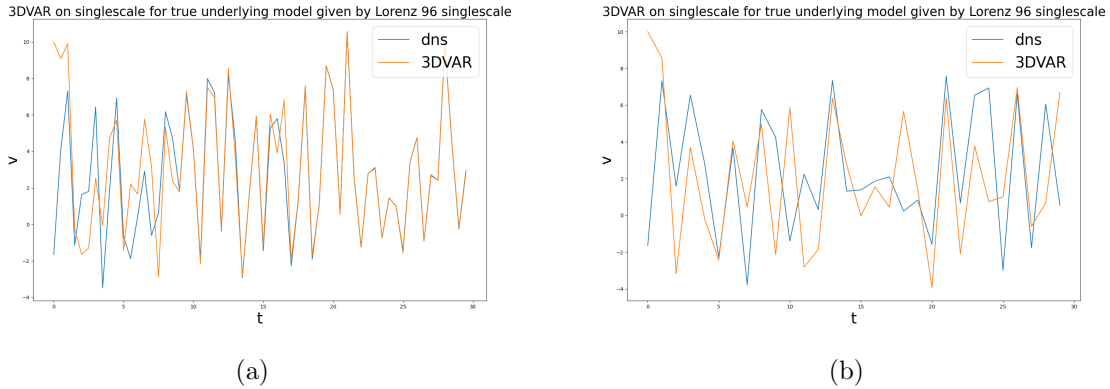


Figure 2.3: In both (a) and (b) the noise variances  $\sigma^2$  and  $\gamma^2$  are set to  $10^{-3}$ . In (a) we display the estimates of  $v_3$  in time produced by 3DVAR against the true dynamics using  $\tau = 5 \cdot 10^{-1}$ , while in (b) using  $\tau = 10^0$ . Again the acronym “dns” refers to direct numerical simulation. 3DVAR successfully synchronizes with the direct numerical simulation at the smaller value of  $\tau$  but fails to do so when  $\tau$  is larger.

but there are clear overshoots and undershoots in the estimates because the noise is larger and not accounted for in the 3DVAR algorithm.

It is intuitive that the synchronization phenomena studied above will depend not only on the size of the noise, but also on the inter-observation time  $\tau$ . Figure 2.3 illustrates the effect

of varying  $\tau$ , in the setting where the variance is  $10^{-3}$ . The simulations show that for  $\tau$  of order  $\mathcal{O}(10^{-1})$ , 3DVAR cannot accurately estimate the true state. ■

A common source of error in data assimilation arises from the fact that the data is not produced by the mathematical model used for assimilation. This is known as *model misspecification*. To illustrate the fact that data assimilation algorithms can be used to address this issue we study it in the context of the Lorenz '96 model. Specifically we will generate data using the Lorenz '96 multiscale model, and assimilate data using the Lorenz '96 singlescale model (2.6). The relationship between the multiscale and singlescale models is detailed in Appendix 7.

**Example 2.2.** To define the multiscale model, let  $v \in C(\mathbb{R}^+, \mathbb{R}^L)$  and  $w \in C(\mathbb{R}^+, \mathbb{R}^{L \times J})$ . Each variable  $v_\ell \in \mathbb{R}$  is coupled to a subgroup of fast variables  $\{w_{\ell,j}\}_{j=1}^J \in \mathbb{R}^J$ . For  $\ell = 1 \dots L$  and  $j = 1 \dots J$ , we write

$$(2.11a) \quad \dot{v}_\ell = f_\ell(v) + h_v \bar{w}_\ell, \quad \bar{w}_\ell = \frac{1}{J} \sum_{j=1}^J w_{\ell,j},$$

$$(2.11b) \quad \dot{w}_{\ell,j} = \frac{1}{\epsilon} r_j(v_\ell, w_\ell)$$

where

$$(2.12a) \quad f_\ell(v) = -v_{\ell-1}(v_{\ell-2} - v_{\ell+1}) - v_\ell + F$$

$$(2.12b) \quad r_j(v_\ell, w_\ell) = -w_{\ell,j+1}(w_{\ell,j+2} - w_{\ell,j-1}) - w_{\ell,j} + h_w v_\ell,$$

and we impose the boundary conditions

$$(2.13) \quad v_{\ell+L} = v_\ell, \quad w_{\ell+L,j} = w_{\ell,j}, \quad w_{\ell,j+J} = w_{\ell+1,j}.$$

Here  $\epsilon > 0$  is a scale-separation parameter,  $h_v, h_w \in \mathbb{R}$  govern the couplings between the fast and slow systems, and  $F > 0$  provides a constant forcing. Note that the equation (2.11a) has the form of the singlescale Lorenz model (2.6) with a coupling to the fast variables replacing the function  $m(\cdot)$ . We set  $L = 9$ ,  $J = 8$ ,  $h_v = -0.8$ ,  $h_w = 1$ ,  $F = 10$  and  $\epsilon = 2^{-7}$  in what follows. In Figure 2.4 we display the dynamics of a slow variable and one associated fast variable of this Lorenz '96 multiscale model; at the parameter values chosen the system is chaotic.

We consider observations  $\{y_n^\dagger\}_{n \in \mathbb{Z}^+}$  arising from the model

$$\begin{aligned} (v_{n+1}^\dagger, w_{n+1}^\dagger) &= \Psi_{\text{mult}}(v_n^\dagger, w_n^\dagger), \\ y_{n+1}^\dagger &= h(v_{n+1}^\dagger), \end{aligned}$$

where  $\Psi_{\text{mult}}$  is the solution operator to the multiscale model (2.11)–(2.13) over the observation time interval  $\tau$ . We then take the data from the multiscale model and assimilate it into the singlescale model (2.6), recalling the relationship between them detailed in Appendix 7, and the importance of the specific function  $m$  shown in Figure 2.1, to the elimination

of the fast variables in favour of a simple closure, using the averaging principle. As in the preceding Example 2.1, we assume that the observation function is linear:  $h(v) = Hv$  for matrix  $H : \mathbb{R}^9 \rightarrow \mathbb{R}^6$  defined by (2.7). As before we choose the gain  $K : \mathbb{R}^6 \rightarrow \mathbb{R}^9$  to be defined by (2.9) and employ the 3DVAR algorithm (2.8) with  $\Psi$  the solution operator over time-interval  $\tau$  for the singlescale model.

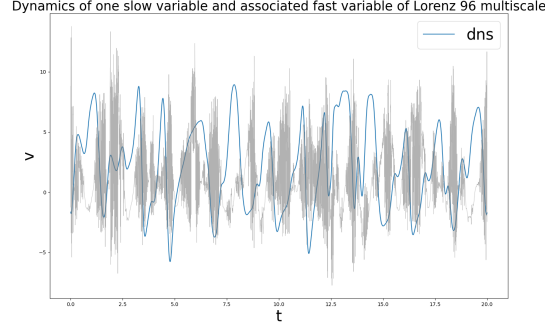


Figure 2.4: Dynamics of a slow variable and an associated fast variable. Here “dns”, in blue, labels the slow variable computed by direct numerical simulation; in grey is the related fast variable.

Again we display the results of 3DVAR on the unobserved component  $v_3$ . Figure 2.5a shows the behavior of the algorithm for  $\tau = 10^{-3}$ . Despite the fact that the data is generated from the multiscale model, whilst assimilation is conducted using the singlescale model, 3DVAR produces an accurate estimate of the true state with, after synchronization, the only discernible errors being slight under and overshoots. Figure 2.5b shows the effect of varying  $\tau$ , the time between observations. As in Example 2.1 the assimilation breaks down when  $\tau$  is larger. ■

The control theoretic approach encapsulated in 3DVAR addresses Objective 1. However, when  $|C_0|$ ,  $|\Gamma|$  and  $|\Sigma|$  are no longer necessarily small, so that the state and observations are subject to noise, it is natural to try and generalize the approach to address Objective 2, and include non-zero covariances; Example 2.1 shows that this may be needed when noise is larger. A natural stochastic generalization of the observer approach is as follows: from current state estimate  $v_n$ , given  $Y_n^\dagger$ , predict the outcome of the model and data from the update equations (2.1), which we denote by  $(\hat{v}_{n+1}, \hat{y}_{n+1})$ ; then correct the state estimate by nudging the mean of the prediction using the mismatch between observed and predicted data  $(y_{n+1}^\dagger, \hat{y}_{n+1})$ . Given  $v_n$  computed from  $Y_n^\dagger$  this results in state estimate  $v_{n+1}$  from  $Y_{n+1}^\dagger$  defined through the following stochastic dynamical system, assumed to hold for all  $n \in \mathbb{Z}^+$ :

(2.14a)

$$\hat{v}_{n+1} = \Psi(v_n) + \xi_n,$$

(2.14b)

$$\hat{y}_{n+1} = h(\hat{v}_{n+1}) + \eta_{n+1},$$

(2.14c)

$$v_{n+1} = \hat{v}_{n+1} + K_n I_n;$$

here  $v_0$ ,  $\xi_n$  and  $\eta_{n+1}$  are random variables given by the known distributions in (2.2) and  $I_n$  is

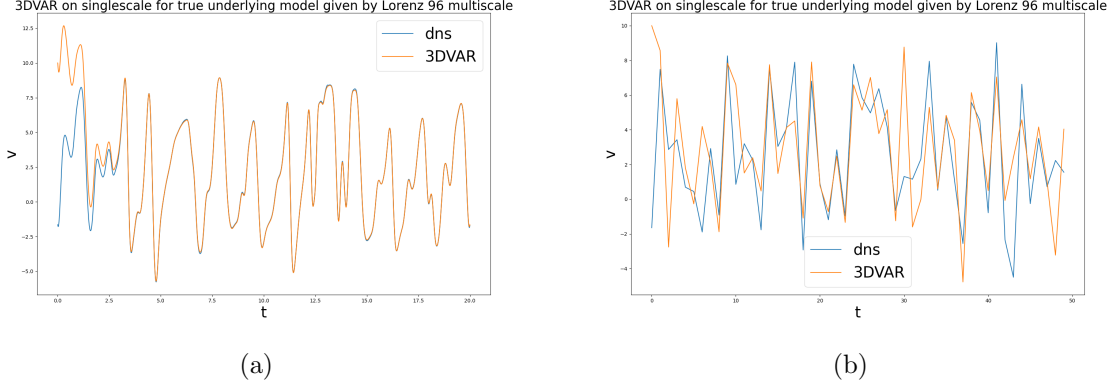


Figure 2.5: In (a) the estimates of  $v_3$  in time produced by 3DVAR using  $\tau = 10^{-3}$  are displayed against the true dynamics. In (b) the estimates of 3DVAR are shown for  $\tau = 10^0$ . Again the acronym “dns” refers to direct numerical simulation. 3DVAR successfully synchronizes with the direct numerical simulation at the smaller value of  $\tau$  but fails to do so when  $\tau$  is larger. It is noteworthy that the synchronization takes place here in the context of model misspecification: the data is generated by the multiscale model, but 3DVAR is applied using the singlescale model.

modified from (2.5) to read

$$(2.15) \quad I_n = y_{n+1}^\dagger - \hat{y}_{n+1}.$$

The data  $\{y_{n+1}^\dagger\}_{n \in \mathbb{Z}^+}$  is a fixed realization of (2.1). Given this data, equations (2.14) then define a random map  $v_n \mapsto v_{n+1}$  which uses knowledge of the model and the observed data to update our state estimate. The predicted state and data  $(\hat{v}_{n+1}, \hat{y}_{n+1})$  are also referred to as the *simulated state and data*. Choice of the *gain matrix*  $K_n$  will complete definition of an algorithm. The key question we proceed to study in subsequent sections concerns the choice of  $\{K_n\}_{n \in \mathbb{Z}^+}$ . We do this in the context of addressing Objective 2. Before doing so we continue our running example, studying the effect of noise on the 3DVAR algorithm, where  $K_n = K$  is constant; this example demonstrates the need for an adaptive choice of  $K_n$  when noise is significant.

**Example 2.3.** We return to the setting of Example 2.1 and consider the effect of including noise in 3DVAR as in (2.14), (2.15). We again study the Lorenz '96 singlescale model (2.6) for unknown  $v \in C(\mathbb{R}^+, \mathbb{R}^L)$ , with  $L = 9$ ,  $h_v = -0.8$  and  $F = 10$ . We let  $\Psi$  denote the solution operator for (2.6) over the observation time interval  $\tau$  and consider observations  $\{y_n^\dagger\}_{n \in \mathbb{Z}^+}$  defined by

$$\begin{aligned} v_{n+1}^\dagger &= \Psi(v_n^\dagger) + \xi_n^\dagger, \\ y_{n+1}^\dagger &= h(v_{n+1}^\dagger) + \eta_{n+1}^\dagger, \end{aligned}$$

where  $\{\xi_n^\dagger\}_{n \in \mathbb{Z}^+}$ ,  $\{\eta_n^\dagger\}_{n \in \mathbb{N}}$  are mutually independent Gaussian sequences

$$\xi_n^\dagger \sim \mathcal{N}(0, \sigma^2 I) \text{ i.i.d.}, \quad \eta_n^\dagger \sim \mathcal{N}(0, \gamma^2 I) \text{ i.i.d.},$$

with  $\sigma^2 = 0.1$  and  $\gamma^2 = 0.1$ . We again assume that the observation function is linear:  $h(v) = Hv$  for matrix  $H : \mathbb{R}^9 \rightarrow \mathbb{R}^6$  defined by (2.7). As in Example 2.1 we choose fixed gain  $K_n \equiv K$  with  $K : \mathbb{R}^6 \rightarrow \mathbb{R}^9$  defined by (2.9).

Figure 2.6 illustrates that this version of noisy 3DVAR does not perform better than the noise-free 3DVAR (2.8), in the setting where true state and true observation noise levels are high. To quantitatively demonstrate this, we compute the mean squared error between the estimates arising from the 3DVAR algorithm (2.8) and the true states, and the mean squared error between the estimates obtained using noisy 3DVAR algorithm (2.14), (2.15) and the true states. Given either method the error  $e$  is computed using the following formula, in which, recall,  $\{v_n^\dagger\}$  is the truth and  $\{v_n\}$  is the output of the 3DVAR or noisy 3DVAR algorithm:

$$(2.16) \quad e = \frac{1}{N \cdot d_v} \sum_{n=1}^N |v_{n+t/\tau}^\dagger - v_{n+t/\tau}|^2$$

where  $N$  is such that  $t + N\tau = T$ . Time  $t$  is chosen to remove error from the incorrect initialization, and focus on quantifying error in statistical steady state;  $T$  is chosen to allow time-averaging over a long enough window to capture this statistical steady state. In this case, we compute this average for the estimates obtained after time  $t = 5$ , up to  $T = 30$ , and report  $e_{\text{3DVAR}} = 1.47 \cdot 10^0$  and  $e_{\text{noisy3DVAR}} = 3.07 \cdot 10^0$ . Clearly use of noisy 3DVAR does not improve the error, in comparison with noise-free 3DVAR. ■

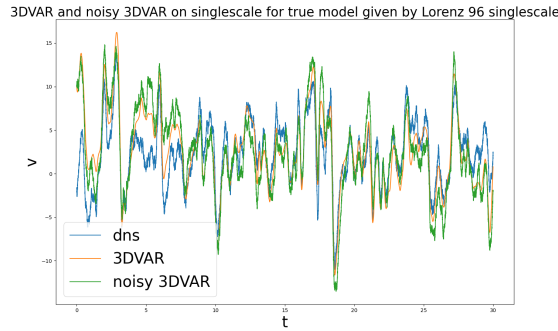


Figure 2.6: In this experiment we set the noise levels  $\sigma^2 = 10^{-1}$ ,  $\gamma^2 = 10^{-1}$ . Again the acronym “dns” refers to direct numerical simulation. We display the estimates of  $v_3$  in time produced by 3DVAR and noisy 3DVAR against the true dynamics using  $\tau = 10^{-3}$ .

Example 2.3 highlights the need to quantify uncertainty and pass to a probabilistic interpretation (Objective 2) of the filtering problem; and, in particular, to make an informed choice of adaptive gain matrices  $K_n$ . We turn to the probabilistic interpretation in the next

subsection; in subsequent subsections we derive algorithms, leading in particular to a specific choice of adaptive gain matrices.

**2.3. Probabilistic Perspective.** We have shown that the 3DVAR methodology can recover the state of a (possibly chaotic) dynamical system, even though the initial condition is not known, by exploiting the observations. However it does not quantify uncertainty in the state estimate. We now introduce a probabilistic perspective which enables us to address this issue. In Subsection 2.3.1 we define the filtering distribution and in Subsection 2.3.2 we establish some notation used throughout the sequel.

**2.3.1. The Filtering Distribution.** To understand how uncertainty may be expressed mathematically we introduce the *filtering distribution*  $\mu_n$ : the distribution of the conditioned random variable  $v_n|Y_n^\dagger$ . This captures the knowledge of the state of the system, and uncertainties in the state, given the observations. It is important to understand how this distribution evolves with  $n$ . In particular, the evolution has a *nonlinear* Markov structure; we emphasize that standard Markov processes are linear, and defined by the linear transition kernel; nonlinearity arises in filtering through the incorporation of data. The map  $\mu_n \mapsto \mu_{n+1}$  is most easily described by defining  $\hat{\mu}_{n+1}$ , the distribution of  $v_{n+1}|Y_n^\dagger$  and  $\nu_{n+1}$ , the distribution of  $(v_{n+1}, y_{n+1})|Y_n^\dagger$ . The map from  $\mu_n$  to  $\hat{\mu}_{n+1}$  is defined by equation (2.3a) and is *linear* as a map from the space of probability measures defined on  $\mathbb{R}^{d_v}$  into itself; the map from  $\hat{\mu}_{n+1}$  to  $\nu_{n+1}$  is defined by (2.3b), and is *linear* as a map from the space of probability measures defined on  $\mathbb{R}^{d_v}$  into the space of probability measures defined on  $\mathbb{R}^{d_v+d_y}$ ; the map from  $\nu_{n+1}$  to  $\mu_{n+1}$  is defined by conditioning  $\nu_{n+1}$  on  $y_{n+1}^\dagger$  and is *nonlinear* as a map from the space of probability measures defined on  $\mathbb{R}^{d_v+d_y}$  into the space of probability measures defined on  $\mathbb{R}^{d_v}$ . We thus have

$$\begin{aligned} (2.17a) \quad & \hat{\mu}_{n+1} = P\mu_n, \\ (2.17b) \quad & \nu_{n+1} = Q\hat{\mu}_{n+1}, \\ (2.17c) \quad & \mu_{n+1} = B_n(\nu_{n+1}), \end{aligned}$$

where  $P$  and  $Q$  are linear maps on measures, whilst  $B_n(\cdot)$  is nonlinear and time dependent. Concatenating we find that

$$(2.18) \quad \mu_{n+1} = B_n(QP\mu_n), \quad \mu_0 = \mathbf{N}(m_0, C_0).$$

This map defines an inhomogeneous nonlinear Markov process on the space of probability measures on  $\mathbb{R}^{d_v}$ . Markovian because it maps probability measures at time  $n$  into probability measures at time  $n+1$ ; nonlinear because of the conditioning operator  $B_n(\cdot)$ ; and inhomogeneous because map  $B_n$  depends on time  $n$  through the time-varying observation  $y_{n+1}^\dagger$ . The map  $B_n(QP\cdot)$  may be decomposed into two maps: the *prediction*  $P$ , which represents application of the dynamical model (2.1a), and application of *Bayes Theorem*<sup>3</sup> through operator  $L_n \cdot := B_n(Q\cdot)$ , which corresponds to use of likelihood defined by the observation model (2.1b).

---

<sup>3</sup>Often referred to as the *analysis* step in the geophysical data assimilation community.

With this notation we thus obtain

$$\begin{aligned} (2.19a) \quad & \hat{\mu}_{n+1} = P\mu_n, \\ (2.19b) \quad & \mu_{n+1} = L_n(\hat{\mu}_{n+1}). \end{aligned}$$

We refer to iteration of (2.19) as the *filtering cycle*. The cycle involves iterative interleaving of prediction, using the dynamical model, a linear operation on measures, and Bayes Theorem, using the observation model, a nonlinear operation on measures.

It is useful, notationally, to work with measures  $\mu_n, \hat{\mu}_n, \nu_n$  rather than their Lebesgue densities; this facilitates clean presentation of particle approximations which employ Dirac measures. However, to define the maps  $P, Q$  and  $L_n$ , we use probability densities arising from the Gaussian nature of the noise appearing in (2.1), summarized in (2.2). To this end, note that (2.1a) is defined by Markov transition kernel  $p(u, v)$ , and the probability of  $y|v$  underlying (2.1b) is defined by kernel  $q(v, y)$ . When  $\Sigma \succ 0, \Gamma \succ 0$ , these are given by

$$(2.20a) \quad p(u, v) = \frac{1}{(2\pi)^{d_v/2} \sqrt{\det(\Sigma)}} \exp\left(-\frac{1}{2}|v - \Psi(u)|_{\Sigma}^2\right),$$

$$(2.20b) \quad q(v, y) = \frac{1}{(2\pi)^{d_y/2} \sqrt{\det(\Gamma)}} \exp\left(-\frac{1}{2}|y - h(v)|_{\Gamma}^2\right).$$

Then we have

$$\begin{aligned} (P\mu)(dv) &= \left( \int_{u \in \mathbb{R}^{d_u}} p(u, v) \mu(du) \right) dv, \\ (Q\mu)(dv, dy) &= q(v, y) \mu(dv) dy, \\ (B_n \nu)(dv) &= \int_{y \in \mathbb{R}^{d_y}} \delta_{y_{n+1}^\dagger}(y) \nu(dv, dy) / \left( \int_{(v, y) \in \mathbb{R}^{d_v} \times \mathbb{R}^{d_y}} \delta_{y_{n+1}^\dagger}(y) \nu(dv, dy) \right) \\ L_n(\mu)(dv) &= q(v, y_{n+1}^\dagger) \mu(dv) / \left( \int_{v \in \mathbb{R}^{d_v}} q(v, y_{n+1}^\dagger) \mu(dv) \right). \end{aligned}$$

It is important to appreciate that there is, in general, no closed form expression for  $\mu_n$  defined by the iteration (2.18); thus (2.18) does not constitute an algorithm. However if  $\Psi$  and  $h$  are linear then, since  $\mu_0 = \mathcal{N}(m_0, C_0)$  is Gaussian, it follows that  $\hat{\mu}_{n+1}, \nu_{n+1}, \mu_{n+1}$  are all Gaussian for all  $n \in \mathbb{Z}^+$ , and closed form expressions, based on dynamical updates of means and covariances, are available; this is the *Kalman filter* discussed in Subsection 2.4.2. Furthermore, the idea of making a Gaussian approximation will play a central role in ensemble Kalman methods, and this perspective is developed in Subsection 2.4.

**2.3.2. Important Repeatedly Used Notation.** Throughout this subsection let  $v_n$  be a random variable distributed according to  $\text{Law}(v_n)$ , let  $\hat{v}_{n+1}$  be random variable with  $\text{Law}(\hat{v}_{n+1}) = P\text{Law}(v_n)$  and let  $(\hat{v}_{n+1}, \hat{y}_{n+1})$  be random variable with law  $Q\text{Law}(\hat{v}_{n+1})$ . Using  $\text{Law}$  avoids a proliferation of notation for the different measures arising from the use of various different algorithms to approximate the filtering cycle.



All of the algorithms are based on a prediction of state, and possibly observation, from  $Law(v_n)$ . To this end recall (2.14) and for all  $n \in \mathbb{Z}^+$ ,

$$(2.21a) \quad \hat{v}_{n+1} = \Psi(v_n) + \xi_n,$$

$$(2.21b) \quad \hat{y}_{n+1} = h(\hat{v}_{n+1}) + \eta_{n+1}.$$

The distribution of  $(\hat{v}_{n+1}, \hat{y}_{n+1})$  given by these equations defines  $PLaw(v_n)$  and  $QLaw(\hat{v}_{n+1})$ . A common theme in this paper is to augment these equations for the predicted state and data with a final map

$$(2.22) \quad \hat{v}_{n+1} \mapsto v_{n+1}, \text{ or } (\hat{v}_{n+1}, \hat{y}_{n+1}) \mapsto v_{n+1}$$

in such a way that, if  $v_n \sim \mu_n$  then  $v_{n+1} \sim \mu_{n+1}$ ; the algorithms we study will be based on approximations of such maps. We refer to equations (2.21, 2.22) as the *sample path perspective*, designed to exactly or approximately reproduce the *probabilistic perspective* encapsulated in the three steps of (2.17). Similarly we will also introduce equations of the form (2.21a, 2.22) to provide sample path exact, or approximate, reproduction of the probabilistic perspective encapsulated in the two steps of (2.19).

In service of designing these approximations, it is useful to define various first and second order statistics computed under the law of  $(\hat{v}_{n+1}, \hat{y}_{n+1})$ . First define mean and covariance of  $\hat{v}_{n+1}$  :

$$(2.23a) \quad \hat{m}_{n+1} = \mathbb{E}\hat{v}_{n+1},$$

$$(2.23b) \quad \hat{C}_{n+1} = \mathbb{E}\left((\hat{v}_{n+1} - \hat{m}_{n+1}) \otimes (\hat{v}_{n+1} - \hat{m}_{n+1})\right).$$

Then define mean of the predicted data, cross-covariance from predicted data to state and covariance of the data:

$$(2.24a) \quad \hat{o}_{n+1} = \mathbb{E}\hat{y}_{n+1},$$

$$(2.24b) \quad \hat{C}_{n+1}^{vy} = \mathbb{E}\left((\hat{v}_{n+1} - \hat{m}_{n+1}) \otimes (\hat{y}_{n+1} - \hat{o}_{n+1})\right),$$

$$(2.24c) \quad \hat{C}_{n+1}^{yy} = \mathbb{E}\left((\hat{y}_{n+1} - \hat{o}_{n+1}) \otimes (\hat{y}_{n+1} - \hat{o}_{n+1})\right).$$

From these covariances we define the matrix

$$(2.25) \quad K_n = \hat{C}_{n+1}^{vy} (\hat{C}_{n+1}^{yy})^{-1}.$$

This particular choice of  $K_n$ , known as the *Kalman gain*, is required for definition of the Kalman filter, and will play a central role in the mean field maps which underpin ensemble Kalman methods through their particle approximations. The origin of this key concept will be described in the next subsection. Note that, if  $\hat{C}_{n+1}^{yy}$  is not invertible, then its action may still be defined through a pseudo-inverse.

We also note that, in view of (2.21b),  $\hat{o}_{n+1} = \mathbb{E}h(\hat{v}_{n+1})$ . It is sometimes useful to express the Kalman gain  $K_n$  in terms of the variable  $h_{n+1} = h(\hat{v}_{n+1})$ . For this purpose we define the

associated correlation matrices

$$(2.26a) \quad \hat{C}_{n+1}^{vh} = \mathbb{E}\left((\hat{v}_{n+1} - \hat{m}_{n+1}) \otimes (\hat{h}_{n+1} - \hat{o}_{n+1})\right),$$

$$(2.26b) \quad \hat{C}_{n+1}^{hh} = \mathbb{E}\left((\hat{h}_{n+1} - \hat{o}_{n+1}) \otimes (\hat{h}_{n+1} - \hat{o}_{n+1})\right),$$

and note that

$$(2.27a) \quad \hat{C}_{n+1}^{vy} = \hat{C}_{n+1}^{vh}, \quad \hat{C}_{n+1}^{yy} = \hat{C}_{n+1}^{hh} + \Gamma,$$

$$(2.27b) \quad K_n = \hat{C}_{n+1}^{vh} \left( \hat{C}_{n+1}^{hh} + \Gamma \right)^{-1}.$$

Note that, if  $\Gamma \succ 0$ ,  $K_n$  is well-defined without recourse to the use of pseudo-inverse.

**2.4. Gaussian Projected Filtering Distribution.** The Gaussian projected filtering distribution is an approximation of the true filtering which leads to a filter which is Gaussian. It is defined by the following steps: (i) taking input Gaussian at time  $n$  as  $Law(v_n)$  and pushing this measure forward under (2.21) to find a (typically non-Gaussian) measure for  $Law(\hat{v}_{n+1}, \hat{y}_{n+1})$ ; (ii) projecting this joint measure onto the nearest Gaussian (in a sense that we will make precise); (iii) then finally conditioning this Gaussian on the data  $y_{n+1}^\dagger$  to find output Gaussian at time  $n+1$ . We note that conditioning a Gaussian random variable on linear functionals of the random variable returns another Gaussian.

The resulting approximation of the filtering distribution plays an important role in motivating the mean field maps, introduced in Section 2.5, whose particle approximations lead to various ensemble Kalman methods introduced in Section 2.6. In Subsection 2.4.1 we introduce the Gaussian projected approximation to the evolution (2.18). In the case where  $\Psi(\cdot)$  and  $h(\cdot)$  are linear the resulting formulae deliver exact solutions of the filtering cycle (2.18), leading to the Kalman filter as derived in Subsection 2.4.2. The Gaussian projected filter leads to a derivation of the Kalman gain (2.25); an alternative derivation, using the minimum variance approach, may be found in Appendix C, Subsection 8.3.

**2.4.1. Gaussian Projected Filtering.** To describe the Gaussian projected approximation to the filtering distribution, we define the following map  $G$ :

**Definition 2.4.** Let  $\mathfrak{P} = \mathfrak{P}(\mathbb{R}^d)$  denote the set of probability measures on  $\mathbb{R}^d$  and let  $\mathfrak{G} = \mathfrak{G}(\mathbb{R}^d)$  denote the set of Gaussian probability measures on  $\mathbb{R}^d$  (including indefinite covariances and hence all Dirac masses) and define  $G : \mathfrak{P} \mapsto \mathfrak{G}$ , for  $u \sim \mu$ , by

$$G\mu = N(m^\mu, C^\mu), \quad m^\mu = \mathbb{E}^\mu u, \quad C^\mu = \mathbb{E}^\mu((u - \mathbb{E}^\mu u) \otimes (u - \mathbb{E}^\mu u)).$$

Thus the map  $G$  applied to measure  $\mu$  simply computes the Gaussian with mean and covariance under  $\mu$ . Notice that  $G$  is the identity on Gaussians. Furthermore  $G \circ G = G$ . We refer to this as a *projection* onto Gaussians because it corresponds to finding the closest point to given measure  $\mu$ , with respect to a Kullback-Leibler divergence<sup>4</sup>:

$$G\mu = \operatorname{argmin}_{\pi \in \mathfrak{G}} d_{\text{KL}}(\mu || \pi).$$

---

<sup>4</sup>For details see the bibliography Subsection 2.7

We now use mapping  $G$  to find an approximation to the evolution (2.17) which generates measures which remain Gaussian; intuitively this will be a good approximation whilst the measures  $\{\mu_n\}$  evolving under (2.18) remain close to Gaussian. To this end we consider random variable  $v_n \sim \mu_n^G$  where the probability measure  $\mu_n^G$  evolves according to

$$(2.28) \quad \mu_{n+1}^G = B_n(GQP\mu_n^G), \quad \mu_0^G = \mathbf{N}(m_0, C_0).$$

This may be decomposed as follows:

$$\begin{aligned} (2.29a) \quad & \hat{\mu}_{n+1}^G = P\mu_n^G, \\ (2.29b) \quad & \nu_{n+1}^G = Q\hat{\mu}_{n+1}^G, \\ (2.29c) \quad & \mu_{n+1}^G = B_n(G\nu_{n+1}^G). \end{aligned}$$

Map (2.28) defines a nonlinear Markov process, similarly to (2.18). It also maps Gaussians into Gaussians. This fact follows from the fact that the nonlinear map  $B_n(\cdot)$ , which represents conditioning, maps Gaussians into Gaussians. The map  $\mu_n^G \mapsto \mu_{n+1}^G$  hence defines a deterministic mapping from the mean  $m_n$  and covariance  $C_n$  of  $\mu_n^G$  into the mean  $m_{n+1}$  and covariance  $C_{n+1}$  of  $\mu_{n+1}^G$ . We now identify this map explicitly.

For  $v_n \sim \mu_n^G$  we introduce the random variables  $\hat{v}_{n+1}, \hat{y}_{n+1}$  defined by (2.21). It then follows that  $\hat{v}_{n+1} \sim \hat{\mu}_{n+1}^G = P\mu_n^G$  and that  $(\hat{v}_{n+1}, \hat{y}_{n+1}) \sim \nu_{n+1}^G = QP\mu_n^G$ . Note also that  $\hat{\mu}_{n+1}^G$  and  $\nu_{n+1}^G$  are not Gaussian, but are defined by the Gaussian  $\mu_n^G$  and hence completely determined by  $m_n$  and  $C_n$ . Thus the mean and covariance under  $\hat{\mu}_{n+1}^G$  are  $(\hat{m}_{n+1}, \hat{C}_{n+1})$  given by (2.23). Furthermore,  $G\nu_{n+1}^G$  is defined by

$$G\nu_{n+1}^G = \mathbf{N}\left(\begin{bmatrix} \hat{m}_{n+1} \\ \hat{o}_{n+1} \end{bmatrix}, \begin{bmatrix} \hat{C}_{n+1} & \hat{C}_{n+1}^{vy} \\ (\hat{C}_{n+1}^{vy})^\top & \hat{C}_{n+1}^{yy} \end{bmatrix}\right),$$

where all relevant quantities are defined in Subsection 2.3.2.

We now condition the Gaussian  $G\nu_{n+1}^G$ , on the second component of the vector taking value  $y_{n+1}^\dagger$ . From this we find the Gaussian measure  $\mu_{n+1}^G = B_n(G\nu_{n+1}^G)$  characterized by mean  $m_{n+1}$  and covariance  $C_{n+1}$  given by the following lemma:

**Lemma 2.5.** *Assume that  $\Gamma \succ 0$ . Let  $m_n$  and  $C_n$  denote the mean and covariance under the Gaussian projected filter. Consider  $\hat{m}_{n+1}, \hat{C}_{n+1}$  given by equations (2.21), (2.23), and the mean of the observed data and covariances given by (2.24). Then  $\hat{C}_{n+1}^{yy} \succ 0$  for all  $n \in \mathbb{Z}^+$  and*

$$\begin{aligned} (2.30a) \quad & m_{n+1} = \hat{m}_{n+1} + \hat{C}_{n+1}^{vy}(\hat{C}_{n+1}^{yy})^{-1}(y_{n+1}^\dagger - \hat{o}_{n+1}), \\ (2.30b) \quad & C_{n+1} = \hat{C}_{n+1} - \hat{C}_{n+1}^{vy}(\hat{C}_{n+1}^{yy})^{-1}(\hat{C}_{n+1}^{vy})^\top, \end{aligned}$$

where  $\{y_n^\dagger\}$  arises from a fixed realization of (2.1).

**Proof.** We first note that  $\hat{C}_{n+1}^{yy} \succ 0$ . Indeed, since by assumption  $\Gamma \succ 0$  and by definition  $\hat{C}_{n+1}^{hh} \succeq 0$ , then  $\hat{C}_{n+1}^{hh} + \Gamma \succ 0$ . Hence by (2.27) we have that  $\hat{C}_{n+1}^{yy} \succ 0$ . By explicitly

formulating the distribution of the Gaussian  $G\nu_{n+1}^G$  conditioned on  $y_{n+1}^\dagger$ , it is possible to conclude that from standard formulae for conditioned Gaussians that  $m_{n+1}$  and  $C_{n+1}$  are given by the expressions in (2.30). ■

Equations (2.21), (2.23), (2.24) and (2.30) define a mapping from  $\mu_n^G$ , characterized by  $(m_n, C_n)$ , into  $\mu_{n+1}^G$ , characterized by  $(m_{n+1}, C_{n+1})$ . They comprise an explicit set of formulae for the mapping (2.28): since Gaussians are determined by mean and covariance, the map on measures is completely determined by the map from  $(m_n, C_n)$  to  $(m_{n+1}, C_{n+1})$ .

We note that (2.30) can also be rewritten as

$$\begin{aligned} (2.31a) \quad & m_{n+1} = \hat{m}_{n+1} + \hat{C}_{n+1}^{vh}(\hat{C}_{n+1}^{hh} + \Gamma)^{-1}(y_{n+1}^\dagger - \hat{o}_{n+1}), \\ (2.31b) \quad & C_{n+1} = \hat{C}_{n+1} - \hat{C}_{n+1}^{vh}(\hat{C}_{n+1}^{hh} + \Gamma)^{-1}(\hat{C}_{n+1}^{vh})^\top. \end{aligned}$$

Equations (2.21), (2.23), (2.26) and (2.31) then also define the mapping from  $\mu_n^G$  into  $\mu_{n+1}^G$  and also comprise an explicit set of formulae for the updates of the mean and covariance which characterize mapping (2.28).

Finally we note that, using the definition (2.25) of Kalman gain, we can rewrite (2.30) as

$$\begin{aligned} m_{n+1} &= \hat{m}_{n+1} + K_n(y_{n+1}^\dagger - \hat{o}_{n+1}), \\ C_{n+1} &= \hat{C}_{n+1} - K_n(\hat{C}_{n+1}^{vy})^\top. \end{aligned}$$

**Remark 2.6.** The preceding explicit formulae for (2.28) involve the computation of expectations under the non-Gaussian measure  $\text{Law}(\hat{v}_{n+1}, \hat{y}_{n+1})$ . For this reason they do not constitute an algorithm. A possible approach to algorithmic implementations involves quadrature to approximate the expectations, leading, for example, to the *unscented Kalman filter* approach; details may be found in the bibliography Subsection 2.7. However the formulation of explicit maps on Gaussians plays a different, important, role in this paper: we use it as a way of explaining the sense in which the distribution of our mean-field models approximate evolution of measures under the true filtering distribution; see Subsection 2.5.5. The explicit map on means and covariances also enables us to derive the Kalman filter, which applies in the linear Gaussian setting, the topic of the next subsection. ■

**2.4.2. The Kalman Filter.** In the setting where  $\Psi(\cdot) = M\cdot$  and  $h(\cdot) = H\cdot$  are both linear, (2.1) becomes

$$\begin{aligned} (2.32a) \quad & v_{n+1} = Mv_n + \xi_n, \\ (2.32b) \quad & y_{n+1} = Hv_{n+1} + \eta_{n+1}. \end{aligned}$$

Furthermore, the mappings (2.18) and (2.28) are identical and the Gaussian projected filter is exact. Then, equations (2.23) give

$$\begin{aligned} (2.33a) \quad & \hat{m}_{n+1} = Mm_n, \\ (2.33b) \quad & \hat{C}_{n+1} = MC_nM^\top + \Sigma; \end{aligned}$$

and (2.24) and (2.30) give

$$\begin{aligned} (2.34a) \quad & m_{n+1} = \hat{m}_{n+1} + \hat{C}_{n+1} H^\top (H \hat{C}_{n+1} H^\top + \Gamma)^{-1} (y_{n+1}^\dagger - H \hat{m}_{n+1}), \\ (2.34b) \quad & C_{n+1} = \hat{C}_{n+1} - \hat{C}_{n+1} H^\top (H \hat{C}_{n+1} H^\top + \Gamma)^{-1} H \hat{C}_{n+1}, \end{aligned}$$

where  $\{y_n^\dagger\}$  arises from a fixed realization of (2.32). The update equations (2.33), (2.34) constitute the Kalman filter, which applies to (2.1) in the linear setting, mapping  $(m_n, C_n)$  to  $(m_{n+1}, C_{n+1})$ . The equations as stated are well-defined if  $\Gamma \succ 0$ .

**2.5. Mean Field Maps.** Note that elements of  $\mathfrak{P}(\mathbb{R}^d)$  are infinite dimensional objects. The preceding subsection provides explicit *finite dimensional maps* which characterize the Gaussian projected filter  $\mu_n^G \mapsto \mu_{n+1}^G$ . This is possible because Gaussians are completely determined by a finite amount of information – the mean and covariance. In this section we have a more ambitious aim: to find maps on finite dimensional spaces with the property that (possibly only approximately) their output is equal in law to the map on measures  $\mu_n \mapsto \mu_{n+1}$  given by the filtering cycle. We achieve this by studying transport maps that achieve (2.22), or approximate it; this leads us to the subject of mean field maps, namely random maps that depend on the law of the state being mapped.

Consider probability measures  $\nu$  and  $\nu'$  on  $\mathbb{R}^d$  and  $\mathbb{R}^{d'}$  respectively, and recall the definition of pushforward of a measure under  $T : \mathbb{R}^d \rightarrow \mathbb{R}^{d'}$ : the statement  $\nu' = T^\# \nu$  is a succinct way of stating that, if  $\text{Law}(v) = \nu$  and  $v' = T(v)$ , then  $\text{Law}(v') = \nu'$ . Given probability measures  $\pi$  and  $\pi'$  on  $\mathbb{R}^d$  and  $\mathbb{R}^{d'}$  respectively, a *transport*  $T : \mathbb{R}^d \rightarrow \mathbb{R}^{d'}$  is a map with property that the pushforward of probability measure  $\pi$  under  $T$ ,  $T^\# \pi$ , is equal to probability measure  $\pi'$ . In the following we refer to  $\pi$  as the *source measure* and  $\pi'$  as the *target measure* defining the transport. In our setting  $\pi'$  will be uniquely determined by  $\pi$ , together with an observed piece of finite dimensional data. Thus  $T$  depends on  $\pi$  and so we may view  $T$  as a mapping  $\mathbb{R}^d \times \mathfrak{P} \rightarrow \mathbb{R}^{d'}$ , suppressing, for the moment, explicit dependence on the observed data. We can compute the pushforward of  $T$  on any measure in  $\mathfrak{P}$ ; but when we compute the pushforward on  $\pi$  we obtain  $\pi'$ . We emphasize that transport maps are not uniquely defined by their source and target measures and require certain conditions for their existence, which we assume here to be satisfied. The underlying mathematical concept is that of coupling of measures. See Subsection 2.7 for discussion of transport, optimal transport and coupling.

We will also consider classes of *approximate transport maps* which do not achieve transport from  $\pi$  to  $\pi'$ , but instead match second order moments information (we will be precise below). Such maps will also depend on  $\pi$ . To be completely clear, the dependence of (possibly approximate) transport  $T$  on a measure in  $\mathfrak{P}$  does not affect the definition of pushforward; we employ the following general definition of pushforward for measure-dependent maps, taken to hold for all  $\pi_1, \pi_2$  regardless of any assumed relationship between them:

$$(2.35) \quad T(\cdot; \pi_1)^\# \pi_2 = T(\cdot; \tilde{\pi})^\# \pi_2 \Big|_{\tilde{\pi}=\pi_1};$$

in particular,

$$(2.36a) \quad T(\cdot; \pi)^\# \pi = T(\cdot; \tilde{\pi})^\# \pi \Big|_{\tilde{\pi}=\pi},$$

$$(2.36b) \quad T(\cdot; \pi)^\#(G\pi) = T(\cdot; \tilde{\pi})^\#(G\pi) \Big|_{\tilde{\pi}=\pi}.$$

In the preceding, pushforward under  $T(\cdot, \tilde{\pi})$  denotes regular pushforward with no relationship assumed between  $\tilde{\pi}$  and measure being pushed forward.

The (approximate) transport maps just identified can be recast as mean field maps when used in the context where source  $\pi$  is the distribution of the input to  $T$ . In this section we identify mean field maps which effect exact filtering (transport maps), or which effect forms of approximate filtering (approximate transport maps). Subsection 2.5.1 introduces two distinct transport approaches which effect exact filtering: one based on the prior to posterior map that constitutes the analysis (Bayesian inference) step of filtering, a transport between probability measures on the same space; and the other based on the conditioning component of the analysis step, a transport between probability measures on different spaces. We refer to these maps which effect exact filtering as *perfect transport*.<sup>5</sup> Subsections 2.5.3 and 2.5.4 are concerned with approximations of these two perfect transports. In these approximations the pushforward under the transport map is designed to match only the first and second order moments of the target measure. For this reason these approximations are closely related to the previously defined Gaussian projected filter; we will elaborate on this connection. Finally, Subsection 2.5.6 applies the ideas of this section to find a mean field formulation of the Kalman filter for linear Gaussian systems.

**2.5.1. Perfect Transport.** Consider the idea of finding a transport map that acts on the joint space of state and data, to effect conditioning with respect to the observed data. To this end we consider the dynamical system, assumed to hold for all  $n \in \mathbb{Z}^+$ :

$$\begin{aligned} (2.37a) \quad & \hat{v}_{n+1} = \Psi(v_n) + \xi_n, \\ (2.37b) \quad & \hat{y}_{n+1} = h(\hat{v}_{n+1}) + \eta_{n+1}, \\ (2.37c) \quad & v_{n+1} = T^S(\hat{v}_{n+1}, \hat{y}_{n+1}; \nu_{n+1}, y_{n+1}^\dagger), \end{aligned}$$

where  $\{y_n^\dagger\}$  arises from a fixed realization of (2.1). The first two equations, which coincide with (2.21), effect the mappings from  $\mu_n$  to  $\hat{\mu}_{n+1}$  and from  $\hat{\mu}_{n+1}$  to  $\nu_{n+1}$ . Map  $T_n^S(\cdot, \cdot) := T^S(\cdot, \cdot; \nu_{n+1}, y_{n+1}^\dagger)$  is then an explicit example of (2.22) defined to effect the desired conditioning of  $\nu_{n+1}$  on  $y_{n+1}^\dagger$  in order to obtain  $\mu_{n+1}$ . The letter  $S$  in  $T^S$  connotes the dependence of the map on the *stochastic* data  $\hat{y}_{n+1}$ . This is a mean-field stochastic dynamical system mapping  $v_n$  to  $v_{n+1}$ : stochastic because of the noise in (2.37a, 2.37b), mean-field because the map  $T^S$  in (2.37c) depends on the law  $\nu_{n+1}$  of  $(\hat{v}_{n+1}, \hat{y}_{n+1})$ , and hence on  $\mu_n$ . The three update steps

---

<sup>5</sup>Perfect transport should not be confused with *optimal transport* which identifies among all (perfect) transport maps the one minimizing a certain cost functional such as the Wasserstein distance. See the bibliography Subsection 2.7 for more details. We use *perfect* here to distinguish from the *approximate* transport maps, based only on matching first and second moment; these approximate methods underpin ensemble Kalman methods.

in this mean field stochastic dynamical system lead to the following maps on measures:

$$\begin{aligned}
 (2.38a) \quad & \hat{\mu}_{n+1} = P\mu_n, \\
 (2.38b) \quad & \nu_{n+1} = Q\hat{\mu}_{n+1}, \\
 (2.38c) \quad & \mu_{n+1} = (T_n^S)^\# \nu_{n+1}.
 \end{aligned}$$

This is simply a restatement of (2.17), noting that  $(T_n^S)^\#$  has been chosen so that pushforward corresponds to conditioning  $\nu_{n+1}$  on data  $y_{n+1}^\dagger$  to obtain  $\mu_{n+1}$ . Note that the implied map from  $\mu_n$  to  $\mu_{n+1}$  is a nonlinear Markov process, because of the dependence of  $T_n^S$  on  $\nu_{n+1}$  and hence on  $\mu_n$ . Furthermore, we have that  $\text{Law}(v_\ell) = \mu_\ell$  for all  $\ell \in \mathbb{Z}^+$ .

Consider now a different approach to transport for filtering: we seek a transport map that acts on the state space only to effect Bayes Theorem, i.e. mapping prior  $\hat{\mu}_{n+1}$  to posterior  $\mu_{n+1}$ . To this end we consider the dynamical system

$$\begin{aligned}
 (2.39a) \quad & \hat{v}_{n+1} = \Psi(v_n) + \xi_n, \\
 (2.39b) \quad & v_{n+1} = T^D(\hat{v}_{n+1}; \hat{\mu}_{n+1}, y_{n+1}^\dagger),
 \end{aligned}$$

again assumed to hold for all  $n \in \mathbb{Z}^+$ . The first equation maps  $v_n \sim \mu_n$  to  $\hat{v}_{n+1} \sim \hat{\mu}_{n+1}$ , thus giving a sample path realization of (2.19a). In the second equation, the map  $T_n^D(\cdot) := T^D(\cdot; \hat{\mu}_{n+1}, y_{n+1}^\dagger)$  is chosen so that, if  $\hat{v}_{n+1} \sim \hat{\mu}_{n+1}$  then  $v_{n+1} \sim \mu_{n+1}$ , thus giving a sample path realization of (2.19b). This is also a mean-field stochastic dynamical system: stochastic because of the noise in (2.39a); mean field because the map  $T^D$  in (2.39b) depends on the law of  $\hat{v}_{n+1}$  itself, and hence on  $\mu_n$ . The symbol  $D$  distinguishes map  $T^D$  from map  $T^S$ : map  $T^D$  is *deterministic* in the sense that it does not require stochastic data  $\hat{y}_{n+1}$ , in contrast to  $T^S$ . Therefore, we again have that  $\text{Law}(v_\ell) = \mu_\ell$  for all  $\ell \in \mathbb{Z}^+$ , where the probability measure  $\mu_n$  evolves according to

$$\begin{aligned}
 (2.40a) \quad & \hat{\mu}_{n+1} = P\mu_n, \\
 (2.40b) \quad & \mu_{n+1} = (T_n^D)^\# \hat{\mu}_{n+1}.
 \end{aligned}$$

This is simply a restatement of (2.19), noting that  $(T_n^D)^\#$  has been chosen so that the pushforward corresponds to the application of Bayes Theorem to incorporate data  $y_{n+1}^\dagger$ . The evolution (2.40) is another nonlinear Markov process, now because of the dependence of  $T_n^D$  on  $\hat{\mu}_{n+1}$ .

The two transport maps  $T^S$  and  $T^D$  introduce an important conceptual approach to algorithms for filtering, but determining the maps can be as hard, or harder, than solving the filtering problem itself. Thus, in the next two subsections, we turn to relaxations of the perfect transport effected by  $T^S$  and  $T^D$ . We instead seek mean field maps which match only first and second order moment information; this relaxation allows for approximate transport maps with simple affine (in senses to be made precise) forms. The perspective of matching first and second order moments naturally suggests working with Gaussians and hence we also relate the approximate transport to the Gaussian projected filter.



**2.5.2. Second Order Transport – Motivation.** To motivate the more general ideas behind second order transport, we study an explicit example. It is well known how to transform samples from a unit centered Gaussian random variable on  $\mathbb{R}$  into samples from a Gaussian random variable with mean  $m \neq 0$  and variance  $\sigma \neq 1$  by a simple scaling and shifting operation. An appropriate generalization of such a procedure leads to the map

$$\begin{aligned}
 (2.41a) \quad & \hat{v}_{n+1} = \Psi(v_n) + \xi_n, \\
 (2.41b) \quad & \hat{y}_{n+1} = h(\hat{v}_{n+1}) + \eta_{n+1}, \\
 (2.41c) \quad & v_{n+1} = m_{n+1} + C_{n+1}^{\frac{1}{2}} \hat{C}_{n+1}^{-\frac{1}{2}} (\hat{v}_{n+1} - \mathbb{E}\hat{v}_{n+1}),
 \end{aligned}$$

where  $m_{n+1}$ ,  $\hat{C}_{n+1}$ , and  $C_{n+1}$  are determined by (2.23), (2.24) and (2.30), using (2.41a) and (2.41b). Here  $\{y_n^\dagger\}$  arises again from a fixed realization of (2.1). The map  $v_n \mapsto v_{n+1}$  defined by (2.41) is a mean-field map because of the dependence of  $m_{n+1}$ ,  $C_{n+1}$  and  $\hat{C}_{n+1}$  on  $QLaw(v_n)$ .

It is clear from (2.41c) that  $\mathbb{E}v_{n+1} = m_{n+1}$  and also that

$$\begin{aligned}
 & \mathbb{E}((v_{n+1} - m_{n+1}) \otimes (v_{n+1} - m_{n+1})) \\
 &= C_{n+1}^{\frac{1}{2}} \hat{C}_{n+1}^{-\frac{1}{2}} \mathbb{E}((v_{n+1} - m_{n+1}) \otimes (v_{n+1} - m_{n+1})) \hat{C}_{n+1}^{-\frac{1}{2}} C_{n+1}^{\frac{1}{2}}, \\
 &= C_{n+1}^{\frac{1}{2}} \hat{C}_{n+1}^{-\frac{1}{2}} \hat{C}_{n+1} \hat{C}_{n+1}^{-\frac{1}{2}} C_{n+1}^{\frac{1}{2}}, \\
 &= C_{n+1}.
 \end{aligned}$$

It is important to recognize that  $v_{n+1}$ , defined by (2.41c), will not be Gaussian distributed since  $\hat{v}_{n+1}$ , defined by (2.41a), will not be Gaussian either, in general. However, although (2.41) does not provide a closed iteration on Gaussians, the map from  $\hat{v}_{n+1}$  to  $v_{n+1}$  agrees with the same step in the Gaussian projected filter, at the level of first and second order moments.

Whilst the mean field map from (2.41) is a relatively transparent way to achieve the goal of matching first and second order moments there is an uncountable set of ways of achieving this objective; the next two subsections demonstrate this, identifying all mean field maps effecting approximate transport from within two specific classes of affine transformations. We will then highlight a small subset that have been used in practice, each of which is useful in certain specific contexts.

**2.5.3. Second Order Transport – Stochastic Case.** The first class of approximate filters determined by mean field maps have the form

$$\begin{aligned}
 (2.42a) \quad & \hat{v}_{n+1} = \Psi(v_n) + \xi_n, \\
 (2.42b) \quad & \hat{y}_{n+1} = h(\hat{v}_{n+1}) + \eta_{n+1}, \\
 (2.42c) \quad & v_{n+1} = \tilde{T}^S(\hat{v}_{n+1}, \hat{y}_{n+1}; \nu_{n+1}, y_{n+1}^\dagger),
 \end{aligned}$$

where  $\{y_n^\dagger\}$  arises from a fixed realization of (2.1). We define<sup>6</sup>  $\nu = \text{Law}(\hat{v}_{n+1}, \hat{y}_{n+1})$  and then identify  $\tilde{T}_n^S : \mathbb{R}^{d_v} \times \mathbb{R}^{d_y} \rightarrow \mathbb{R}^{d_v}$ , where  $\tilde{T}_n^S(\cdot) = \tilde{T}^S(\cdot; \nu, y^\dagger)$  approximates an exact transport map  $T_n^S(\cdot) = T^S(\cdot; \nu, y^\dagger)$  by matching the first and second order moments. To be precise we assume that the exact and approximate transport maps satisfy, respectively,

$$(2.43a)$$

$$(T_n^S)^\# \nu = B_n(\nu),$$

$$(2.43b)$$

$$G((\tilde{T}_n^S)^\# \nu) = B_n(G\nu),$$

for all measures  $\nu$  on the product space  $\mathbb{R}^{d_v} \times \mathbb{R}^{d_y}$ . Of course  $T_n^S$  and  $\tilde{T}_n^S$  will depend on  $\nu$  and then pushforward is to be interpreted as in (2.35), (2.36). We ask that for all measures  $\nu$  on the space  $\mathbb{R}^{d_v} \times \mathbb{R}^{d_y}$  either (2.43a) holds (perfect transport) or (2.43b) holds (second order transport). Whilst achieving (2.43a) may be harder than solving the filtering problem directly, achieving (2.43b) is straightforward and leads to computationally tractable methods. This gain in tractability comes at the price of only achieving (2.43b), rather than (2.43a); however it is intuitive that this price will not be high for settings in which the filtering distribution, and the predictive distribution on state and data, is not too far from Gaussian; we flesh out this idea in Subsection 2.5.5 below.

To find tractable approximate transport we seek  $\tilde{T}^S$  in the form

$$(2.44) \quad \tilde{T}^S(\hat{v}_{n+1}, \hat{y}_{n+1}; \nu, y^\dagger) := A\hat{v}_{n+1} + B\hat{y}_{n+1} + a.$$

We allow the matrices/vectors  $A, B, a$  to depend on  $(\nu, y^\dagger)$ ; however, they are assumed to be independent of  $(\hat{v}_{n+1}, \hat{y}_{n+1})$ . Making this assumption ensures that the transport map is affine with respect to the realization of  $(\hat{v}_{n+1}, \hat{y}_{n+1})$  (but not their law). This in turn leads to tractable computations to determine  $A, B, a$  on the basis of matching second order moments of perfect transport. In addition to computational tractability, the affine form of the transport map  $\tilde{T}^S$  is motivated by the following which shows that the approximate transport is perfect when applied to Gaussian source:

**Lemma 2.7.** *Let  $\tilde{T}_n^S := \tilde{T}^S(\hat{v}_{n+1}, \hat{y}_{n+1}; \nu, y^\dagger)$  have the form (2.44) and satisfy (2.43b). Then  $\tilde{T}^S$  depends on  $\nu$  only through  $G\nu$ . Furthermore,*

$$(\tilde{T}_n^S)^\#(G\nu) = B_n(G\nu);$$

thus, if  $\nu$  is Gaussian, equation (2.43b) implies (2.43a).

*Proof.* We first note that (2.43b) is equivalent to insisting that

$$(2.45) \quad G((\tilde{T}_n^S)^\# G\nu) = B_n(G\nu)$$

for all measures  $\nu$ ; this follows because, noting the definition (2.35) and consequence (2.36), the first and second moments of  $(\tilde{T}_n^S)^\# G\nu$  and  $(\tilde{T}_n^S)^\# \nu$  agree, because of the affine form (2.44) assumed for  $\tilde{T}_n^S$ . From the identity (2.45), it is clear that  $\tilde{T}_n^S$  only depends on  $\nu$  through  $G\nu$

---

<sup>6</sup>We temporarily drop explicit notational dependence on  $n+1$  in  $\nu$  and in  $y^\dagger$ . This should not cause confusion as the approximate map we derive is concerned simply with finding a push forward which approximates conditioning of  $\text{Law}(\hat{v}_{n+1}, \hat{y}_{n+1})$  on  $\hat{y}_{n+1} = y^\dagger$ .

because changing  $\nu \rightarrow G\nu$  leaves the identity invariant, as  $G \circ G = G$ . Now note that, because Gaussians are preserved under affine transformations,

$$(\tilde{T}^S(\hat{v}_{n+1}, \hat{y}_{n+1}; \nu, y^\dagger))^\sharp(G\nu) = G\left((\tilde{T}^S(\hat{v}_{n+1}, \hat{y}_{n+1}; \nu, y^\dagger))^\sharp\nu\right),$$

or, in compact notational form,

$$(\tilde{T}_n^S)^\sharp(G\nu) = G((\tilde{T}_n^S)^\sharp\nu).$$

The desired display in the lemma is then immediate from (2.43b). ■

An affine transport map of the form (2.44), when combined with particle approximations, leads to practical implementable algorithms and achieves (2.43b) by ensuring that  $(\tilde{T}_n^S)^\sharp\nu$  has first and second moments which agree with those of the Gaussian projected filter, given by equations (2.23), (2.24) and (2.30) when  $\nu$  is the law of  $(\hat{v}_{n+1}, \hat{y}_{n+1})$ .

In Appendix C, Subsection 8.1, we identify the (uncountable) set of all possible  $A, B, a$  which achieve the desired matching of first and second order moments. Here we focus on the two specific choices given in Example 8.5 from that Appendix. The first that we highlight corresponds to the choice

$$\tilde{T}^S(\hat{v}_{n+1}, \hat{y}_{n+1}; \tilde{\nu}_{n+1}, y_{n+1}^\dagger) := \hat{v}_{n+1} + K_n(y_{n+1}^\dagger - \hat{y}_{n+1}),$$

with  $K_n = K_n(\nu_{n+1})$  given by (2.25). Thus we obtain the following mean-field dynamical system, which corresponds to (2.14) with the Kalman gain  $K_n$  defined by (2.25):

(2.46a)

$$\hat{v}_{n+1} = \Psi(v_n) + \xi_n,$$

(2.46b)

$$\hat{y}_{n+1} = h(\hat{v}_{n+1}) + \eta_{n+1},$$

(2.46c)

$$v_{n+1} = \hat{v}_{n+1} + \hat{C}_{n+1}^{vy}(\hat{C}_{n+1}^{yy})^{-1}(y_{n+1}^\dagger - \hat{y}_{n+1}),$$

where  $\{y_n^\dagger\}$  arises from a fixed realization of (2.1). We refer to this as *Kalman transport*, noting that it serves as a derivation of the Kalman gain, beyond the linear Gaussian setting.

The second transport map from Example 8.5 corresponds to the choice

$$\tilde{T}^S(\hat{v}_{n+1}, \hat{y}_{n+1}; \nu_{n+1}, y_{n+1}^\dagger) := m_{n+1} + C_{n+1}^{\frac{1}{2}} \hat{C}_{n+1}^{-\frac{1}{2}}(\hat{v}_{n+1} - \mathbb{E}\hat{v}_{n+1}),$$

leading to the mean field map (2.41). A key difference between the mean field models (2.46) and (2.41) is that the former involves inversion of matrices in data space, and the latter in state space. The relative dimensions of the two spaces will determine which mean field model is more appropriate as the basis of algorithms. Note also that the mean field model (2.41) does not require generation of the stochastic data  $\hat{y}_{n+1}$  because we may employ the identity  $\mathbb{E}\hat{y}_{n+1} = \mathbb{E}h(\hat{v}_{n+1})$  and use (2.26), (2.27) to compute  $m_{n+1}, C_{n+1}$  and  $\hat{C}_{n+1}$ . Motivated by this observation, the next subsection studies a wide class of approximate transport maps with the property that they do not require generation of stochastic data.

**2.5.4. Second Order Transport – Deterministic Case.** We now turn our attention to approximate filters determined by deterministic mean field maps. We define, for  $\hat{v}_{n+1}$  given by (2.21b),  $\hat{\mu} = \text{Law}(\hat{v}_{n+1})$ , as in the previous subsection dropping explicit  $n$ -dependence on the measure  $\hat{\mu}$  and on the data  $y^\dagger$ . We seek to approximate the exact transport (2.39) by mean field maps in the form

(2.47a)

$$\hat{v}_{n+1} = \Psi(v_n) + \xi_n,$$

(2.47b)

$$v_{n+1} = \tilde{T}^D(\hat{v}_{n+1}; \hat{\mu}_{n+1}, y_{n+1}^\dagger),$$

where  $\{y_n^\dagger\}$  arises from a fixed realization of (2.1). Analogously to the previous subsection, we seek an approximation  $\tilde{T}^D$  which, in comparison with the true transport map  $T^D$ , satisfies

(2.48a)

$$(T_n^D)^\# \hat{\mu} = B_n(Q\hat{\mu}),$$

(2.48b)

$$G((\tilde{T}_n^D)^\# \hat{\mu}) = B_n(GQ\hat{\mu}),$$

for all measures  $\hat{\mu}$  on the state space  $\mathbb{R}^{d_v}$ . Here  $\tilde{T}_n^D : \mathbb{R}^{d_v} \rightarrow \mathbb{R}^{d_v}$  is defined by  $\tilde{T}_n^D(\cdot) = \tilde{T}^D(\cdot; \hat{\mu}, y^\dagger)$ , and similarly for  $T_n^D$ . As in the previous subsection, where we studied approximate stochastic transport, we again seek maps with a specific affine form. Concretely, the maps are assumed to be affine in the pair  $(\hat{v}_{n+1}, \hat{h}_{n+1})$ , with  $\hat{h}_{n+1} = h(\hat{v}_{n+1})$ , leading to the assumed form  $\tilde{T}_n^D(\cdot) = \tilde{T}^D(\cdot; \mu, y^\dagger)$  with

$$\tilde{T}^D(\hat{v}_{n+1}, \hat{h}_{n+1}; \mu, y^\dagger) := R\hat{v}_{n+1} + S\hat{h}_{n+1} + r,$$

for  $(\hat{\mu}, y^\dagger)$ -dependent matrices/vectors  $R, S, r$  of appropriate dimensions. Note, however, that  $R, S, r$  are assumed to be independent of the realization  $(\hat{v}_{n+1}, \hat{h}_{n+1})$ , depending only on its law, so that the transport map is affine in  $(\hat{v}_{n+1}, \hat{h}_{n+1})$ . With this restriction, which will lead to practical implementable algorithms, we simply ask that (2.48b) holds: the first and second moments of the output map agree with those of the Gaussian projected filter, given by equations (2.23), (2.26) and (2.31).

As in the previous subsection, there are uncountably many choices of  $R, S, r$  which we identify in Appendix C, Subsection 8.2; Example 8.12 highlights two important cases. The first coincides with (2.41) since  $S = 0$ , but the second leads to a new mean field map. To formulate this new map we first define  $\tilde{K}_n = \tilde{K}_n(\hat{\mu})$  by

(2.49)

$$\tilde{K}_n = \hat{C}_{n+1}^{vh} \left( (\hat{C}_{n+1}^{hh} + \Gamma) + \Gamma^{1/2} (\hat{C}_{n+1}^{hh} + \Gamma)^{1/2} \right)^{-1}.$$

We then make the choice

$$\tilde{T}^D(\hat{v}_{n+1}, \hat{h}_{n+1}; \hat{\mu}, y^\dagger) := \hat{v}_{n+1} - \tilde{K}_n(\hat{h}_{n+1} - \mathbb{E}\hat{h}_{n+1}) + K_n(y^\dagger - \mathbb{E}\hat{h}_{n+1}),$$

with  $K_n$  given by (2.27) and  $\tilde{K}_n$  by (2.49). This leads to the mean field map

$$\begin{aligned} (2.50a) \quad & \hat{v}_{n+1} = \Psi(v_n) + \xi_n, \\ (2.50b) \quad & \hat{h}_{n+1} = h(\hat{v}_{n+1}), \\ (2.50c) \quad & v_{n+1} = \hat{v}_{n+1} - \tilde{K}_n(\hat{h}_{n+1} - \mathbb{E}\hat{h}_{n+1}) + K_n(y_{n+1}^\dagger - \mathbb{E}\hat{h}_{n+1}), \end{aligned}$$

where  $K_n$  and  $\tilde{K}_n$  are computed under  $Law(\hat{v}_{n+1})$ .

**Remark 2.8.** If the ensemble spread is such that the size of  $\hat{C}_{n+1}^{hh}$  is much smaller than the size of the observational covariance  $\Gamma$  then we may invoke the approximation  $\hat{C}_{n+1}^{hh} + \Gamma \approx \Gamma$ . With this approximation it follows that  $\tilde{K}_n \approx \frac{1}{2}K_n$  in (2.49). Some deterministic ensemble Kalman filters are derived from mean-field dynamics which exploit this approximation by setting  $\tilde{K}_n = \frac{1}{2}K_n$  in (2.50). We then replace (2.50c) by the compact updating step

$$v_{n+1} = \hat{v}_{n+1} + K_n \left( y_{n+1}^\dagger - \frac{1}{2}(\mathbb{E}\hat{h}_{n+1} + \hat{h}_{n+1}) \right).$$

Such a formulation corresponds to the control-theoretic perspective of (2.14), with  $K_n$  given by (2.27) and the innovation (2.15) replaced by

$$(2.51) \quad I_n = y_{n+1}^\dagger - \frac{1}{2}(\mathbb{E}\hat{h}_{n+1} + \hat{h}_{n+1}).$$

Filters based on this mean-field dynamics thus invoke an additional approximation of perfect transport, over and above that stemming from matching only first and second moments, assume further that the observational noise dominates ensemble variation. However we will see that, in the continuous time limit described in Section 3, this form of the innovation arises naturally and does not constitute an additional approximation. ■

**2.5.5. Second Order Transport – Summary.** It is helpful at this point to take stock of two approximations to filtering that we have introduced, Gaussian projected filtering and approximate transport, and discuss their inter-relations. For simplicity we do this in the context of mean field stochastic maps, but similar considerations extend to mean field deterministic maps.

With this goal in mind, let  $\mu^{MF}$  denote the measure associated with using the mean-field map  $\tilde{T}_n^S$  to approximate the conditioning step in (2.17). Notice that

$$\begin{aligned} (2.52a) \quad & \mu_{n+1} = B_n(QP\mu_n), \quad \mu_0 = \mathbf{N}(m_0, C_0), \\ (2.52b) \quad & \mu_{n+1}^G = B_n(GQP\mu_n^G), \quad \mu_0^G = \mathbf{N}(m_0, C_0), \end{aligned}$$

and that, by (2.43b),

$$\begin{aligned} (2.53a) \quad & \mu_{n+1}^G = G((\tilde{T}_n^S)^\#(QP\mu_n^G)), \quad \mu_0^G = \mathbf{N}(m_0, C_0), \\ (2.53b) \quad & \mu_{n+1}^{MF} = (\tilde{T}_n^S)^\#(QP\mu_n^{MF}), \quad \mu_0^{MF} = \mathbf{N}(m_0, C_0). \end{aligned}$$

These maps show that  $\{\mu_n^{MF}\}$  is close to  $\{\mu_n^G\}$ , if the Gaussian projection in (2.53a) is close to the identity where it acts, and that  $\{\mu_n^G\}$  is close to  $\{\mu_n\}$  if the Gaussian projection in (2.52b) is close to the identity where it acts. Together these two facts suggest that  $\{\mu_n^{MF}\}$ ,  $\{\mu_n^G\}$  and  $\{\mu_n\}$  are all close to one another if the two Gaussian projections can be viewed as being close to the identity map, where they appear in (2.52), (2.53). This provides a potential path for analysis of the mean field model, away from the linear setting where it is exact.

**2.5.6. Mean Field Formulation of the Kalman Filter.** Application of the Kalman transport map (2.46) in the linear Gaussian setting leads to the following:

**Theorem 2.9.** *Assume that  $v_0 \sim \mathcal{N}(m_0, C_0)$ ,  $\Psi(\cdot) = M \cdot$  and  $h(\cdot) = H \cdot$  and that  $\Gamma \succ 0$ . The mean field stochastic dynamical system (2.46) takes the form*

$$\begin{aligned} (2.54a) \quad & \hat{v}_{n+1} = Mv_n + \xi_n, \\ (2.54b) \quad & \hat{y}_{n+1} = H\hat{v}_{n+1} + \eta_{n+1}, \\ (2.54c) \quad & v_{n+1} = \hat{v}_{n+1} + \hat{C}_{n+1}H^\top (H\hat{C}_{n+1}H^\top + \Gamma)^{-1}(y_{n+1}^\dagger - \hat{y}_{n+1}), \end{aligned}$$

where  $\{y_n^\dagger\}$  arises from a fixed realization of (2.32) and where  $C_n$  is the covariance of  $v_n$  and  $\hat{C}_{n+1} = MC_nM^\top + \Sigma$  is the covariance of  $\hat{v}_{n+1}$ . The resulting dynamics are identical in law to the Kalman filter in that  $v_n \sim \mathcal{N}(m_n, C_n)$  where  $m_n, C_n$  are as given in Subsection 2.4.2.

*Proof.* The map defined by (2.5.3) is well-defined since  $\Gamma \succ 0$ . Lemma 2.7 shows that the approximate transport is exact in this Gaussian setting.  $\blacksquare$

Similar ideas can be applied to (2.41) and (2.50) to determine other mean field models with law equal to that of the Kalman filter. Furthermore we observe that the formulation based on (2.41) can be symmetrized to obtain, in the linear setting of Theorem 2.9,

$$\begin{aligned} (2.55a) \quad & \hat{v}_{n+1} = Mv_n + \xi_n, \quad n \in \mathbb{Z}^+, \\ (2.55b) \quad & v_{n+1} = m_{n+1} + A_n(\hat{v}_{n+1} - \hat{m}_{n+1}), \\ (2.55c) \quad & A_n = (C_{n+1})^{1/2} \left[ (C_{n+1})^{1/2} \hat{C}_{n+1} (C_{n+1})^{1/2} \right]^{-1/2} (C_{n+1})^{1/2}, \end{aligned}$$

with  $(\hat{m}_{n+1}, \hat{C}_{n+1}, \hat{C}_{n+1}^{vh}, \hat{C}_{n+1}^{hh})$  defined by (2.4.1) and  $(m_{n+1}, C_{n+1})$  defined by (2.30). We note that the second component of the map may be written in gradient form and corresponds to an optimal transport from  $\hat{\mu}_{n+1}$  into  $\mu_{n+1}$  in the sense of the Euclidean Wasserstein distance of optimal transportation (see Subsection 2.7 for details); indeed this is true of for an entire family of weighted Wasserstein distances – see Example 8.7. To recognize the gradient structure define

$$\Phi_n(v) := \langle m_{n+1}, v \rangle + \frac{1}{2} \langle A_n(v - \hat{m}_{n+1}), v - \hat{m}_{n+1} \rangle$$

and note that then

$$\begin{aligned} (2.56a) \quad & \hat{v}_{n+1} = Mv_n + \xi_n, \quad n \in \mathbb{Z}^+, \\ (2.56b) \quad & v_{n+1} = \nabla \Phi_n(\hat{v}_{n+1}). \end{aligned}$$

**2.6. Ensemble Kalman Methods.** In this subsection we take the mean field models from Subsection 2.5 and use particle approximations to derive implementable numerical algorithms. We start, in Subsection 2.6.1, with the setting in which transport is perfect; these algorithms are not, in general, implementable since determining perfect transport is itself a difficult computational task and the subject of ongoing research; see the bibliography Subsection 2.7. Thus we turn to particle approximations of the transports designed to match first and second order statistics. This leads to the (stochastic) *ensemble Kalman filter* in Subsection 2.6.2, and to (deterministic) *ensemble square root filters* in Subsection 2.6.3. The methods derived in this subsection involve approximating the Kalman gain by computing covariances under the empirical measure defined by the ensemble of particles. To avoid overloading notation, in the rest of this subsection  $C_{n+1}$ ,  $\hat{C}_{n+1}$ ,  $\hat{C}_{n+1}^{vy}$  and  $\hat{C}_{n+1}^{yy}$  will denote covariances computed with expectation under the empirical measure. With this notation in place, in the rest of this subsection  $K_n$  will directly refer to the particle approximation of the Kalman gain, computed using the covariances with respect to the empirical measure, without further specification needed. Throughout this section  $\{y_n^\dagger\}$  arises from a fixed realization of (2.1).

**2.6.1. Perfect Particle Filters.** The mean-field equations (2.37) could, in principle, be approximated through a particle approximation of the mean-field leading to the following conceptual (because map  $T_n^S$  is not known explicitly) algorithm: let  $J = \{1, \dots, J\}$  and consider, for  $(n, j) \in \mathbb{Z}^+ \times J$ , the interacting particle dynamical system

$$\begin{aligned}
 (2.57a) \quad & \hat{v}_{n+1}^{(j)} = \Psi(v_n^{(j)} + \xi_n^{(j)}), \\
 (2.57b) \quad & \hat{y}_{n+1}^{(j)} = h(\hat{v}_{n+1}^{(j)}) + \eta_{n+1}^{(j)}, \\
 (2.57c) \quad & v_{n+1}^{(j)} = T^S(\hat{v}_{n+1}^{(j)}, \hat{y}_{n+1}^{(j)}; \nu_{n+1}^J, y_{n+1}^\dagger), \\
 (2.57d) \quad & \nu_{n+1}^J = \frac{1}{J} \sum_{j=1}^J \delta_{(\hat{v}_{n+1}^{(j)}, \hat{y}_{n+1}^{(j)})}.
 \end{aligned}$$

This evolves the particles  $\{v_n^{(j)}\}_{j \in J}$  into  $\{v_{n+1}^{(j)}\}_{j \in J}$ . Here the  $\{\xi_n^{(j)}\}$  are, for each  $j$ , random variables given by the known distribution of  $\xi_n$  specified in (2.2) and, furthermore, are drawn independently with respect to each  $(n, j) \in \mathbb{Z}^+ \times J$ . Similar considerations apply to the  $\{\eta_n^{(j)}\}$  which, additionally, are independent of the  $\{\xi_n^{(j)}\}$ . It is intuitive that the large  $J$  limit of this system recovers the mean-field dynamics (2.37) and, in particular,

$$(2.58) \quad \mu_n^J = \frac{1}{J} \sum_{j=1}^J \delta_{v_n^{(j)}} \approx \mu_n.$$

Applying a similar idea to (2.39) leads to the following conceptual (because map  $T_n^D$  is not known explicitly) algorithm. Consider, for  $(n, j) \in \mathbb{Z}^+ \times J$ , the interacting particle dynamical



system

$$(2.59a)$$

$$\hat{v}_{n+1}^{(j)} = \Psi(v_n^{(j)} + \xi_n^{(j)}),$$

$$(2.59b)$$

$$v_{n+1}^{(j)} = T^D(\hat{v}_{n+1}^{(j)}; \hat{\mu}_{n+1}^J, y_{n+1}^\dagger),$$

$$(2.59c)$$

$$\hat{\mu}_{n+1}^J = \frac{1}{J} \sum_{j=1}^J \delta_{\hat{v}_{n+1}^{(j)}}.$$

This evolves the particles  $\{v_n^{(j)}\}_{j \in J}$  into  $\{v_{n+1}^{(j)}\}_{j \in J}$ . The same assumptions are made about the  $\{\xi_n^{(j)}\}$  as for the preceding interacting particle dynamical system. It is again intuitive that the large  $J$  limit of this system recovers the mean field dynamics (2.39), and the evolution (2.40). In particular it is intuitive that (2.58) holds for this particle approximation too. We reiterate that in practice these algorithms are, in general, not easy to use. More specifically, finding particle based approximations  $T_J^S$  and  $T_J^D$  to the desired transport maps such that

$$\lim_{J \rightarrow \infty} T_J^S = T^S, \quad \lim_{J \rightarrow \infty} T_J^D = T^D$$

in an appropriate sense is a computationally challenging task and the subject of ongoing research. This leads to the next two subsections in which we replace  $T^S$  and  $T^D$ , in the interacting particles systems (2.57) and (2.59), by the previously introduced approximate transports  $\tilde{T}^S$  and  $\tilde{T}^D$ , respectively.

**2.6.2. Stochastic Ensemble Kalman Filters.** Particle approximation of the mean field dynamical system (2.46), effecting Kalman transport, bring us to the stochastic EnKF (*ensemble Kalman filter*). This method may be derived by writing down a particle approximation of the mean field stochastic dynamics defined by (2.46). We evolve the particles  $\{v_n^{(j)}\}_{j \in J}$  into  $\{v_{n+1}^{(j)}\}_{j \in J}$  according to the following stochastic interacting particle system, holding for  $(n, j) \in \mathbb{Z}^+ \times J$ :

$$(2.60a)$$

$$\hat{v}_{n+1}^{(j)} = \Psi(v_n^{(j)} + \xi_n^{(j)}), \quad n \in \mathbb{Z}^+,$$

$$(2.60b)$$

$$\hat{y}_{n+1}^{(j)} = h(\hat{v}_{n+1}^{(j)}) + \eta_{n+1}^{(j)}, \quad n \in \mathbb{Z}^+,$$

$$(2.60c)$$

$$v_{n+1}^{(j)} = \hat{v}_{n+1}^{(j)} + K_n(y_{n+1}^\dagger - \hat{y}_{n+1}^{(j)}),$$

$$(2.60d)$$

$$\nu_{n+1}^J = \frac{1}{J} \sum_{j=1}^J \delta_{(\hat{v}_{n+1}^{(j)}, \hat{y}_{n+1}^{(j)})}.$$

Here the Kalman gain from (2.25) is approximated using the empirical measure  $\nu_{n+1}^J$  and but is still denoted by  $K_n$ ; details follow below. The same assumptions regarding  $\{\xi_n^{(j)}\}$  and  $\{\eta_{n+1}^{(j)}\}$  are made as for (2.57). We let  $\mathbb{E}_n^J$  denote expectation under  $\nu_n^J$ . For the basic implementation of EnKF (2.60) the desired covariance matrices, and Kalman gain (2.25) are

then approximated by expectation under  $\nu_{n+1}^J$ , so that <sup>7</sup>

$$\begin{aligned}\widehat{C}_{n+1}^{vy} &= \mathbb{E}_{n+1}^J \left( (\widehat{v}_{n+1} - \mathbb{E}_{n+1}^J \widehat{v}_{n+1}) \otimes (\widehat{y}_{n+1} - \mathbb{E}_{n+1}^J \widehat{y}_{n+1}) \right), \\ \widehat{C}_{n+1}^{yy} &= \mathbb{E}_{n+1}^J \left( (\widehat{y}_{n+1} - \mathbb{E}_{n+1}^J \widehat{y}_{n+1}) \otimes (\widehat{y}_{n+1} - \mathbb{E}_{n+1}^J \widehat{y}_{n+1}) \right).\end{aligned}$$

An alternative is to use a particle approximation in formula (2.27b), leading to the use of

$$\begin{aligned}\widehat{C}_{n+1}^{vh} &= \mathbb{E}_{n+1}^J \left( (\widehat{v}_{n+1} - \mathbb{E}_{n+1}^J \widehat{v}_{n+1}) \otimes (\widehat{y}_{n+1} - \mathbb{E}_{n+1}^J h(\widehat{v}_{n+1})) \right), \\ \widehat{C}_{n+1}^{hh} &= \mathbb{E}_{n+1}^J \left( (\widehat{y}_{n+1} - \mathbb{E}_{n+1}^J h(\widehat{v}_{n+1})) \otimes (\widehat{y}_{n+1} - \mathbb{E}_{n+1}^J h(\widehat{v}_{n+1})) \right) + \Gamma\end{aligned}$$

in computation of the gain  $K_n$ . The advantage of this latter formulation is that it ensures positivity, and hence invertibility, of the covariance in data space, if  $\Gamma$  is assumed positive-definite.

Pseudo-code for the stochastic EnKF may be found as Algorithm 6.2 in Appendix 6.

**Example 2.10.** We return to the set-up of Example 2.1, and now demonstrate performance of the stochastic EnKF on the same Lorenz '96 model. Indeed, we again study the Lorenz '96 (singlescale) model for unknown  $v \in C(\mathbb{R}^+, \mathbb{R}^L)$  satisfying the equations (2.6) with  $L = 9$ ,  $h_v = -0.8$  and  $F = 10$ . We consider observations  $\{y_n^\dagger\}_{n \in \mathbb{Z}^+}$  arising from the model

$$\begin{aligned}v_{n+1}^\dagger &= \Psi(v_n^\dagger) + \xi_n^\dagger, \\ y_{n+1}^\dagger &= h(v_{n+1}^\dagger) + \eta_{n+1}^\dagger,\end{aligned}$$

where  $\Psi$  is the solution operator for (2.6) over the observation time interval  $\tau$ , and  $\{\xi_n^\dagger\}_{n \in \mathbb{Z}^+}$ ,  $\{\eta_n^\dagger\}_{n \in \mathbb{N}}$  are mutually independent Gaussian sequences defined by

$$\xi_n^\dagger \sim \mathcal{N}(0, \sigma^2 I) \text{ i.i.d.}, \quad \eta_n^\dagger \sim \mathcal{N}(0, \gamma^2 I) \text{ i.i.d.},$$

with  $\sigma^2 = 0.1$  and  $\gamma^2 = 0.1$ . We again assume that the observation function is linear:  $h(v) = Hv$  for matrix  $H : \mathbb{R}^9 \rightarrow \mathbb{R}^6$  defined by (2.7).

Figures 2.7a and 2.7b demonstrate the performance of stochastic EnKF in this experimental setting with  $\tau = 10^{-3}$  and using  $J = 10^2$  and  $J = 10^3$ , respectively, against the performance of 3DVAR with no noise; note that the EnKF uses a time-varying estimate of the gain  $K_n$ , whilst 3DVAR uses the fixed  $K$  given in Example 2.1. These experiments illustrate that using sufficiently large ensembles, the ensemble Kalman filter outperforms 3DVAR on such a non-linear filtering problem where the true state and observational noise levels are high. To quantitatively demonstrate this improvement, we compute the mean squared error between the estimates yielded by 3DVAR and the true states and the mean squared error between the estimates obtained by computing the ensemble mean of the stochastic EnKF and comparing with the true states. In particular we report time-averaged mean squared errors

---

<sup>7</sup>The empirical covariance computations are often modified to accommodate the widely adopted convention of scaling by  $1/(J-1)$ , instead of  $1/J$ , in view of the matrix being computed from  $J-1$  independent increments about the mean.

obtained from both 3DVAR and stochastic EnKF given by use of formula (2.16) from Example 2.3 using  $t = 5$  and  $T = 20$ . An ensemble size of  $J = 10^2$  yields  $e_{\text{EnKF}} = 8.20 \cdot 10^{-1}$ , while for  $J = 10^3$  we obtain  $e_{\text{EnKF}} = 4.91 \cdot 10^{-1}$ . For comparison, the error obtained using 3DVAR is  $e_{\text{3DVAR}} = 1.45 \cdot 10^0$ .

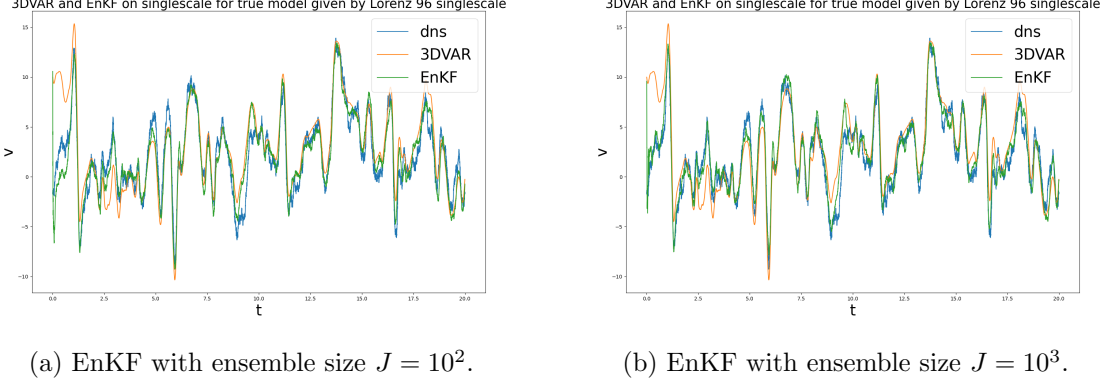


Figure 2.7: In this experiment we set the noise levels  $\sigma^2 = 10^{-1}, \gamma^2 = 10^{-1}$ . We display the estimates of  $v_3$  in time produced by EnKF and 3DVAR against the true dynamics using  $\tau = 10^{-3}$ . Again “dns” refers to direct numerical simulation.

**2.6.3. Ensemble Square Root Filters.** The variants on the EnKF described in this subsection are known as ensemble square root filters; they are based on mean field maps (2.41) and (2.50), approximated by interacting particle systems. They are also sometimes referred to as deterministic ensemble Kalman filters, to distinguish them from their stochastic counterparts described in the preceding subsection. We introduce two families of square root filters: of adjustment and transform type. We emphasize again that the choice of which method to use in practice is determined by implementations details such as the number of particles  $J$ , the dimension of state space  $d_v$ , and the dimension of the observation space  $d_y$ .

*Ensemble Adjustment Kalman Filters.* As in the previous subsection the methods evolve particle ensemble  $\{v_n^{(j)}\}_{j \in J}$  into  $\{v_{n+1}^{(j)}\}_{j \in J}$ , via the predictive ensemble  $\{\hat{v}_{n+1}^{(j)}\}_{j \in J}$ . However they do not employ simulated data  $\{\hat{y}_{n+1}^{(j)}\}_{j \in J}$ , rather they make use of  $\{\hat{h}_{n+1}^{(j)}\}_{j \in J}$ , where  $\hat{h}_n^{(j)} = h(\hat{v}_n^{(j)})$ . To define the methods it helps to introduce new notation. Slightly modifying the notation in the preceding subsection, we now let  $\mathbb{E}_n^J$  denote expectation with respect to the empirical measure

$$\hat{\mu}_n^J = \frac{1}{J} \sum_{j=1}^J \delta_{\hat{v}_n^{(j)}}.$$

We let  $\hat{v}_{n+1}$  denote the random variable with this distribution and, as before,  $\hat{h}_{n+1} = h(\hat{v}_{n+1})$ .

Next we define matrix  $\widehat{V}_n$  comprising scaled ensemble deviations in state space:

$$\widehat{V}_n = \frac{1}{\sqrt{J}} \left( \widehat{v}_n^{(1)} - \mathbb{E}_n^J \widehat{v}_n, \widehat{v}_n^{(2)} - \mathbb{E}_n^J \widehat{v}_n, \dots, \widehat{v}_n^{(J)} - \mathbb{E}_n^J \widehat{v}_n \right) \in \mathbb{R}^{d_v \times J},$$

we then define the analogous matrix  $\widehat{H}_n$  in observation space

$$\widehat{H}_n = \frac{1}{\sqrt{J}} \left( \widehat{h}_n^{(1)} - \mathbb{E}_n^J \widehat{h}_n, \widehat{h}_n^{(2)} - \mathbb{E}_n^J \widehat{h}_n, \dots, \widehat{h}_n^{(J)} - \mathbb{E}_n^J \widehat{h}_n \right) \in \mathbb{R}^{d_y \times J}.$$

For later use we also define

$$V_n = \frac{1}{\sqrt{J}} \left( v_n^{(1)} - \mathbb{E}_{*,n}^J v_n, v_n^{(2)} - \mathbb{E}_{*,n}^J v_n, \dots, v_n^{(J)} - \mathbb{E}_{*,n}^J v_n \right) \in \mathbb{R}^{d_v \times J},$$

where, here, expectation  $\mathbb{E}_{*,n}^J$  is with respect to the empirical measure (2.58) and  $v_n$  is a random variable with this distribution.

With these notations in hand, we have, with expectations computed under  $\mathbb{E}_n^J$ ,

$$(2.61a) \quad \widehat{C}_n^{vh} = \widehat{V}_n \widehat{H}_n^\top,$$

$$(2.61b) \quad \widehat{C}_n^{hh} = \widehat{H}_n \widehat{H}_n^\top$$

and the ensemble-based approximation of the Kalman gain matrix is <sup>8</sup>

$$(2.62) \quad K_n = \widehat{V}_{n+1} \widehat{H}_{n+1}^\top (\widehat{H}_{n+1} \widehat{H}_{n+1}^\top + \Gamma)^{-1}.$$

This is a linear algebraic reformulation of the Kalman gain approximation resulting from (2.6.2). By making a particle approximation of (2.41) we obtain

$$(2.63a) \quad \widehat{v}_{n+1}^{(j)} = \Psi(v_n^{(j)}) + \xi_n^{(j)}, \quad n \in \mathbb{Z}^+,$$

$$(2.63b) \quad \widehat{m}_{n+1} = \mathbb{E}_{n+1}^J \widehat{v}_{n+1},$$

$$(2.63c) \quad m_{n+1} = \widehat{m}_{n+1} + K_n (y_{n+1}^\dagger - \mathbb{E}_{n+1}^J \widehat{h}_{n+1}),$$

$$(2.63d) \quad v_{n+1}^{(j)} = m_{n+1} + C_{n+1}^{\frac{1}{2}} \widehat{C}_{n+1}^{-\frac{1}{2}} \left( \widehat{v}_{n+1}^{(j)} - \widehat{m}_{n+1} \right),$$

where  $K_n$  is given by (2.62), whilst  $\widehat{C}_{n+1}$  and  $C_{n+1}$  are computed empirically using

$$(2.64) \quad \widehat{C}_{n+1} = \widehat{V}_{n+1} \widehat{V}_{n+1}^\top, \quad C_{n+1} = \widehat{V}_{n+1} \left( I + \widehat{H}_{n+1}^\top \Gamma^{-1} \widehat{H}_{n+1} \right)^{-1} \widehat{V}_{n+1}^\top.$$

The first of these two formulae follows similarly to (2.61); the second of these two formulae is

---

<sup>8</sup>Here too, the empirical covariance computations are often modified to accommodate the widely adopted convention of scaling by  $1/(J-1)$ , instead of  $1/J$ .

derived as follows: <sup>9</sup>

$$\begin{aligned}
(2.65a) \quad C_{n+1} &= \hat{C}_{n+1} - \hat{C}_{n+1}^{vh} (\hat{C}_{n+1}^{hh} + \Gamma)^{-1} (\hat{C}_{n+1}^{vh})^\top \\
(2.65b) \quad &= \hat{V}_{n+1} \hat{V}_{n+1}^\top - \hat{V}_{n+1} \hat{H}_{n+1}^\top (\hat{H}_{n+1} \hat{H}_{n+1}^\top + \Gamma)^{-1} \hat{H}_{n+1} \hat{V}_{n+1}^\top, \\
(2.65c) \quad &= \hat{V}_{n+1} \left( I - \hat{H}_{n+1}^\top (\hat{H}_{n+1} \hat{H}_{n+1}^\top + \Gamma)^{-1} \hat{H}_{n+1} \right) \hat{V}_{n+1}^\top \\
(2.65d) \quad &= \hat{V}_{n+1} \left( I + \hat{H}_{n+1}^\top \Gamma^{-1} \hat{H}_{n+1} \right)^{-1} \hat{V}_{n+1}^\top.
\end{aligned}$$

Similarly, we may apply a particle approximation to the mean field dynamical system (2.50) to obtain

$$\begin{aligned}
(2.66a) \quad & \hat{v}_{n+1}^{(j)} = \Psi(v_n^{(j)}) + \xi_n^{(j)}, \quad n \in \mathbb{Z}^+, \\
(2.66b) \quad & \hat{h}_{n+1}^{(j)} = h(\hat{v}_{n+1}^{(j)}), \\
(2.66c) \quad & \hat{m}_{n+1} = \mathbb{E}_{n+1}^J \hat{v}_{n+1}, \\
(2.66d) \quad & m_{n+1} = \hat{m}_{n+1} + K_n (y_{n+1}^\dagger - \mathbb{E}_{n+1}^J \hat{h}_{n+1}), \\
(2.66e) \quad & v_{n+1}^{(j)} = m_{n+1} + (\hat{v}_{n+1}^{(j)} - \hat{m}_{n+1}) - \tilde{K}_n (\hat{h}_{n+1}^{(j)} - \mathbb{E}_{n+1}^J \hat{h}_{n+1}).
\end{aligned}$$

By making an empirical approximation of the formula (2.49) the matrix  $\tilde{K}_n$  is defined using the identification

$$\tilde{K}_n = \hat{V}_{n+1} \hat{H}_{n+1}^\top \left[ (\hat{H}_{n+1} \hat{H}_{n+1}^\top + \Gamma) + (\hat{H}_{n+1} \hat{H}_{n+1}^\top + \Gamma)^{1/2} \Gamma^{1/2} \right]^{-1}$$

The key difference between (2.63) and (2.66) is that the former involves inversion in state space, and the latter in data space. The relative size of the two dimensions dictates which is preferable. Both methods are examples of a general class of algorithms known as *ensemble adjustment Kalman filters*: EAKF.

**Ensemble Transform Kalman Filters.** The ensemble adjustment Kalman filters involve application, and inversion, of matrices which are applied on the left and act on state space. A different class of algorithms, known as *ensemble transform Kalman filters* (ETKF), involve matrix multiplication from the right and consequently inversions take place in the ensemble space of dimension  $J$ . In many applications this is far smaller than the dimension of the state or data spaces, and then use of this version of the methodology is preferred. The aim is to determine matrix  $Z_n \in \mathbb{R}^{J \times J}$ , and to derive Kalman gain  $K_n$  from  $Z_n$ , so that the following interacting particle system produces an ensemble of particles  $\{v_{n+1}^{(j)}\}_{j \in J}$  with empirical

<sup>9</sup>Using, in the last line, the identity  $I - W^\top (W W^\top + I)^{-1} W = (I + W^\top W)^{-1}$  which holds for all (not necessarily square) matrices  $W$ .

covariance  $C_{n+1}$  defined by the second item in display (2.64):

$$\begin{aligned}
 (2.67a) \quad & \hat{v}_{n+1}^{(j)} = \Psi(v_n^{(j)}) + \xi_n^{(j)}, \quad n \in \mathbb{Z}^+, \\
 (2.67b) \quad & \hat{m}_{n+1} = \mathbb{E}_{n+1}^J \hat{v}_{n+1}, \\
 (2.67c) \quad & m_{n+1} = \hat{m}_{n+1} + K_n (y_{n+1}^\dagger - \mathbb{E}_{n+1}^J \hat{h}_{n+1}), \\
 (2.67d) \quad & v_{n+1}^{(j)} = m_{n+1} + \sum_{i=1}^J \left( \hat{v}_{n+1}^{(i)} - \hat{m}_{n+1} \right) (Z_n)_{ij}.
 \end{aligned}$$

It follows from (2.67d) that

$$(2.68) \quad V_{n+1} = \hat{V}_{n+1} Z_n.$$

If we define

$$(2.69) \quad Z_n = \left( I + \hat{H}_{n+1}^\top \Gamma^{-1} \hat{H}_{n+1} \right)^{-1/2} \in \mathbb{R}^{J \times J}.$$

then, as desired,  $V_{n+1} V_{n+1}^\top = C_{n+1}$  as defined by (2.64), by virtue of (2.65). The calculations in (2.65) can also be utilized to verify that the empirical Kalman gain matrix defined by (2.62) satisfies

$$K_n = \hat{V}_{n+1} Z_n^2 \hat{H}_{n+1}^\top \Gamma^{-1}.$$

Using this formula for  $K_n$  in (2.63) leads to an algorithm which matches first and second order statistics of the Gaussian projected filter, at  $n+1$ , requiring only matrix inversions in space of dimension defined by the number of particles  $J$ .

We finally note that (2.67c) and (2.67d) can be combined into a single transformation step of the form

$$(2.70) \quad v_{n+1}^{(j)} = \sum_{i=1}^J \hat{v}_{n+1}^{(i)} (S_n)_{ij}$$

where  $S_n \in \mathbb{R}^{J \times J}$  replaces the matrix  $Z_n$  in (2.67d) such that

$$m_{n+1} = \sum_{j=1}^J v_{n+1}^{(j)} = \sum_{i,j=1}^J \hat{v}_{n+1}^{(i)} (S_n)_{ij}$$

holds in addition to (2.68) with  $Z_n$  replaced by  $S_n$ . Formulation (2.70) has a number of attractive features. First, it clearly reveals that the analysis  $\{v_{n+1}^{(j)}\}_{j \in J}$  lies in the span of the space spanned by the predictions  $\{\hat{v}_{n+1}^{(j)}\}_{j \in J}$ , which is relevant whenever  $J < d_v$ . Second, all particle implementations of the ensemble Kalman filter and many of its extensions can be put into the framework (2.70) with the (possibly random) matrix  $S_n$  chosen appropriately. Third, it encodes a coupling between the prediction  $\{\hat{v}_{n+1}^{(j)}\}_{j \in J}$  and the analysis  $\{v_{n+1}^{(j)}\}_{j \in J}$  at the level of their associated empirical measures  $\hat{\mu}_n^J$  and  $\mu_n^J$ , respectively. See the bibliographic Section 2.7 below for more details.

**2.7. Bibliographical Notes.** For the control theoretic approach to the state estimation problem see Luenberger (1964) and Luenberger (1971). Recent analysis of the closely related 3DVAR method rests heavily on ideas introduced in Olson & Titi (2003), Hayden *et al.* (2011) and Foias *et al.* (2016); the papers Law & Stuart (2012), Law *et al.* (2012), Law *et al.* (2016a) and Sanz-Alonso & Stuart (2015) essentially establish the stability of these deterministic results to small noise perturbations. In the context of using observations to control the instability of chaotic systems, all of this work may be seen as building on the study of synchronization, reviewed in Ashwin (2003).

The Kalman filter (Kalman, 1960) is perhaps the first systematic analysis of an algorithm for incorporation of discrete time data into estimation of a discrete time stochastic dynamical system; it applies only to linear Gaussian systems. The monograph Jazwinski (2007) provides an introduction to nonlinear filtering both in discrete and continuous time.

Particle-based extensions of the classical Kalman filter to nonlinear filtering problems include the unscented Kalman filter and the ensemble Kalman filter. While this review focuses primarily on ensemble Kalman filter techniques, the unscented Kalman filter is an approach based on application of quadrature to the Gaussian projected filter; see Julier *et al.* (2000) as well as Särkkä (2013). A discussion and evaluation in the context of ensemble square root filters may be found in Wang *et al.* (2004).

The books Reich & Cotter (2015), Asch *et al.* (2016), Law *et al.* (2015), Harlim & Majda (2010), Abarbanel (2013), and Evensen *et al.* (2022) provide overviews of a variety of filtering methods, and ensemble Kalman methods in particular. The numerical implementation of ensemble Kalman methods is a very rich subject on its own with many important details which are beyond the scope of this mathematical survey paper. We refer the reader to the excellent monographs by Asch *et al.* (2016) and Evensen *et al.* (2022) for texts with emphasis on these implementation details. These include techniques such as inflation and localization, which we do not cover in this mathematical survey. Here we wish to only point to two particular aspects. First, the matrix  $Z_n$  in (2.68) is not uniquely defined by the requirement  $V_{n+1}V_{n+1}^\top = C_{n+1}$ . Formula (2.69) constitutes one possible choice, which leads to a symmetric  $Z_n$ . See Livings *et al.* (2008) for more details. Second, finite particle implementations of the stochastic EnKF entail that the random realizations  $\hat{y}_{n+1}^{(j)}$  appear both in the Kalman gain  $K_n$  as well as in the innovation term in (2.60c). As first observed by Houtekamer & Mitchell (2005), this leads to a systematic underestimation of the ensemble spread, which vanishes in the  $J \rightarrow \infty$  limit; but can affect the performance of the EnKF for small particle sizes. In Subsection 4.6 we will highlight the same effect when discussing finite particle implementations (Nüsken & Reich, 2019; Garbuno-Inigo *et al.*, 2020a) of the ensemble Kalman sampler for Bayesian inversion, based on the mean field model proposed in Garbuno-Inigo *et al.* (2020b).

Much of the development of ensemble Kalman methods reflects the historical roots of the subject in the geophysical sciences, the atmosphere-ocean sciences in particular, including Lagrangian data assimilation, and in the modeling of subsurface flow (Burgers *et al.*, 1998; Houtekamer & Mitchell, 1998; Anderson, 2001; Bishop *et al.*, 2001; Whitaker & Hamill, 2002; Tippett *et al.*, 2003; Hunt *et al.*, 2007; Li & Reynolds, 2009; Sakov *et al.*, 2012; Bocquet & Sakov, 2014; Evensen, 2019; Bocquet & Sakov, 2012; Bocquet *et al.*, 2017; Gurumoorthy *et al.*, 2017; Sampson *et al.*, 2021; Kuznetsov *et al.*, 2003; Salman *et al.*, 2006). We also mention



the randomized maximum likelihood (RML) approach to Bayesian inference which is closely related to the analysis step of a stochastic EnKF and has also been developed primarily through application in the geophysical sciences [Kitanidis \(1995\)](#), [Oliver \*et al.\* \(1997\)](#), and [Oliver \*et al.\* \(2008\)](#).

The following papers concern analysis and development of ensemble methods with an emphasis on applications in complex and turbulent flows: [Grooms \*et al.\* \(2014\)](#), [Grooms \*et al.\* \(2015\)](#), [Robinson \*et al.\* \(2018\)](#), [Lee \*et al.\* \(2017\)](#), [Gottwald & Majda \(2013\)](#), [Kelly \*et al.\* \(2015\)](#), [Tong \*et al.\* \(2016\)](#), [Tong \*et al.\* \(2015\)](#), [Kelly \*et al.\* \(2015\)](#), [Harlim \*et al.\* \(2014\)](#), [Majda & Tong \(2018\)](#), [Fertig \*et al.\* \(2007\)](#), [Harlim & Hunt \(2007b\)](#), [Harlim & Hunt \(2007a\)](#). The conceptual fluid dynamics models of Lorenz ([Lorenz, 1996](#)) (often referred to, collectively, as Lorenz '96 models) have been particularly influential in germinating this body of work and we use them exclusively in our illustrative Examples [2.1](#), [2.2](#), [2.3](#), [2.10](#) and [4.21](#). Furthermore we will make use of the relationship between the multiscale and singlescale version of the model as developed in ([Fatkullin & Vanden-Eijnden, 2004](#)).

Recently ensemble Kalman methods have been developed for potential use in machine learning ([Haber \*et al.\*, 2018](#); [Kovachki & Stuart, 2019](#); [Guth \*et al.\*, 2020](#); [Grooms, 2021](#); [Gottwald & Reich, 2021](#); [Yang & Grooms, 2021](#); [Pidstrigach & Reich, 2021](#)); see also [Bocquet \*et al.\* \(2017\)](#), [Chen \*et al.\* \(2022\)](#) for research at the intersection of machine learning with ensemble Kalman methodology.

While we have started from mean field equations in this survey and then discretized by  $J$  particles, it remains to be demonstrated that the arising discrete formulations converge to the mean field equations in the  $J \rightarrow \infty$  limit. This has indeed been established for the standard ensemble Kalman filter formulations by [Le Gland \*et al.\* \(2011\)](#), [Mandel \*et al.\* \(2011\)](#), and [Kwiatkowski & Mandel \(2015\)](#); see [Law \*et al.\* \(2016b\)](#) for related work studying ensemble Kalman methods in the context of non-Gaussian problems. The papers [Ding \*et al.\* \(2020\)](#), [Ding & Li \(2021a,b\)](#) study particle approximation of mean-field limits beyond the Gaussian setting, primarily in the context of the solution of inverse problems; see the discussion in Subsection [4.6](#). The papers [Hoel \*et al.\* \(2016\)](#); [Chernov \*et al.\* \(2021\)](#) study the use of multilevel approximation of the mean field limit, coupling ensemble approximations at different levels of space or time discretization.

The non-uniqueness of second order transport maps is studied in continuous time, for linear Gaussian stochastic differential equations, in [Taghvaei & Mehta \(2020\)](#); this work is closely related to our analysis in the first two subsections of Section [8](#). Non-Gaussian extensions are discussed in [Taghvaei & Hosseini \(2022\)](#). We also highlight that it is possible to construct second order transport maps  $\tilde{T}$ , which satisfy conditions different from [\(2.43b\)](#) and [\(2.48b\)](#), respectively. For example, one could request that

$$G((\tilde{T}_n^S)^\# \nu) = GB_n(\nu).$$

This approximation has been utilized by [Lei & Bickel \(2011\)](#). The analog deterministic approach has been put forward by [Tödter & Ahrens \(2015\)](#) and has been explored further, for example, in [Acevedo \*et al.\* \(2017\)](#). Alternatively, one can also replace the definition [\(2.4.1\)](#) of the Gaussian projection operator  $G$ . To this end, recall that the Kullback–Leibler divergence

between probability measures  $\mu$  and  $\pi$  on  $\mathbb{R}^d$  is defined as

$$d_{\text{KL}}(\mu||\pi) = \int \pi(du) \log \frac{d\pi}{d\mu}(u);$$

it is not symmetric in its two arguments. Gaussian variational inference [Bishop \(2011\)](#) is for example based of the definition

$$(2.71) \quad G\mu = \operatorname{argmin}_{\pi \in \mathcal{G}} d_{\text{KL}}(\pi||\mu)$$

in place of (2.4.1); note, however, that the minimizer of (2.71) may not be unique, whilst the minimizer of (2.4.1) is always unique.

While we follow the moment matching perspective on the derivation of ensemble Kalman filter methods in this survey, we mention in passing that there is an alternative perspective based on linear minimum variance estimators. See [van Leeuwen \(2020\)](#) in the context of the stochastic ensemble Kalman filter and the Appendix 8.3 as well as [Lei & Bickel \(2011\)](#) for nonlinear extensions.

Even in the mean field limit  $J \rightarrow \infty$ , the ensemble Kalman filter provides approximations only to approximate transport based filters. As mentioned in Subsection 1.1, sequential Monte Carlo methods can be designed to be consistent with the underlying nonlinear filtering problem as defined, for example, by perfect transport based filters. Foundational analysis of these particle methods is undertaken in [Crisan \*et al.\* \(1998\)](#) and [del Moral \(2004\)](#); but we reiterate that, in contrast to ensemble Kalman based methods, they do not scale well to high dimensions. We also point to [Del Moral \*et al.\* \(2006\)](#) for an application of the sequential Monte Carlo method to Bayesian inference problems; the approach therein is closely related to iterative implementations of the EnKF that were subsequently developed in the papers [Li & Reynolds \(2009\)](#), [Gu & Oliver \(2007\)](#), [Sakov \*et al.\* \(2012\)](#).

Despite only providing approximations to the exact filtering distribution, accuracy and stability results for the ensemble Kalman filter, viewed as a state estimator, have been derived, for example, in [González-Tokman & Hunt \(2013\)](#), [Kelly \*et al.\* \(2014\)](#), [Tong \*et al.\* \(2015\)](#), and [Tong \*et al.\* \(2016\)](#). Mechanisms for finite time filter divergence have also been identified ([Gottwald & Majda, 2013](#); [Kelly \*et al.\*, 2015](#)).

Extending the ensemble Kalman filter to strongly nonlinear and high dimensional state estimation problems constitute an area of active ongoing research. The current state of the art has been summarized in [van Leeuwen \*et al.\* \(2019\)](#) in the context of high dimensional geophysical applications. Extensions of the transport framework (2.39), which build on approximating the perfect transport maps  $T^D$  in (2.39b) in an asymptotically consistent manner, include the work by [Reich \(2013\)](#), [Cheng & Reich \(2015\)](#), [Spantini \*et al.\* \(2019b\)](#), and [Zech & Marzouk \(2022\)](#). In an alternative line of research there have been several proposals to construct hybrid methods, which aim to adaptively bridge between the ensemble Kalman and particle filters; including the work by [Stordal \*et al.\* \(2011\)](#), [Frei & Künsch \(2013\)](#), and [Chustagulprom \*et al.\* \(2016\)](#).

In this context, the transformation formula (2.70) proves to be rather useful since most existing particle based methods can be covered by appropriate choices of  $S_n$ , where  $S_n$  is typically the realization of a random matrix. See [Reich & Cotter \(2015\)](#) for more details. For

example, a resampling step in a sequential Monte Carlo method gives rise to a matrix  $S_n$  with a single non-zero entry equal to one in each of its columns. More generally, it holds that

$$\sum_{i \in J} (S_n)_{ij} = 1.$$

The subject of optimal transport is given a comprehensive treatment in Villani (2008); see also Villani (2021). Computational aspects of the subject are discussed in Peyré *et al.* (2019). Ideas from the field are impacting filtering and Bayesian inference (Corenflos *et al.*, 2021), building on the computational tractability of entropy-regularized optimal transport (Cuturi, 2013). This regularization is linked to the Schrödinger bridge problem, and connections with data assimilation are developed in Reich (2019). See also Subsection 1.1 for discussion of transport-based methodologies within the context of ensemble Kalman methods. See Example 8.7 and Reich & Cotter (2015) for the connection between the map (2.56) and optimal transport. For a derivation of the standard formulae for mean and covariance of conditioned Gaussians used in the proof of Lemma 2.5 see Eaton (2007).

**3. Continuous Time.** This section is devoted to deriving, and studying properties of, continuous time analogues of concepts introduced in the previous section. We start in Subsection 3.1 defining the set-up. Thereafter the subsections mirror those from the previous section, describing the relevant continuous time analogues; in particular we conclude with Subsection 3.7 containing bibliographic notes.

All problems arising in practice are implemented as algorithms in discrete time, so it is important to establish motivation for the continuous time formulations. There are two primary reasons for introducing them. The first is that continuous time limits of the discrete algorithms provide a way to understand and interpret the behavior of the discrete algorithms; results about accuracy, stability and uncertainty quantification, which shed light on the relative merits of different algorithmic approaches, are often cleanest in the continuous time setting. The second is that many problems arising in practice involve physical processes which evolve in continuous time; when the data informing these models is discrete in time, but very high frequency, it is insightful to consider the idealization of continuous time data. Both of these motivations underlie the developments in this section.

We introduce a small increment in time, denoted by  $\Delta t$ . Recalling the map  $\Psi(\cdot)$  defining the systematic component of the state dynamics, we now define an infinitesimal analogue  $f(\cdot)$ ; we also introduce the rescaled observation operators  $h(\cdot)$  from the original nonlinear observation operator  $h(\cdot)$ ; and we introduce state/observational covariances  $(\Gamma, \Sigma)$  by rescaling  $(\Gamma, \Sigma)$ :

$$(3.1a) \quad \Psi(v) = v + \Delta t f(v), \quad h(v) = \Delta t h(v),$$

$$(3.1b) \quad \Sigma = \Delta t \Sigma, \quad \Gamma = \Delta t \Gamma.$$

In the linear setting  $\Psi(\cdot) = M \cdot, h(\cdot) = H \cdot$  we will also introduce an infinitesimal vector field

$f(\cdot) = F \cdot$  for matrix  $F$ , and rescaled linear observation operator  $H$  <sup>10</sup>

$$M = \text{Id} + \Delta t F, \quad H = \Delta t H.$$

The observation  $\{y_n\}$  is best thought of, in the scalings we introduce, as capturing increments of a process  $\{z_n\}$ . To capture this, and extend it to the specific realization of the data appearing in the algorithms, and the artificial data used in some algorithms, we introduce the variables  $z_n, z_n^\dagger, \widehat{z}_n$  by assuming that

$$(3.2a) \quad y_{n+1} := z_{n+1} - z_n = \Delta z_{n+1},$$

$$(3.2b) \quad y_{n+1}^\dagger := z_{n+1}^\dagger - z_n^\dagger = \Delta z_{n+1}^\dagger,$$

$$(3.2c) \quad \widehat{y}_{n+1} := \widehat{z}_{n+1} - \widehat{z}_n = \Delta \widehat{z}_{n+1}.$$

Note that  $z_n, z_n^\dagger, \widehat{z}_n$  have dimension  $d_z = d_y$ . We assume that  $z_0 = z_0^\dagger = \widehat{z}_0 = 0$ . Then  $z_n, z_n^\dagger, \widehat{z}_n$  are uniquely defined from  $y_n, y_n^\dagger, \widehat{y}_n$ , respectively.

In the following we set  $t_n = n\Delta t$ . With this definition, and the scaling above in hand, we may view the state  $v_n$  and observation  $y_n$  as relating to approximations of continuous time processes  $v(\cdot)$  and  $z(\cdot)$ :  $v_n \approx v(t_n)$ ,  $z_n \approx z(t_n)$ . We also introduce continuous time process  $\widehat{v}(\cdot)$ , which we will be used in the prediction part of algorithms developed in what follows, and  $(z^\dagger(\cdot), \widehat{z}(\cdot))$ , denoting the continuous time observed data, which we are conditioning on, and predicted data, used in the algorithm. We assume that  $z(0) = z^\dagger(0) = \widehat{z}(0) = 0$ . Under the rescalings above, and in the limit  $\Delta t \rightarrow 0$ , the data assimilation problem may be reformulated in terms of SDEs; and the related mappings on measures, and discrete-time algorithms that stem from them, may be reformulated in terms of SDEs and SPDEs; we now go on to identify these continuous time stochastic processes.

**3.1. Set-Up.** We turn our attention to deriving the continuous-time analogue of the discrete-time set-up (2.1) for state-observation coevolution: for all  $n \in \mathbb{Z}^+$  we have

$$\begin{aligned} v_{n+1} &= \Psi(v_n) + \xi_n, \\ y_{n+1} &= h(v_{n+1}) + \eta_{n+1}; \end{aligned}$$

recall that we assume that  $v_0, \{\xi_n\}_{n \in \mathbb{Z}^+}$  and  $\{\eta_n\}_{n \in \mathbb{N}}$  are mutually independent Gaussians defined by

$$v_0 \sim \mathbf{N}(m_0, C_0), \quad \xi_n \sim \mathbf{N}(0, \Sigma) \text{ i.i.d.}, \quad \eta_n \sim \mathbf{N}(0, \Gamma) \text{ i.i.d.}.$$

Applying the rescalings in (3.1) and the reparametrization of  $y_{n+1}$  in (3.2), we obtain the system

$$(3.3a) \quad v_{n+1} = v_n + \Delta t f(v_n) + \xi_n,$$

$$(3.3b) \quad z_{n+1} = z_n + \Delta t h(v_{n+1}) + \eta_{n+1},$$

---

<sup>10</sup>Note the difference between the discrete time objects  $(h(\cdot), H, \Gamma, \Sigma)$  and the related continuous time objects  $(h(\cdot), \mathbf{H}, \Gamma, \Sigma)$ .

for all  $n \in \mathbb{Z}^+$ , where we assume  $v_0, \{\xi_n\}_{n \in \mathbb{Z}^+}$  and  $\{\eta_n\}_{n \in \mathbb{N}}$  are mutually independent Gaussians defined by

$$v_0 \sim \mathbf{N}(m_0, C_0), \quad \xi_n \sim \mathbf{N}(0, \Delta t \Sigma) \text{ i.i.d.}, \quad \eta_n \sim \mathbf{N}(0, \Delta t \Gamma) \text{ i.i.d.}.$$

Note that (3.3) is a variant on the Euler-Maruyama discretization of an SDE. Indeed, by taking the  $\Delta t \rightarrow 0$  limit it is clear that the natural continuous time analogue of equations (2.1) is the pair of coupled SDEs

$$(3.4a) \quad dv = f(v)dt + \sqrt{\Sigma}dW, \quad v_0 \sim \mathbf{N}(m_0, C_0)$$

$$(3.4b) \quad dz = h(v)dt + \sqrt{\Gamma}dB, \quad z(0) = 0,$$

taken to hold for all  $t \in \mathbb{R}^+$ . The vector fields  $f(\cdot)$  and  $h(\cdot)$  describe the systematic, deterministic components of the dynamics and observation processes and are assumed known. The systematic components of the model are subjected to unit Brownian motions  $W$  and  $B$ , in  $\mathbb{R}^{d_v}$  and  $\mathbb{R}^{d_z}$  respectively, and the initial condition for  $v$  is Gaussian. Analogous to the discrete time setting, we assume that

$$(3.5) \quad C_0 \succeq 0, \quad \Sigma \succeq 0, \quad \Gamma \succ 0,$$

where  $v_0, W$  and  $B$  are mutually independent random variables. Note that, for each fixed  $t \in \mathbb{R}^+$ , the state  $v(t) \in \mathbb{R}^{d_v}$  and the observations  $z(t) \in \mathbb{R}^{d_z}$ .

Throughout we use  $\dagger$  again to denote a specific realization of a process, as in the discrete time setting. We assume that we have available to us a sample path  $\{z^\dagger(t)\}_{t \in \mathbb{R}^+}$  of the observation coordinates of a realization of the SDE (3.4), from which we wish to recover the true realization of the state  $\{v^\dagger(t)\}_{t \in \mathbb{R}^+}$ . These observation and state sample paths are generated by  $v_0^\dagger, \{W^\dagger\}_{t \in \mathbb{R}^+}$  and  $\{B^\dagger\}_{t \in \mathbb{R}^+}$ , specific realizations of the initial condition and the Brownian motions driving the state and observation components of (3.4). We also introduce  $Z^\dagger(t) = \{z^\dagger(s)\}_{0 \leq s \leq t}$ . It is natural to think about our objective in two different ways:

- Objective 1: design an algorithm producing output  $v(t)$  from  $Z^\dagger(t)$  so that  $\{v(t)\}_{t \in \mathbb{R}^+}$  estimates  $\{v^\dagger(t)\}_{t \in \mathbb{R}^+}$ , the true signal generated by (3.4a);
- Objective 2: design an algorithm which estimates the distribution of random variable  $v(t)|Z^\dagger(t)$ .

In both cases we are interested in Markovian formulations which update the estimate  $v(t)$ , or the distribution  $v(t)|Z^\dagger(t)$ , sequentially as the data is acquired. All of the algorithms we describe depend only on the increments of the process  $z^\dagger(t)$ , hence the fixing of  $z^\dagger(0) = 0$  is immaterial. In the next two subsections we describe control theoretic and probabilistic approaches to this problem which, respectively, provide the basis for algorithms addressing Objectives 1 and 2. Following the road-map from the previous section in the discrete time setting, we then proceed to study exact transport leading to mean-field equations related to these Objective 2; we then study second order approximations of exact transport, and finally reach ensemble Kalman methods through particle approximations.

**3.2. Control Theory Perspective.** As for the time-discrete problem, we again start with the control theoretical approach based on the small uncertainty assumption. Specifically

we assume that the three covariances appearing in (3.5) are small so that the states and observations can be well approximated as deterministic. Thus we initially set  $\Sigma$  and  $\Gamma$  to zero. Applying the rescalings (3.1) to (2.3) we obtain, in the deterministic setting,

$$(3.6a) \quad \hat{v}_{n+1} = v_n + \Delta t f(v_n),$$

$$(3.6b) \quad \hat{z}_{n+1} = \hat{z}_n + \Delta t h(\hat{v}_{n+1}),$$

$$(3.6c) \quad v_{n+1} = \hat{v}_{n+1} + K(\Delta z_{n+1}^\dagger - \Delta \hat{z}_{n+1}).$$

Equations (3.6) define a deterministic map  $v_n \mapsto v_{n+1}$  using the observed increments from (3.2b) so that

$$\Delta z_{n+1}^\dagger := z^\dagger((n+1)\Delta t) - z^\dagger(n\Delta t),$$

derived from a specific fixed realization of (3.4). Taking the continuous time limit, and eliminating  $\hat{z}$ , we obtain the following estimator  $v$  for  $v^\dagger$  given  $Z^\dagger$ :

$$(3.7) \quad \boxed{dv = f(v)dt + K(dz^\dagger - h(v)dt),}$$

where  $z^\dagger$  (the data) is obtained from a specific fixed realization of (3.4):

$$(3.8a) \quad dv^\dagger = f(v^\dagger)dt + \sqrt{\Sigma}dW^\dagger, \quad v_0 \sim \mathbf{N}(m_0, C_0)$$

$$(3.8b) \quad dz^\dagger = h(v^\dagger)dt + \sqrt{\Gamma}dB^\dagger, \quad z(0) = 0.$$

This is a continuous time analog of the 3DVAR algorithm (2.4). Equation (3.7) is a controlled ordinary differential equation (ODE); typically it is initialized with  $v(0) \sim \mathbf{N}(m_0, C_0)$ .

We now include the effect of uncertainty, allowing for non-zero covariances in (3.5). Accounting for noise in the expressions for  $\hat{v}_{n+1}$  and  $\hat{z}_{n+1}$  in (3.6) we obtain the following rescaling of (2.14):

$$\hat{v}_{n+1} = v_n + \Delta t f(v_n) + \xi_n,$$

$$\hat{z}_{n+1} = \hat{z}_n + \Delta t h(\hat{v}_{n+1}) + \eta_{n+1},$$

$$v_{n+1} = \hat{v}_{n+1} + K_n(\Delta z_{n+1}^\dagger - \Delta \hat{z}_{n+1}),$$

for all  $n \in \mathbb{Z}^+$ , where we assume  $v_0, \{\xi_n\}_{n \in \mathbb{Z}^+}$  and  $\{\eta_n\}_{n \in \mathbb{N}}$  are mutually independent Gaussians defined by (3.1). We may now formally take the  $\Delta t \rightarrow 0$  limit and obtain the following continuous time analog of (2.14), namely the controlled SDE formulation:

$$(3.9a) \quad \boxed{dv = f(v)dt + \sqrt{\Sigma}dW + K(dz^\dagger - d\hat{z}),}$$

$$(3.9b) \quad \boxed{d\hat{z} = h(v)dt + \sqrt{\Gamma}dB.}$$

where  $z^\dagger$  is given by (3.8). The unit Brownian motions  $W, W^\dagger, B$  and  $B^\dagger$ , in  $\mathbb{R}^{d_v}, \mathbb{R}^{d_v}, \mathbb{R}^{d_z}$  and  $\mathbb{R}^{d_z}$  respectively, are all independent of one another. As in the discrete time analog, encapsulated in (2.14), the choice of a time-dependent gain matrix  $K$  remains to be determined. We adopt a mean-field perspective for determination of  $K$  in continuous time, as we did in discrete time. To this end we progress to discuss the evolution of probability measures describing the conditional distribution of  $v(t)|Z^\dagger(t)$ .

### 3.3. Probabilistic Perspective.

**3.3.1. The Filtering Distribution.** The derivation of continuous time limits in the previous two subsections is relatively straightforward. However, there is an important practical and theoretical issue which we need to address. Instead of continuous time observations  $z^\dagger(t)$  one typically has access to the data at discrete time instances  $\tau_k = k\delta$ ,  $\delta > 0$ ,  $k = 1, \dots$  only. In order to make use of continuous time algorithms and theory it is then useful to construct a continuous time approximation  $z^{\dagger,\delta}$ ; to be concrete we will use piecewise linear interpolation. With this set-up we need to deal with two small parameters; the time-step  $\Delta t$  used in (3.1) to obtain a continuous time limit, and the data sampling interval  $\delta$ . There are results for continuous time filtering which imply that the desired limiting equation can be found in either Itô or Stratonovich forms by considering different orders of the limits  $\Delta t \rightarrow 0$  and  $\delta \rightarrow 0$  – see the bibliographic remarks in Subsection 3.7. However most theoretical results are derived by first taking  $\delta \rightarrow 0$  and then  $\Delta t \rightarrow 0$ . From a practical and theoretical perspective it is sometimes more convenient to first consider  $\Delta t \rightarrow 0$  followed by  $\delta \rightarrow 0$ . We will utilize the later sequence of limits in the following subsection in order to derive a set of evolution equations for the conditional probability measure  $\mu(v, t)$  solving Objective 2. These equations will in turn guide our choice of the gain matrix  $K$  in (3.9a). Finally, when the data  $z^\dagger$  arises itself from numerical simulations, then it is most convenient to set  $\delta = \Delta t$ , and hence  $\tau_k = t_k$ ; this is implicitly used in the derivation of the continuous time sample path equations in the two preceding subsections.

Our starting point here is the iteration on measures, the filtering cycle, defined by (2.19), under the scalings (3.1). We assume that  $\delta$  is an integer multiple of  $\Delta t$  so that the  $\{\tau_k\}$  are a subset of the  $\{t_n\}$ . We replace the true observation path  $z^\dagger(t)$  by its piecewise linear approximation  $z^{\dagger,\delta}(t)$  based on linear interpolation of values  $\{z^\dagger(\tau_k)\}$ . We then have that the implied observation increments  $\Delta z_{n+1}^\dagger$  are constant over the time intervals  $[t_n, t_{n+1}]$  and are given by

$$\Delta z_{n+1}^\dagger = \frac{dz^{\dagger,\delta}}{dt}(t_n)\Delta t.$$

In this setting, the operators  $P$  and  $L_n$ , defined by (2.19a) and (2.19b), respectively, become

$$(3.10a) \quad (P\mu)(dv) = \left( \int_{u \in \mathbb{R}^{d_v}} p(u, v) \mu(du) \right) dv,$$

$$(3.10b) \quad L_n(\mu)(dv) = q(v, \Delta z_{n+1}^\dagger) \mu(dv) / \left( \int_{\mathbb{R}^{d_v}} q(v, \Delta z_{n+1}^\dagger) \mu(dv) \right),$$

where

$$(3.11a) \quad p(u, v) = \frac{1}{(2\pi\Delta t)^{d_v/2} \sqrt{\det(\Sigma)}} \exp\left(-\frac{1}{2\Delta t} |v - u - \Delta t f(u)|_\Sigma^2\right),$$

$$(3.11b) \quad q(v, \Delta z) = \frac{1}{(2\pi\Delta t)^{d_y/2} \sqrt{\det(\Gamma)}} \exp\left(-\frac{1}{2\Delta t} |\Delta z - \Delta t h(v)|_\Gamma^2\right).$$

With these scalings, we now derive the continuous time analog of (2.19), for  $\mu(v, t)$ . For ease of exposition we assume that  $\mu$  has density  $\rho$  and derive the equation satisfied by  $\rho$ . To



do this we employ the *split-step principle*: we find the continuous time evolution equation associated with each of  $P$  and  $L_n$  (equations (3.10a) and (3.10b) respectively) separately, and then add the right-hand sides of the resulting evolution equations to obtain the desired continuous time limit resulting from the composition of  $L_n$  and  $P$ . We use  $r$  as a dummy variable to denote the density being evolved, for both of the split-steps, and in both discrete ( $r_n$ ) and continuous ( $r(t)$ ) time, in what follows.

First consider the continuous time limit of the evolution associated to  $P$  as described by (3.10a) and (3.11a). Since the underlying continuous time limit of the sample paths is given by the SDE (3.4a), the time evolution of the probability density  $r$  is given by the Fokker–Planck equation<sup>11</sup>

$$(3.12) \quad \partial_t r = -\nabla \cdot (rf) + \frac{1}{2} \nabla \cdot (\nabla \cdot (r\Sigma)).$$

Consider now the second component of the split-step argument: we determine a continuous time limit of the evolution associated to  $L_n$  as described by (3.10b) and (3.11b). The following lemma presents an evolution equation for  $r$  associated to  $L_n$ , describing how observation of the piecewise continuous interpolated data  $z^{\dagger,\delta}(t)$  changes the density  $r(t, v)$ .

**Lemma 3.1.** *Assume that  $\Gamma \succ 0$ . The continuous time limit of the evolution associated to  $L_n$ , as described by (3.10b) and (3.11b), is given by*

$$(3.13) \quad \partial_t r = \left\langle \mathbf{h} - \mathbb{E}\mathbf{h}, \frac{dz^{\dagger,\delta}}{dt} \right\rangle_{\Gamma} r - \frac{1}{2} \left\{ |\mathbf{h}|_{\Gamma}^2 - \mathbb{E} |\mathbf{h}|_{\Gamma}^2 \right\} r.$$

*Proof.* Consider the discrete-time evolution  $r_{n+1} = L_n r_n$ , where  $L_n$  is defined by (3.10b) and (3.11b). By Taylor expansion we have

$$\exp \left( -\frac{1}{2\Delta t} \left| \Delta z_{n+1}^{\dagger} - \Delta t \mathbf{h}(v) \right|_{\Gamma}^2 \right) = 1 - \frac{\Delta t}{2} \left| \frac{\Delta z_{n+1}^{\dagger}}{\Delta t} - \mathbf{h}(v) \right|_{\Gamma}^2 + \mathcal{O}(\Delta t^2);$$

then, using expressions (3.10b) and (3.11b), we obtain

$$(3.14) \quad L_n r_n = \frac{1}{C} \left( 1 - \frac{\Delta t}{2} \left| \frac{\Delta z_{n+1}^{\dagger}}{\Delta t} - \mathbf{h}(v) \right|_{\Gamma}^2 + \mathcal{O}(\Delta t^2) \right) r_n,$$

where

$$C = \int_{\mathbb{R}^{dv}} \left( 1 - \frac{\Delta t}{2} \left| \frac{\Delta z_{n+1}^{\dagger}}{\Delta t} - \mathbf{h}(v) \right|_{\Gamma}^2 + \mathcal{O}(\Delta t^2) \right) r_n dv.$$

---

<sup>11</sup>Here, and in what follows, we use the standard notation from continuum mechanics for the divergence of vector and second order tensor fields, and for the gradient of scalar and vector fields; see the bibliography Subsection 3.7 for references.

By integrating and noting that  $r_n$  is a density, it follows that

$$(3.15) \quad C = 1 - \frac{\Delta t}{2} \mathbb{E} \left| \frac{\Delta z_{n+1}^\dagger}{\Delta t} - \mathbf{h}(v) \right|_\Gamma^2 + \mathcal{O}(\Delta t^2),$$

where expectation is with respect to  $v$  distributed as random variable with density  $r_n$ . Hence, multiplying numerator and denominator in (3.14) by  $1 + \frac{\Delta t}{2} \mathbb{E} \left| \frac{\Delta z_{n+1}^\dagger}{\Delta t} - \mathbf{h} \right|_\Gamma^2$  we obtain

$$r_{n+1} = r_n \left\{ 1 + \Delta t \left\langle \mathbf{h} - \mathbb{E}\mathbf{h}, \frac{dz_{n+1}^{\dagger, \delta}}{dt} \right\rangle_\Gamma - \frac{\Delta t}{2} \left\{ |\mathbf{h}|_\Gamma^2 - \mathbb{E} |\mathbf{h}|_\Gamma^2 \right\} + \mathcal{O}(\Delta t^2) \right\},$$

using that the data increments  $\Delta z_{n+1}^\dagger$  are given by (3.3.1) for fixed  $\delta$ . Taking the time continuous limit  $\Delta t \rightarrow 0$  with fixed observation interval  $\delta > 0$  leads to the evolution equation (3.13). ■

Now taking the  $\delta \rightarrow 0$  limit in (3.13), we obtain the following nonlocal nonlinear stochastic evolution equation for density  $r(v, t)$ :

$$(3.16) \quad dr = \left\langle \mathbf{h} - \mathbb{E}\mathbf{h}, \circ dz^\dagger \right\rangle_\Gamma r - \frac{1}{2} \left\{ |\mathbf{h}|_\Gamma^2 - \mathbb{E} |\mathbf{h}|_\Gamma^2 \right\} r dt.$$

Here  $\circ$  denotes Stratonovitch integration; this form of integration arises in the limit  $\delta \rightarrow 0$  because the equation is derived by making a smooth approximation  $z^{\dagger, \delta}$  of  $z^\dagger$  and passing to the limit. Recall that  $z^\dagger$  is given by (3.8). The equation is nonlocal and nonlinear because  $\mathbb{E}$  denotes expectation at time  $t$  with respect to density  $r(\cdot, t)$ .

We now wish to invoke the split-step principle and combine the evolutions (3.12) and (3.16). However before doing this we proceed to convert the equation (3.16) into its more common Itô representation. For this, the following lemma is crucial. Here we provide a streamlined proof using known abstract results about covariation of correlated stochastic processes; in Appendix 9 we provide explicit calculations for the reader who is interested in understanding the details of the conversion by means of the definitions of Itô and Stratonovitch integrals as limits. In particular, the concepts underlying the covariation calculations in the following are derived from first principles in Lemma 9.1.

**Lemma 3.2.** *Assume that  $\Gamma \succ 0$  and that  $z^\dagger$  is given by (3.8). The Itô and Stratonovich interpretations of the stochastic forcing term in (3.16) are related through*

$$\begin{aligned} dr &= \left\langle \mathbf{h} - \mathbb{E}\mathbf{h}, \circ dz^\dagger \right\rangle_\Gamma r - \frac{1}{2} \left\{ |\mathbf{h}|_\Gamma^2 - \mathbb{E} |\mathbf{h}|_\Gamma^2 \right\} r dt \\ &= \left\langle \mathbf{h} - \mathbb{E}\mathbf{h}, dz^\dagger - \mathbb{E}\mathbf{h} dt \right\rangle_\Gamma r. \end{aligned}$$

*Proof.* Using the formula for the Itô–Stratonovich conversion between two semimartingales, we have

$$(3.17) \quad \int_0^t r \left\langle \mathbf{h} - \mathbb{E}\mathbf{h}, \circ dz^\dagger \right\rangle_\Gamma = \int_0^t r \left\langle \mathbf{h} - \mathbb{E}\mathbf{h}, dz^\dagger \right\rangle_\Gamma + \frac{1}{2} \int_0^t d \left[ \left\langle r(\mathbf{h} - \mathbb{E}\mathbf{h}), z^\dagger \right\rangle_\Gamma \right],$$

where  $[\langle \cdot, \cdot \rangle]$  denotes covariation. Note that the covariation between  $r$  and  $z^\dagger$  satisfies  $d[r, z^\dagger] = r(\mathbf{h} - \mathbb{E}\mathbf{h})dt$ . Hence the covariation in (3.17) satisfies

$$\begin{aligned} d[\langle r(\mathbf{h} - \mathbb{E}\mathbf{h}), z^\dagger \rangle_\Gamma] &= \langle \mathbf{h} - \mathbb{E}\mathbf{h}, d[r, z^\dagger] \rangle_\Gamma - r d[\langle \mathbb{E}\mathbf{h}, z^\dagger \rangle_\Gamma] \\ &= r |\mathbf{h} - \mathbb{E}\mathbf{h}|_\Gamma^2 dt - r \int \langle \mathbf{h}, d[r, z^\dagger] \rangle_\Gamma dv \\ &= r |\mathbf{h} - \mathbb{E}\mathbf{h}|_\Gamma^2 dt - r \mathbb{E} \langle \mathbf{h}, (\mathbf{h} - \mathbb{E}\mathbf{h}) \rangle_\Gamma dt \\ &= r \left\{ |\mathbf{h} - \mathbb{E}\mathbf{h}|_\Gamma^2 - \mathbb{E} |\mathbf{h} - \mathbb{E}\mathbf{h}|_\Gamma^2 \right\} dt. \end{aligned}$$

Upon rearranging, we find that

$$r \left\langle \mathbf{h} - \mathbb{E}\mathbf{h}, \circ dz^\dagger \right\rangle_\Gamma - \frac{1}{2} \left\{ |\mathbf{h}|_\Gamma^2 - \mathbb{E} |\mathbf{h}|_\Gamma^2 \right\} r dt = r \left\langle \mathbf{h} - \mathbb{E}\mathbf{h}, dz^\dagger - \mathbb{E}h dt \right\rangle_\Gamma,$$

which in turn leads to the following Itô representation of (3.16):

$$dr = r \left\langle \mathbf{h} - \mathbb{E}\mathbf{h}, dz^\dagger - \mathbb{E}h dt \right\rangle_\Gamma. \quad \blacksquare$$

Using the Itô form of the equation from the preceding lemma, the Fokker-Planck equation (3.12) and the split-step principle delivers:

**Theorem 3.3.** *Assume that  $\Gamma \succ 0$  and that  $z^\dagger$  is given by (3.8). The time evolution of the density  $\rho(\cdot, t)$  for the random variable  $v(t)|Z^\dagger(t)$  is characterized by the SPDE*

$$(3.18) \quad d\rho = -\nabla \cdot (\rho f) dt + \frac{1}{2} \nabla \cdot (\nabla \cdot (\rho \Sigma)) dt + \left\langle \mathbf{h} - \mathbb{E}\mathbf{h}, dz^\dagger - \mathbb{E}h dt \right\rangle_\Gamma \rho.$$

This is known as the Kushner–Stratonovich equation. The equation (3.18) should now be interpreted in the Itô sense with respect to the driving noise  $z^\dagger(t)$ . The corresponding Stratonovich formulation follows immediately from (3.16) in combination with (3.12).

**3.3.2. Important Repeatedly Used Notation.** In discrete time expectations may be taken under the law of the (possibly approximate) discretely evolving mean-field model, or under the predictive distribution found from pushing this law forward under the model. This distinction disappears in continuous time and we simply need to compute expectations under the (possibly approximate) continuously evolving mean-field models that we will introduce later. To this end we define, with  $m := \mathbb{E}v$ ,

$$\begin{aligned} (3.19a) \quad C &= \mathbb{E}((v - m) \otimes (v - m)), \\ (3.19b) \quad C^{vf} &= \mathbb{E}((v - m) \otimes (f(v) - \mathbb{E}f(v))), \\ (3.19c) \quad C^{vh} &= \mathbb{E}((v - m) \otimes (h(v) - \mathbb{E}h(v))). \end{aligned}$$

All expectations are under the mean-field model for  $v$ . The covariances should be viewed as functions of time  $t$ . In deriving continuous time models from discrete time models, we will also use discrete time analogs, computed under the law of random variable  $v_n$  and denoted  $C_n, C_n^{vf}$  and  $C_n^{vh}$ .

**3.4. Gaussian Projected Filtering Distribution.** As in discrete time, the Gaussian projected filtering distribution plays an important conceptual role in understanding later filtering algorithms. We derive this Gaussian filter in Subsection 3.4.1, and specialize to the setting of linear-Gaussian dynamics-observation in Subsection 3.4.2 where we obtain the Kalman-Bucy filter.

**3.4.1. Gaussian Projected Filtering.** The evolution equations for the mean  $m$  and the covariance matrix  $C$  follow naturally from a continuous time limit of the associated discrete time filtering formulations. We summarize the resulting equations in the following:

**Theorem 3.4.** *Assume that  $\Gamma \succ 0$ . and that  $z^\dagger$  is given by (3.8). Consider the map from  $(m_n, C_n)$  to  $(m_{n+1}, C_{n+1})$  defined by choosing  $v_n \sim \mathbf{N}(m_n, C_n)$  and then using (2.21), (2.23), (2.26) and (2.31). Under the rescalings (3.1), and in the limit  $\Delta t \rightarrow 0$ , we obtain the following continuous-time analogue of this map:*

$$\begin{aligned} (3.20a) \quad & dm = \mathbb{E}f(v)dt + C^{vh}\Gamma^{-1}(dz^\dagger - \mathbb{E}h(v)dt) \\ (3.20b) \quad & dC = C^{vf}dt + (C^{vf})^\top dt + \Sigma dt - C^{vh}\Gamma^{-1}(C^{vh})^\top dt, \end{aligned}$$

where the expectation is computed under  $\mathbf{N}(m(t), C(t))$  and where  $z^\dagger$  is given by (3.8).

**Remark 3.5.** Note that the preceding equation implicitly defines gain matrix

$$(3.21) \quad K = C^{vh}\Gamma^{-1}.$$

This specific choice of gain will play a central role in what follows. ■

**Proof.** (Lemma 3.4) The Gaussian projected filter is defined by evolution of mean and covariance given by equations (2.23), (2.26) and (2.31), repeated and reordered here for convenience:

$$\begin{aligned} \hat{m}_{n+1} &= \mathbb{E}\Psi(v_n), \\ \hat{C}_{n+1} &= \mathbb{E}\left((\Psi(v_n) - \hat{m}_{n+1}) \otimes (\Psi(v_n) - \hat{m}_{n+1})\right) + \Sigma, \\ m_{n+1} &= \hat{m}_{n+1} + \hat{C}_{n+1}^{vh}(\hat{C}_{n+1}^{hh} + \Gamma)^{-1}(y_{n+1}^\dagger - \mathbb{E}\hat{h}_{n+1}), \\ C_{n+1} &= \hat{C}_{n+1} - \hat{C}_{n+1}^{vh}(\hat{C}_{n+1}^{hh} + \Gamma)^{-1}(\hat{C}_{n+1}^{vh})^\top, \\ \hat{C}_{n+1}^{vh} &= \mathbb{E}\left((\hat{v}_{n+1} - \mathbb{E}\hat{v}_{n+1}) \otimes (\hat{h}_{n+1} - \mathbb{E}\hat{h}_{n+1})\right), \\ \hat{C}_{n+1}^{hh} &= \mathbb{E}\left((\hat{h}_{n+1} - \mathbb{E}\hat{h}_{n+1}) \otimes (\hat{h}_{n+1} - \mathbb{E}\hat{h}_{n+1})\right). \end{aligned}$$

Recall that  $\hat{h}_{n+1} := h(\hat{v}_{n+1})$ . Expectations in the prediction step are with respect to the law of  $v_n \sim \mathbf{N}(m_n, C_n)$ ; and expectations in the analysis step are with respect to the law of  $\hat{v}_{n+1}$  given by (2.21a), assuming that  $v_n \sim \mathbf{N}(m_n, C_n)$ ; thus  $Law(\hat{v}_{n+1}) = PLaw(v_n)$ .

We now impose the rescalings (3.1) on these equations. Note that, under the rescalings

and using that  $\xi_{n+1} = \mathcal{O}(\Delta t^{\frac{1}{2}})$  has mean zero,

$$\begin{aligned}\widehat{C}_{n+1}^{vh} &= \Delta t \mathbb{E} \left( (v_n - \mathbb{E}v_n + \xi_n + \mathcal{O}(\Delta t)) \otimes (h(v_n) - \mathbb{E}h(v_n) + Dh(v_n)\xi_n + \mathcal{O}(\Delta t)) \right) \\ &= \Delta t \mathbb{E} \left( (v_n - \mathbb{E}v_n) \otimes (h(v_n) - \mathbb{E}h(v_n)) \right) + \mathcal{O}(\Delta t^2) \\ &= \Delta t C_n^{vh} + \mathcal{O}(\Delta t^2).\end{aligned}$$

Similarly

$$\begin{aligned}\widehat{C}_{n+1}^{hh} + \Gamma &= \Delta t^2 \mathbb{E} \left( (h(v_n) - \mathbb{E}h(v_n) + \mathcal{O}(\Delta t^{\frac{1}{2}})) \otimes (h(v_n) - \mathbb{E}h(v_n) + \mathcal{O}(\Delta t^{\frac{1}{2}})) \right) + \Delta t \Gamma \\ &= \Delta t \Gamma + \mathcal{O}(\Delta t^2).\end{aligned}$$

Thus

$$(3.22a) \quad \widehat{C}_{n+1}^{vh} (\widehat{C}_{n+1}^{hh} + \Gamma)^{-1} = C_n^{vh} \Gamma^{-1} + \mathcal{O}(\Delta t),$$

$$(3.22b) \quad \widehat{C}_{n+1}^{vh} (\widehat{C}_{n+1}^{hh} + \Gamma)^{-1} \widehat{C}_{n+1}^{vh} = \Delta t C_n^{vh} \Gamma^{-1} (C_n^{vh})^\top + \mathcal{O}(\Delta t^2).$$

Furthermore

$$\begin{aligned}\mathbb{E} \left( (\Psi(v_n) - \widehat{m}_{n+1}) \otimes (\Psi(v_n) - \widehat{m}_{n+1}) \right) \\ &= \mathbb{E} \left( (v_n + \Delta t f(v_n) - \mathbb{E}v_n - \Delta t \mathbb{E}f(v_n)) \otimes (v_n + \Delta t f(v_n) - \mathbb{E}v_n - \Delta t \mathbb{E}f(v_n)) \right) \\ &= C_n + \Delta t C_n^{vf} + \Delta t (C_n^{vf})^\top + \mathcal{O}(\Delta t^2).\end{aligned}$$

Using these approximations, and the fact that  $\Delta z_{n+1}^\dagger = \mathcal{O}(\Delta t^{\frac{1}{2}})$ , we obtain

$$\begin{aligned}\widehat{m}_{n+1} &= m_n + \Delta t \mathbb{E}f(v_n), \\ \widehat{C}_{n+1} &= C_n + \Delta t C_n^{vf} + \Delta t (C_n^{vf})^\top + \Delta t \Sigma + \mathcal{O}(\Delta t^2), \\ m_{n+1} &= \widehat{m}_{n+1} + C_n^{vh} \Gamma^{-1} (\Delta z_{n+1}^\dagger - \Delta t \mathbb{E}h(\widehat{v}_{n+1})) + \mathcal{O}(\Delta t^{\frac{3}{2}}), \\ C_{n+1} &= \widehat{C}_{n+1} - \Delta t C_n^{vh} \Gamma^{-1} (C_n^{vh})^\top + \mathcal{O}(\Delta t^2), \\ C_n^{vf} &= \mathbb{E}((v_n - m_n) \otimes (f(v_n) - \mathbb{E}f(v_n))), \\ C_n^{vh} &= \mathbb{E}((v_n - m_n) \otimes (h(v_n) - \mathbb{E}h(v_n))).\end{aligned}$$

In the following  $C^{vh}, C^{vf}$  are functions of time, defined by (3.19), and  $C_n^{vh}, C_n^{vf}$  are discrete time analogs computed under the law of  $v_n$ .

Combining the prediction and analysis steps we find that

$$\begin{aligned}m_{n+1} &= m_n + \Delta t \mathbb{E}f(v_n) + C_n^{vh} \Gamma^{-1} (\Delta z_{n+1}^\dagger - \Delta t \mathbb{E}h(\widehat{v}_{n+1})) + \mathcal{O}(\Delta t^{\frac{3}{2}}) \\ C_{n+1} &= C_n + \Delta t C_n^{vf} + \Delta t (C_n^{vf})^\top + \Delta t \Sigma - \Delta t C_n^{vh} \Gamma^{-1} (C_n^{vh})^\top + \mathcal{O}(\Delta t^2).\end{aligned}$$

Taking the  $\Delta t \rightarrow 0$  limit, we deduce the continuous-time analogue of the equations (2.23), (2.26) as stated. ■

**3.4.2. The Kalman-Bucy Filter.** We consider the setting where  $f(\cdot) = F\cdot$  and  $h(\cdot) = H\cdot$  in equations (3.4) so that

$$(3.23a) \quad dv = Fvdt + \sqrt{\Sigma}dW, \quad v_0 \sim \mathbf{N}(m_0, C_0)$$

$$(3.23b) \quad dz = Hvdt + \sqrt{\Gamma}dB, \quad z(0) = 0.$$

Now consider data  $z^\dagger(t)$  generated by

$$(3.24a) \quad dv^\dagger = Fv^\dagger dt + \sqrt{\Sigma}dW^\dagger, \quad v_0 \sim \mathbf{N}(m_0, C_0)$$

$$(3.24b) \quad dz^\dagger = Hv^\dagger dt + \sqrt{\Gamma}dB^\dagger, \quad z(0) = 0.$$

The filtering distribution for  $v(t)|Z^\dagger(t)$  is Gaussian and is given by the Kalman-Bucy filter, which is the continuous time analog of what appears in Subsection 2.4.2. It may be obtained from the continuous time Gaussian projected filter, which is exact in this setting, and also yields a solution of the Kushner-Stratonovich equation. The following summarizes the result.

**Theorem 3.6.** *Assume that  $\Gamma \succ 0$  in (3.23). The density  $\rho(\cdot, t)$  for the random variable  $v(t)|Z^\dagger(t)$ , with  $z^\dagger$  given by (3.24), is Gaussian with mean  $m(\cdot)$  and covariance  $C(\cdot)$  solving*

$$(3.25a) \quad dm = Fm dt + CH^\top \Gamma^{-1} (dz^\dagger - Hm dt),$$

$$(3.25b) \quad dC = FC dt + CF^\top dt + \Sigma dt - CH^\top \Gamma^{-1} HC dt.$$

Furthermore, if  $\rho|_{t=0}$  is Gaussian then the Kushner-Stratonovich equation (3.18) has solution given by the Gaussian  $\mathbf{N}(m(t), C(t))$ .

*Proof.* Under (3.1), (3) the limiting Gaussian projected filter from Theorem 3.4 gives (3.25). This equation thus reproduces the true filtering distribution in the linear-Gaussian setting. ■

**3.5. Mean Field Evolution Equations.** In Subsection 3.5.1 we describe work concerning the derivation of explicit mean-field SDEs equal in law to the filtering distribution; this is a departure from our discussion of this topic in discrete time where no explicit maps were identified in the general setting. Subsections 3.5.2 and 3.5.3 describe a variety of explicit approximate mean-field SDEs, based on matching first and second order moment information, and arising from rescaling of the discrete time setting. We conclude in Subsection 3.5.4 by identifying a mean-field SDE which is equal in law to the Kalman-Bucy filter.

**3.5.1. Perfect Transport.** Here we seek a mean field dynamical system with law given by that of the Kushner-Stratonovich equation. The analog of the discrete-time transport map  $T_n^S$ , is to find transport evolution equations for  $v$  and  $\hat{z}$  in the form a mean-field SDE. We will seek to achieve this in the specific form

$$(3.26a) \quad dv = f(v)dt + \sqrt{\Sigma}dW + a(v; \rho)dt + K(v; \rho)(dz^\dagger - d\hat{z}),$$

$$(3.26b) \quad d\hat{z} = h(v)dt + \sqrt{\Gamma}dB,$$

where  $\rho$  is the time-dependent density of  $v$ . The goal is to chose drift  $a$  and gain  $K$  such that the induced time evolution of the density  $\rho$  of  $v$  agrees with the density  $\rho$  given by the Kushner-Stratonovich equation (3.18). We thus find a controlled SDE, similar in form to that proposed in (3.9) but with an additional drift term and with mean field dependence. We emphasize that, as in the discrete-time transport formulation, there is a considerable degree of non-uniqueness in the choice of transport in general, and here in the choice of  $a$  and  $K$  specifically. We make specific, simple, choices in the theorem that follows. Working in continuous time enables very explicit identification of exact mean-field models; this is not possible in discrete time.

**Theorem 3.7.** *Assume that  $\Gamma \succ 0$  and that there exists  $K = K(v; \rho)$  satisfying the identity*

$$(3.27) \quad -\nabla \cdot (\rho K^\top) = \rho \Gamma^{-1} (\mathbf{h} - \mathbb{E} \mathbf{h}).$$

*Consider the stochastic mean-field dynamics given by*

$$(3.28a) \quad dv = f(v)dt + \sqrt{\Sigma}dW + \nabla \cdot (K \Gamma K^\top)dt - K \Gamma \nabla \cdot K^\top dt + K(dz^\dagger - d\hat{z}),$$

$$(3.28b) \quad d\hat{z} = \mathbf{h}(v)dt + \sqrt{\Gamma}dB,$$

where  $z^\dagger$  given by (3.8). Assume that solution  $v$  has law with smooth density and that the Kushner-Stratonovich equation (3.18) has smooth density as solution. Then the law of  $v$  has density given by the Kushner-Stratonovich equation (3.18).

*Proof.* To simplify calculations we will first look at choosing  $a$  and  $K$  to get agreement, at the level of densities of  $v$ , with (5); a straightforward modification, using the split-step principle again, then provides the generalization to (3.18). This enables us to consider the case where  $f(\cdot) \equiv 0$  and  $\Sigma = 0$ .

Note that, in (3.26),  $z^\dagger$  is a fixed, given, trajectory and we are interested in the evolution of the probability density induced for  $v$  by the randomness over the distribution on trajectories  $\hat{z}$ . Using (3.26b) in (3.26a) and setting  $f$  and  $\Sigma$  to zero we obtain

$$(3.29) \quad dv = a(v; \rho)dt + K(v; \rho)(dz^\dagger - \mathbf{h}(v)dt - \sqrt{\Gamma}dB).$$

Applying Fokker-Planck analysis, modified to the mean-field setting, shows that the time evolution of the density  $\rho$  of  $v$  under (3.26) is provided by the nonlinear (because of dependence of  $a, K$  on  $\rho$ ) SPDE<sup>12</sup> to be interpreted in the Itô sense:

$$(3.30) \quad d\rho = -\nabla \cdot (\rho(a - K\mathbf{h}))dt - \langle \nabla \cdot (\rho K^\top), dz^\dagger \rangle + \nabla \cdot (\nabla \cdot (\rho K \Gamma K^\top))dt.$$

Note that, although  $z^\dagger$  is a fixed trajectory, it contributes to the diffusion term in this Fokker-Planck equation, explaining the factor 1 rather than 1/2. This arises as a contribution from the quadratic variation of the path of  $z^\dagger$  to the evolution of  $\rho$ . For further details on the

---

<sup>12</sup>Here we use the standard convention from continuum mechanics that the divergence of a matrix is to be interpreted via computation of derivatives with respect to the second index; see Subsection 3.7 for references to relevant continuum mechanics textbooks. Strictly speaking equation (3.30) is an SPDE only if we now view  $z^\dagger$  as a random variable rather than a fixed realization.



derivation of (3.30) see Lemma 9.2 in Appendix 9. Comparing with (5) we find that to get agreement  $a$  and  $K$  have to be chosen such that

$$\begin{aligned} \rho \langle (\mathbf{h} - \mathbb{E}\mathbf{h}), \Gamma^{-1}(dz^\dagger - \mathbb{E}\mathbf{h}dt) \rangle = \\ - \nabla \cdot (\rho(a - K\mathbf{h}))dt - \langle \nabla \cdot (\rho K^\top), dz^\dagger \rangle + \nabla \cdot (\nabla \cdot (\rho K \Gamma K^\top))dt. \end{aligned}$$

Equating the two terms involving the data  $z^\dagger$  shows immediately that  $K(v; \rho)$  has to satisfy the (vector-valued) PDE (3.27). From this, equating the terms that do not involve the data  $z^\dagger$ , it follows that  $a(v; \rho)$  has to satisfy

$$\begin{aligned} \nabla \cdot (\rho a) &= \nabla \cdot (\nabla \cdot (\rho K \Gamma K^\top)) + \nabla \cdot (\rho K(\mathbf{h} - \mathbb{E}\mathbf{h})) \\ &= \nabla \cdot (\nabla \cdot (\rho K \Gamma K^\top)) - \nabla \cdot (K \Gamma \nabla \cdot (\rho K^\top)) \\ &= \nabla \cdot \left( \rho \left( \nabla \cdot (K \Gamma K^\top) - K \Gamma \nabla \cdot K^\top \right) \right). \end{aligned}$$

A natural choice for  $a$  is provided by asking that the term on which the divergence acts is zero. This yields

$$(3.31) \quad a = \nabla \cdot (K \Gamma K^\top) - K \Gamma \nabla \cdot K^\top,$$

a solution for  $a$  with no explicit dependence on  $\rho$ ; note, however, that  $a$  does depend on  $\rho$  implicitly through the dependence of  $K$  on  $\rho$ .

With these choices of  $a, K$ , and applying the split-step principle so that the mean-field dynamics are consistent with (3.18) rather than (5), we obtain a version of the *feedback particle filter*; in particular we find the equation in its stochastic mean-field formulation given by (3.28) where  $K = K(v; \rho)$  solves (3.27) and  $\rho$  evolves according to the Kushner-Stratonovich equation (3.18), an equation which also defines the law of  $v$ . ■

**Remark 3.8.** There is an interesting interpretation of the contribution  $a$  to the drift term in (3.28): it is simply the Itô-to-Stratonovich-like correction with regard to the  $v$ -dependence in  $K(v; \rho)$ ; however there is a subtlety that the equation for  $\rho$  itself depends on the data  $z^\dagger$  and the correction does not account for the  $\rho$ -dependence of  $K(v; \rho)$  – the Stratonovich correction is only with respect to  $v$ -dependence of the drift; an Itô interpretation is retained with respect to the  $\rho$  dependence. We refer to Appendix 9.2 for an in-depth discussion concerning this unusual form of stochastic integration. In that section we also derive the full Stratonovich correction (with respect to both  $v$  and  $\rho$  dependence) of the exact mean-field model. ■

**Remark 3.9.** The mean field equations (3.28) require a gain  $K(v; \rho)$  which satisfies (3.27). Let  $\mathbb{E}$  denote expectation with respect to random variable  $v$  distributed according to probability measure with density  $\rho$ . Using appropriately regular test functions  $\psi : \mathbb{R}^{d_v} \rightarrow \mathbb{R}^{d_v}$ , chosen to have mean-zero under  $\mathbb{E}$ , equation (3.27) can be rephrased in the weak form <sup>13</sup>

$$(3.32) \quad \mathbb{E} \left( K^\top \nabla \psi \right) = \Gamma^{-1} C^h \psi;$$

<sup>13</sup>Recall that the conventions from continuum mechanics that we use to define the divergence and gradient of vector fields are discussed in the bibliography Subsection 3.7.

here  $C^{h\psi}$  denotes the covariance between  $h$  under  $\mathbb{E}$  and, in what follows, we also let  $C^{vh}$  denote covariance between  $v$  and  $h$ .

The particular choice  $\psi(v) = v - \mathbb{E}v$  leads to

$$\mathbb{E}K = C^{vh}\Gamma^{-1}.$$

This relation will be central to the subsequent discussion concerning second order transport methods in continuous time. Note, in particular, that it can be satisfied by making the *constant gain* ansatz that  $K$  is independent of  $v$  and is then given by  $K = C^{vh}\Gamma^{-1}$ , as derived for the Gaussian projected filter in Remark 3.5. More generally speaking, we note that (3.32) is amenable to numerical approximations. This will be discussed further in Subsection 3.6.1 below. ■

We close this subsection with the mean field formulation using deterministic innovations:

$$(3.33) \quad dv = f(v)dt + \sqrt{\Sigma}dW + \nabla \cdot (K\Gamma K^\top)dt - K\Gamma\nabla \cdot K^\top dt + K \left( dz^\dagger - \frac{1}{2}(h + \mathbb{E}h)dt \right),$$

where  $z^\dagger$  is given by (3.8). The relationship between this equation and (3.28), is analogous to the relationship between innovation terms (2.51) and (2.15) already encountered in the discrete time setting.

**3.5.2. Second Order Transport – Stochastic Case.** Recall that, in the discrete-time setting, there are an uncountable set of maps which effect approximate transport, in the sense of matching the first and second order statistics of the analysis map, using either stochastic or deterministic models. These are elucidated in Appendix 8. We, however, concentrated in the main text on a handful of examples. In this and the next subsection we study continuous time analogs of some of these examples, starting with the Kalman transport map (2.46) recalled here, and reformulated, for convenience:<sup>14</sup>

$$(3.34a) \quad \hat{v}_{n+1} = \Psi(v_n) + \mathbf{N}(0, \Sigma),$$

$$(3.34b) \quad \hat{y}_{n+1} = h(\hat{v}_{n+1}) + \mathbf{N}(0, \Gamma),$$

$$(3.34c) \quad v_{n+1} = \hat{v}_{n+1} + \hat{C}_{n+1}^{vh}(\hat{C}_{n+1}^{hh} + \Gamma)^{-1}(y_{n+1}^\dagger - \hat{y}_{n+1}).$$

We now apply the rescaling (3.1) to obtain, using (3.22a),

$$\begin{aligned} \hat{v}_{n+1} &= v_n + \Delta t f(v_n) + \sqrt{\Delta t} \mathbf{N}(0, \Sigma), \\ \hat{z}_{n+1} &= \hat{z}_n + \Delta t h(\hat{v}_{n+1}) + \sqrt{\Delta t} \mathbf{N}(0, \Gamma), \\ v_{n+1} &= \hat{v}_{n+1} + C_n^{vh}\Gamma^{-1}(\Delta z_{n+1}^\dagger - \Delta \hat{z}_{n+1}) + \mathcal{O}(\Delta t^{3/2}). \end{aligned}$$

The preceding calculation, leading to  $\mathcal{O}(\Delta t^{3/2})$  error, uses the fact that the noises entering the equations for  $\hat{v}_{n+1}$ ,  $\hat{z}_{n+1}$  and  $z_{n+1}^\dagger$  are independent. Taking the continuous time limit we

---

<sup>14</sup>The notation for the first two equations, which we use variants of in what follows, is shorthand for the first two equations appearing in (2.14), together with the assumptions detailed following those equations. Thus we use  $\mathbf{N}(0, \Sigma)$  to denote an i.i.d. realization from the stated Gaussian distribution, and similarly for other variables.

obtain

$$(3.35a) \quad dv = f(v)dt + \sqrt{\Sigma}dW + C^{vh}\Gamma^{-1}(dz^\dagger - d\hat{z}),$$

$$(3.35b) \quad d\hat{z} = h(v)dt + \sqrt{\Gamma}dB.$$

Again  $W, B$  are independent unit Brownian motions of appropriate dimensions and  $z^\dagger$  is given by (3.8).

*Remark 3.10.* Note the recurrence of the continuous time gain  $K$  first identified in Remark 3.5. We have derived the mean field equations (3.35) from the associated stochastic discrete time formulation (3.34). However there is another way to derive them. If we make the assumption that the gain  $K = K(\rho)$  is independent of  $v$  then the equations (3.35) follow directly from the general framework (3.28) if (3.9) is invoked. This is because both divergence terms drop out in (3.28) if  $K$  is independent of  $v$ , and (3.9) simply gives  $K = C^{vh}\Gamma^{-1}$ . ■

**3.5.3. Second Order Transport – Deterministic Case.** We may apply a similar analysis to (2.46), rewritten and reformulated here for convenience:

$$\begin{aligned} \hat{v}_{n+1} &= \Psi(v_n) + \mathbf{N}(0, \Sigma), \quad \hat{h}_{n+1} = h(\hat{v}_{n+1}), \\ v_{n+1} &= \hat{v}_{n+1} - \tilde{K}_n(\hat{h}_{n+1} - \mathbb{E}\hat{h}_{n+1}) + K_n(y_{n+1}^\dagger - \mathbb{E}\hat{h}_{n+1}), \end{aligned}$$

where

$$K_n = \hat{C}_{n+1}^{vh} \left( \hat{C}_{n+1}^{hh} + \Gamma \right)^{-1}, \quad \tilde{K}_n = \hat{C}_{n+1}^{vh} \left( (\hat{C}_{n+1}^{hh} + \Gamma) + \Gamma^{1/2}(\hat{C}_{n+1}^{hh} + \Gamma)^{1/2} \right)^{-1}.$$

Applying the rescalings (3.1) gives

$$\begin{aligned} \hat{v}_{n+1} &= v_n + \Delta t f(v_n) + \sqrt{\Delta t} \mathbf{N}(0, \Sigma), \\ v_{n+1} &= \hat{v}_{n+1} + C_n^{vh} \Gamma^{-1} \left( \Delta z_{n+1}^\dagger - \frac{1}{2} (h(\hat{v}_{n+1}) + \mathbb{E}h(\hat{v}_{n+1})) \right) + \mathcal{O}(\Delta t^2), \end{aligned}$$

where we have used

$$K_n = C_n^{vh} \Gamma^{-1} + \mathcal{O}(\Delta t^{3/2}), \quad \tilde{K}_n = \frac{1}{2} C_n^{vh} \Gamma^{-1} + \mathcal{O}(\Delta t^{3/2}).$$

Taking the continuous time limit we obtain

$$(3.36) \quad dv = f(v)dt + \sqrt{\Sigma}dW + C^{vh}\Gamma^{-1} \left( dz^\dagger - \frac{1}{2} (h(v) + \mathbb{E}h(v))dt \right),$$

where, once again,  $z^\dagger$  is given by (3.8).

These mean field equations can also be derived directly from the general mean field equation (3.33), assuming a deterministic innovation, invoking the constant gain approximation  $K = K(\rho)$  and using (3.9). The reasoning is similar to that in Remark 3.10.

### 3.5.4. Mean Field Formulation of the Kalman-Bucy Filter.

**Theorem 3.11.** *Assume that  $\Gamma \succ 0$  and consider the evolution of random variable  $v$  initialized at a Gaussian and satisfying*

$$\begin{aligned} (3.37a) \quad & dv = Fvdt + \sqrt{\Sigma}dW + CH^\top \Gamma^{-1}(dz^\dagger - d\hat{z}), \\ (3.37b) \quad & d\hat{z} = Hvd t + \sqrt{\Gamma}dB, \end{aligned}$$

where  $C$  is the covariance of  $v$  and where  $z^\dagger$  is given by (3.24). Then the mean and covariance of  $v$  satisfy equations (3.25).

*Proof.* We consider the setting where  $f(\cdot) = F\cdot$  and  $h(\cdot) = H\cdot$  with  $F$  and  $H$  as defined in (3.1). The mean field models become exact in this setting and have mean and covariance satisfying (3.25). With this in mind we note that under the linearity assumptions (3.35) gives (3.37). ■

Similar considerations, starting at (3.36), give the following variant of the preceding theorem:

**Theorem 3.12.** *Assume that  $\Gamma \succ 0$  and consider the evolution of random variable  $v$  initialized at a Gaussian and satisfying*

$$(3.38) \quad dv = Fvdt + \sqrt{\Sigma}dW + CH^\top \Gamma^{-1}\left(dz^\dagger - \frac{1}{2}H(v+m)dt\right),$$

where  $(m, C)$  are the mean and covariance of  $v$  and where  $z^\dagger$  is given by (3.24). Then the mean and covariance of  $v$  satisfy equations (3.25).

**3.6. Ensemble Kalman Methods.** We now discuss several particle approximations to the mean field equations derived in the preceding subsections. We start with the mean field equations (3.28), based on perfect transport, before considering particle approximations for time continuous approximate transport formulations. Throughout this subsection  $z^\dagger$  is given by (3.24).

**3.6.1. Perfect Particle Filters.** As in Subsection 2.6.1 we define  $J := \{1, \dots, J\}$ . The desired approximation to the mean field model (3.28) evolves particle ensemble  $\{v^{(j)}\}_{j \in J}$  and its associated empirical measure

$$(3.39) \quad \mu^J(t) = \frac{1}{J} \sum_{j=1}^J \delta_{v^{(j)}}$$

according to the interacting particle system

$$\begin{aligned} (3.40a) \quad & dv^{(j)} = f(v^{(j)})dt + a^{(j)}dt + \sqrt{\Sigma}dW^{(j)} + K^{(j)}(dz^\dagger - d\hat{z}^{(j)}), \\ (3.40b) \quad & d\hat{z}^{(j)} = h(v^{(j)})dt + \sqrt{\Gamma}dB^{(j)}, \end{aligned}$$

where  $z^\dagger$  is given by (3.8) and the  $\{W^{(j)}\}_{j \in J}$  and  $\{B^{(j)}\}_{j \in J}$  are mutually independent collections of i.i.d. Brownian motions in  $\mathbb{R}^{d_v}$  and  $\mathbb{R}^{d_y}$  respectively. The interaction between the

particles arises from the gain matrices

$$(3.41) \quad K^{(j)} := K^J(v^{(j)}; \mu^J),$$

$j \in J$ , where the matrix valued function  $K^J$  approximates the solution  $K$  of (3.27); the drift term  $a^{(j)}$  is defined by (3.31) with  $K(v)$  replaced by  $K^J(v; \mu^J)$  and then evaluated at  $v = v^{(j)}$ . To be self-consistent we require that the empirical measure (3.39) becomes the desired particle approximation for the law of  $v$  satisfying (3.28).

The key challenge for implementing a particle approximation of the mean field model (3.28) lies in the numerical approximation of (3.27), or its weak formulation (3.32). We start with the numerical approximation of the weak formulation (3.32). Let  $\mathcal{F}$  denote a space of vector-valued functions mapping  $\mathbb{R}^{d_v}$  into  $\mathbb{R}^d$  and assumed to have mean zero with respect to expectation  $\mathbb{E}$  under density  $\rho$ .<sup>15</sup> We make the ansatz that  $K^\top = \nabla \Psi$ , for some  $\Psi \in \mathcal{F}$ . Then (3.32) can be rewritten as

$$\mathbb{E}(\nabla \Psi \nabla \psi) = \Gamma^{-1} C^{\text{h}\psi},$$

assumed to hold for all  $\psi \in \mathcal{F}$ . In order to obtain the desired numerical approximation  $K^J$  let  $\mathbb{E}^J$  denote expectation with respect to the empirical measure (3.39) and consider  $(K^J)^\top = \nabla \Psi^J$  and

$$(3.42) \quad \mathbb{E}^J(\nabla \Psi^J \nabla \psi) = \Gamma^{-1} C^{\text{h}\psi}$$

with the correlation  $C^{\text{h}\psi}$  approximated by

$$C^{\text{h}\psi} = \mathbb{E}^J \left( (\text{h}(v) - \mathbb{E}^J \text{h}(v)) \otimes (\psi(v) - \mathbb{E}^J \psi(v)) \right).$$

The final step in the numerical approximation is to choose an appropriate finite dimensional subspace  $\mathcal{F}^L \subset \mathcal{F}$  of dimension  $L \ll J$  and to determine  $\Psi^J \in \mathcal{F}^L$  such that (3.42) holds for all  $\psi \in \mathcal{F}^L$ .

We return to the strong formulation (3.27) again making the ansatz  $K^\top = \nabla \Psi$  and giving rise to the equivalent formulation

$$\mathcal{L}_\rho \Psi = -\Gamma^{-1}(\text{h} - \mathbb{E}\text{h})$$

with differential operator  $\mathcal{L}_\rho$  defined by

$$\mathcal{L}_\rho \Psi = \rho^{-1} \nabla \cdot (\rho \nabla \Psi) = \nabla^2 \Psi + \nabla \Psi \nabla \log \rho.$$

Note that in the case of scalar observations,  $\mathcal{L}_\rho$  is the infinitesimal generator of a diffusion process with invariant density  $\rho$ ; in the vector case the same statement holds component-by-component. This fact may be used to approximate the action of  $\mathcal{L}_\rho$  via its heat semigroup, and this may be used as the basis for numerical approximations. See the bibliography Subsection 3.7 for references to the relevant literature.

---

<sup>15</sup>We will consider different choices for  $d$  but use the same notation for the space.

While we have discussed two general approaches to approximate the gain matrix in (3.41) numerically so far, we now return to the constant gain approximation; that is, we make  $K^J(\cdot; \mu^J)$  independent of its first argument so that  $K^{(j)} = K^J$  for some  $K^J$  depending only on  $\mu^J$ . In doing so we recover an empirical version of (3.21), the continuous time gain first identified in discussion of the Gaussian projected filter in Remark 3.5, and arising again in second order transport as discussed in Remark 3.10. In the current context the identification of  $K^J$  arises from (3.42), by making the choice  $\Psi(v) = (K^J)^\top (v - \mathbb{E}^J v)$  and  $\psi(v) = v - \mathbb{E}^J v$ . These choices result in

$$(3.43) \quad K^J = C^{vh} \Gamma^{-1},$$

where

$$C^{vh} = \mathbb{E}^J \left( (v - \mathbb{E}^J v) \otimes (h(v) - \mathbb{E}^J h(v)) \right).$$

Note that the constant gain approximation (3.43) also implies that the drift term  $a^{(j)}$  in (3.40) vanishes. We summarize numerical implementation details in the following two subsections.

**3.6.2. Stochastic Ensemble Kalman Filters.** We now consider the mean-field model (3.35) and its numerical approximation. Since the drift correction  $a$  does not appear here, the only significant difference to the interacting particle approximation (3.40) arises from the choice of the interaction term, that is,  $K^{(j)}$ , which is now independent of  $j$  and determined by (3.43). In summary, we obtain the following

$$(3.44a) \quad dv^{(j)} = f(v^{(j)})dt + \sqrt{\Sigma}dW^{(j)} + C^{vh}\Gamma^{-1}(dz^\dagger - d\hat{z}^{(j)}),$$

$$(3.44b) \quad d\hat{z}^{(j)} = h(v^{(j)})dt + \sqrt{\Gamma}dB^{(j)},$$

**3.6.3. Deterministic Ensemble Kalman Filters.** We make an empirical approximation of the mean-field model (3.36) as follows: for  $j \in J := \{1, \dots, J\}$  we consider

$$(3.45) \quad dv^{(j)} = f(v^{(j)})dt + \sqrt{\Sigma}dW^{(j)} + C^{vh}\Gamma^{-1} \left( dz^\dagger - \frac{1}{2}(h(v^{(j)}) + \mathbb{E}^J h(v))dt \right).$$

The notation is as in the preceding subsection and, in particular, the formula (3.39) again gives the particle approximation of the approximate filter; now the relevant approximate filter is defined by the distribution of (3.45).

**3.7. Bibliographical Notes.** This chapter is framed in the language of SDEs; see Evans (2012), Oksendal (2013) for background in this area. In passing from discrete to continuous time we often invoke ideas from the numerical solution of SDEs; see Kloeden & Platen (1991) and Higham (2001) for introductions to this area. The conventions from continuum mechanics, that we use to define the divergence and gradient of vector fields, are the same as those adopted, and described in detail, in Gonzalez & Stuart (2008), Gurtin (1982).

The Kalman-Bucy filter (Kalman & Bucy, 1961) contains what is perhaps the first systematic derivation and analysis of an algorithm for the incorporation of continuous time data

into estimation of a sample path of an SDE. Its extension to nonlinear and non-Gaussian distributions is provided by the Kushner-Stratonovich equation (3.18). An heuristic derivation of both the Kalman-Bucy filter as well as the Kushner-Stratonovich equation can be found in Jazwinski (2007) while Bain & Crisan (2008) covers the field of continuous time filtering in full detail.

The idea of Strang-splitting, which we use to derive the Kushner-Stratonovich equation, originates in Strang (1968); for an overview of splitting methods see McLachlan & Quispel (2002). Furthermore, we rely on robustness results for continuous time filtering (Clark & Crisan, 2005), which imply that smooth approximations  $z^{\dagger,\delta}$  to stochastic observations  $z^\dagger$  are justified and that the order of taking limits  $\Delta t \rightarrow 0$  and  $\delta \rightarrow 0$  can be accounted for by appropriate Stratonovich to Itô correction terms. An introduction to the required covariation formulae used in proof of Lemma 3.2 can be found in Eberle (2013). We note that robustness results do not carry over to associated mean field equations and filtering problems with correlated noise (Coghi *et al.*, 2021).

A mean field approach to the Kushner-Stratonovich equation (3.18) appeared first in the work of Crisan & Xiong (2010), which utilizes robustness results and smoothed data  $z^{\dagger,\delta}$  in the  $\delta \rightarrow 0$  limit. The mean field equations (3.36) were proposed in Yang *et al.* (2013) while the stochastic counterpart appeared first in Reich (2019). The mathematical relationship between the various mean field formulations has been analyzed in Pathiraja *et al.* (2021). The continuous time ensemble Kalman filter formulations (3.44) and (3.45) appeared first in Bergemann & Reich (2012). These formulations are based on earlier work on homotopy formulations of the Bayesian inference step by Bergemann & Reich (2010b) and Reich (2011). Rigorous derivation of continuous time ensemble Kalman filter formulations from their discrete time counterparts can be found in Lange & Stannat (2019), Lange & Stannat (2021), Blömker *et al.* (2018) and Blömker *et al.* (2021). Derivation and analysis of the properties of continuous time limits in the context of solving inverse problems may be found in Schillings & Stuart (2017). Numerical time-stepping methods for continuous time ensemble Kalman filter formulations are analyzed in Amezcua *et al.* (2014).

The numerical approximation of the Kushner-Stratonovich equation (3.18) has a long history. The paper Crisan & Lyons (1999) demonstrated how (3.18) can be approximated by a particle method; this is a generalization of the bootstrap particle filter to continuous time Crisan *et al.* (1998). See also Bain & Crisan (2008) for a detailed discussion of alternative approximation techniques. The paper Hu *et al.* (2002) discussed solution of the unnormalized and linear version of the Kushner-Stratonovich equation known as the Zakai equation. Numerical implementations of the mean field equations (3.28) are discussed in Taghvaei *et al.* (2017) while Taghvaei *et al.* (2020) provides a detailed analysis of the diffusion map approximation discussed after (3.6.1). The constant gain approximation  $K = C^{vh}\Gamma$ , which corresponds to the ensemble Kalman filter, arises as a particular scaling limit from the diffusion map approach as discussed, for example, in Taghvaei *et al.* (2017). The papers Ding *et al.* (2020); Ding & Li (2021a,b) undertake a systematic analysis of the link between interacting particle systems and mean-field systems in continuous time, mostly focused on the solution of inverse problems; however the methods developed are more widely applicable. Similar to the stochastic ensemble Kalman filter, particle implementation (3.44) leads to undesirable correlations via the synthetic data  $\hat{z}^{(j)}$ , which appear both in the gain  $K^J = C^{vh}\Gamma^{-1}$  and the innovation term



$dI = dz^\dagger - d\hat{z}^{(j)}$  effectively giving rise to colored noise. These numerically induced correlations vanish in the limit  $J \rightarrow \infty$ .

Theoretical analysis of the continuous time 3DVAR algorithm (3.7) may be found in [Law et al. \(2012\)](#), [Blömker et al. \(2013\)](#), [Azouani et al. \(2014\)](#), [Gesho et al. \(2016\)](#), [Olson & Titi \(2003\)](#), [Mondaini & Titi \(2018\)](#) and [Larios & Pei \(2017\)](#). Well-posedness, stability, and accuracy results for the ensemble Kalman filter have been derived, for example, in [Kelly et al. \(2014\)](#), [de Wiljes et al. \(2018\)](#), [Del Moral & Tugaut \(2018\)](#), and [de Wiljes & Tong \(2020\)](#).

**4. Inverse Problems.** Inverse problems may be solved by using ideas from filtering in stochastic dynamical systems, by the application of ideas arising in ensemble Kalman methods, and by the conjunction of the two. The power of the resulting methods is that they are derivative-free, requiring the forward model only as a black box. After commencing, in Subsection 4.1, with definitions of the classical (optimization) and Bayesian (probabilistic) perspectives on the inverse problems, we proceed to study three approaches to inversion based on ideas from filtering and ensemble Kalman methodology. These are:

- In Subsection 4.2 we show how the Bayesian formulation of the inverse problem may be tackled by introducing a transport from prior to posterior, underpinned by a stochastic dynamical system with filtering distribution given by the posterior, at step  $N$ , when initiated at the prior, at step 0. Algorithms to approximate the filtering distribution may then be employed, leading to a variety of approaches to Bayesian inversion, and in particular to ensemble Kalman based filtering approaches to inversion.
- Subsection 4.3 establishes a connection between the Kalman type mean field equations from Subsection 4.2 and gradient descent methods used in optimization. In particular, continuous time Kalman mean field equations naturally lead to preconditioned mean field gradient descent formulations which enjoy the property of affine invariance. Furthermore, it is demonstrated that these mean field equations possess a gradient flow structure in the space of probability measures. This leads to a generalization of the well-known Wasserstein gradient flow structure, which we refer to as a *Kalman-Wasserstein* gradient flow. While these structures rely on an exact computation of gradients, an attractive feature of Kalman type gradient descent methods lies in their ability to approximate gradients using only evaluations of the forward problem, and no adjoint calculations. Such approximations can be justified via statistical linearization and are now used in a wide range of applications.
- Subsection 4.4 is based on finding partially and noisily observed stochastic dynamical systems with filtering distribution that is ergodic and delivers a solution of the inverse problem in statistical steady state; ensemble Kalman methods may then be iterated to find this statistical steady state. The starting point is a stochastic dynamical system for which the steady state of the filtering distribution is equal, for linear Gaussian inverse problems, to a Gaussian with mean given by a regularized least squares solution to the inverse problem, or with Gaussian equal to the posterior distribution. This property does not hold exactly in the nonlinear case, but the assumptions under which it does hold, namely linear and Gaussian structure, are precisely those under which the ensemble Kalman second-order transport filters are exact. It is thus self-consistent to apply ensemble Kalman methods to filter the stochastic dynamical system to solve



problems beyond the linear Gaussian setting, by studying large time asymptotic behavior of the filtering distribution.

Throughout these three subsections we present ideas based on the road-map of Figure 1.1. Furthermore in each subsection we study both discrete and continuous time; the latter is useful for insight whilst the former provides the basis for practical algorithms. Since Sections 2 and 3 show in detail how to derive a variety of ensemble Kalman methods from mean-field models based on second order transport, the focus of the work in this section is on: a) the identification of appropriate dynamical systems with filtering distribution linked to the inverse problem; b) the properties of mean-field models derived from the filtering problem arising from the dynamical systems; c) the derivation of other novel mean-field models arising from the concept of statistical linearization. Once mean-field models have been identified in b) and c), application of ideas from Sections 2 and 3 is straightforward. However, in Subsection 4.5 we present applications of ensemble Kalman methodology to some specific mean-field models identified for inversion; and we include a simple illustrative example, building on the Lorenz '96 model considered earlier, to show the methods is use for inverse problems arising in parameter estimation for dynamical systems. We conclude in Subsection 4.6, containing bibliographic notes.

**4.1. Set-up.** Consider the inverse problem of finding unknown parameter  $u \in \mathbb{R}^{d_u}$  from data  $w \in \mathbb{R}^{d_w}$ , when  $w$  is related to  $u$  via the equation

$$(4.1) \quad \boxed{w = G(u) + \gamma.}$$

Here  $G : \mathbb{R}^{d_u} \rightarrow \mathbb{R}^{d_w}$  is the *forward model* and  $\gamma$  represents noise polluting the data. We assume that  $G$  is bounded on compact subsets of  $\mathbb{R}^{d_u}$ .

We consider the *Bayesian* approach to this inverse problem. To be concrete we assume as prior  $u \sim \mathcal{N}(m_0, C_0)$ , that  $\gamma \sim \mathcal{N}(0, \Gamma)$  and that  $u$  and  $\gamma$  are independent; thus the likelihood  $w|u \sim \mathcal{N}(G(u), \Gamma)$ . Throughout this section we assume that  $C_0 \succ 0$  and  $\Gamma \succ 0$ . We may then define

$$\begin{aligned} \Phi(u) &= \frac{1}{2} |w - G(u)|_{\Gamma}^2, \\ \Phi_R(u) &= \Phi(u) + \frac{1}{2} |u - m_0|_{C_0}^2. \end{aligned}$$

Under the stated assumptions, application of Bayes Theorem shows that the *posterior distribution* on  $u|w$  is measure  $\mu^w$  given by

$$(4.2a) \quad \boxed{\mu^w(du) = \frac{1}{\mathcal{Z}} \exp(-\Phi_R(u)) du,}$$

$$(4.2b) \quad \boxed{\mathcal{Z} = \int_{\mathbb{R}^{d_u}} \exp(-\Phi_R(u)) du.}$$

We will also discuss least-squares based optimization approaches to the inverse problem. These revolve around minimization of  $\Phi$  or  $\Phi_R$ . Minimizing  $\Phi$  is a *maximum likelihood approach*; minimizing  $\Phi_R$  is a *maximum a posteriori approach*. In the latter context it is useful

to observe that we may write

$$\Phi_R(u) = \frac{1}{2} |w_R - G_R(u)|_{\Gamma_R}^2,$$

where

$$(4.3) \quad w_R := \begin{pmatrix} w \\ m_0 \end{pmatrix}, \quad G_R(u) := \begin{pmatrix} G(u) \\ u \end{pmatrix}, \quad \Gamma_R := \begin{pmatrix} \Gamma & 0 \\ 0 & C_0 \end{pmatrix}.$$

Thus the regularized least squares problem associated with the inverse problem (4.1) may be viewed as an unregularized least squares problem arising from the modified inverse problem

$$w_R = G_R(u) + \gamma_R,$$

with  $\gamma_R \sim \mathbf{N}(0, \Gamma_R)$ .

In the case of linear  $G(\cdot) = L \cdot$  we define

$$(4.4) \quad L_R := \begin{pmatrix} L \\ I \end{pmatrix}$$

and note that, with this definition,  $G_R(\cdot) = L_R \cdot$ . Note also that, since  $C_0 \succ 0$ ,  $\Phi_R$  has a unique minimizer if  $G$  is linear. Since, in this linear setting,

$$\Phi_R(u) = \frac{1}{2} |w_R - L_R u|_{\Gamma_R}^2,$$

we deduce that the posterior covariance  $C_R$  of the Gaussian posterior  $\mu^w$  is given via its precision, the Hessian of  $\Phi_R$ :

$$(4.5) \quad C_R^{-1} = L_R^\top \Gamma_R^{-1} L_R.$$

The equilibrium mean  $m_R$  solves the *normal equations*

$$(4.6) \quad C_R^{-1} m_R = L_R^\top \Gamma_R^{-1} w_R.$$

The following subsections are devoted to the derivation and study of mean field methods, which are therefore the basis for ensemble Kalman methods, to sample from  $\mu^w$ , or to study the related least squares optimization problems of minimizing  $\Phi(\cdot)$  or  $\Phi_R(\cdot)$ .

**4.2. Transporting Prior To Posterior.** The basic idea used in this subsection, to address the solution of inverse problems, is rooted in a sequential formulation of Bayesian inference. To understand this, define for integer  $N > 1$ ,

$$(4.7) \quad \Phi_{R,n}(u) = \frac{1}{N} \sum_{j=1}^n \Phi(u) + \frac{1}{2} |u - m_0|_{C_0}^2,$$

noting that  $\Phi_{R,N}(u) = \Phi_R(u)$ . Now consider the sequence  $\mu_n$  of probability measures with negative log density given (up to an additive constant with respect to variation of  $u$ ) by

$\Phi_{R,n}(u)$ . Then the Bayesian inference problem (4.2) can be reformulated as a sequence of  $N$  Bayesian inference steps where the prior  $\mu_n$  is morphed into posterior  $\mu_{n+1}$  using the data likelihood  $\exp(-\Phi(u)/N)$  in each step:

$$\mu_{n+1}(du) \propto \exp\left(-\frac{1}{N}\Phi(u)\right)\mu_n(du).$$

The initial prior is set to  $\mu_0 = \mathbf{N}(m_0, C_0)$  and the  $N^{\text{th}}$  posterior  $\mu_N$  delivers the desired Bayesian solution to the inverse problem, given in (4.2). A variant on this idea is to morph from prior to posterior by (possibly artificially) considering the data  $w$  as sequentially acquired and incrementally including components of the data at each step  $n$ .

These sequential formulations of Bayesian inversion are well known and have, for example, been exploited in the use of sequential Monte Carlo methods for Bayesian inference; see Subsection 4.6 for details. However these sequential Monte Carlo methods do not always scale well to high dimensions, as for state estimation. Consequently ensemble Kalman variants of them have an important place in the field. In the following subsections we use (4.7) as the basis for ensemble Kalman filtering frameworks in discrete time, and subsequently (in the limit  $N \rightarrow \infty$ ) in continuous time.

**4.2.1. Bayesian Inversion Using Discrete Time Filtering.** Consider the combined state-observation system in the form, for  $n \in \{0, \dots, N-1\}$ ,

(4.8a)

$$u_{n+1} = u_n,$$

(4.8b)

$$w_{n+1} = G(u_{n+1}) + \frac{1}{\sqrt{\Delta t}}\gamma_{n+1},$$

where  $\{\gamma_{n+1}\}_{n=0}^{N-1}$  is an i.i.d. sequence with variance  $\mathbf{N}(0, \Gamma)$ . It is intuitive that, if  $N\Delta t = 1$ ,  $u_0 \sim \mathbf{N}(m_0, C_0)$  and  $w_{n+1} = w$  for all  $n \in \{0, \dots, N-1\}$ , then  $u_N$  conditioned on  $\{w_{n+1}\}_{n=0}^{N-1}$  is distributed as  $\mu^w$ . This follows since use of (4.8b) for  $n \in \{0, \dots, N-1\}$  corresponds to making  $N$  independent noisy observations of  $G(u_0)$ , all with noise variance  $\Delta t^{-1}\Gamma$ ; this is statistically equivalent to a single noisy observation of  $G(u_0)$  with noise variance  $\Gamma$ . Since  $u_0$  is initialized as  $\mathbf{N}(m_0, C_0)$  (the prior) the problem reduces to the Bayesian inverse problem for  $u|w$ .

This intuition may be substantiated using the discussion above, following equation (4.7). We prove the desired result but, before doing so, and in order to avail ourselves of the results from Sections 2 and 3, we rescale the observation equation in (4.8) to obtain

(4.9a)

$$u_{n+1} = u_n,$$

(4.9b)

$$y_{n+1} = \Delta t G(u_{n+1}) + \eta_{n+1},$$

with  $\eta_{n+1} \sim \mathbf{N}(0, \Delta t \Gamma)$  and  $y_{n+1} = \Delta t w_{n+1}$ . Let  $Y_n^\dagger = \{y_\ell\}_{\ell=1}^n$ . We may then show the following:

**Theorem 4.1.** *Assume that  $C_0 \succ 0$ ,  $\Gamma \succ 0$  and  $N\Delta t = 1$ . Assume also that  $u_0 \sim \mathbf{N}(m_0, C_0)$  and  $\eta_{n+1} \sim \mathbf{N}(0, \Delta t \Gamma)$ ; furthermore, assume that  $\{\eta_n\}_{n=1}^N$  forms an i.i.d. sequence, independent of  $u_0$ . Then  $\mu_N$ , the law of  $u_N|Y_N^\dagger$ , is equal to the posterior distribution  $\mu^w$  if the data is chosen as  $y_n = \Delta t w$ , for  $n \in \{1, \dots, N\}$ .*

*Proof.* Let  $\mu_n$  be the law of  $u_n|Y_n^\dagger$ . Since (in the notation of Section 2)  $\hat{\mu}_{n+1} = \mu_n$  we see that the mapping  $\mu_n$  to  $\mu_{n+1}$  is simply given by Bayes theorem:  $\mu_{n+1} = L_n(\mu_n)$ . This observation yields the identity, expressed in terms of  $\rho_n$  the Lebesgue density of measure  $\mu_n$ :

$$\begin{aligned} \log \rho_{n+1} - \log \rho_n &= -\frac{1}{2\Delta t} |y_n - \Delta t G(u)|_\Gamma^2 + \text{const}, \\ &= -\frac{\Delta t}{2} |w - G(u)|_\Gamma^2 + \text{const}. \end{aligned}$$

Summing over  $n \in \{0, \dots, N-1\}$ , using the fact that

$$\log \rho_0 = -\frac{1}{2} |u - m_0|_{C_0}^2 + \text{const},$$

and exponentiating we obtain the desired result. We also deduce that

$$\log \rho_n = -\Phi_{R,n} + \text{const},$$

with  $\Phi_{R,n}$  given by (4.7). ■

Thus we may approach the problem of sampling from  $\mu^w$  by (approximately) solving the filtering problem for  $\mu_n$ , until discrete time  $n = N$ , using ensemble Kalman methods. To illustrate this idea we describe the Gaussian projected filter in this setting, and then the mean field model of Kalman transport form, both applied to the specific state-observation model (4.9); particle approximations of the mean field models lead to Kalman based algorithms for the inverse problem. We discuss both the discrete and continuous time settings and, to this end, we first study the continuous limit of (4.9) found by sending  $\Delta t \rightarrow 0$ , with  $N\Delta t = 1$  fixed.

**4.2.2. Bayesian Inversion Using Continuous Time Filtering.** The reparametrization (3.2a) yields the continuum limit of (4.9) in the form of the SDE

$$(4.10a)$$

$$du = 0,$$

$$(4.10b)$$

$$dz = G(u)dt + \sqrt{\Gamma}dB.$$

with  $B$  a unit Brownian motion in  $\mathbb{R}^{d_z}$ . We define  $Z^\dagger(t) = \{z^\dagger(s)\}_{0 \leq s \leq t}$ , and consider the filtering distribution for the random variable  $u(t)|Z^\dagger(t)$ . However there is a twist on the standard filtering setting: we are interested in the case where the data has constant derivative:  $dz^\dagger(t)/dt = w$ . Since the path  $z^\dagger$  has zero quadratic variation the probability distribution is found by setting  $z^\dagger(t) = tw$  within the Stratonovich formulation of the non-local evolution equation for the density. Referring to (3.16) we see that this yields the following evolution for density  $\rho(u, t)$  of  $u(t)|Z^\dagger(t)$ :

$$(4.11) \quad \partial_t \rho = \langle G - \mathbb{E}G, w \rangle_\Gamma \rho - \frac{1}{2} \left\{ |G|_\Gamma^2 - \mathbb{E} |G|_\Gamma^2 \right\} \rho.$$

Here  $\mathbb{E}$  denotes integration with respect to density  $\rho(\cdot, t)$  so that the equation is non-local with respect to variable  $u$ . This is the analogue of the Kushner-Stratonovich equation for the

filtering problem defined by (4.10), since the unconditioned variable  $u$  has trivial dynamics and since we are studying the case where the data has zero quadratic variation and is in fact differentiable.

We may then show the following:

**Theorem 4.2.** *Assume that  $C_0 \succ 0$ ,  $\Gamma \succ 0$  and  $u_0 \sim \mathbf{N}(m_0, C_0)$ . Let  $\mu(t)$  be the law of  $u(t)|Z^\dagger(t)$ , with data chosen as  $z^\dagger(t) = tw$ , for  $t \in (0, 1)$ . Then  $\mu(t)$  has density  $\rho(\cdot, t)$  satisfying (4.11), with solution given by the formulae*

$$(4.12a) \quad \rho(u, t) = \frac{1}{\mathcal{Z}(t)} \exp(-t\Phi(u)) \rho_0(u),$$

$$(4.12b) \quad \mathcal{Z}(t) = \int_{\mathbb{R}^{d_u}} \exp(-t\Phi(u)) \rho_0(u) du;$$

in particular  $\mu(1)$  is equal to the posterior distribution  $\mu^w$ .

*Proof.* Let  $\rho_0$  denote the probability density function of the prior  $\mathbf{N}(m_0, C_0)$ . Recall that  $\mu(t)$  has density given by equation (4.11) with initial condition  $\rho|_{t=0} = \rho_0$ . First note that (4.12b) gives

$$\frac{d\mathcal{Z}}{dt} = -\mathbb{E}\Phi \mathcal{Z}$$

and hence that (4.12a) gives

$$\begin{aligned} \partial_t \rho &= -(\Phi - \mathbb{E}\Phi) \rho, \\ &= (\langle w, G \rangle_\Gamma - \frac{1}{2}|G|_\Gamma^2) \rho - \mathbb{E}(\langle w, G \rangle_\Gamma - \frac{1}{2}|G|_\Gamma^2) \rho, \\ &= \langle G - \mathbb{E}G, w \rangle_\Gamma \rho - \frac{1}{2} \left\{ |G|_\Gamma^2 - \mathbb{E}|G|_\Gamma^2 \right\} \rho. \end{aligned}$$

Thus  $\rho$  given by (4.12) solves (4.11), and since (4.11) characterizes the law of  $u(t)|Z^\dagger(t)$  when  $\frac{dz^\dagger}{dt} = w$ , the result is proven. ■

**4.2.3. Gaussian Projected Filter: Discrete Time.** We now apply the ideas from Subsection 2.4, on the Gaussian projected filter in the general setting, to the specific setting of (4.2). Let  $\mathbb{E}$  denote expectation under  $u \sim \mathbf{N}(m_n, C_n)$  and define

$$(4.13a) \quad C_n^{uG} = \mathbb{E} \left( (u - \mathbb{E}u) \otimes (G(u) - \mathbb{E}G(u)) \right),$$

$$(4.13b) \quad C_n^{GG} = \mathbb{E} \left( (G(u) - \mathbb{E}G(u)) \otimes (G(u) - \mathbb{E}G(u)) \right).$$

Noting that prediction under (4.2a) is trivial it follows that the predicted mean and covariance satisfy  $\hat{m}_{n+1} = m_n$  and  $\hat{C}_{n+1} = C_n$ . Hence, using (2.31) in the specific setting of (4.2), yields

$$(4.14a) \quad m_{n+1} = m_n + \Delta t C_n^{uG} (\Gamma + \Delta t C_n^{GG})^{-1} (w - \mathbb{E}G(u)),$$

$$(4.14b) \quad C_{n+1} = C_n - \Delta t C_n^{uG} (\Gamma + \Delta t C_n^{GG})^{-1} (C_n^{uG})^\top.$$

Note that the difference between the data  $w$  and the mean of  $G(u)$  under the Gaussian at step  $n$  acts as a forcing term in the evolution of the mean from  $n$  to  $n+1$ , promoting a Gaussian which agrees with the data. This forcing term is weighted by covariance information. The covariance of the Gaussian projected filter decreases from step to step since  $\langle u, C_{n+1}u \rangle \leq \langle u, C_n u \rangle$  for all  $u \in \mathbb{R}^{d_u}$ ; this reflects the fact that more information is received at each step  $n \mapsto n+1$  as the unknown  $u$  is repeatedly observed.

In the setting of linear inverse problems, where  $G(u) = Lu$ , the equations reduce to

$$\begin{aligned} (4.15a) \quad & m_{n+1} = m_n + \Delta t C_n L^\top (\Gamma + \Delta t L C_n L^\top)^{-1} (w - L m_n), \\ (4.15b) \quad & C_{n+1} = C_n - \Delta t C_n L^\top (\Gamma + \Delta t L C_n L^\top)^{-1} L C_n. \end{aligned}$$

We know from Section 2 that this is simply the Kalman filter applied to our specific linear and Gaussian dynamical system, and that it exactly solves the filtering problem:

**Lemma 4.3.** *Assume that  $C_0 \succ 0$ ,  $\Gamma \succ 0$  and that  $G(u) = Lu$  for  $L \in \mathbb{R}^{d_w \times d_u}$ . Then the posterior measure  $\mu^w$  is Gaussian with mean  $m_N$  and covariance matrix  $C_N$  given by (4.15).*

*Proof.* Theorem 4.1 shows that, if  $w_n \equiv w$  for  $n \in \{1, \dots, N\}$ , then the filtering distribution for (4.8) at time  $N$  equals the posterior distribution  $\mu^w$ . Since  $G$  is linear this posterior distribution is Gaussian and the filtering distribution for (4.8) is Gaussian. In Section 2 we show that the Gaussian projected filter gives the exact filtering distribution in the linear Gaussian setting, and hence the desired result follows. ■

**4.2.4. Gaussian Projected Filter: Continuous Time.** To further elucidate the structure of Gaussian projected filtering for the inverse problem, we study its continuous time formulation from Subsection 3.4 when applied to the specific state-observation model (4.9), and its continuous time limit (4.10). Taking the limit  $\Delta t \rightarrow 0$  in (4.14) we obtain the following evolution equations for mean and covariance:

$$\begin{aligned} (4.16a) \quad & \frac{dm}{dt} = C^u G \Gamma^{-1} (w - \mathbb{E} G(u)) \\ (4.16b) \quad & \frac{dC}{dt} = -C^u G \Gamma^{-1} (C^u G)^\top, \\ (4.16c) \quad & C^u G = \mathbb{E} \left( (u - \mathbb{E} u) \otimes (G(u) - \mathbb{E} G(u)) \right) \end{aligned}$$

and in which all where expectations are computed under  $\mathbf{N}(m(t), C(t))$ .

We complete this subsection by solving equations (4.16) explicitly in the setting of linear  $G$ . Consider  $\rho$  solving the Kushner-Stratonovich equation (4.11), with solution given by (4.12). In the general linear setting we know that the Gaussian projected filter is exact. In the current inverse problem setting this leads to Lemma 4.4 below. For this we note that, in the linear setting  $G(u) = Lu$ , the Gaussian projected filter (4.16) becomes

$$\begin{aligned} (4.17a) \quad & \frac{dm}{dt} = C L^\top \Gamma^{-1} (w - L m) \\ (4.17b) \quad & \frac{dC}{dt} = -C L^\top \Gamma^{-1} L C, \\ (4.17c) \quad & C = \mathbb{E} \left( (u - \mathbb{E} u) \otimes (u - \mathbb{E} u) \right), \end{aligned}$$

and again all expectations are computed under  $N(m(t), C(t))$ .

**Lemma 4.4.** *Assume that  $C_0 \succ 0$ ,  $\Gamma \succ 0$  and that  $G(u) = Lu$  for  $L \in \mathbb{R}^{d_w \times d_u}$ . Then  $\rho$  solving equation (4.11) is given by the Gaussian  $N(m(t), C(t))$  where  $m(t), C(t)$  solve the Gaussian projected filter equations (4.17). In particular the posterior measure  $\mu^w$  is Gaussian and given by  $N(m(1), C(1))$ .*

*Proof.* From Theorem 4.2, and in particular equation (4.12), we see that, in the linear case  $G(\cdot) = L \cdot$ , the solution of (4.11) is given by

$$(4.18) \quad \rho(u, t) \propto \exp\left(-\frac{t}{2}|w - Lu|_\Gamma^2 - \frac{1}{2}|u - m_0|_{C_0}^2\right).$$

Completing the square shows that this density corresponds to Gaussian  $N(m(t), C(t))$  with mean and covariance satisfying

$$(4.19a) \quad C(t)^{-1}m(t) = tL^\top \Gamma^{-1}w + C_0^{-1}m_0,$$

$$(4.19b) \quad C(t)^{-1} = C_0^{-1} + tL^\top \Gamma^{-1}L.$$

Note that since  $C_0 \succ 0$  it follows that  $C_0^{-1} \succ 0$  and hence (4.19b) shows that, for all  $t \geq 0$ ,  $C(t)^{-1} \succ 0$  and hence that  $C(t) \succ 0$  for all  $t \geq 0$ ; hence  $C(t)$  is well-defined by (4.19b) and  $m(t)$  is well-defined by (4.19a). It simply remains to show that  $m(t)$  and  $C(t)$  given by these formulae solve (4.17) when  $m(0) = m_0$  and  $C(0) = C_0$ .

We thus turn our attention to the equations (4.17). Note that  $C(t)$  solving (4.17b) satisfies  $C(0) = C_0 \succ 0$ . Hence  $C(0)^{-1} \succ 0$ . Thus, by continuity,  $C(t)$  remains invertible for some positive interval of time  $t \in [0, \tau)$  and, on this interval, direct computation with (4.17b) shows that

$$(4.20) \quad \frac{dC^{-1}}{dt} = L^\top \Gamma^{-1}L.$$

From this it follows by integration that  $C^{-1}(t) \succeq C_0^{-1} \succ 0$  for all  $t$  and hence that we may take  $\tau = \infty$ . Furthermore, the integration also shows that the solution of (4.20), solving (4.17b), delivers (4.19b) as desired.

We then notice that, from (4.17a),

$$\begin{aligned} C^{-1} \frac{dm}{dt} &= L^\top \Gamma^{-1}w - L^\top \Gamma^{-1}Lm, \\ &= L^\top \Gamma^{-1}w - \frac{dC^{-1}}{dt}m. \end{aligned}$$

It follows that

$$\frac{d}{dt}(C^{-1}m) = L^\top \Gamma^{-1}w$$

and integration, together with use of the initial conditions, shows that (4.17a) delivers the desired identity (4.19a). ■

*Remark 4.5.* It is also possible to establish the preceding result by studying the discrete time problem and taking a limit. Recall that the solution  $\rho$  of (4.11) is given by (4.18) in the linear setting. By Theorem 4.2 we know that  $\rho(\cdot, 1)$  is the density of the posterior distribution. Furthermore, for any  $t > 0$ ,  $\rho(u, t)$  is the posterior distribution for the Bayesian inference problem with scaled likelihood function  $\exp(-\frac{t}{2}|w - Lu|_F^2)$ . The associated posterior mean  $m(t)$  and covariance matrix  $C(t)$  satisfy (4.19); application of the Woodbury matrix identity shows that

$$\begin{aligned} m(t) &= m_0 + C_0 L^\top (LC_0 L^\top + t^{-1} \Gamma)^{-1} (w - Lm_0), \\ C(t) &= C_0 - C_0 L^\top (LC_0 L^\top + t^{-1} \Gamma)^{-1} LC_0; \end{aligned}$$

these expressions also follow from the Kalman filter update formulae (2.34) with  $\Gamma$  being replaced by  $\Gamma/t$ , and identifications of the predictive distribution in (2.34) with the prior here, and observation operator  $H$  in (2.34) with  $L$  here. Furthermore, we may take  $\mathbf{N}(m(t), C(t))$  as prior and apply the scaled likelihood  $\exp(-\frac{\Delta t}{2}|w - Ly|_F^2)$  to obtain posterior  $\mathbf{N}(m(t + \Delta t), C(t + \Delta t))$  with associated Kalman update formula

$$\begin{aligned} m(t + \Delta t) &= m(t) + C(t) L^\top (LC(t) L^\top + \Delta t^{-1} \Gamma)^{-1} (w - Lm(t)), \\ C(t + \Delta t) &= C(t) - C(t) L^\top (LC(t) L^\top + \Delta t^{-1} \Gamma)^{-1} LC(t), \end{aligned}$$

again using (2.34). It simply remains to show that taking the limit  $\Delta t \rightarrow 0$  yields evolution equations (4.17), which indeed follow trivially from observing

$$C(t) L^\top (LC(t) L^\top + \Delta t^{-1} \Gamma)^{-1} = \Delta t C(t) L^\top \Gamma^{-1} + \mathcal{O}(\Delta t^2). \quad \blacksquare$$

**4.2.5. Kalman Transport: Discrete Time.** Recall that we introduce Gaussian projected filtering in Section 2 as a stepping stone to mean field dynamical systems. These mean field models in turn lead to ensemble Kalman methods through particle approximation. In this Section 4, devoted to inverse problems, we simply highlight use of one of the mean field models, namely the stochastic *Kalman transport* model. We leave details of particle approximations of it to the reader, to the brief discussions of the topic in Subsection 4.5 and to Appendix 6 for related pseudo code. The adaptation of deterministic Kalman transport filter models to inverse problems is briefly discussed in Subsection 4.2.7 below.

Employing the state-observation model (4.9) within (2.46) we obtain the mean-field dynamical system, for i.i.d. unit Gaussian sequence  $\{\xi_n\}$  in  $\mathbb{R}^{d_w}$ ,

$$\begin{aligned} (4.21a) \quad & u_{n+1} = u_n + \Delta t C_n^{uG} (\Delta t C_n^{GG} + \Gamma)^{-1} \left( w - G(u_n) - \sqrt{\frac{\Gamma}{\Delta t}} \xi_n \right), \\ (4.21b) \quad & C_n^{uG} = \mathbb{E} \left( (u_n - \mathbb{E} u_n) \otimes (G(u_n) - \mathbb{E} G(u_n)) \right), \\ (4.21c) \quad & C_n^{GG} = \mathbb{E} \left( (G(u_n) - \mathbb{E} G(u_n)) \otimes (G(u_n) - \mathbb{E} G(u_n)) \right). \end{aligned}$$

Note that, here, expectation  $\mathbb{E}$  is computed under the law of  $u_n$  itself. The ideas of Section 2 show that random variable  $u_N$  provides an approximation to the posterior distribution  $\mu^w$ , provided that  $u_0 \sim \mathbf{N}(m_0, C_0)$ , the prior distribution. More can be said in the linear case:



**Lemma 4.6.** Assume that  $C_0 \succ 0$  and  $\Gamma \succ 0$  and that  $G(u) = Lu$  for  $L \in \mathbb{R}^{d_w \times d_u}$ . Then the solution of the mean field model (4.21) satisfies  $u_N \sim \mu^w$ .

*Proof.* In the linear setting equation (4.21) defines a closed evolution in the set of Gaussian probability measures. Furthermore, some calculation confirms that the mean and covariance of  $u_N$  then coincide with the Gaussian projected filter, in this linear case, given by equations (4.15). Indeed, by taking the expectation under the law of  $u_n$  of (4.21a), it is readily checked that in the linear setting

$$(4.22) \quad m_{n+1} = m_n + \Delta t C_n L^\top (\Gamma + \Delta t L C_n L^\top)^{-1} (w - L m_n).$$

To obtain the evolution equation of the covariance, we first recall that

$$(4.23) \quad C_{n+1} = \mathbb{E} \left( (u_{n+1} - m_{n+1}) \otimes (u_{n+1} - m_{n+1}) \right).$$

Substituting into (4.23) the expression for  $u_{n+1}$ , given by (4.21a) in the linear setting, and the expression for  $m_{n+1}$ , given by (4.22), and then computing the expectation yields

$$(4.24) \quad C_{n+1} = C_n - \Delta t C_n L^\top (\Gamma + \Delta t L C_n L^\top)^{-1} L C_n.$$

Thus equations (4.22), (4.24) are identical to (4.15) and it follows from Lemma 4.3 that  $u_N \sim \mu^w$ . ■

**4.2.6. Kalman Transport: Continuous Time.** We now study the inverse problem using Kalman transport in continuous time. Upon taking the continuous time limit of (4.21) we formally obtain

(4.25a)

(4.25b)

(4.25c)

$$\begin{aligned} du &= C^{uG} \Gamma^{-1} (w dt - d\hat{z}), \\ d\hat{z} &= G(u) dt + \sqrt{\Gamma} dB, \\ C^{uG} &= \mathbb{E} \left( (u - \mathbb{E}u) \otimes (G(u) - \mathbb{E}G(u)) \right). \end{aligned}$$

Here  $B \in \mathbb{R}^{d_w}$  is a unit Brownian motion and expectation is under the law of  $u$  itself. The SDE (4.25) may also be seen as a consequence of (3.35) applied to the specific case of state-observation model (4.9). However, special care is required since the observations  $z^\dagger$  in Section 3 were assumed to have non vanishing quadratic variation while  $dz^\dagger/dt = w$  in this section.

To obtain further insight into this mean-field dynamical system we once again consider the linear setting:

**Lemma 4.7.** Assume that  $C_0 \succ 0$  and  $\Gamma \succ 0$ . Consider the SDE (4.25) in the setting where  $G(u) = Lu$  for matrix  $L \in \mathbb{R}^{d_w \times d_u}$ . Then  $u(1) \sim \mu^w$ .

*Proof.* The Gaussian projected filter is exact in the linear setting, by Lemma 4.4, and hence delivers the desired posterior at time  $t = 1$ , by Theorem 4.2. Thus it suffices to show that the mean and covariance of  $u$  from (4.25) satisfy the Gaussian projected filter in the linear setting; this is given by (4.17).

We first note that

$$du = CL^\top \Gamma^{-1} (w dt - Lu dt - \sqrt{\Gamma} dB)$$

where  $C$  is the covariance of  $u$  under its law. By the Itô formula,  $m = \mathbb{E}u$  satisfies (4.17a). It follows that  $e = u - m$  satisfies

$$de = -CL^\top \Gamma^{-1} Le dt - CL^\top \Gamma^{-1/2} dB.$$

A second use of the Itô formula shows that  $C = \mathbb{E}(e \otimes e)$  satisfies (4.17b). The proof is complete.  $\blacksquare$

**4.2.7. Non-Stochastic Transports.** We briefly summarize corresponding deterministic transport formulations, both in discrete and continuous time. Following the approximation (2.8), which holds in our case provided  $\Delta t$  is small enough, and choosing  $K_n$  as implicitly defined in (4.21), we obtain

$$u_{n+1} = u_n + \Delta t C_n^{uG} (\Delta t C_n^{GG} + \Gamma)^{-1} \left( w - \frac{1}{2} (G(u_n) + \mathbb{E}G(u_n)) \right).$$

Furthermore, taking the  $\Delta t \rightarrow 0$  limit results in the mean field ODE formulation

$$(4.26) \quad \frac{du}{dt} = C^{uG} \Gamma^{-1} \left( w - \frac{1}{2} (G(u) + \mathbb{E}G(u)) \right).$$

Analogously to Lemma 4.7 we have

**Lemma 4.8.** *Assume that  $C_0 \succ 0$  and  $\Gamma \succ 0$ . Consider the mean field model (4.26) in the setting where  $G(u) = Lu$  for matrix  $L \in \mathbb{R}^{d_w \times d_u}$ . Then  $u(1) \sim \mu^w$ .*

*Proof.* The Gaussian projected filter is exact in the linear setting, by Lemma 4.4, and hence delivers the desired posterior at time  $t = 1$ , by Theorem 4.2. Thus it suffices to show that the mean and covariance of  $u$  from (4.26) satisfy the Gaussian projected filter in the linear setting; this is given by (4.17).

We first note that the mean under (4.26) satisfies

$$\frac{dm}{dt} = CL^T \Gamma^{-1} (w - Lm),$$

which is (4.17a). Using this it also follows that

$$\frac{d}{dt}(u - m) = -\frac{1}{2} CL^T \Gamma^{-1} L(u - m)$$

from which it follows that the variance satisfies (4.17b).  $\blacksquare$

**4.3. Geometric Structure in Kalman Transport, Optimization and Sampling.** So far we have taken a Bayesian perspective on solving inverse problems, considering both discrete and continuous time transport approaches in Subsection 4.2. The methods were characterized by the requirement that either  $n = 1, \dots, N$  subject to  $N\Delta t = 1$  or  $t \in [0, 1]$ , and must be initialized at the prior. In this subsection, we lift these restrictions and consider the behavior of continuous time Kalman transport methods in the asymptotic limit  $t \rightarrow \infty$ , leading to algorithms which can be initialized freely. Analogous investigations could be conducted for the discrete time formulations with  $\Delta t$  fixed and iteration index  $N \rightarrow \infty$  and are left to the

reader; furthermore the following Subsection 4.4 also covers discrete time methods based on iterating to infinity.

We show that Kalman transport methods, when viewed from such an asymptotic perspective, are closely related to gradient descent methods for optimization. However, the resulting methodologies lead to new perspectives: firstly, Kalman transport methods possess the property of *affine invariance* leading, for linear inverse problems, to methods with convergence rate that is independent of the conditioning of the problem; second, they constitute mean field equations and give rise to a novel gradient flow structure in the space of probability measures; third, the mean field equations are gradient free while still being closely related to gradient based optimization methods; and fourth the ideas can be generalized from optimization to sampling.

In Subsection 4.3.1 we study gradient descent, making connections to affine invariance via a mean field preconditioning. In Subsection 4.3.2 we show how *statistical linearization* can be used to define ensemble Kalman variants on numerous iterative methods for least squares problems. And in Subsection 4.3.3 we combine the two preceding subsections by introducing a derivative-free approximation of mean field preconditioned gradient flow, obtained by statistical linearization. In Subsection 4.3.4 we generalize the foregoing considerations from gradient descent to the Langevin equation, via development of Kalman-Wasserstein gradient flow in the space of probability measures.

**4.3.1. Gradient Flow Structures In Parameter Space.** We start by recalling some properties of standard gradient descent when applied to an objective function  $\Psi : \mathbb{R}^d \rightarrow \mathbb{R}^+$  and given symmetric positive-definite preconditioner  $B \in \mathbb{R}^{d_u \times d_u}$ :

$$(4.27) \quad \frac{du}{dt} = -B\nabla\Psi(u).$$

Note that, along solutions of (4.27),

$$\begin{aligned} \frac{d}{dt}\Psi(u) &= \left\langle \nabla\Psi(u), \frac{du}{dt} \right\rangle \\ &= -\left\langle B^{-1}\frac{du}{dt}, \frac{du}{dt} \right\rangle \\ &= -|B^{\frac{1}{2}}\nabla\Psi(u)|^2 \leq 0. \end{aligned}$$

In particular we highlight that

$$\frac{d}{dt}\Psi(u) = -\left|\frac{du}{dt}\right|_B^2.$$

Equation (4.27) is said to possess a gradient flow structure in parameter space  $\mathbb{R}^{d_u}$  because the vector field driving the evolution of  $u$  is tangential to the gradient of the objective function in a Euclidean metric weighted by  $B$ ; this is behind the non-increasing property of  $\Psi(u)$  along trajectories.

Consider now the affine transformation  $u \mapsto \tilde{u}$  given by

$$(4.28) \quad \tilde{u} = Au + b,$$

where  $A$  is an invertible matrix and  $b$  a vector. An important issue in all vector space optimization problems is the relative scaling of the components of the vector. A highly desirable feature of an algorithm is that it be insensitive to such scaling issues. This can be addressed by looking at differences between: (i) the algorithm for  $u$  rewritten in terms of  $\tilde{u}$  given by (4.28); (ii) the same algorithm applied directly to variable  $\tilde{u}$  optimizing  $\tilde{\Psi}(\tilde{u})$ , with the latter defined by

$$(4.29) \quad \tilde{\Psi}(\tilde{u}) = \Psi\left(A^{-1}(\tilde{u} - b)\right).$$

When these two ways of using reparametrization (4.28) lead to the same algorithm, for all choices of  $A, b$ , we say that the algorithm is *affine invariant*. Such algorithms are highly desirable as they are not sensitive to the scaling of the variables which, at the optimum, may be unknown *a priori*.

Applying the transformation (4.28) to (4.27) leads to

$$(4.30) \quad \frac{d\tilde{u}}{dt} = -AB\nabla\Psi\left(A^{-1}(\tilde{u} - b)\right),$$

the descent approach underlying algorithm viewed as in (i). In contrast, applying the same gradient descent to  $\tilde{\Psi}$  given by (4.29), leads to the the descent approach underlying algorithms viewed as in (ii):

$$(4.31) \quad \frac{d\tilde{u}}{dt} = -BA^{-\top}\nabla\Psi\left(A^{-1}(\tilde{u} - b)\right).$$

The two equations (4.30), (4.31) only agree if

$$AB = BA^{-\top}$$

and such an identity cannot hold for all  $A$ , for a fixed  $B$ . Thus the basic gradient descent (4.27) is not affine invariant. However it is a remarkable fact that, by generalizing (4.27) to allow for mean-field dependence, we can achieve affine invariance.

To this end consider the mean-field generalization of (4.27)

$$(4.32) \quad \frac{du}{dt} = -B(\rho)\nabla\Psi(u),$$

where  $\rho(\cdot, t)$  is the probability density function associated with the law of  $u$ , assuming that  $u$  is initialized from probability density function  $\rho_0(\cdot)$ . If we assume that  $B(\cdot)$  is positive-definite symmetric for all possible input densities, then similar arguments to before show that  $\Psi(u)$  is non-increasing along trajectories of (4.32). Furthermore similar arguments to before show that the algorithm is affine invariant if, for all invertible  $A \in \mathbb{R}^{d_u \times d_u}$ ,

$$AB(\rho) = B(\tilde{\rho})A^{-\top},$$

where  $\tilde{\rho}$  is the density of  $\tilde{u}$  related to  $u$ , with density  $\rho$ , by (4.28). This identity holds if  $B(\cdot)$  is chosen to be the covariance associated with its argument. We have thus discovered the affine

invariant mean field gradient descent

$$(4.33) \quad \boxed{\frac{du}{dt} = -C\nabla\Psi(u),}$$

where  $C$  is the covariance operator under the law of  $u(t)$  and  $u(0)$  is chosen at random from probability measure with density  $\rho_0$ .

Algorithms based on solving (4.33) are not themselves ensemble Kalman methods, although we have drawn inspiration from the power of mean field methods to motivate the approach. In the next subsection we introduce the idea of statistical linearization, leading to a variety of ensemble Kalman methods for optimization; and in the subsection following it we use this idea to approximate (4.33) by an ensemble Kalman version of gradient descent which obviates the need for computing adjoints of the forward model.

**4.3.2. Statistical Linearization.** A basic building block in the Gaussian projected filter and mean-field models for inverse problems that we have presented in Subsection 4.2 is the object

$$(4.34) \quad C^{uG} = \mathbb{E}\left((u - \mathbb{E}u) \otimes (G(u) - \mathbb{E}G(u))\right),$$

evolving in both discrete and continuous time, and its regularized analog arising when  $G_R$ , as defined in (4.3), is used in place of  $G$ . In a methodology based on exact properties only for first and second order statistics, it is natural that  $C^{uG}$  should appear when solving the inverse problem: the correlation between the parameter  $u$ , which we wish to estimate, and  $G(u)$  to which we have access when evaluated at a noise-polluted version of the true value, is a fundamental object. One way of understanding its role in algorithms for inversion is through the idea of statistical linearization, providing a link between ensemble methods and derivatives of the objective function. The underlying principle is that the differences used in ensemble methods, and covariances in particular, act as a surrogate for derivatives.

The expectation defining (4.34) is computed under the distribution of a Gaussian (for the Gaussian projected filter) or a more general distribution (mean-field model). To get some insight into the connection between ensemble methods and derivatives, we first consider the setting where  $u \sim \mathbf{N}(m, C)$ . Note that such  $u$  can be written as  $u = m + \sqrt{C}\xi$  where  $\xi \sim \mathbf{N}(0, I)$ . Thus (4.34) may be reformulated as

$$(4.35) \quad C^{uG} = \mathbb{E}\left((\sqrt{C}\xi) \otimes (G(m + \sqrt{C}\xi) - \mathbb{E}G(m + \sqrt{C}\xi))\right), \quad \xi \sim \mathbf{N}(0, I).$$

Using this we obtain the following connection between  $C^{uG}$  and derivatives of  $G$ :

**Lemma 4.9.** *Assume that the second derivative of  $G$  is small: there is  $\epsilon \ll 1$  such that*

$$\sup_{u \in \mathbb{R}^{d_u}} |D^2G(u)[\zeta, \zeta]| \leq \epsilon |\zeta|^2.$$

*Then  $C^{uG}$  given by (4.35) satisfies*

$$C^{uG} = CDG(m)^\top + \mathcal{O}(\epsilon).$$

Thus, when  $C^{-1} \succ \lambda I$ , for some  $\lambda > 0$  independent of  $\epsilon$ ,

$$(4.36) \quad DG(m) = (C^{uG})^\top C^{-1} + \mathcal{O}(\epsilon).$$

*Proof.* Note that

$$\begin{aligned} G(m + \sqrt{C}\xi) &= G(m) + DG(m)\sqrt{C}\xi + \mathcal{O}(\epsilon), \\ \mathbb{E}G(m + \sqrt{C}\xi) &= G(m) + \mathcal{O}(\epsilon). \end{aligned}$$

From (4.35)

$$C^{uG} = \mathbb{E}\left((\sqrt{C}\xi) \otimes (DG(m)\sqrt{C}\xi + \mathcal{O}(\epsilon))\right), \quad \xi \sim \mathcal{N}(0, I),$$

and the desired result follows. ■

*Remark 4.10.* Another perspective on the preceding lemma is via Stein's identity. This states that

$$C^{uG} = C(\mathbb{E}DG)^\top$$

for (4.35) when expectation is computed under a Gaussian measure  $\mathcal{N}(m, C)$ . The identity can be verified via integration by parts. Given the assumption stated in Lemma 4.9,  $\mathbb{E}DG(u) = DG(m) + \mathcal{O}(\epsilon)$  and the approximation result (4.36) also follows. ■

When  $D^2G$  is indeed small it is not unreasonable to use (4.36) as the basis for an approximation to  $DG(\cdot)$  at points in an  $\mathcal{O}(1)$  ball around the mean. We now take this idea further and consider random variable  $u \in \mathbb{R}^{d_u}$  (not necessarily Gaussian) and compute  $C$  and  $C^{uG}$  as covariance of  $u$  and cross-covariance of  $u$  with  $G(u)$  respectively. We refer to use of the approximation

$$(4.37) \quad DG(u) \approx (C^{uG})^\top C^{-1}, \quad \text{for all } u \in \mathbb{R}^{d_u},$$

as *statistical linearization*. The approximation can be invoked to replace the derivative within any standard optimization or sampling algorithm to solve the inverse problem (4.1). Doing so results in a mean-field algorithm; that algorithm in turn can be approximated by particle methods. This philosophy allows the conversion of standard single particle optimization and sampling algorithms for inverse problems, with dependence on the derivative of the forward model, into derivative-free interacting particle system optimizers and samplers. An important application of this methodological approach is in the development of ensemble Kalman approximations of Gauss-Newton and Levenberg-Marquadt algorithms; pointers to the literature will be given in the bibliography Subsection 4.6. We now turn to the use of statistical linearization in gradient descent, perhaps the most basic setting in which it can be used for optimization.

**4.3.3. Gradient Descent and Statistical Linearization.** We provide further insight into the statistical linearization approach from the previous subsection by applying it in the context of gradient descent. We consider the unregularized least squares function so that  $\Psi(u) = \Phi(u)$

in (4.27); but similar ideas may be developed in the regularized setting where  $\Psi(u) = \Phi_R(u)$ . In the unregularized setting

$$(4.38) \quad \nabla \Phi(u) = DG(u)^\top \Gamma^{-1}(G(u) - w),$$

and we obtain, from (4.27),

$$\frac{du}{dt} = DG(u)^\top \Gamma^{-1}(w - G(u)).$$

Similarly, the covariance preconditioned gradient flow (4.33) becomes

$$(4.39) \quad \frac{du}{dt} = CDG(u)^\top \Gamma^{-1}(w - G(u)),$$

We now approximate this equation using statistical linearization.

From (4.37) we deduce the equivalent (assuming  $C$  is invertible) approximation

$$CDG(u)^\top \approx C^{uG}, \quad \text{for all } u \in \mathbb{R}^{d_u}.$$

Combining this with (4.38) we obtain

$$(4.40) \quad C\nabla \Phi(u) \approx C^{uG} \Gamma^{-1}(G(u) - w).$$

Making this approximation in (4.39) gives the following ensemble Kalman approximation of mean field gradient descent:

$$(4.41) \quad \boxed{\frac{du}{dt} = C^{uG} \Gamma^{-1}(w - G(u)).}$$

*Remark 4.11.* We note that equation (4.41) is identical to (4.25) with the Brownian motion simply set to zero. This provides a new perspective on Kalman transport for inverse problems, namely that it may be thought of as a noisy version of an approximation of mean-field gradient descent based on statistical linearization; building on this idea we note that equation (4.26) may also be viewed as a different approximation of mean-field gradient descent, also using statistical linearization. Furthermore the Gaussian projected filter, in continuous time, has a related structure which is apparent from comparing (4.16) and (4.41).

It may be verified that the affine invariance of (4.33) is preserved under the statistical linearization ansatz and, hence, (4.25), (4.26) and (4.41) are also affine invariant. In fact, this property holds for all Kalman transport formulations from Subsection 4.2. ■

We now observe that statistical linearization, and (4.40) in particular, become exact for linear  $G(u) = Lu$ . In this setting we may hence study the asymptotic behavior of the mean field gradient descent model (4.33) by studying (4.26) or (4.41). To carry this out we study the deterministic continuous time Kalman transport formulation (4.26), noting that it delivers perfect transport in the linear setting. Furthermore, when initialized with  $u(0) \sim \mathcal{N}(m_0, C_0)$ ,

we know that  $u(t)$  is Gaussian distributed with mean  $m(t)$  and covariance matrix  $C(t)$  satisfying the modified Kalman formulae (4.5), by Lemma 4.8. If we assume that  $L$  is invertible and hence that the desired minimizer  $u^\dagger$  of  $\Phi$  is given by  $u^\dagger = L^{-1}w$  then (4.5) reduce to

$$(4.42a) \quad m(t) = m_0 - C_0 L^\top (L C_0 L^\top + t^{-1} \Gamma)^{-1} L (m_0 - u^\dagger),$$

$$(4.42b) \quad C(t) = C_0 - C_0 L^\top (L C_0 L^\top + t^{-1} \Gamma)^{-1} L C_0.$$

The following lemma characterizes the asymptotic behavior of the associated mean field equations as  $t \rightarrow \infty$ .

**Lemma 4.12.** *Assume that  $\Gamma \succ 0$ . Consider the mean-field ODE (4.26) and assume further that  $G(u) = Lu$  for invertible matrix  $L \in \mathbb{R}^{d_u \times d_y}$ , so that  $\Phi$  is given by*

$$\Phi_L(u) = \frac{1}{2} |Lu^\dagger - Lu|_\Gamma^2$$

with  $u^\dagger = L^{-1}w$ . Then the equation (4.26) for  $u(t)$  may be written in the form

$$(4.43) \quad \frac{du}{dt} = -CL^\top \Gamma^{-1} L \left( \frac{1}{2}(u + m) - u^\dagger \right),$$

where  $C$  is the covariance of  $u(t)$  and  $m$  its mean. Furthermore, if  $u(0)$  is Gaussian then  $u(t)$  is Gaussian with mean  $m(t)$  and covariance  $C(t)$  satisfying (4.42). Since  $B := L^\top \Gamma^{-1} L \succ 0$ ,  $u(t)$  converges to the mean  $m(t)$  at an algebraic rate  $t^{-1/2}$ :  $d(t) = u(t) - m(t)$ , satisfies

$$(4.44) \quad |B^{1/2}d(t)|^2 \leq \frac{1}{t} |B^{1/2}d(0)|^2.$$

The mean,  $m(t)$ , converges to the minimizer  $u^\dagger$  at an algebraic rate  $t^{-1}$ :

$$(4.45) \quad m(t) - u^\dagger = t^{-1} L^{-1} \Gamma (L C_0 L^\top + t^{-1} \Gamma)^{-1} L (m(0) - u^\dagger).$$

**Proof.** The mean  $m(t)$  satisfies (4.42a) and straightforward algebraic manipulations lead to (4.45). Furthermore, the mean field equation (4.43) and the corresponding evolution equation for the mean

$$\frac{dm}{dt} = -CL^\top \Gamma^{-1} L (m - u^\dagger)$$

imply that

$$\frac{d}{dt}(u - m) = -\frac{1}{2} CL^\top \Gamma^{-1} L (u - m).$$

Hence

$$(4.46) \quad \frac{d}{dt} |B^{1/2}d|^2 = -d^\top B C B d \leq -\frac{1}{t} |B^{1/2}d|^2,$$

where  $d = u - m$  and we have used

$$t^{-1} I \succ B^{1/2} C B^{1/2};$$



this last matrix inequality follows from (4.42b) and its equivalent form

$$C(t)^{-1} = C_0^{-1} + tB,$$

which may be established using the Woodbury matrix identity. The estimate (4.44) follows from the differential inequality (4.46) by integration. ■

*Remark 4.13.* The same algebraic rates also apply to the mean field gradient descent formulation (4.41). This algebraic rate of convergence is an undesirable feature of algorithms based on the mean field model (4.41); algorithms based on discretization of such continuous-time algorithms are not recommended in practice unless used in combination with stochastic approximations to the cost function  $\Psi(u)$  (*stochastic gradient descent*), or if used with adaptive time-stepping and a stopping criterion; see discussions in Subsection 4.6. However by considering a stochastic analogue of the methodology we arrive, in the next Subsection 4.3.4, at the mean field model (4.51); this has exponential convergence rates to the posterior. Furthermore in Subsection 4.4.1 we will also exhibit discrete-time algorithms for optimization which exhibit exponential convergence. ■

**4.3.4. Gradient Flow Structures in Spaces of Probability Measures.** In this subsection, we investigate the geometric properties of the mean field gradient descent equations (4.33) in some more detail. We assume that  $u(t)$  has smooth probability density  $\rho(u, t)$  for all  $t \geq 0$  and denote the manifold of all smooth probability density functions on  $\mathbb{R}^{d_u}$  by  $\mathcal{P}_+$ . Then  $\rho$  satisfies the Liouville equation

$$(4.47) \quad \partial_t \rho = \nabla \cdot (\rho C \nabla \Psi).$$

Note that the appearance of the covariance matrix  $C = \mathcal{C}(\rho)$  renders (4.47) a nonlinear and nonlocal partial differential equation on  $\mathcal{P}_+$ . We will show that the evolution of  $\rho$  on  $\mathcal{P}_+$  has gradient flow structure. In order to do so, we first need to identify the functional  $\mathcal{E}(\rho)$  on  $\mathcal{P}_+$  which is being minimized. In case of (4.33), this functional is simply

$$\mathcal{E}(\rho) = \int_{\mathbb{R}^{d_u}} \Psi(u) \rho(u) du,$$

namely the expected value of  $\Psi(u)$ . Note that the Fréchet derivative<sup>16</sup> of  $\mathcal{E}$  is given by

$$\frac{\delta \mathcal{E}}{\delta \rho} = \Psi.$$

Hence we can rewrite (4.47) as

$$(4.48) \quad \partial_t \rho = \nabla \cdot \left( \rho \mathcal{C}(\rho) \nabla \frac{\delta \mathcal{E}}{\delta \rho} \right).$$

The desired gradient flow structure on  $\mathcal{P}_+$  requires an appropriate metric tensor  $g_{\rho, \mathcal{C}} : T_\rho \mathcal{P}_+ \times T_\rho \mathcal{P}_+ \rightarrow \mathbb{R}$  on the tangent space  $T_\rho \mathcal{P}_+$  at  $\rho \in \mathcal{P}_+$ :

$$T_\rho \mathcal{P}_+ = \left\{ \sigma \in C^\infty(\mathbb{R}^{d_u}) : \int_{\mathbb{R}^{d_u}} \sigma du = 0 \right\}.$$

---

<sup>16</sup>Identified by writing  $\mathcal{E}(\rho + \sigma) - \mathcal{E}(\rho)$  as a linear operator acting on  $\sigma \in T_\rho \mathcal{P}_+$  plus higher order terms.

The metric tensor itself is defined by

$$g_{\rho, \mathcal{C}}(\sigma_1, \sigma_2) := \int_{\mathbb{R}^{d_u}} \langle \nabla \psi_1, \mathcal{C}(\rho) \nabla \psi_2 \rangle \rho \, du,$$

where  $\sigma_i = -\nabla \cdot (\rho \mathcal{C}(\rho) \nabla \psi_i) \in T_\rho \mathcal{P}_+$  for  $i = 1, 2$ .<sup>17</sup> The equation (4.48) takes gradient flow structure in  $(\mathcal{P}_+, g_{\rho, \mathcal{C}})$ :

$$(4.49) \quad \frac{d}{dt} \mathcal{E}(\rho) = -g_{\rho, \mathcal{C}}(\partial_t \rho, \partial_t \rho).$$

It is interesting to compare the gradient structure (4.49) on  $\mathcal{P}_+$  to the gradient flow structure (4.3.1) on  $\mathbb{R}^{d_u}$ . To establish (4.49) note that

$$\begin{aligned} \frac{d}{dt} \mathcal{E}(\rho) &= \int_{\mathbb{R}^{d_u}} \frac{\delta \mathcal{E}}{\delta \rho} \partial_t \rho \, du \\ &= - \int_{\mathbb{R}^{d_u}} \rho \left| \mathcal{C}(\rho)^{\frac{1}{2}} \nabla \frac{\delta \mathcal{E}}{\delta \rho} \right|^2 \, du \\ &= - \int_{\mathbb{R}^{d_u}} \langle \nabla \psi, \mathcal{C}(\rho) \nabla \psi \rangle \rho \, du \\ &= -g_{\rho, \mathcal{C}}(\sigma, \sigma), \end{aligned}$$

where

$$\sigma = -\nabla \cdot (\rho \mathcal{C}(\rho) \nabla \psi), \quad \psi = \frac{\delta \mathcal{E}}{\delta \rho}.$$

Thus  $\sigma = -\partial_t \rho$  and the gradient flow identity is established.

The established machinery is very powerful and demonstrates that any evolution equation of type (4.48) with appropriate potential  $\mathcal{E}$  induces a gradient flow on  $\mathcal{P}_+$ . A particularly significant example follows from the choice

$$\mathcal{E}(\rho) = \int (\Phi_R + \ln \rho) \rho \, du$$

with Fréchet derivative given by<sup>18</sup>

$$\frac{\delta \mathcal{E}}{\delta \rho} = \Phi_R + \ln \rho.$$

In this case the associated evolution equation (4.48) becomes

$$(4.50) \quad \partial_t \rho = \nabla \cdot (\rho \mathcal{C}(\rho) \nabla \Phi_R) + \nabla \cdot (\mathcal{C}(\rho) \nabla \rho).$$

---

<sup>17</sup>A precise mathematical treatment requires further assumptions on the considered set  $\mathcal{P}_+$  of probability functions ensuring that the required potentials  $\psi$  indeed exists for all  $\sigma \in T_\rho \mathcal{P}_+$ . See the bibliography for references and discussion of open questions in this area.

<sup>18</sup>Formal calculations give rise to an additional constant term which is irrelevant and in fact zero if the Fréchet derivative is computed using  $\sigma \in T_\rho \mathcal{P}_+$ .

The mean-field SDE model for which this is the nonlinear and nonlocal Fokker-Planck equation is

$$(4.51) \quad du = -C\nabla\Phi_R(u)dt + \sqrt{2C}dW,$$

where we reverted to the notation  $C$ , for the covariance, as used previously in all mean field models. Theory concerning this equation is contained in the following bibliography section. We note here that it may be verified that (4.51) is invariant under affine transformations of type (4.28) and that the posterior distribution  $\rho^w$  is stationary, that is,  $\rho = \rho^w$  leads to  $\partial_t \rho = 0$  in (4.50). Thus (4.51) provides an attractive generalization of standard Langevin dynamics for sampling from the posterior distribution; furthermore it may be approximated by statistical linearization to obtain a derivative-free methodology. For (4.50) the desired posterior distribution is approached only in the limit  $t \rightarrow \infty$ . The relative efficiency of methods based on this approach, in comparison with the transport methods considered in Subsection 4.2, depends on the nature of this convergence; the fact that it is exponential in many settings make the approach potentially competitive. However discrete time versions of the approach of iterating mean field models to infinity can exhibit greater competitiveness and are explored in the following subsection.

We conclude this subsection by noting that the Kalman-Wasserstein gradient flow structure for the Liouville and Fokker-Planck equations considered here is not maintained under statistical linearization: they are not of gradient descent type in  $\mathcal{P}_+$  unless  $G(u)$  is linear.

**4.4. Steady State Filtering Distribution and Inversion.** The transport of prior to posterior in  $N$  steps, or one time unit, the subject of Subsection 4.2, provides an attractive framework within which to derive algorithms for approximate Bayesian inversion from state estimation and filtering of a dynamical system. However it is a somewhat rigid approach, requiring specific initialization of the variable  $u_0$  at the prior; and it does not possess any strong stability property that might be used to control the errors arising from using second order, rather than exact, transport, or inexact initialization. On the other hand, Subsection 4.3 shows that Kalman-inspired methods may be used to solve optimization and sampling problems, which may be initialized arbitrarily but require iteration to infinity to address their respective goals. In this subsection we further explore the idea of iterating to infinity with Kalman methods. As in Subsection 4.2, the methods also employ state estimation and filtering of a dynamical system. However, instead of transporting an initial prior to the posterior at a fixed time (discrete or continuous), we instead seek an underlying partially and noisily observed dynamical system with filtering distribution that has as steady state a solution to the inverse problem; in brief we work in settings where the filtering distribution is ergodic and use the statistical steady state to extract information about the inverse problem.

Subsections 4.4.1 and 4.4.2 approach this problem from the optimization perspective on inversion, and provide an intuitive introduction to the use of ergodic filtering distributions. However the approach we adopt does not lead to affine invariant methods and so, in Subsections 4.4.3 and 4.4.4 we introduce a different filtering distribution. Identifying filtering distributions with statistical steady state which solves the inverse problem is difficult in general, and so we build the methodology by adopting the more limited goal of using a dynamical system which achieves this goal exactly in the linear Gaussian setting; we then deploy it

beyond the linear Gaussian setting. The approach is consistent with the use of second order transport, rather than exact transport, underlying the application of ensemble Kalman methods: second order transport is also exact only in the linear Gaussian setting, but is used beyond this setting. In the first two subsections concerned with optimization the underlying partially and noisily observed dynamical system used is, like (2.1) or (3.4), not of mean-field form. However, in the subsequent two subsections concerned with the Bayesian approach, the underlying partially and noisily observed dynamical system used is itself of mean-field form; indeed it is an unusual mean-field model that depends on its own filtering distribution and it is this fact that facilitates the derivation of an affine invariant methods. Note that in Sections 2 and 3 respectively, the underlying dynamical system ((2.1) or (3.4) respectively), to which ensemble methods are applied, was not of mean-field form: mean-field was only introduced to construct ensemble Kalman methods.

#### 4.4.1. Steady State Filtering Distribution and Classical Inversion: Discrete Time.

With the goal of solving least-squares based optimization problems using ideas from filtering, consider now the stochastic dynamical system

$$\begin{aligned} (4.52a) \quad & u_{n+1} = \alpha u_n + (1 - \alpha)r_0 + \xi_n, \\ (4.52b) \quad & w_{n+1} = G(u_{n+1}) + \eta_{n+1}. \end{aligned}$$

Here  $\alpha \in (0, 1]$ ,  $\xi_n \sim \mathbf{N}(0, \sigma' \Sigma)$ ,  $\sigma' \geq 0$  and  $\eta_{n+1} \sim \mathbf{N}(0, \gamma' \Gamma)$ ,  $\gamma' > 0$ ; we assume that  $\Sigma, \Gamma \succ 0$ . Unlike the transport setting of Subsection 4.2 we do not require that  $u_0$  is initialized at the prior, although this is a reasonable choice of initialization. Let  $W_n = \{w_\ell\}_{\ell=1}^n$  and consider the filtering distribution defined by random variable  $u_n | W_n$ . The following theorem provides motivation for the study of this distribution, and its limiting behavior as  $n \rightarrow \infty$ , to obtain information about the least squares optimization approach to the inverse problem.

**Lemma 4.14.** *Consider the filtering distribution  $u_n | W_n$  of (4.52), and assume that  $u_0$  is initialized at a Gaussian  $\mathbf{N}(m_0, C_0)$ .<sup>19</sup> Assume that  $C_0, \Gamma, \Sigma \succ 0$ ,  $\sigma' \geq 0$ ,  $\gamma' > 0$ , and  $\alpha \in (0, 1]$  and consider the setting where  $G(u) = Lu$  for matrix  $L \in \mathbb{R}^{d_w \times d_u}$ . Then the filtering distribution is Gaussian  $\mathbf{N}(m_n, C_n)$ . Furthermore, if  $w_n \equiv w$  then any positive-definite steady solution  $C_\infty$  of the covariance update equation satisfies*

$$(4.53a) \quad C_\infty^{-1} = \frac{1}{\gamma'} L^\top \Gamma^{-1} L + \hat{C}_\infty^{-1},$$

$$(4.53b) \quad \hat{C}_\infty = \alpha^2 C_\infty + \sigma' \Sigma,$$

where, note,  $\hat{C}_\infty$  is also positive-definite. Furthermore, the associated steady state mean  $m_\infty$  is the minimizer of the Tikhonov-Phillips regularized least squares functional  $\Phi_{TP}$  given by

$$\Phi_{TP}(m) := \frac{1}{2\gamma'} |w - Lm|_\Gamma^2 + \frac{1-\alpha}{2} |m - r_0|_{\hat{C}_\infty}^2.$$

---

<sup>19</sup>For simplicity of exposition we denote this as  $\mathbf{N}(m_0, C_0)$  but emphasize that here it need not be the prior distribution.

*Proof.* We first identify the update equations for  $(m_n, C_n)$ . Note that the predictive mean  $\hat{m}_{n+1}$  and covariance  $\hat{C}_{n+1}$  defined by (4.52a) satisfy

$$\begin{aligned}\hat{m}_{n+1} &= \alpha m_n + (1 - \alpha)r_0, \\ \hat{C}_{n+1} &= \alpha^2 C_n + \sigma' \Sigma.\end{aligned}$$

To find  $(m_{n+1}, C_{n+1})$  it is possible to simply use (2.34); however it is convenient to derive the formulae in a different form, using precisions rather than covariance. To this end we view the Gaussian  $\mathcal{N}(\hat{m}_{n+1}, \hat{C}_{n+1})$  as prior distribution for the linear inverse problem defined by (4.52b) with  $w_{n+1} = w$ . Note that the likelihood, since linear and Gaussian, is conjugate to the prior so that the posterior on  $u_{n+1}|W_{n+1}$  is Gaussian with mean and covariance  $(m_{n+1}, C_{n+1})$  which can be found by completing the square:

$$\begin{aligned}C_{n+1}^{-1} &= \frac{1}{\gamma'} L^\top \Gamma^{-1} L + \hat{C}_{n+1}^{-1}, \\ C_{n+1}^{-1} m_{n+1} &= \frac{1}{\gamma'} L^\top \Gamma^{-1} w + \hat{C}_{n+1}^{-1} \hat{m}_{n+1}.\end{aligned}$$

The equation satisfied by the steady state covariance  $C_\infty$  follows, along with the definition of  $\hat{C}_\infty$ . The steady state mean satisfies

$$C_\infty^{-1} m_\infty = \frac{1}{\gamma'} L^\top \Gamma^{-1} w + \hat{C}_\infty^{-1} (\alpha m_\infty + (1 - \alpha)r_0).$$

Using the equation (4.53a) to replace  $C_\infty$  by  $\hat{C}_\infty$  we may rewrite this as

$$\hat{C}_\infty^{-1} m_\infty = \frac{1}{\gamma'} L^\top \Gamma^{-1} (w - L m_\infty) + \hat{C}_\infty^{-1} (\alpha m_\infty + (1 - \alpha)r_0).$$

This in turn may be reorganized as

$$(1 - \alpha) \hat{C}_\infty^{-1} (m_\infty - r_0) = \frac{1}{\gamma'} L^\top \Gamma^{-1} (w - L m_\infty)$$

which is patently the equation found by setting the gradient of  $\Phi_{TP}$  to 0. Finally note that the Hessian of  $\Phi_{TP}$  is  $(1 - \alpha) \hat{C}_\infty^{-1} + \frac{1}{\gamma'} L^\top \Gamma^{-1} L \succ 0$ . Thus the critical point is indeed a minimizer as asserted. ■

*Remark 4.15.* Assume either that  $\alpha \in (0, 1)$  or that, if  $\alpha = 1$  then assume additionally that the range of  $G^\top$  is  $\mathbb{R}^{d_u}$ , the entire parameter space, and that the noise in the prediction is positive  $\sigma' > 0$ . Then, although we do not prove it here, the equilibrium solutions of the filtering distribution are, in the linear setting, unique (within the class of solutions with positive-definite covariance) and exponentially attracting. This gives methodology based on application of filtering to (4.52) a robustness that the transport methods of Subsection 4.2 do not possess. We give details in the bibliography Subsection 4.6. These results suggest that we should use  $\alpha \in (0, 1)$  except in situations where the number of observations is greater than or equal to the dimension of the parameter space  $\mathbb{R}^{d_w} \geq \mathbb{R}^{d_u}$  when it is plausible to use  $\alpha = 1$ ; indeed empirical evidence (see papers cited in Subsection 4.6) suggests that such a choice often works well for over-determined inverse problems. ■

*Remark 4.16.* The Tikhonov-Phillips regularized least squares function  $\Phi_{TP}$  corresponds to regularization of the inverse problem (4.1), with  $G(\cdot) = L\cdot$ , stemming from Gaussian prior  $\mathcal{N}(r_0, (1-\alpha)^{-1}\hat{C}_\infty)$ . This is non-standard from the point of view of inverse problems because the prior covariance is proportional to  $\hat{C}_\infty$  which depends on the forward model  $L$ . ■

Returning to the general nonlinear inverse problem (4.52), and applying the Kalman transport mean field model (2.46) we obtain

$$\begin{aligned} (4.54a) \quad & \hat{u}_{n+1} = \alpha u_n + (1-\alpha)r_0 + \xi_n, \\ (4.54b) \quad & \hat{w}_{n+1} = G(u_{n+1}) + \eta_{n+1}, \\ (4.54c) \quad & u_{n+1} = \hat{u}_{n+1} + \hat{C}_{n+1}^{uG}(\hat{C}_{n+1}^{GG} + \gamma'\Gamma)^{-1}(w - \hat{w}_{n+1}). \end{aligned}$$

Here

$$\begin{aligned} \hat{C}_{n+1}^{uG} &= \mathbb{E}\left((\hat{u}_{n+1} - \mathbb{E}\hat{u}_{n+1}) \otimes (G(\hat{u}_{n+1}) - \mathbb{E}G(\hat{u}_{n+1}))\right), \\ \hat{C}_{n+1}^{GG} &= \mathbb{E}\left((G(\hat{u}_{n+1}) - \mathbb{E}G(\hat{u}_{n+1})) \otimes (G(\hat{u}_{n+1}) - \mathbb{E}G(\hat{u}_{n+1}))\right), \end{aligned}$$

and, recall,  $\alpha \in (0, 1)$ ,  $\xi_n \sim \mathcal{N}(0, \sigma'\Sigma)$  and  $\eta_{n+1} \sim \mathcal{N}(0, \gamma'\Gamma)$ .

#### 4.4.2. Steady State Filtering Distribution and Classical Inversion: Continuous Time.

We now study the inverse problem using steady state optimization in a continuous time limit. We set  $\alpha = 1 - a\Delta t$ ,  $\sigma' = \Delta t$  and  $\gamma' = \Delta t^{-1}$  in (4.52) to obtain the continuous time limit

$$\begin{aligned} (4.55a) \quad & du = -a(u - r_0)dt + \sqrt{\Sigma}dW, \\ (4.55b) \quad & dz = G(u)dt + \sqrt{\Gamma}dB \end{aligned}$$

where  $W, B$  are independent unit Brownian motions of appropriate dimensions. We are interested in the filtering distribution  $u(t)|Z^\dagger(t)$  in the case where  $\frac{dz^\dagger}{dt} \equiv w$ .

Taking the continuous time limit in equation (4.54), we obtain the following mean field Kalman transport model for the inverse problem:

$$\begin{aligned} (4.56a) \quad & du = -a(u - r_0)dt + C^{uG}\Gamma^{-1}(w dt - d\hat{z}) + \sqrt{\Sigma}dW, \\ (4.56b) \quad & d\hat{z} = G(u)dt + \sqrt{\Gamma}dB, \\ (4.56c) \quad & C^{uG} = \mathbb{E}\left((u - \mathbb{E}u) \otimes (G(u) - \mathbb{E}G(u))\right). \end{aligned}$$

Again  $W, B$  are independent unit Brownian motions of appropriate dimensions and expectation  $\mathbb{E}$  is under the law of  $u$  itself. The resulting algorithm nudges  $G(u)$  towards the data, does so in direction informed by  $C^{uG}$ , and has additional noise and reversion to a prescribed point  $r_0$ . It is of interest to consider this continuous time limit in the context of Remark 4.11. It too has at its core an approximate mean field gradient descent, defined via statistical linearization. However the additional noise term in state-space, and the reversion to  $r_0$ , lead to a loss of affine invariance.

We now generalize the ideas in the previous subsection from the optimization approach to the Bayesian approach to inversion. Following the same philosophy as the last subsection, we first identify a dynamical system with steady state filtering distribution given by solution of the Bayesian inverse problem. As in the optimization setting of the preceding subsection this is difficult in general, but may be achieved for linear Gaussian inverse problems. And, as in the optimization setting, we can then use the approach in the nonlinear setting noting that this invokes an approximation that is consistent with the use of second order, rather than exact, transport to derive the mean-field models. Since these mean-field models are the basis for our ensemble Kalman algorithms this approach to inversion is based on a self-consistent set of approximations. The resulting methodology leads to affine invariant dynamics.

**4.4.3. Steady State Filtering Distribution and Bayesian Inversion: Discrete Time.** The previous two subsections study the idea of iterating to infinity to solve optimization approaches to the inverse problem. The methods do not solve the Bayesian inverse problem defined by (4.3), (4.1) and, furthermore, are not affine invariant. In this and the next subsection we address these two issues, generalizing the ideas of the preceding two subsections. To this end, consider the dynamical system

(4.57a)

$$u_{n+1} = u_n + \xi_n,$$

(4.57b)

$$w_{n+1} = G_R(u_{n+1}) + \eta_{n+1}.$$

Let  $W_n = \{w_\ell\}_{\ell=1}^n$  and consider the filtering distribution defined by random variable  $u_n|W_n$ , and let  $C_n$  denote the covariance of this random variable. Choose  $\alpha > 0$  and assume that  $\xi_n \sim \mathcal{N}(0, \alpha C_n)$  and that  $\eta_{n+1} \sim \mathcal{N}(0, (1 + \alpha^{-1})\Gamma_R)$ . Note a *fundamental difference with all the other state-observation models* considered in this paper: this is a mean-field model. Everywhere else in the paper we only introduce mean-field models when we construct transport maps for approximate filtering. Furthermore, (4.57) with  $\xi_n \sim \mathcal{N}(0, \alpha C_n)$  and  $C_n$  as defined is a non-standard mean-field stochastic dynamical system which depends not on its own law, but rather on the law of its own filtering distribution  $\mu_n$ . Although the filtering distribution depends on the history  $W_n$ , equation (4.57) can be rendered Markovian by coupling it to the Markovian evolution of the filtering distribution  $\mu_n \mapsto \mu_{n+1}$ , and noting that  $C_n$  is computed under  $\mu_n$ .

Recall  $w_R$  defined by (4.3). The non-standard mean-field dynamical system we have just introduced has a highly desirable property in the linear setting:

**Lemma 4.17.** *Assume that  $C_0 \succ 0$  and  $\Gamma \succ 0$ . Consider the filtering distribution  $u_n|W_n^\dagger$  for the mean-field dynamical system (4.57) in the setting where  $w_n^\dagger \equiv w_R$  and in the setting where  $u_0$  is initialized at a Gaussian.<sup>20</sup> Assume that  $G(\cdot) = L\cdot$  so that  $u_n|W_n^\dagger$  is Gaussian  $\mathcal{N}(m_n, C_n)$ . Then the steady state mean  $m_R$  and precision matrix  $C_R^{-1}$  of the filter are those of the posterior distribution (4.2) arising from the Bayesian inverse problem defined by (4.1), in this linear setting.*

<sup>20</sup>Again, for simplicity of exposition, we denote this Gaussian as  $\mathcal{N}(m_0, C_0)$  but emphasize that here it need not be the prior distribution.

*Proof.* Under the dynamics (4.57a) the predictive mean and covariance are given by

$$\hat{m}_{n+1} = m_n, \quad \hat{C}_{n+1} = (1 + \alpha)C_n.$$

Taking  $(\hat{m}_{n+1}, \hat{C}_{n+1})$  as prior for the inverse problem defined by (4.57b) we deduce that, by completing the square analogously to the same step in the proof of Lemma 4.14,

$$\begin{aligned} C_{n+1}^{-1} &= \hat{C}_{n+1}^{-1} + \frac{\alpha}{1 + \alpha} L_R^\top \Gamma_R^{-1} L_R, \\ C_{n+1}^{-1} m_{n+1} &= \hat{C}_{n+1}^{-1} \hat{m}_{n+1} + \frac{\alpha}{1 + \alpha} L_R^\top \Gamma_R^{-1} w_R; \end{aligned}$$

here  $L_R$  is defined in (4.4). The equilibrium covariance is defined by  $C_R^{-1} = L_R^\top \Gamma_R^{-1} L_R$  and the equilibrium mean  $m_R$  solves the equation

$$L_R^\top \Gamma_R^{-1} L_R m_\infty = L_R^\top \Gamma_R^{-1} w_R;$$

the discussion following (4.4) shows that these are the desired expressions for posterior mean and covariance given by (4.5) and (4.6).  $\blacksquare$

*Remark 4.18.* As for the classical inversion methodology introduced in Subsection 4.4.1 the convergence to equilibrium is exponential; see Subsection 4.6 for details.  $\blacksquare$

Motivated by this property, we may use Kalman transport algorithms applied to (4.57) to solve the Bayesian inverse problem defined by (4.1) in the general nonlinear setting. Of course, because Kalman transport is only exact up to second order moments, this does not produce the exact filtering distribution. Furthermore, to make resulting algorithms tractable we will predict in (4.57a) using the covariance  $C_n$  of the Kalman transport algorithm, rather than the covariance under the true filtering distribution. The previous lemma shows that in the linear case, though, these do coincide. With these considerations in hand, application of the Kalman transport mean field model (2.46) to (4.57) yields

$$\begin{aligned} (4.58a) \quad & \hat{u}_{n+1} = u_n + \xi_n, \\ (4.58b) \quad & \hat{w}_{n+1} = G_R(u_{n+1}) + \eta_{n+1}, \\ (4.58c) \quad & u_{n+1} = \hat{u}_{n+1} + \hat{C}_{R,n+1}^{uG} (\hat{C}_{R,n+1}^{GG} + (1 + \alpha^{-1})\Gamma_R)^{-1} (w_R - \hat{w}_{n+1}). \end{aligned}$$

Here  $\alpha > 0$ ,  $\xi_n \sim \mathcal{N}(0, \alpha C_n)$ ,  $\eta_{n+1} \sim \mathcal{N}(0, (1 + \alpha^{-1})\Gamma_R)$  and

$$\begin{aligned} C_n &= \mathbb{E}((u_n - \mathbb{E}u_n) \otimes (u_n - \mathbb{E}u_n)), \\ \hat{C}_{R,n+1}^{uG} &= \mathbb{E}((\hat{u}_{n+1} - \mathbb{E}\hat{u}_{n+1}) \otimes (G_R(\hat{u}_{n+1}) - \mathbb{E}G_R(\hat{u}_{n+1}))), \\ \hat{C}_{R,n+1}^{GG} &= \mathbb{E}((G_R(\hat{u}_{n+1}) - \mathbb{E}G_R(\hat{u}_{n+1})) \otimes (G_R(\hat{u}_{n+1}) - \mathbb{E}G_R(\hat{u}_{n+1}))). \end{aligned}$$

We note that the stochastic dynamics in (4.58a) can be replaced by the deterministic update

$$(4.59) \quad \hat{u}_{n+1} = \mathbb{E}u_n + \sqrt{1 + \alpha} (u_n - \mathbb{E}u_n)$$



leading to an equivalent dynamical behavior, in law, in the case of linear Gaussian Bayesian inverse problems. The form of (4.59) is closely related to multiplicative ensemble inflation as widely used in ensemble Kalman filtering. Similarly, the stochastic Kalman update step (4.58c) could be replaced by a corresponding deterministic one. In this context, it is noteworthy that  $\sigma' > 0$  in (4.52) is related to the concept of additive ensemble inflation as also widely used in ensemble Kalman filtering. See the Bibliography 4.6 for appropriate references.

#### 4.4.4. Steady State Filtering Distribution and Bayesian Inversion: Continuous Time.

We now study continuous time limit of the original state-observation system, and the second-order Kalman transport algorithm applied to it. We set  $\alpha = \Delta t$  in (4.57) to obtain the continuous time limit

(4.60a)

$$du = \sqrt{C}dW,$$

(4.60b)

$$dz = G_R(u)dt + \sqrt{\Gamma_R}dB$$

where  $W, B$  are independent unit Brownian motions of appropriate dimensions and  $C$  is covariance computed under the filtering distribution of  $u(t)|Z(t)$  where  $Z(t) = \{z(s)\}_{0 \leq s \leq t}$ . We are interested in the filtering distribution  $u(t)|Z^\dagger(t)$  in the case where  $\frac{dz^\dagger}{dt} \equiv w_R$ . Now taking the continuous time limit in equation (4.58), as before setting  $\alpha = \Delta t$ , we obtain the following mean field Kalman transport model for the inverse problem:

(4.61a)

$$du = C_R^{uG}(\Gamma_R)^{-1}(w_R dt - d\hat{z}) + \sqrt{C}dW,$$

(4.61b)

$$d\hat{z} = G_R(u)dt + \sqrt{\Gamma_R}dB,$$

(4.61c)

$$C = \mathbb{E}((u - \mathbb{E}u) \otimes (u - \mathbb{E}u)),$$

(4.61d)

$$C_R^{uG} = \mathbb{E}\left((u - \mathbb{E}u) \otimes (G_R(u) - \mathbb{E}G_R(u))\right).$$

Again  $W, B$  are independent unit Brownian motions of appropriate dimensions, and expectation  $\mathbb{E}$  is under the law of  $u$  itself.

*Remark 4.19.* We discuss the continuous time mean-field model (4.61) in the context of Remark 4.11. It again has the character of an approximation of mean-field gradient descent, using statistical linearization; but now the regularized objective function  $\Phi_R$  is used in place of  $\Phi$ . Furthermore, in contrast to the continuous time model (4.56), it is affine invariant. And finally, in the linear, Gaussian setting where statistical linearization is exact, we note that the underlying dynamics differs from (4.51), but nonetheless has the same steady state, equal to the posterior distribution. ■

We now study the steady state of (4.61) in the linear Gaussian setting; analogous calculations for (4.51) may be found in the papers cited in Subsection 4.6.

**Lemma 4.20.** *Assume that  $C_0 \succ 0$  and  $\Gamma \succ 0$ . Consider the filtering distribution  $u(t)|Z^\dagger(t)$  for the mean-field dynamical system (4.60) in the setting where  $z^\dagger(t) = tw_R$  for all  $t \geq 0$ . and where  $u(0)$  is initialized at a Gaussian.<sup>21</sup> Assume that  $G(\cdot) = L \cdot$  so that  $u(t)|Z^\dagger(t)$  is Gaussian*

<sup>21</sup>Again, for simplicity of exposition, we denote this Gaussian as  $\mathbf{N}(m_0, C_0)$  but emphasize that here it need not be the prior distribution.

$\mathbf{N}(m(t), C(t))$ . Then the mean-field model (4.61) has a steady state mean  $m_R$  and precision matrix  $C_R^{-1}$  given by those of the posterior distribution (4.2) arising from the Bayesian inverse problem defined by (4.1).

*Proof.* In this linear setting the law of  $u$  given by (4.61) solves the filtering problem and  $u$  itself evolves according to the SDE

$$du = CL_R^\top \Gamma_R^{-1} (w_R - L_R u - \sqrt{\Gamma_R} dB) + \sqrt{C} dW,$$

where  $C$  is the covariance of  $u$ . Solution  $u$  is Gaussian  $\mathbf{N}(m(t), C(t))$  and use of the Itô formula reveals that

$$\begin{aligned} (4.62a) \quad & \frac{dm}{dt} = CL_R^\top \Gamma_R^{-1} (w_R - L_R m) \\ (4.62b) \quad & \frac{dC}{dt} = -CL_R^\top \Gamma_R^{-1} L_R C + C. \end{aligned}$$

Setting the right hand sides to zero, and seeking a solution with non-zero covariance, gives the desired result that  $(m_R, C_R)$  as defined by (4.6) and (4.5), the posterior mean and covariance in this linear setting. ■

**4.5. Ensemble Kalman Methods For Inversion.** In this section we make a brief foray into ensemble approximations of the mean field models introduced in our discussion of inverse problems. We illustrate, in a succinct fashion, both the transport and iterative approaches of Subsections 4.2 and 4.4 respectively. By working in specific parametric regimes we illustrate them both by application of a single algorithm, and we demonstrate the use of that algorithm in an example.

We note that particle approximations of the mean field models (4.21) and (4.54) yield implementable schemes for inversion. These are described in Algorithms 6.3 and 6.4, respectively. Clearly, these two algorithmic frameworks reduce to one another in the cases  $\Delta t = 1$  in Algorithm 6.3 and  $\alpha = 1$ ,  $\sigma' = 0$  and  $\gamma' = 1$  in Algorithm 6.4, and are then both derived from ensemble approximations of the mean field model

$$\begin{aligned} (4.63a) \quad & u_{n+1} = u_n + C_n^{uG} (C_n^{GG} + \Gamma)^{-1} (w + \xi_n - G(u_n)), \\ (4.63b) \quad & C_n^{uG} = \mathbb{E} \left( (u_n - \mathbb{E} u_n) \otimes (G(u_n) - \mathbb{E} G(u_n)) \right), \\ (4.63c) \quad & C_n^{GG} = \mathbb{E} \left( (G(u_n) - \mathbb{E} G(u_n)) \otimes (G(u_n) - \mathbb{E} G(u_n)) \right), \end{aligned}$$

where  $\xi_n \sim \mathbf{N}(0, \Gamma)$  and the expectation  $\mathbb{E}$  is computed under the law of  $u_n$  itself. Algorithm 6.5 describes a particle approximation of (4.63).

In general we recommend using methodology based on (4.54) with  $\sigma' > 0$ . Furthermore for methodology based on (4.21) we recommend using  $\Delta t < 1$ . However for the specific example we consider below the algorithm performs well with  $\sigma' = 0$  (for (4.54)) and with  $\Delta t = 1$  (for (4.21)). Thus by considering ensemble Kalman approximation of (4.63) we are able to illustrate both transport and iterative approaches to inversion within a single numerical experiment.

Regarding the connection to transport, we note that the mean field model (4.63) can be derived by setting  $\Delta t = 1$  in (4.21), initialized at the prior and iterated to  $N$  such that  $N\Delta t = 1$  and so  $N = 1$ . Indeed, iterating (4.63) initialized at the prior once then yields an approximate sample from the posterior  $\mu^w$ . The mean field model (4.63) can also be derived from the iterative optimization approach (4.54) by setting  $\alpha = 1$ ,  $\sigma' = 0$  and  $\gamma' = 1$ . In this setting (4.63) can be initialized anywhere and needs to be iterated to convergence. These observations explain that implementing a particle approximation of (4.63), initialized at the prior, will yield an approximate ensemble of samples from  $\mu^w$  after one iteration; and by iterating beyond one step it will provide approximate solution to classical optimization based framing of the inverse problem. In the optimization context particle collapse (consensus) may be taken as a proxy for convergence and used as a stopping criterion, as demonstrated in the continuous time setting, for linear inverse problems, in Lemma 4.12.

The mean field model (4.63) thus constitutes the basis for an implementable algorithm that can be employed to solve the inverse problem (4.1) by either Bayesian or optimization approaches. Indeed, a particle approximation of (4.63) leads to the specific ensemble Kalman inversion method described in Algorithm 6.5. We have chosen to highlight ensemble Kalman methods based on (4.63) because it allows illustration of both the transport and iterative approaches to solving inverse problems within a single example. Since this coincidence of the two methods requires the choice  $\alpha = 1$  in (4.54) it is natural (see Remark 4.15) to consider an over-determined inverse problem. The following illustrative example has precisely this property. In it we study application of Algorithm 6.5, and then compare with application of Algorithm 6.3 with a choice of  $\Delta t < 1$ .

**Example 4.21.** We again consider the Lorenz '96 (singlescale) model for  $v \in C(\mathbb{R}^+, \mathbb{R}^L)$  satisfying the equations

$$(4.64a) \quad \dot{v}_\ell = -v_{\ell-1}(v_{\ell-2} - v_{\ell+1}) - v_\ell + u + h_v m(v_\ell), \quad \ell = 1 \dots L,$$

$$(4.64b) \quad v_{\ell+L} = v_\ell, \quad \ell = 1 \dots L.$$

As before we set  $L = 9$ ,  $h_v = -0.8$  and  $u = 10$ . We recall that function  $m$  is shown in Figure 2.1. We have used the notation  $u$  instead of  $F$ , for the forcing parameter, to align with the notation for the unknown parameter used through the section concerning inverse problems. Our objective is to recover parameter  $u$  from time-averaged data. We consider an observation  $w \in \mathbb{R}^2$  arising from the model

$$(4.65) \quad w = G_T(u) + \gamma,$$

where  $\gamma \sim N(0, \Gamma)$  represents the noise polluting the data,  $G_T : \mathbb{R} \rightarrow \mathbb{R}^2$  is the forward model that outputs, given forcing parameter  $u$ , a two-dimensional vector consisting of the averages over the  $L$  variables, of the mean and variance over time  $T$  of the state of system (4.64). In particular, considering the state of the system  $v^\dagger$  to evolve according to

$$(4.66) \quad v_{n+1}^\dagger = \Psi(v_n^\dagger),$$

where  $\Psi$  is the solution operator for (4.64) over the observation time interval  $\tau$ , the action of

forward operator  $G_T$  on  $u$  is defined as

$$G_T(u) = \begin{pmatrix} w_1 \\ w_2 \end{pmatrix},$$

with

$$w_1 = \frac{1}{L} \sum_{l=1}^L \bar{v}_l^\dagger \quad w_2 = \frac{1}{L \cdot T/\tau} \sum_{n=1}^{T/\tau} \sum_{l=1}^L (v_{n;l}^\dagger - \bar{v}_l^\dagger)^2, \quad \bar{v}_l^\dagger = \frac{1}{T/\tau} \sum_{n=1}^{T/\tau} v_{n;l}^\dagger,$$

where we have used  $v_{n;l}^\dagger$  to denote the  $l^{th}$  variable in vector  $v_n^\dagger$ , and where the states  $v_n^\dagger$  evolve according to (4.64) with true forcing parameter  $u$ , in discrete time form (4.66). We note that  $G_T$  also depends on the initialization of the system but, by ergodicity, this effect will be small if  $T$  is large enough compared with the Lyapunov time of the system; for this reason we neglect it, notationally.

To solve the parameter estimation problem consisting of inferring unknown forcing parameter  $u$  from data  $w$  given by (4.65) we use ensemble Kalman methods as formulated in Algorithms 6.3 and 6.5. The data  $w$  is generated with  $T = 10$ ; the algorithms are implemented with  $T = 20$ . In each instance of the evaluation of  $G_T$  the initial condition is chosen at random from a Gaussian distribution with mean 0 and variance 40. We initialize an ensemble of size 30 from a prior Gaussian of mean 0 and variance 10.

In Figure 4.1 we show application of Algorithm 6.5, running for 15 steps. In Figure 4.2 we show application of Algorithm 6.3 with  $\Delta t$  set to  $5 \cdot 10^{-2}$ , running for 40 steps. Notice that, in the first figure, step 1 of the algorithm outputs an ensemble Kalman approximation of the posterior and in the second figure it is at step 20 that the algorithm does so; the output of both algorithms at these specific steps corresponds to approximation of the posterior distribution, given by formula (4.12) at time  $t = 1$ . In both cases we also iterate beyond  $t = 1$  which takes the algorithms into the realm of approximate minimization of  $\Phi$ , as formula (4.12) shows as  $t \rightarrow \infty$ . The left panel of both figures shows evolution of the ensemble mean as the iteration progresses; furthermore the ensemble spread is summarized in the shading, which denotes a one standard deviation band around the mean. The right panel shows the distribution of the particles after 1 and 20 steps respectively, and a Gaussian fit with the mean and variance of the particles; in principle this is an approximation of the posterior distribution. Clearly both algorithms behave well as an iterative method to solve the inverse problems from an optimization perspective: the true value of the parameter is captured well by the ensemble mean; and ensemble collapse, which is a form of consensus in the interacting particle system, is shown by the shrinking of the ensemble standard deviation as the iteration progresses (left-hand panels). The right hand panels illustrate that the putative Bayesian samples from the posterior should be interpreted with some caution: the distribution is very different for the two different values of  $\Delta t$  that are used and cannot both be good approximations of the true posterior.

**4.6. Bibliographical Notes.** Sequential Monte Carlo methods may be used to approximately morph one probability distribution (source) into another (target), using empirical approximation and a discrete-time homotopy (Del Moral *et al.*, 2006; Chopin & Papaspiliopoulos,

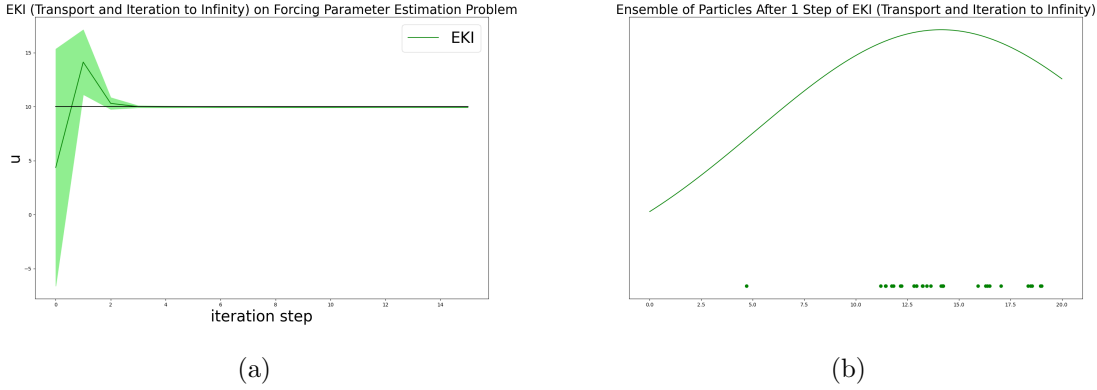


Figure 4.1: The plot in (a) displays the results obtained applying Ensemble Kalman Inversion (Transport and Iteration to Infinity), i.e. Algorithm 6.5, to the forcing parameter estimation problem. The value of the true forcing parameter is displayed in black. The green line represents the parameter estimates given by the ensemble averages, while the shaded light green region quantifies one standard deviation around the ensemble mean. The plot in (b) displays the values of the particles in the ensemble after one iteration step of Algorithm 6.5 and a Gaussian fit with the mean and variance of the particles. This ensemble represents an ensemble Kalman approximate set of samples from the posterior.

2020). In general the methodology does not scale well to high dimensional problems (Beskos *et al.*, 2014). However some success has been achieved in this direction (Kantas *et al.*, 2014), and a basic underlying theory is described in Beskos *et al.* (2015). Our presentation in this paper is confined to the setting of ensemble Kalman methods because of their empirical success and scalability to high dimensions.

The development of ensemble Kalman methods for inverse problems was pioneered in the study of reservoir simulation, in the context of learning subsurface properties from localized flow measurements (Chen & Oliver, 2002; Gu & Oliver, 2007; Li & Reynolds, 2009; Emerick & Reynolds, 2013a,b; Evensen, 2018). Subsequent work has studied parameter estimation in chaotic dynamical systems, such as those arising in weather forecasting using ensemble methods for joint state and parameter estimation (Pulido *et al.*, 2018; Bocquet *et al.*, 2020), and by matching to time-averaged statistics (Schneider *et al.*, 2017; Cleary *et al.*, 2021; Dunbar *et al.*, 2020), motivated by climate modeling. The chaotic dynamics that underlie weather and climate models lead to complicated energy landscapes for minimization and sampling (Lea *et al.*, 2000). The papers Huang *et al.* (2022b); Duncan *et al.* (2021) demonstrate the benefits of using ensemble methods, rather than computing exact derivatives, for such problems: the ensemble approach smoothes the energy landscape.

The idea of transporting prior to posterior, as developed in Subsection 4.2, is widely used in the statistics literature; see Del Moral *et al.* (2006) for a unified perspective and for citations to earlier works which characterize the deformation of one measure to the other

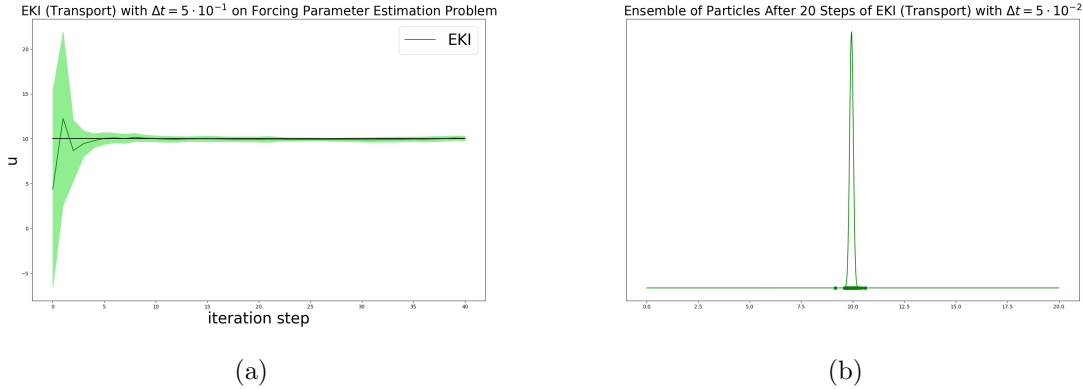


Figure 4.2: The plot in (a) displays the results obtained applying Ensemble Kalman Inversion (Transport), i.e. Algorithm 6.3, with  $\Delta t = 5 \cdot 10^{-2}$  to the forcing parameter estimation problem. The value of the true forcing parameter is displayed in black. The green line represents the parameter estimates given by the ensemble averages, while the shaded light green region quantifies one standard deviation around the ensemble mean. The plot in (b) displays the values of the particles in the ensemble after 20 steps and a Gaussian fit with the mean and variance of the particles. This ensemble represents an ensemble Kalman approximate set of samples from the posterior; note that it differs substantially from that obtained with  $\Delta t = 1$  in Figure 4.1.

either through incrementally building up the available data, or through a temperature like annealing parameter in the likelihood. In the context of data assimilation, and ensemble Kalman methods in particular, these ideas were developed by Li & Reynolds (2009), Gu & Oliver (2007), and Sakov *et al.* (2012). Their continuous time limits were first derived in Bergemann & Reich (2010a) and Bergemann & Reich (2010b) and further explored in the context of continuous time transport in Reich (2011). A connection between the non-stochastic Kalman transport equations (4.26) and preconditioned gradient descent was first identified in Bergemann & Reich (2010b) for finite ensemble sizes and in Reich & Cotter (2015) for the mean field limit. See also Yang *et al.* (2014) for related formulations based on the feedback particle filter approach to continuous time filtering.

The papers Schillings & Stuart (2017) and Schillings & Stuart (2018) studied the use of ensemble Kalman methods for optimization problems, taking a continuous time limit and making a connection to preconditioned gradient descent. This led to work on approximate sampling from the preconditioned Langevin equation in Garbuno-Inigo *et al.* (2020b), Garbuno-Inigo *et al.* (2020a), Nüsken & Reich (2019) and Liu *et al.* (2022); in particular the papers Nüsken & Reich (2019); Garbuno-Inigo *et al.* (2020a) demonstrated an important finite ensemble size correction to the mean field limit introduced in Garbuno-Inigo *et al.* (2020b). The paper Garbuno-Inigo *et al.* (2020b) used the non-standard Kalman-Wasserstein metric, first introduced in Reich & Cotter (2015), to provide a framework to analyze the preconditioned

Langevin equation. It remains open to fully develop the mathematical foundations of gradient flows using this metric. These papers demonstrate the role that the ensemble plays in preconditioning the dynamics. This makes a link to the important paper [Goodman & Weare \(2010\)](#) which introduced the concept of affine invariant ensemble samplers, an idea developed further in [Leimkuhler \*et al.\* \(2018\)](#).

Filtering using dynamical systems with equilibrium filtering distribution which solves the inverse problem, the approach adopted in Subsection 4.4, is an idea developed for optimization in [Huang \*et al.\* \(2022b\)](#) and for sampling in [Huang \*et al.\* \(2022a\)](#). See those papers for details concerning uniqueness of, and exponential convergence to, steady state solutions in the linear Gaussian setting, as discussed in Remarks 4.15, 4.18. See also [Pidstrigach & Reich \(2021\)](#) for related formulations in the time continuous setting. The stochastic perturbations utilized in (4.52a) and (4.57a) are closely related to additive and multiplicative, respectively, ensemble inflation methods as widely used in ensemble Kalman filter implementations ([Asch \*et al.\*, 2016](#); [Evensen \*et al.\*, 2022](#)).

The optimization and sampling approaches for inverse problems, in both discrete and continuous time, can in principle be combined with ideas from stochastic annealing ([Kushner & Yin, 2003](#)), and stochastic gradient descent ([Goodfellow \*et al.\*, 2016](#)). The papers by [Haber \*et al.\* \(2018\)](#); [Kovachki & Stuart \(2019\)](#); [Pidstrigach & Reich \(2021\)](#) demonstrate the use of ensemble Kalman methods for inversion, when combined with stochastic gradient descent, and mini-batching in particular, as well as the application of ensemble Kalman methods beyond the setting of the  $L_2$ -loss functions  $\Phi$  and  $\Phi_R$  considered here.

However, despite the growing use of ensemble Kalman methods to solve inverse problems, it is important to appreciate that they all invoke approximations which amount to matching only first and second order statistics, at some point in the algorithmic development. For this reason the methods are intuitively only useful as samplers for problems with posterior distribution close to a Gaussian. This idea is carefully explained in [Ernst \*et al.\* \(2015\)](#). As is the case for state estimation, analysis is required to justify use of ensemble Kalman methods beyond the linear and Gaussian regime.

The idea of using ensemble methods for performing the optimization step within variational data assimilation was introduced in [Zupanski \(2005\)](#). The connection between iterative applications of the ensemble Kalman filter and optimization were first investigated in [Iglesias \*et al.\* \(2013\)](#) and developed to include constraints in [Albers \*et al.\* \(2019\)](#), [Chada \*et al.\* \(2019\)](#) and Tikhonov regularization [Chada \*et al.\* \(2020b\)](#). Recall from Remark 4.13 the algebraic rates of convergence inherent in mean-field gradient descent. This undesirable feature of optimization methods based on statistical linearization of mean-field gradient descent can be ameliorated to some extent by the use of the use adaptive time-steps, connections to the Levenberg-Marquadt algorithm, and the use of stopping criteria; see [Iglesias \(2015\)](#), [Iglesias \(2016\)](#), and [Iglesias & Yang \(2021\)](#). The recent paper [Chada \*et al.\* \(2020a\)](#) overviews the optimization perspective and provides a unifying framework, going beyond gradient descent-based methods. In particular, framing ensemble Kalman based optimization methods in terms of statistical linearization, as we do in Subsection 4.3, originates in that paper.

Other interacting particle system approaches to optimization have been proposed, including feedback particle ([Zhang \*et al.\*, 2017](#)) and unscented Kalman approaches ([Huang \*et al.\*, 2022b,a](#)). Furthermore the papers [Reich & Weissmann \(2021\)](#) and [Pavliotis \*et al.\* \(2021\)](#) show



how to construct a derivative free Langevin sampler using localized ensembles. An alternative interacting particle system approach to solving inverse problems and optimization tasks is the use of consensus based methods (Tsianos *et al.*, 2012; Ha *et al.*, 2021; Fornasier *et al.*, 2021; Carrillo *et al.*, 2018, 2021; Chen *et al.*, 2020; Pinnau *et al.*, 2017; Fornasier *et al.*, 2020).

The papers Ding *et al.* (2020), Ding & Li (2021a,b) undertake a systematic analysis of the link between interacting particle systems and mean-field systems, mostly focused on the solution of inverse problems; however the methods developed are more widely applicable.

Finally we note that Kalman methods have been related to approximate Bayesian computation (ABC) methodologies, utilizing a linear regression ansatz (Sisson *et al.*, 2018; Nott *et al.*, 2012). Such methods are in turn closely related to Bayes linear and best linear unbiased estimators (BLUE) as discussed in Goldstein & Rougier (2006), Goldstein & Wooff (2007), Lei & Bickel (2011), Nott *et al.* (2012), Snyder (2014), Goldstein (2014), Reich & Cotter (2015), and Latz (2016). BLUE is discussed in more detail in Appendix 8.3.

**5. Conclusions and Open Problems.** This paper presents a unifying perspective on the derivation, interpretation and analysis of ensemble Kalman methods through use of the ideas of mean field models, second order approximate transport and particle approximation. Both state estimation and parameter estimation (inverse problems) are studied, and similar ideas may be developed for joint parameter-state estimation problems. Furthermore, ideas have been presented in discrete time and, through specific parametric scalings, continuous time limits have been identified. Our unifying approach constitutes a novel presentation of the subject, and creates a framework for the mathematical development of the subject area.

Ensemble Kalman methods have been enormously impactful in the geosciences, where they originated, and are starting to be used in numerous other application domains. However, if they are to realize their potential for widespread adoption and application, many research challenges remain. These challenges are both in mathematical analysis and in the development of methodology. One of the biggest challenges is the following: some theory, and abundant numerical evidence, show that ensemble Kalman methods perform well at state estimation and at parameter estimation; however, there is very little theory, or empirical evidence, which identifies situations in which the statistical information in the ensemble constitutes valid approximate Bayesian inference.

In mathematical analysis a number of substantial challenges are presented by ensemble Kalman methods, which we list here.

- Determine conditions, related to small noise scenarios, under which the true state is well-approximated by the mean or sample path of mean field models based on second order transport; find sharp error estimates.
- More generally, determine conditions under which the filtering distribution is well-approximated by mean field models based on second order transport; find sharp error estimates and appropriate metrics for the analysis; furthermore, identify which problems satisfy these conditions.
- For inverse problems, determine conditions under which the optimizer of a (to-be-identified) loss function is well-approximated by the mean or sample path of mean field models based on second order transport; find sharp error estimates.
- Again, more generally, for inverse problems, determine conditions under which the



Bayesian posterior is well-approximated by mean field models based on second order transport, in both the transport and iterative approaches to inversion; find sharp error estimates and appropriate metrics for the analysis; furthermore, identify which inverse problems satisfy these conditions.

- For all of the preceding four scenarios derive error bounds for particle approximations of the mean-field models; when low-rank structure is present in covariances prove that ensemble Kalman methods can correctly identify it, and exploit the low-rank structure in the analysis of particle approximations.
- In all of the particle methods arising above, compare the cost/error trade-off with that arising for other competitive methods, to determine when ensemble Kalman methods are competitive.
- All of the algorithms in the paper are studied in idealized scenarios, in the absence of widely employed techniques such as covariance inflation and localization; developing analyses which account for covariance inflation and localization will be highly desirable.

On the methodology side there are also a number of significant challenges, which we also list here.

- Given ability to compute an ensemble of evaluations of the combined state-observation dynamical system, what is the optimal way to combine them to either estimate the state given an observation sequence, or the filtering distribution.
- Given ability to compute an ensemble of evaluations of the forward model, what is the optimal way to combine them to either estimate the parameter given an observation, or the posterior distribution, for the corresponding inverse problem.
- What role might be played by machine learning in addressing the design of algorithms, and in particular in addressing the preceding questions.
- Develop an overarching interacting particle and mean field framework that subsumes ensemble Kalman and alternative particle filters as well as derivative-free and consensus based optimization methods and use the framework to create new methods.
- Develop principles for the deployment of covariance inflation, and generalizations of localization, so that the resulting methodology is widely applicable and does not need application-specific principles to be applied.
- Expand the preceding scenarios beyond the additive error models discussed in the survey, to include classification and other machine learning tasks.

**Acknowledgments** EC is grateful to the Kortschak Scholars Program within the CMS Department at Caltech for financial support. The work of SR was supported by Deutsche Forschungsgemeinschaft (DFG) - Project-ID 318763901 - SFB1294.. The work of AMS is supported by NSF award AGS1835860, the Office of Naval Research award N00014-17-1-2079 and by a Department of Defense Vannevar Bush Faculty Fellowship. The authors are grateful to Dmitry Burov for helpful advice regarding the numerical experiments; they are also grateful to Ricardo Baptista and Daniel Sanz-Alonso for helpful discussions which improved the paper.

## REFERENCES

- ABARBANEL, H. (2013) *Predicting the future: Completing models of observed complex systems*. Springer.
- ABDULLE, A., WEINAN, E., ENGQUIST, B. & VANDEN-EIJNDEN, E. (2012) The heterogeneous multiscale method. *Acta Numerica*, **21**, 1–87.
- ACEVEDO, W., DE WILJES, J. & REICH, S. (2017) Second-order accurate ensemble transform particle filters. *SIAM J. Sci. Comput.*, **39**, A1834–A1850.
- AGAPIOU, S., PAPASPILIOPOULOS, O., SANZ-ALONSO, D. & STUART, A. (2017) Importance sampling: Intrinsic dimension and computational cost. *Statistical Science*, 405–431.
- ALBERS, D. J., BLANCQUART, P.-A., LEVINE, M. E., SEYLABI, E. E. & STUART, A. (2019) Ensemble Kalman methods with constraints. *Inverse Problems*, **35**, 095007.
- AMEZCUA, J., KALNAY, E., IDE, K. & REICH, S. (2014) Ensemble transform Kalman-Bucy filters. *Q.J.R. Meteor. Soc.*, **140**, 995–1004.
- ANDERSON, B. D. & MOORE, J. B. (2012) *Optimal filtering*. Courier Corporation.
- ANDERSON, J. L. (2001) An ensemble adjustment Kalman filter for data assimilation. *Monthly weather review*, **129**, 2884–2903.
- ASCH, M., BOCQUET, M. & NODET, M. (2016) *Data assimilation: Methods, algorithms, and applications*. SIAM.
- ASHWIN, P. (2003) Synchronization from chaos. *Nature*, **422**, 384–385.
- AZOUANI, A., OLSON, E. & TITI, E. S. (2014) Continuous data assimilation using general interpolant observables. *Journal of Nonlinear Science*, **24**, 277–304.
- BAIN, A. & CRISAN, D. (2008) *Fundamentals of stochastic filtering*, vol. 60. Springer Science & Business Media.
- BERGEMANN, K. & REICH, S. (2010a) A localization technique for ensemble Kalman filters. *Quarterly Journal of the Royal Meteorological Society: A journal of the atmospheric sciences, applied meteorology and physical oceanography*, **136**, 701–707.
- BERGEMANN, K. & REICH, S. (2010b) A mollified ensemble Kalman filter. *Quarterly Journal of the Royal Meteorological Society*, **136**, 1636–1643.
- BERGEMANN, K. & REICH, S. (2012) An ensemble Kalman-Bucy filter for continuous data assimilation. *Meteorologische Zeitschrift*, **21**, 213.
- BESKOS, A., CRISAN, D. & JASRA, A. (2014) On the stability of sequential monte carlo methods in high dimensions. *The Annals of Applied Probability*, **24**, 1396–1445.
- BESKOS, A., JASRA, A., MUZAFFER, E. A. & STUART, A. M. (2015) Sequential monte carlo methods for bayesian elliptic inverse problems. *Statistics and Computing*, **25**, 727–737.
- BICKEL, P., LI, B. & BENGTSOON, T. (2008) Sharp failure rates for the bootstrap particle filter in high dimensions. *Pushing the limits of contemporary statistics: Contributions in honor of Jayanta K. Ghosh*. Institute of Mathematical Statistics, pp. 318–329.
- BISHOP, C., ETHERTON, B. & MAJUMDAR, S. (2001) Adaptive sampling with the ensemble transform Kalman filter. Part I: Theoretical aspects. *Monthly Weather Review*, **129**, 420–436.
- BISHOP, C. (2011) *Pattern Recognition and Machine Learning*, 2nd edn. New York: Springer-Verlag.
- BLÖMKER, D., LAW, K., STUART, A. M. & ZYGALAKIS, K. C. (2013) Accuracy and stability of the continuous-time 3DVAR filter for the Navier–Stokes equation. *Nonlinearity*, **26**, 2193.
- BLÖMKER, D., SCHILLINGS, C. & WACKER, P. (2018) A strongly convergent numerical scheme from ensemble Kalman inversion. *SIAM Journal on Numerical Analysis*, **56**, 2537–2562.
- BLÖMKER, D., SCHILLINGS, C., WACKER, P. & WEISSMANN, S. (2021) Continuous time limit of the stochastic ensemble Kalman inversion: Strong convergence analysis. *Technical Report*. arXiv:2107.14508.
- BOCQUET, M., GURUMOORTHY, K. S., APTE, A., CARRASSI, A., GRUDZIEN, C. & JONES, C. K. (2017) Degenerate Kalman filter error covariances and their convergence onto the unstable subspace. *SIAM/ASA Journal on Uncertainty Quantification*, **5**, 304–333.
- BOCQUET, M., BRAJARD, J., CARRASSI, A. & BERTINO, L. (2020) Bayesian inference of chaotic dynamics by merging data assimilation, machine learning and expectation-maximization. *Foundations of Data Science*, **2**, 55–80.
- BOCQUET, M. & SAKOV, P. (2012) Combining inflation-free and iterative ensemble Kalman filters for strongly nonlinear systems. *Nonlinear Processes in Geophysics*, **19**, 383–399.
- BOCQUET, M. & SAKOV, P. (2014) An iterative ensemble Kalman smoother. *Q. J. R. Meteorol. Soc.*, **140**, 1521–1535.

- BURGERS, G., VAN LEEUWEN, P. & EVENSEN, G. (1998) Analysis scheme in the ensemble Kalman filter. *Monthly Weather Review*, **126**, 1719–1724.
- BUROV, D., GIANNAKIS, D., MANOHAR, K. & STUART, A. (2021) Kernel analog forecasting: Multiscale test problems. *Multiscale Modeling & Simulation*, **19**, 1011–1040.
- CARRILLO, J., HOFFMANN, F., STUART, A. & VAES, U. (2021) Consensus based sampling. *arXiv preprint arXiv:2106.02519*.
- CARRILLO, J. A., CHOI, Y.-P., TOTZECK, C. & TSE, O. (2018) An analytical framework for consensus-based global optimization method. *Mathematical Models and Methods in Applied Sciences*, **28**, 1037–1066.
- CHADA, N. K., SCHILLINGS, C. & WEISSMANN, S. (2019) On the incorporation of box-constraints for ensemble Kalman inversion. *arXiv preprint arXiv:1908.00696*.
- CHADA, N. K., CHEN, Y. & SANZ-ALONSO, D. (2020a) Iterative ensemble Kalman methods: a unified perspective with some new variants. *arXiv preprint arXiv:2010.13299*.
- CHADA, N. K., STUART, A. M. & TONG, X. T. (2020b) Tikhonov regularization within ensemble Kalman inversion. *SIAM Journal on Numerical Analysis*, **58**, 1263–1294.
- CHEN, J., JIN, S. & LYU, L. (2020) A consensus-based global optimization method with adaptive momentum estimation. *arXiv preprint arXiv:2012.04827*.
- CHEN, Y., SANZ-ALONSO, D. & WILLETT, R. (2022) Autodifferentiable Ensemble Kalman filters. *SIAM Journal on Mathematics of Data Science*, **4**, 801–833.
- CHEN, Y. & OLIVER, D. (2002) Ensemble randomized maximum likelihood method as an iterative ensemble smoother. *Mathematical Geosciences*, **44**, 1–26.
- CHENG, Y. & REICH, S. (2015) Data assimilation: A coupling of measure perspective. *Frontiers in Applied Dynamical Systems*, vol. 2. New York: Springer-Verlag.
- CHERNOV, A., HOEL, H., LAW, K. J., NOBILE, F. & TEMPONE, R. (2021) Multilevel ensemble kalman filtering for spatio-temporal processes. *Numerische Mathematik*, **147**, 71–125.
- CHOPIN, N. & PAPASPILIOPOULOS, O. (2020) *An Introduction to Sequential Monte Carlo*. Cham, Switzerland: Springer Nature Switzerland AG.
- CHUSTAGULPROM, N., REICH, S. & REINHARDT, M. (2016) A hybrid ensemble transform filter for nonlinear and spatially extended dynamical systems. *SIAM/ASA J. Uncertainty Quantification*, **4**, 592–608.
- CLARK, J. & CRISAN, D. (2005) On a robust version of the integral representation formula of nonlinear filtering. *Probab. Theory Relat. Fields*, **133**, 43–56.
- CLEARY, E., GARBUNO-INIGO, A., LAN, S., SCHNEIDER, T. & STUART, A. M. (2021) Calibrate, emulate, sample. *Journal of Computational Physics*, **424**, 109716.
- COGHI, M., NILSSEN, T., NÜSKEN, N. & REICH, S. (2021) Rough McKean–Vlasov dynamics for robust ensemble Kalman filtering. *Technical Report*. arXiv:2107.06621.
- CORENFLOS, A., THORNTON, J., DELIGIANNIDIS, G. & DOUCET, A. (2021) Differentiable particle filtering via entropy-regularized optimal transport. *International Conference on Machine Learning*. PMLR, pp. 2100–2111.
- COTTER, C. & REICH, S. (2013) Ensemble filter techniques for intermittent data assimilation. *Radon Ser. Comput. Appl. Math.*, **13**, 91–134.
- CRISAN, D., DEL MORAL, P. & LYONS, T. (1998) *Discrete filtering using branching and interacting particle systems*. Citeseer.
- CRISAN, D. & LYONS, T. (1999) A particle approximation of the solution of the kushner–stratonovitch equation. *Probability Theory and Related Fields*, **115**, 549–578.
- CRISAN, D. & XIONG, J. (2010) Approximate McKean–Vlasov representations for a class of SPDEs. *Stochastics*, **82**, 53–68.
- CUTURI, M. (2013) Sinkhorn distances: Lightspeed computation of optimal transport. *Advances in neural information processing systems*, **26**.
- DAUM, F., HUANG, J. & NOUSHIN, A. (2010) Exact particle flow for nonlinear filters. *Signal Processing, Sensor Fusion, and Target Recognition XIX* (I. Kadar ed.), vol. 7697. International Society for Optics and Photonics, SPIE, pp. 92 – 110.
- DE WILJES, J., REICH, S. & STANNAT, W. (2018) Long-time stability and accuracy of the ensemble Kalman–Bucy filter for fully observed processes and small measurement noise. *SIAM Journal on Applied Dynamical Systems*, **17**, 1152–1181.
- DE WILJES, J. & TONG, X. (2020) Analysis of a localised nonlinear ensemble Kalman Bucy filter with

- complete and accurate observations. *Nonlinearity*, **33**, 4752–4782.
- DEL MORAL, P. (2004) *Feynman–Kac Formulae: Genealogical and Interacting Particle Systems with Applications*. New York: Springer-Verlag.
- DEL MORAL, P., DOUCET, A. & JASRA, A. (2006) Sequential Monte Carlo samplers. *Journal of the Royal Statistical Society: Series B (Statistical Methodology)*, **68**, 411–436.
- DEL MORAL, P. & TUGAUT, J. (2018) On the stability and the uniform propagation of chaos properties of ensemble Kalman–Bucy filters. *The Annals of Applied Probability*, **28**, 790–850.
- DING, Z., LI, Q. & LU, J. (2020) Ensemble Kalman inversion for nonlinear problems: weights, consistency, and variance bounds. *arXiv preprint arXiv:2003.02316*.
- DING, Z. & LI, Q. (2021a) Ensemble Kalman inversion: mean-field limit and convergence analysis. *Statistics and Computing*, **31**, 1–21.
- DING, Z. & LI, Q. (2021b) Ensemble Kalman sampler: Mean-field limit and convergence analysis. *SIAM Journal on Mathematical Analysis*, **53**, 1546–1578.
- DOUCET, A., DE FREITAS, N. & GORDON, N. (2001) An introduction to sequential Monte Carlo methods. *Sequential Monte Carlo Methods in Practice*. Springer, pp. 3–14.
- DUNBAR, O. R., GARBUNO-INIGO, A., SCHNEIDER, T. & STUART, A. M. (2020) Calibration and uncertainty quantification of convective parameters in an idealized GCM. *arXiv preprint arXiv:2012.13262*.
- DUNCAN, A., STUART, A. & WOLFRAM, M.-T. (2021) Ensemble inference methods for models with noisy and expensive likelihoods. *arXiv preprint arXiv:2104.03384*.
- EATON, M. L. (2007) Multivariate statistics: A vector space approach. *Lecture Notes-Monograph Series*, **53**, i–512.
- EBERLE, A. (2013) Stochastic analysis. *Technical Report*. Lecture Notes, University of Bonn.
- EL MOSELHY, T. A. & MARZOUK, Y. M. (2012) Bayesian inference with optimal maps. *Journal of Computational Physics*, **231**, 7815–7850.
- EMERICK, A. A. & REYNOLDS, A. C. (2013a) Ensemble smoother with multiple data assimilation. *Computers & Geosciences*, **55**, 3–15.
- EMERICK, A. & REYNOLDS, A. (2013b) Investigation of the sampling performance of ensemble-based methods with a simple reservoir model. *Computational Geosciences*, **17**, 325–350.
- ERNST, O. G., SPRUNGK, B. & STARKLOFF, H.-J. (2015) Analysis of the ensemble and polynomial chaos Kalman filters in bayesian inverse problems. *SIAM/ASA Journal on Uncertainty Quantification*, **3**, 823–851.
- EVANS, L. C. (2012) *An introduction to stochastic differential equations*, vol. 82. American Mathematical Soc.
- EVENSEN, G. (1994) Sequential data assimilation with a nonlinear quasi-geostrophic model using Monte Carlo methods to forecast error statistics. *Journal of Geophysical Research: Oceans*, **99**, 10143–10162.
- EVENSEN, G. (2018) Analysis of iterative ensemble smoothers for solving inverse problems. *Computational Geosciences*, **22**, 885–908.
- EVENSEN, G. (2019) Accounting for model errors in iterative ensemble smoothers. *Computational Geosciences*, **23**, 761–775.
- EVENSEN, G., VOSSEPOEL, F. & VAN LEEUWEN, P. (2022) *Data Assimilation Fundamentals: A unified Formulation of the State and Parameter Estimation Problem*. Cham, Switzerland: Springer Nature Switzerland AG.
- FATKULLIN, I. & VANDEN-EIJNDEN, E. (2004) A computational strategy for multiscale systems with applications to Lorenz 96 model. *Journal of Computational Physics*, **200**, 605–638.
- FERTIG, E. J., HARLIM, J. & HUNT, B. R. (2007) A comparative study of 4D-VAR and a 4D ensemble Kalman filter: Perfect model simulations with Lorenz-96. *Tellus A: Dynamic Meteorology and Oceanography*, **59**, 96–100.
- FOIAS, C., MONDAINI, C. F. & TITI, E. S. (2016) A discrete data assimilation scheme for the solutions of the two-dimensional Navier–Stokes equations and their statistics. *SIAM Journal on Applied Dynamical Systems*, **15**, 2109–2142.
- FORNASIER, M., HUANG, H., PARESCHI, L. & SÜNNEN, P. (2020) Consensus-based optimization on hypersurfaces: Well-posedness and mean-field limit. *Mathematical Models and Methods in Applied Sciences*, **30**, 2725–2751.
- FORNASIER, M., KLOCK, T. & RIEDL, K. (2021) Consensus-based optimization methods converge globally

- in mean-field law. *arXiv preprint arXiv:2103.15130*.
- FREI, M. & KÜNSCH, H. R. (2013) Bridging the ensemble Kalman and particle filters. *Biometrika*, **100**, 781–800.
- GARBUNO-INIGO, A., NÜSKEN, N. & REICH, S. (2020a) Affine invariant interacting Langevin dynamics for bayesian inference. *SIAM Journal on Applied Dynamical Systems*, **19**, 1633–1658.
- GARBUNO-INIGO, A., HOFFMANN, F., LI, W. & STUART, A. M. (2020b) Interacting Langevin diffusions: Gradient structure and ensemble Kalman sampler. *SIAM Journal on Applied Dynamical Systems*, **19**, 412–441.
- GESHO, M., OLSON, E. & TITI, E. S. (2016) A computational study of a data assimilation algorithm for the two-dimensional Navier–Stokes equations. *Communications in Computational Physics*, **19**, 1094–1110.
- GHIL, M., COHN, S., TAVANTZIS, J., BUBE, K. & ISAACSON, E. (1981) Applications of estimation theory to numerical weather prediction. *Dynamic meteorology: Data assimilation methods*. Springer, pp. 139–224.
- GOLDSTEIN, M. (2014) Bayes linear analysis. *Wiley StatsRef: Statistics Reference Online*, 1–7.
- GOLDSTEIN, M. & ROUGIER, J. (2006) Bayes linear calibrated prediction for complex systems. *Journal of the American Statistical Association*, **101**, 1132–1143.
- GOLDSTEIN, M. & WOOFF, D. (2007) *Bayes linear statistics: Theory and methods*, vol. 716. John Wiley & Sons.
- GONZALEZ, O. & STUART, A. M. (2008) *A first course in continuum mechanics*. Cambridge University Press.
- GONZÁLEZ-TOKMAN, C. & HUNT, B. R. (2013) Ensemble data assimilation for hyperbolic systems. *Physica D: Nonlinear Phenomena*, **243**, 128–142.
- GOODFELLOW, I., BENGIO, Y., COURVILLE, A. & BENGIO, Y. (2016) *Deep learning*, vol. 1. MIT press Cambridge.
- GOODMAN, J. & WEARE, J. (2010) Ensemble samplers with affine invariance. *Communications in applied mathematics and computational science*, **5**, 65–80.
- GOTTWALD, G. A. & MAJDA, A. J. (2013) A mechanism for catastrophic filter divergence in data assimilation for sparse observation networks. *Nonlinear Processes in Geophysics*, **20**, 705–712.
- GOTTWALD, G. A. & REICH, S. (2021) Supervised learning from noisy observations: Combining machine-learning techniques with data assimilation. *Physica D: Nonlinear Phenomena*, **423**, 132911.
- GROOMS, I., LEE, Y. & MAJDA, A. J. (2014) Ensemble Kalman filters for dynamical systems with unresolved turbulence. *Journal of Computational Physics*, **273**, 435–452.
- GROOMS, I., LEE, Y. & MAJDA, A. J. (2015) Ensemble filtering and low-resolution model error: Covariance inflation, stochastic parameterization, and model numerics. *Monthly Weather Review*, **143**, 3912–3924.
- GROOMS, I. (2021) Analog ensemble data assimilation and a method for constructing analogs with variational autoencoders. *Quarterly Journal of the Royal Meteorological Society*, **147**, 139–149.
- GU, Y. & OLIVER, D. S. (2007) An iterative ensemble Kalman filter for multiphase fluid flow data assimilation. *SPE Journal*, **12**, 438–446.
- GURTIN, M. E. (1982) *An introduction to continuum mechanics*. Academic press.
- GURUMOORTHY, K. S., GRUDZIEN, C., APTE, A., CARRASSI, A. & JONES, C. K. (2017) Rank deficiency of Kalman error covariance matrices in linear time-varying system with deterministic evolution. *SIAM Journal on Control and Optimization*, **55**, 741–759.
- GUTH, P. A., SCHILLINGS, C. & WEISSMANN, S. (2020) Ensemble Kalman filter for neural network based one-shot inversion. *arXiv preprint arXiv:2005.02039*.
- HA, S.-Y., JIN, S. & KIM, D. (2021) Convergence and error estimates for time-discrete consensus-based optimization algorithms. *Numerische Mathematik*, **147**, 255–282.
- HABER, E., LUCKA, F. & RUTHOTTO, L. (2018) Never look back - The EnKF method and its application to the training of neural networks without back propagation. *arXiv preprint arXiv:1805.08034*.
- HARLIM, J., MAHDI, A. & MAJDA, A. J. (2014) An ensemble Kalman filter for statistical estimation of physics constrained nonlinear regression models. *Journal of Computational Physics*, **257**, 782–812.
- HARLIM, J. & HUNT, B. R. (2007a) Four-dimensional local ensemble transform Kalman filter: Numerical experiments with a global circulation model. *Tellus A: Dynamic Meteorology and Oceanography*, **59**, 731–748.
- HARLIM, J. & HUNT, B. R. (2007b) A non-Gaussian ensemble filter for assimilating infrequent noisy observations. *Tellus A: Dynamic Meteorology and Oceanography*, **59**, 225–237.



- HARLIM, J. & MAJDA, A. J. (2010) Filtering turbulent sparsely observed geophysical flows. *Monthly Weather Review*, **138**, 1050–1083.
- HAYDEN, K., OLSON, E. & TITI, E. S. (2011) Discrete data assimilation in the Lorenz and 2D Navier–Stokes equations. *Physica D: Nonlinear Phenomena*, **240**, 1416–1425.
- HIGHAM, D. J. (2001) An algorithmic introduction to numerical simulation of stochastic differential equations. *SIAM review*, **43**, 525–546.
- HOEL, H., LAW, K. J. & TEMPONE, R. (2016) Multilevel ensemble kalman filtering. *SIAM Journal on Numerical Analysis*, **54**, 1813–1839.
- HOUTEKAMER, P. & MITCHELL, H. (2005) Ensemble Kalman filtering. *Q. J. Royal Meteorological Soc.*, **131**, 3269–3289.
- HOUTEKAMER, P. & MITCHELL, M. (1998) Data assimilation using an ensemble Kalman filter techniques. *Monthly Weather Review*, **126**, 796–811.
- HU, Y., KALLIANPUR, G. & XIONG, J. (2002) An approximation for the Zakai equation. *Applied Mathematics and Optimization*, **45**, 23–44.
- HUANG, D. Z., HUANG, J., REICH, S. & STUART, A. M. (2022a) Efficient derivative-free bayesian inference for large-scale inverse problems. *arXiv preprint arXiv:2204.04386*.
- HUANG, D. Z., SCHNEIDER, T. & STUART, A. M. (2022b) Iterated Kalman methodology for inverse problems. *Journal of Computational Physics*, **463**, 111262.
- HUNT, B., KOSTELICH, E. & SZUNYOGH, I. (2007) Efficient data assimilation for spatiotemporal chaos: A local ensemble transform Kalman filter. *Physica D*, **230**, 112–126.
- IGLESIAS, M. A., LAW, K. J. & STUART, A. M. (2013) Ensemble Kalman methods for inverse problems. *Inverse Problems*, **29**, 045001.
- IGLESIAS, M. A. (2015) Iterative regularization for ensemble data assimilation in reservoir models. *Computational Geosciences*, **19**, 177–212.
- IGLESIAS, M. A. (2016) A regularizing iterative ensemble Kalman method for pde-constrained inverse problems. *Inverse Problems*, **32**, 025002.
- IGLESIAS, M. & YANG, Y. (2021) Adaptive regularisation for ensemble Kalman inversion. *Inverse Problems*, **37**, 025008.
- JAZWINSKI, A. H. (2007) *Stochastic processes and filtering theory*. Courier Corporation.
- JULIER, S., UHLMANN, J. & DURRANT-WHYTE, H. F. (2000) A new method for the nonlinear transformation of means and covariances in filters and estimators. *IEEE Transactions on Automatic Control*, **45**, 477–482.
- KAPIO, J. & SOMERSALO, E. (2006) *Statistical and computational inverse problems*, vol. 160. Springer Science & Business Media.
- KALMAN, R. E. (1960) A New Approach to Linear Filtering and Prediction Problems. *Journal of Basic Engineering*, **82**, 35–45.
- KALMAN, R. E. & BUCY, R. S. (1961) New Results in Linear Filtering and Prediction Theory. *Journal of Basic Engineering*, **83**, 95–108.
- KANTAS, N., BESKOS, A. & JASRA, A. (2014) Sequential monte carlo methods for high-dimensional inverse problems: A case study for the navier–stokes equations. *SIAM/ASA Journal on Uncertainty Quantification*, **2**, 464–489.
- KELLY, D., MAJDA, A. J. & TONG, X. T. (2015) Concrete ensemble Kalman filters with rigorous catastrophic filter divergence. *Proceedings of the National Academy of Sciences*, **112**, 10589–10594.
- KELLY, D. T., LAW, K. J. & STUART, A. M. (2014) Well-posedness and accuracy of the ensemble Kalman filter in discrete and continuous time. *Nonlinearity*, **27**, 2579.
- KITANIDIS, P. K. (1995) Quasi-linear geostatistical theory for inversion. *Water Resour. Res.*, **31**, 2411–2419.
- KLOEDEN, P. & PLATEN, E. (1991) *Numerical methods for stochastic differential equations*. New York: Springer.
- KOVACHKI, N. B. & STUART, A. M. (2019) Ensemble Kalman inversion: A derivative-free technique for machine learning tasks. *Inverse Problems*, **35**, 095005.
- KUSHNER, H. & YIN, G. G. (2003) *Stochastic approximation and recursive algorithms and applications*, vol. 35. Springer Science & Business Media.
- KUZNETSOV, L., IDE, K. & JONES, C. K. (2003) A method for assimilation of Lagrangian data. *Monthly Weather Review*, **131**, 2247–2260.
- KWIATKOWSKI, E. & MANDEL, J. (2015) Convergence of the square root ensemble Kalman filter in the large

- ensemble limit. *SIAM/ASA Journal on Uncertainty Quantification*, **3**, 1–17.
- LANGE, T. & STANNAT, W. (2019) On the continuous time limit of Ensemble Square Root Filters. *arXiv preprint arXiv:1910.12493*.
- LANGE, T. & STANNAT, W. (2021) On the continuous time limit of the ensemble Kalman filter. *Mathematics of Computation*, **90**, 233–265.
- LARIOS, A. & PEI, Y. (2017) Nonlinear continuous data assimilation. *arXiv preprint arXiv:1703.03546*.
- LATZ, J. (2016) Bayes linear methods for inverse problems. *Ph.D. thesis*, Master's thesis, University of Warwick.
- LAW, K., STUART, A. & ZYGALAKIS, K. (2015) Data assimilation. *Cham, Switzerland: Springer*, **214**.
- LAW, K., SANZ-ALONSO, D., SHUKLA, A. & STUART, A. (2016a) Filter accuracy for the Lorenz 96 model: Fixed versus adaptive observation operators. *Physica D: Nonlinear Phenomena*, **325**, 1–13.
- LAW, K. J., SHUKLA, A. & STUART, A. M. (2012) Analysis of the 3DVAR filter for the partially observed Lorenz'63 model. *arXiv preprint arXiv:1212.4923*.
- LAW, K. J., TEMBINE, H. & TEMPONE, R. (2016b) Deterministic mean-field ensemble kalman filtering. *SIAM Journal on Scientific Computing*, **38**, A1251–A1279.
- LAW, K. J. & STUART, A. M. (2012) Evaluating data assimilation algorithms. *Monthly Weather Review*, **140**, 3757–3782.
- LE GLAND, F., MONBET, V. & TRAN, V.-D. (2011) Large sample asymptotics for the ensemble Kalman filter. Oxford: Oxford Univ. Press, pp. 598–631.
- LEA, D. J., ALLEN, M. R. & HAINE, T. W. (2000) Sensitivity analysis of the climate of a chaotic system. *Tellus A: Dynamic Meteorology and Oceanography*, **52**, 523–532.
- LEE, Y., MAJDA, A. J. & QI, D. (2017) Preventing catastrophic filter divergence using adaptive additive inflation for baroclinic turbulence. *Monthly Weather Review*, **145**, 669–682.
- LEI, J. & BICKEL, P. (2011) A moment matching ensemble filter for nonlinear non-Gaussian data assimilation. *Monthly Weather Review*, **139**, 3964–3973.
- LEIMKUEHLER, B., MATTHEWS, C. & WEARE, J. (2018) Ensemble preconditioning for markov chain monte carlo simulation. *Statistics and Computing*, **28**, 277–290.
- LI, G. & REYNOLDS, A. C. (2009) An iterative ensemble Kalman filter for data assimilation. Society of Petroleum Engineers, pp. 496–505.
- LIU, Z., STUART, A. & WANG, Y. (2022) Second order ensemble Langevin method for sampling and inverse problems. *arXiv:2208.04506*.
- LIVINGS, D., DANCE, S. & NICHOLS, N. (2008) Unbiased ensemble square root filters. *Physica D*, **237**, 1021–1028.
- LORENZ, E. N. (1996) Predictability: A problem partly solved. *Proc. Seminar on Predictability*, vol. 1. ECMWF.
- LUENBERGER, D. (1971) An introduction to observers. *IEEE Transactions on automatic control*, **16**, 596–602.
- LUENBERGER, D. G. (1964) Observing the state of a linear system. *IEEE transactions on military electronics*, **8**, 74–80.
- MAJDA, A. J. & TONG, X. T. (2018) Performance of ensemble Kalman filters in large dimensions. *Communications on Pure and Applied Mathematics*, **71**, 892–937.
- MANDEL, J., COBB, L. & BEEZLEY, J. (2011) On the convergence of the ensemble Kalman filter. *Appl Math*, **56**, 533–541.
- MCLACHLAN, R. I. & QUISPEL, G. R. W. (2002) Splitting methods. *Acta Numerica*, **11**, 341–434.
- MONDAINI, C. F. & TITI, E. S. (2018) Uniform-in-time error estimates for the postprocessing Galerkin method applied to a data assimilation algorithm. *SIAM Journal on Numerical Analysis*, **56**, 78–110.
- NOTT, D. J., MARSHALL, L. & NGOC, T. M. (2012) The ensemble Kalman filter is an ABC algorithm. *Statistics and Computing*, **22**, 1273–1276.
- NÜSKEN, N. & REICH, S. (2019) Note on interacting Langevin diffusions: Gradient structure and ensemble Kalman sampler by Garbuno-Inigo, Hoffmann, Li and Stuart. *arXiv preprint arXiv:1908.10890*.
- OKSENDAL, B. (2013) *Stochastic differential equations: an introduction with applications*. Springer Science & Business Media.
- OLIVER, D., REYNOLDS, A. & LIU, N. (2008) *Inverse Theory for Petroleum Reservoir Characterization and History Matching*. Cambridge: Cambridge University Press.
- OLIVER, D. S., CUNHA, L. B. & REYNOLDS, A. C. (1997) Markov chain Monte Carlo methods for condi-

- tioning a permeability field to pressure data. *Mathematical Geology*, **29**, 61–91.
- OLSON, E. & TITI, E. S. (2003) Determining modes for continuous data assimilation in 2D turbulence. *Journal of statistical physics*, **113**, 799–840.
- PATHIRAJA, S., REICH, S. & STANNAT, W. (2021) McKean-Vlasov SDEs in nonlinear filtering. *SIAM J Control and Optimization*, **59**, 4188–4212.
- PAVLIOTIS, G., STUART, A. & VAES, U. (2021) Derivative-free Bayesian inversion using multiscale dynamics. *arXiv preprint arXiv:2102.00540*.
- PAVLIOTIS, G. & STUART, A. (2008) *Multiscale methods: Averaging and homogenization*. Springer Science & Business Media.
- PEYRÉ, G., CUTURI, M. *et al.* (2019) Computational optimal transport: With applications to data science. *Foundations and Trends® in Machine Learning*, **11**, 355–607.
- PIDSTRIGACH, J. & REICH, S. (2021) Affine-invariant ensemble transform methods for logistic regression. *arXiv preprint arXiv:2104.08061*.
- PINNAU, R., TOTZECK, C., TSE, O. & MARTIN, S. (2017) A consensus-based model for global optimization and its mean-field limit. *Mathematical Models and Methods in Applied Sciences*, **27**, 183–204.
- PULIDO, M., TANDEO, P., BOCQUET, M., CARRASSI, A. & LUCINI, M. (2018) Stochastic parameterization identification using ensemble Kalman filtering combined with maximum likelihood methods. *Tellus A*, **70**, 1442099.
- REBESCHINI, P. & VAN HANDEL, R. (2015) Can local particle filters beat the curse of dimensionality? *The Annals of Applied Probability*, **25**, 2809–2866.
- REICH, S. (2011) A dynamical systems framework for intermittent data assimilation. *BIT Numerical Mathematics*, **51**, 235–249.
- REICH, S. (2013) A nonparametric ensemble transform method for Bayesian inference. *SIAM J. Sci. Comput.*, **35**, A2013–A2024.
- REICH, S. (2019) Data assimilation: the schrödinger perspective. *Acta Numerica*, **28**, 635–711.
- REICH, S. & COTTER, C. (2015) *Probabilistic forecasting and Bayesian data assimilation*. Cambridge University Press.
- REICH, S. & WEISSMANN, S. (2021) Fokker-Planck particle systems for Bayesian inference: Computational approaches. *SIAM/ASA J. Uncertain. Quantification*, **9**, 446–482.
- ROBINSON, G., GROOMS, I. & KLEIBER, W. (2018) Improving particle filter performance by smoothing observations. *Monthly Weather Review*, **146**, 2433–2446.
- SAKOV, P., OLIVER, D. S. & BERTINO, L. (2012) An iterative EnKF for strongly nonlinear systems. *Mon. Wea. Rev.*, **140**, 1988–2004.
- SAKOV, P. & OKE, P. (2008) A deterministic formulation of the ensemble Kalman filter: An alternative to ensemble square root filters. *Tellus A*, **60**, 361–371.
- SALMAN, H., KUZNETSOV, L., JONES, C. & IDE, K. (2006) A method for assimilating Lagrangian data into a shallow-water-equation ocean model. *Monthly Weather Review*, **134**, 1081–1101.
- SAMPSON, C., CARRASSI, A., AYDOĞDU, A. & JONES, C. K. (2021) Ensemble Kalman filter for nonconservative moving mesh solvers with a joint physics and mesh location update. *Quarterly Journal of the Royal Meteorological Society*, **147**, 1539–1561.
- SANZ-ALONSO, D. & STUART, A. M. (2015) Long-time asymptotics of the filtering distribution for partially observed chaotic dynamical systems. *SIAM/ASA Journal on Uncertainty Quantification*, **3**, 1200–1220.
- SÄRKKÄ, S. (2013) *Bayesian Filtering and Smoothing*. Cambridge: Cambridge University Press.
- SCHILLINGS, C. & STUART, A. M. (2017) Analysis of the ensemble Kalman filter for inverse problems. *SIAM Journal on Numerical Analysis*, **55**, 1264–1290.
- SCHILLINGS, C. & STUART, A. M. (2018) Convergence analysis of ensemble Kalman inversion: The linear, noisy case. *Applicable Analysis*, **97**, 107–123.
- SCHNEIDER, T., LAN, S., STUART, A. M. & TEIXEIRA, J. (2017) Earth system modeling 2.0: A blueprint for models that learn from observations and targeted high-resolution simulations. *Geophysical Research Letters*, **44**, 12–396.
- SISSON, S. A., FAN, Y. & BEAUMONT, M. (2018) *Handbook of approximate Bayesian computation*. CRC Press.
- SNYDER, C., BENGTSSON, T., BICKEL, P. & ANDERSON, J. (2008) Obstacles to high-dimensional particle filtering. *Monthly Weather Review*, **136**, 4629–4640.



- SNYDER, C. (2014) Introduction to the Kalman filter. *Advanced Data Assimilation for Geosciences, Lecture Notes of the Les Houches School of Physics, June 2012*. Oxford University Press.
- SPANTINI, A., BAPTISTA, R. & MARZOUK, Y. (2019a) Coupling techniques for nonlinear ensemble filtering. *arXiv preprint arXiv:1907.00389*.
- SPANTINI, A., BAPTISTA, R. & MARZOUK, Y. (2019b) Coupling techniques for nonlinear ensemble filtering. *arXiv preprint arXiv:1907.00389*.
- STORDAL, A., KARLSEN, H., NÆVDAL, G., SKAUG, H. & VALLÉS, B. (2011) Bridging the ensemble Kalman filter and particle filters: the adaptive Gaussian mixture filter. *Comput. Geosci.*, **15**, 293–305.
- STRANG, G. (1968) On the construction and comparison of difference schemes. *SIAM journal on numerical analysis*, **5**, 506–517.
- STUART, A. M. (2010) Inverse problems: a bayesian perspective. *Acta numerica*, **19**, 451–559.
- TAGHVAEI, A., DE WILJES, J., MEHTA, P. & REICH, S. (2017) Kalman filter and its modern extensions for the continuous-time nonlinear filtering problem. *ASME. J. Dyn. Sys., Meas., Control.*, **140**, 030904–030904–11.
- TAGHVAEI, A., MEHTA, P. & MEYN, S. (2020) Diffusion map-based algorithm for gain function approximation in the feedback particle filter. *SIAM/ASA J. Uncertain. Quantif.*, **8**, 1090–1117.
- TAGHVAEI, A. & HOSSEINI, B. (2022) An optimal transport formulation of bayes’ law for nonlinear filtering algorithms. *arXiv preprint arXiv:2203.11869*.
- TAGHVAEI, A. & MEHTA, P. G. (2020) An optimal transport formulation of the ensemble kalman filter. *IEEE Transactions on Automatic Control*, **66**, 3052–3067.
- TIPPETT, M., ANDERSON, J., BISHOP, C., HAMILL, T. & WHITAKER, J. (2003) Ensemble square root filters. *Mon. Weather Rev.*, 1485–1490.
- TÖDTER, J. & AHRENS, B. (2015) A second-order exact ensemble square root filter for nonlinear data assimilation. *Mon. Wea. Rev.*, **143**, 1347–1367.
- TONG, X. T., MAJDA, A. J. & KELLY, D. (2015) Nonlinear stability of the ensemble Kalman filter with adaptive covariance inflation. *arXiv preprint arXiv:1507.08319*.
- TONG, X. T., MAJDA, A. J. & KELLY, D. (2016) Nonlinear stability and ergodicity of ensemble based Kalman filters. *Nonlinearity*, **29**, 657.
- TSIANOS, K. I., LAWLOR, S. & RABBAT, M. G. (2012) Consensus-based distributed optimization: Practical issues and applications in large-scale machine learning. *2012 50th annual allerton conference on communication, control, and computing (allerton)*. IEEE, pp. 1543–1550.
- VAN LEEUWEN, P., KÜNSCH, H., NERGER, L., POTTHAST, R. & REICH, S. (2019) Particle filters for high-dimensional geoscience applications: A review. *Q. J. Royal Meteorol. Soc.*, **145**, 2335–2365.
- VAN LEEUWEN, P. J. (2020) A consistent interpretation of the stochastic version of the Ensemble Kalman filter. *Quarterly Journal of the Royal Meteorological Society*, **146**, 2815–2825.
- VAN LEEUWEN, P. J. & EVENSEN, G. (1996) Data assimilation and inverse methods in terms of a probabilistic formulation. *Monthly Weather Review*, **124**, 2898–2913.
- VANDEN-EIJNDEN, E. *et al.* (2003) Fast communications: Numerical techniques for multi-scale dynamical systems with stochastic effects. *Communications in Mathematical Sciences*, **1**, 385–391.
- VILLANI, C. (2008) *Optimal transport: Old and new*, vol. 338. Springer Science & Business Media.
- VILLANI, C. (2021) *Topics in optimal transportation*, vol. 58. American Mathematical Soc.
- WANG, X., BISHOP, C. & JULIER, S. (2004) Which is better, an ensemble of positive-negative pairs or a centered spherical simplex ensemble? *Monthly Weather Review*, **132**, 1590–1605.
- WELCH, G., BISHOP, G. *et al.* (1995) An introduction to the Kalman filter.
- WHITAKER, J. & HAMILL, T. (2002) Ensemble data assimilation without perturbed observations. *Monthly Weather Review*, **130**, 1913–1924.
- YANG, L. M. & GROOMS, I. (2021) Machine learning techniques to construct patched analog ensembles for data assimilation. *arXiv preprint arXiv:2103.00318*.
- YANG, T., MEHTA, P. G. & MEYN, S. P. (2013) Feedback particle filter. *IEEE Trans. Automat. Control*, **58**, 2465–2480.
- YANG, T., BLUM, H. A. P. & MEHTA, P. G. (2014) The continuous-discrete time feedback particle filter. *IEEE*, pp. 648–653.
- ZECH, J. & MARZOUK, Y. (2022) Sparse approximation of triangular transports, part I: The finite-dimensional case. *Constructive Approximation*, **55**, 919–986.

ZHANG, C., TAGHVAEI, A. & MEHTA, P. G. (2017) A controlled particle filter for global optimization. *Technical Report*. arXiv:1701.02413.

ZUPANSKI, M. (2005) Maximum likelihood ensemble filter: Theoretical aspects. *Mon. Weath. Rev.*, **133**, 1710–1726.

**6. Appendix A (Pseudo-Code).** In this appendix we provide pseudo-code describing several of the algorithms that we present and deploy in this paper. Algorithms 6.1 and 6.2, 3DVAR and the ensemble Kalman filter (EnKF) respectively, are presented in the context of the problem of state estimation for discrete time dynamical systems presented in Section 2. The scheme 3DVAR is employed in Examples 2.1, 2.2, 2.3 and 2.10. The ensemble Kalman filter is applied in the context of Example 2.10. Ensemble Kalman methods for inversion, as shown in Algorithms 6.3, 6.4 and 6.5, are presented in Section 4 and applied in the context of Example 4.21. We refer to Algorithm 6.3 as Ensemble Kalman Inversion (Transport), as it arises from the approach to inversion described in Subsection 4.2; we refer to Algorithm 6.4 as Ensemble Kalman Inversion (Iteration to Infinity), as it arises from the approach to inversion described in Subsection 4.4; Algorithm 6.5 corresponds to particular cases of Algorithms 6.3 and 6.4 where they coincide as explained in Subsection 4.5.

---

**Algorithm 6.1** 3DVAR

---

**Input:** Initial  $v_0 \in \mathbb{R}^{d_v}$  and fixed gain matrix  $K \in \mathbb{R}^{d_v \times d_y}$ .

**for**  $n = 0$  to  $N - 1$  **do**

**Prediction:**

$$\hat{v}_{n+1} = \Psi(v_n).$$

**Analysis:**

$$v_{n+1} = \hat{v}_{n+1} + K \left( y_{n+1}^\dagger - h(\hat{v}_{n+1}) \right).$$

**end for**

**Output:** Estimates  $\{v_n\}_{n=0}^N$ .

---

**7. Appendix B (Lorenz '96 Multiscale).** To illustrate the problems of both state estimation and parameter estimation we use, throughout this paper, variants on the Lorenz '96 model. In particular we use both the Lorenz '96 multiscale system and a singlescale closure derived from it in the scale-separated case; see Subsection 2.7, and the developments in this section, for bibliographic details. If we generate data with the singlescale model, and assimilate using this model, we are able to test algorithms in their basic (perfect model) form. If we generate data with the multiscale model, and assimilate using the singlescale model, this will also allow us to study the effect of model misspecification on data assimilation.

**7.1. Lorenz '96 Multiscale Model.** Let  $v \in C(\mathbb{R}^+, \mathbb{R}^L)$  and  $w \in C(\mathbb{R}^+, \mathbb{R}^{L \times J})$ . Each variable  $v_\ell \in \mathbb{R}$  is coupled to a subgroup of fast variables  $\{w_{\ell,j}\}_{j=1}^J \in \mathbb{R}^J$ . For  $\ell = 1 \dots L$  and  $j = 1 \dots J$ , the multiscale model is defined by equations (2.11) and (2.12); the boundary conditions (2.13) complete definition of the equations and provide further couplings beyond those in the differential equations themselves. Here  $\epsilon > 0$  is a scale-separation parameter,  $h_v, h_w \in \mathbb{R}$  govern the couplings between the fast and slow systems, and  $F > 0$  provides a constant forcing.

**Algorithm 6.2** EnKF

**Input:** Ensemble size  $J$ , initial ensemble  $\{v_0^{(j)}\}_{j=1}^J$ .

**for**  $n = 0$  to  $N - 1$  **do**

**Prediction:** for  $j = 1, \dots, J$  **do**

$$\begin{aligned}\xi_n^{(j)} &\sim \mathcal{N}(0, \Sigma), \quad \eta_n^{(j)} \sim \mathcal{N}(0, \Gamma) \\ \hat{v}_{n+1}^{(j)} &= \Psi(v_n^{(j)}) + \xi_n^{(j)}, \\ \hat{y}_{n+1}^{(j)} &= h(\hat{v}_{n+1}^{(j)}) + \eta_n^{(j)}.\end{aligned}$$

    Compute

$$\begin{aligned}\hat{m}_{n+1} &= \frac{1}{J} \sum_{j=1}^J \hat{v}_{n+1}^{(j)}, \quad \hat{o}_{n+1} = \frac{1}{J} \sum_{j=1}^J h(\hat{v}_{n+1}^{(j)}), \\ \hat{C}_{n+1}^{vh} &= \frac{1}{J} \sum_{j=1}^J (\hat{v}_{n+1}^{(j)} - \hat{m}_{n+1}) \otimes (\hat{v}_{n+1}^{(j)} - \hat{o}_{n+1}), \\ \hat{C}_{n+1}^{hh} &= \frac{1}{J} \sum_{j=1}^J (\hat{v}_{n+1}^{(j)} - \hat{o}_{n+1}) \otimes (\hat{v}_{n+1}^{(j)} - \hat{o}_{n+1}), \\ K_{n+1} &= \hat{C}_{n+1}^{vh} (\hat{C}_{n+1}^{hh} + \Gamma)^{-1}.\end{aligned}$$

**Analysis:** for  $j = 1, \dots, J$  **do**

$$v_{n+1}^{(j)} = \hat{v}_{n+1}^{(j)} + K_{n+1} (y_{n+1}^{(j)} - h(\hat{v}_{n+1}^{(j)})).$$

**end for**

**Output:** Ensembles  $\{v_n^{(j)}\}_{j=1}^J$  for  $n = 0, \dots, N$ .

**7.2. Lorenz '96 Singlescale Model.** If  $\epsilon \ll 1$  then the dynamics for the  $w = \{w_{\ell,j}\}$  governed (2.11b) evolve on a much faster timescale than the dynamics for the  $v = \{v_\ell\}$  governed by (2.11a). Thus it is a reasonable approximation to think of  $v$  as frozen in (2.11b). In the following let  $\bar{w} = \{\bar{w}_\ell\}$ . If we assume that the dynamics of  $w$  with  $v$  frozen is ergodic with invariant measure  $\mu^v(dw)$  (a measure in  $w$ , parameterized by  $v$ ) then the averaging principle Vanden-Eijnden *et al.* (2003); Abdulle *et al.* (2012); Pavliotis & Stuart (2008) suggests that we may make the approximation

$$\bar{w} \approx M(v) := \int \bar{w} \mu^v(dw).$$

If we also invoke the approximation  $M_\ell(v) \approx m(v_\ell)$ , which is shown to be valid for large  $J$  in Fatkullin & Vanden-Eijnden (2004), then we arrive at the singlescale Lorenz '96 model (2.6). This program of analysis for the Lorenz '96 model, and studies of the validity of the resulting

**Algorithm 6.3** Ensemble Kalman Inversion (Transport)

**Input:** Data  $w$ ,  $N$  and  $\Delta t$  such that  $N\Delta t = 1$ , ensemble size  $J$ , initial ensemble  $\{u_0^{(j)}\}_{j=1}^J$ .  
**for**  $n = 0$  to  $N - 1$  **do**

**Prediction:** for  $j = 1, \dots, J$  **do**

$$\begin{aligned}\eta_n^{(j)} &\sim \mathcal{N}\left(0, \frac{\Gamma}{\Delta t}\right) \\ \hat{u}_{n+1}^{(j)} &= u_n^{(j)} \\ \hat{w}_{n+1}^{(j)} &= w + \eta_n^{(j)}.\end{aligned}$$

    Compute

$$\begin{aligned}\hat{m}_{n+1} &= \frac{1}{J} \sum_{j=1}^J \hat{u}_{n+1}^{(j)}, \quad \hat{o}_{n+1} = \frac{1}{J} \sum_{j=1}^J G(\hat{u}_{n+1}^{(j)}), \\ \hat{C}_{n+1}^{uG} &= \frac{1}{J} \sum_{j=1}^J (\hat{u}_{n+1}^{(j)} - \hat{m}_{n+1}) \otimes (G(\hat{u}_{n+1}^{(j)}) - \hat{o}_{n+1}), \\ \hat{C}_{n+1}^{GG} &= \frac{1}{J} \sum_{j=1}^J (G(\hat{u}_{n+1}^{(j)}) - \hat{o}_{n+1}) \otimes (G(\hat{u}_{n+1}^{(j)}) - \hat{o}_{n+1}).\end{aligned}$$

**Analysis:** for  $j = 1, \dots, J$  **do**

$$u_{n+1}^{(j)} = \hat{u}_{n+1}^{(j)} + \Delta t \hat{C}_{n+1}^{uG} \left( \Delta t \hat{C}_{n+1}^{GG} + \Gamma \right)^{-1} (\hat{w}_{n+1}^{(j)} - G(\hat{u}_{n+1}^{(j)})).$$

**end for**

**Output:** Ensembles  $\{u_n^{(j)}\}_{j=1}^J$  for  $n = 0, \dots, N$ .

singlescale approximation, was established in the paper [Fatkullin & Vanden-Eijnden \(2004\)](#). The function  $m(\cdot)$  is not given explicitly, but may be fit to data in various different ways, as explained in [Fatkullin & Vanden-Eijnden \(2004\)](#). Figure 2.1 shows such an  $m$ , fit using Gaussian process regression methodology as detailed in Subsection 4.3 of [Burov \*et al.\* \(2021\)](#).

**8. Appendix C (Mean Field Maps).** In Subsection 8.1 we discuss the existence, form and properties of mean field maps which carry out the program of approximate transport described in Subsection 2.5.3; these maps require access to simulated data and are hence referred as stochastic second order transport maps. In Subsection 8.2 we discuss the existence, form and properties of mean field maps which carry out the program of approximate transport described in Subsection 2.5.4; these maps do not require access to simulated data and are hence referred as deterministic second order transport maps. The two approaches provide fundamental underpinnings of ensemble Kalman methods as we develop them here, but were

**Algorithm 6.4** Ensemble Kalman Inversion (Iteration to Infinity)

**Input:** Data  $w$ ,  $N$ ,  $\alpha \in (0, 1)$ ,  $r_0$ ,  $\sigma', \gamma'$  ensemble size  $J$ , initial ensemble  $\{u_0^{(j)}\}_{j=1}^J$ .

**for**  $n = 0$  to  $N - 1$  **do**

**Prediction:** for  $j = 1, \dots, J$  **do**

$$\begin{aligned}\xi_n^{(j)} &\sim \mathcal{N}(0, \sigma' \Sigma), \quad \eta_n^{(j)} \sim \mathcal{N}(0, \gamma' \Gamma) \\ \hat{u}_{n+1}^{(j)} &= \alpha u_n^{(j)} + (1 - \alpha) r_0 + \xi_n^{(j)} \\ \hat{w}_{n+1}^{(j)} &= w + \eta_n^{(j)}.\end{aligned}$$

**Compute**

$$\begin{aligned}\hat{m}_{n+1} &= \frac{1}{J} \sum_{j=1}^J \hat{u}_{n+1}^{(j)}, \quad \hat{o}_{n+1} = \frac{1}{J} \sum_{j=1}^J G(\hat{u}_{n+1}^{(j)}), \\ \hat{C}_{n+1}^{uG} &= \frac{1}{J} \sum_{j=1}^J (\hat{u}_{n+1}^{(j)} - \hat{m}_{n+1}) \otimes (G(\hat{u}_{n+1}^{(j)}) - \hat{o}_{n+1}), \\ \hat{C}_{n+1}^{GG} &= \frac{1}{J} \sum_{j=1}^J (G(\hat{u}_{n+1}^{(j)}) - \hat{o}_{n+1}) \otimes (G(\hat{u}_{n+1}^{(j)}) - \hat{o}_{n+1}).\end{aligned}$$

**Analysis:** for  $j = 1, \dots, J$  **do**

$$u_{n+1}^{(j)} = \hat{u}_{n+1}^{(j)} + \hat{C}_{n+1}^{uG} \left( \hat{C}_{n+1}^{GG} + \gamma' \Gamma \right)^{-1} (\hat{w}_{n+1}^{(j)} - G(\hat{u}_{n+1}^{(j)})).$$

**end for**

**Output:** Ensembles  $\{u_n^{(j)}\}_{j=1}^J$  for  $n = 0, \dots, N$ .

not adopted in its historical development. Subsection 8.3 is devoted to the minimum variance approximation, a way of deriving the Kalman transport map (2.46), which is part of the historical development of the subject, but which does not play a central role in our presentation and analysis of the subject.

We note that the maps of interest in Subsection 8.1 take  $\text{Law}(\hat{v}_{n+1}, \hat{y}_{n+1})$  into  $\text{Law}(v_{n+1})$  and hence we may drop the subscript  $n + 1$  throughout the analysis. Similar considerations apply in Subsection 8.2 and in Subsection 8.3.

**8.1. Mean Field Maps – Simulated Data.** Let  $(\hat{v}, \hat{y}) \sim \nu$  where

$$G\nu = \mathcal{N}\left(\begin{bmatrix} \hat{m} \\ \hat{o} \end{bmatrix}, \begin{bmatrix} \hat{C} & \hat{C}^{vy} \\ (\hat{C}^{vy})^\top & \hat{C}^{yy} \end{bmatrix}\right).$$

**Algorithm 6.5** Ensemble Kalman Inversion (Transport and Iteration to Infinity)

**Input:** Data  $w$ , ensemble size  $J$ , initial ensemble  $\{u_0^{(j)}\}_{j=1}^J$ .

**for**  $n = 0$  to  $N - 1$  **do**

**Prediction:** for  $j = 1, \dots, J$  **do**

$$\begin{aligned}\eta_n^{(j)} &\sim \mathcal{N}(0, \Gamma) \\ \hat{u}_{n+1}^{(j)} &= u_n^{(j)} \\ \hat{w}_{n+1}^{(j)} &= w + \eta_n^{(j)}.\end{aligned}$$

    Compute

$$\begin{aligned}\hat{m}_{n+1} &= \frac{1}{J} \sum_{j=1}^J \hat{u}_{n+1}^{(j)}, \quad \hat{o}_{n+1} = \frac{1}{J} \sum_{j=1}^J G(\hat{u}_{n+1}^{(j)}), \\ \hat{C}_{n+1}^{uG} &= \frac{1}{J} \sum_{j=1}^J (\hat{u}_{n+1}^{(j)} - \hat{m}_{n+1}) \otimes (G(\hat{u}_{n+1}^{(j)}) - \hat{o}_{n+1}), \\ \hat{C}_{n+1}^{GG} &= \frac{1}{J} \sum_{j=1}^J (G(\hat{u}_{n+1}^{(j)}) - \hat{o}_{n+1}) \otimes (G(\hat{u}_{n+1}^{(j)}) - \hat{o}_{n+1}).\end{aligned}$$

**Analysis:** for  $j = 1, \dots, J$  **do**

$$u_{n+1}^{(j)} = \hat{u}_{n+1}^{(j)} + \hat{C}_{n+1}^{uG} \left( \hat{C}_{n+1}^{GG} + \Gamma \right)^{-1} (\hat{w}_{n+1}^{(j)} - G(\hat{u}_{n+1}^{(j)})).$$

**end for**

**Output:** Ensembles  $\{u_n^{(j)}\}_{j=1}^J$  for  $n = 0, \dots, N$ .

Define

(8.1a)

$$m = \hat{m} + \hat{C}^{vy} (\hat{C}^{yy})^{-1} (y^\dagger - \hat{o}),$$

(8.1b)

$$C = \hat{C} - \hat{C}^{vy} (\hat{C}^{yy})^{-1} (\hat{C}^{vy})^\top.$$

Note that these are the mean and covariance of the Gaussian random variable  $\hat{v}$  conditioned on  $\hat{y} = y^\dagger$  under Gaussian measure  $G\nu$ ; see (2.30). The quantities in the above identities are as defined in Subsection 2.3.2, with the exception that the subscripts  $n+1$  have been dropped for clarity of exposition.

Our goal is to identify maps of the form

$$(8.2) \quad v = A\hat{v} + B\hat{y} + a$$

so that, if  $(\hat{v}, \hat{y}) \sim \nu$ , then  $v$  has mean  $m$  and covariance  $C$  given by (8.1). We make the following assumptions on the covariance under  $G\nu$  and on the matrices  $A, B$  and vector  $a$ :

*Assumptions 8.1.* The covariance under  $G\nu$  is invertible. The matrices  $A, B$  and vector  $a$  may depend on  $y^\dagger$  and measure  $\nu$  but not on the random variables  $(\hat{v}, \hat{y})$ . ■

Recall the discussion of pushforward of measures in the introduction to Subsection 2.5. Under Assumptions 8.1 pushforward under the map (8.2), when chosen to match the desired first and second order statistics, defines a nonlinear map on the space of measures, and in particular on  $\nu$  itself. In what follows all expectations are computed under  $\nu$ . Since the covariance under  $G\nu$  is strictly positive-definite so are the marginal covariances  $\hat{C}$  and  $\hat{C}^{yy}$  (see Stuart (2010)[Lemma 6.21]). Thus we may define the conditional mean and covariance by (8.1), as well as Kalman gain  $K$ , and conditional covariance  $\tilde{C}$ , given by

$$K = \hat{C}^{vy}(\hat{C}^{yy})^{-1},$$

$$\tilde{C} = \hat{C}^{yy} - (\hat{C}^{vy})^\top (\hat{C})^{-1} \hat{C}^{vy};$$

we note that the conditional covariances  $C$  and  $\tilde{C}$  are also strictly positive-definite (see Stuart (2010)[Lemma 6.21]). From equations (8.1a) and (8.2) the following is immediate:

*Lemma 8.2.* Let Assumptions 8.1 hold and let  $(\hat{v}, \hat{y}) \sim \nu$ . If  $v$  given by (8.2) has mean given by (8.1a) then

$$a = (I - A)\mathbb{E}\hat{v} + Ky^\dagger - (B + K)\mathbb{E}\hat{y}.$$

As a consequence it follows that

$$(8.3) \quad v = \mathbb{E}\hat{v} + A(\hat{v} - \mathbb{E}\hat{v}) + B(\hat{y} - \mathbb{E}\hat{y}) + K(y^\dagger - \mathbb{E}\hat{y}).$$

and that

$$\mathbb{E}\left((v - \mathbb{E}v) \otimes (v - \mathbb{E}v)\right) = A\hat{C}A^\top + B\hat{C}^{yy}B^\top + A\hat{C}^{vy}B^\top + B(\hat{C}^{vy})^\top A.$$

Thus, to match the covariance of the conditioned random variable, we obtain

$$(8.4) \quad C = A\hat{C}A^\top + B\hat{C}^{yy}B^\top + A\hat{C}^{vy}B^\top + B(\hat{C}^{vy})^\top A.$$

*Theorem 8.3.* Let Assumptions 8.1 hold and let  $(\hat{v}, \hat{y}) \sim \nu$ . If  $a$  is given by Lemma 8.2 then  $v$  defined by (8.2) has covariance (8.1b) if and only if real-valued matrices  $A$  and  $B$  are related by the identity

$$(8.5) \quad F\hat{C}^{-1}F^\top = C - B\tilde{C}B^\top,$$

where

$$(8.6) \quad F = A\hat{C} + B(\hat{C}^{vy})^\top.$$

*Proof.* We complete the square on the right hand side of (8.4) to obtain

$$(A\hat{C} + B(\hat{C}^{vy})^\top)\hat{C}^{-1}(A\hat{C} + B(\hat{C}^{vy})^\top)^\top = C'.$$

where

$$C' = C - B\tilde{C}B^\top.$$

Rearranging gives the desired result. ■

Define

$$\mathcal{B} = \{B \in \mathbb{R}^{d_v \times d_y} : C' \succ 0\},$$

noting that this set is non-empty, and contains an open (and hence uncountable) set of  $B$ , since  $C \succ 0$ . For  $B \in \mathcal{B}$  consider the eigenvalue problem

$$\begin{aligned} C' \varphi^{(i)} &= (s^{(i)})^2 \varphi^{(i)}, \\ \langle \varphi^{(i)}, \varphi^{(j)} \rangle &= \delta_{ij}. \end{aligned}$$

Note that this has  $d_v$  real solutions, up to sign changes in the eigenvectors and assuming the  $s^{(i)}$  to be non-negative. We now seek to express  $F$  in terms of  $B \in \mathcal{B}$ . Writing the SVD  $F\hat{C}^{-\frac{1}{2}} = U\Sigma V^\top$ , where  $U, V \in \mathbb{R}^{d_v \times d_v}$  are orthogonal matrices and  $\Sigma \in \mathbb{R}^{d_v \times d_v}$  is a diagonal matrix, we see from (8.5) that

$$U\Sigma^2U^\top = C'$$

so that  $U$  has columns given by the  $\{\varphi^{(i)}\}_{i=1}^{d_v}$  and corresponding diagonal entries of  $\Sigma$ ,  $\pm s^{(i)}$ . We define

$$(8.7) \quad U = (\varphi^{(1)}, \dots, \varphi^{(d_v)}), \quad \Sigma = \text{diag}(\pm s^{(1)}, \dots, \pm s^{(d_v)}).$$

**Corollary 8.4.** *For every  $B \in \mathcal{B}$  the choices of  $A$  such that the pair  $(A, B)$  satisfies the criterion of Theorem 8.3 are defined as follows. For  $U, \Sigma$  as given in (8.7), set*

$$F = U\Sigma V^\top \hat{C}^{\frac{1}{2}}$$

where  $V$  is an arbitrary orthogonal matrix in  $\mathbb{R}^{d_v \times d_v}$ . Then

$$A = \left(F - B(\hat{C}^{vy})^\top\right) \hat{C}^{-1}.$$

**Example 8.5.** Among the uncountably many possible solutions for pairs  $(A, B)$  we highlight two. The choice  $B = 0$  is interesting because it does not require the data variable  $\hat{y}$  in the definition of  $v$ . The choice  $A = I$  is interesting because it does not require action of an operator acting on  $\hat{v}$ .

The first, with  $B = 0$ , allows the choice  $F = C^{\frac{1}{2}} \hat{C}^{\frac{1}{2}}$  and then  $A = C^{\frac{1}{2}} \hat{C}^{-\frac{1}{2}}$ . Thus the map (8.3) becomes

$$\begin{aligned} v &= \mathbb{E}\hat{v} + C^{\frac{1}{2}} \hat{C}^{-\frac{1}{2}} (\hat{v} - \mathbb{E}\hat{v}) + \hat{C}^{vy} (\hat{C}^{yy})^{-1} (y^\dagger - \mathbb{E}\hat{y}) \\ &= m + C^{\frac{1}{2}} \hat{C}^{-\frac{1}{2}} (\hat{v} - \mathbb{E}\hat{v}). \end{aligned}$$

The second comes from setting  $B = -K$  which leads to the possible choice  $F = C$  and  $A = I$  under which the map (8.3) becomes

$$v = \hat{v} + \hat{C}^{vy} (\hat{C}^{yy})^{-1} (y^\dagger - \hat{y}).$$

We refer to this as the *Kalman transport* solution. ■



Given the plethora of solutions for matrices  $(A, B)$ , all of which effect the desired measure transport from  $\nu$  into the conditional, it is natural to ask how to choose a specific pair  $(A, B)$ . One possibility is to use optimal transport. To this end we define, for positive definite  $W \in \mathbb{R}^{d_v \times d_v}$ ,

$$I_W(A, B) = \frac{1}{2} \mathbb{E} \langle (v - \hat{v}), W(v - \hat{v}) \rangle.$$

**Theorem 8.6.** *Let  $v$  be given by (8.3). Consider the problem of finding minimizers of  $I_W(A, B)$  over pairs  $(A, B)$  satisfying (8.5), (8.6); we refer to the resulting map evaluated at such an  $(A, B)$  as an optimal transport in the  $W$ -weighted Euclidean distance. For any positive definite  $W$ , such minimizers satisfy  $B = 0$ . In particular the Kalman transport solution is not an optimal transport solution.*

*Proof.* We formulate the optimization problem over the pair  $(F, B)$  since, because  $\hat{C}$  is invertible, there is a bijection between  $(A, B)$  and  $(F, B)$ . Let  $:$  denotes the Frobenius inner-product. Then, under constraint (8.6),

$$(8.8a) \quad I_W(A, B) = J_W(F) + \text{const},$$

$$(8.8b) \quad J_W(F) = -F : W,$$

where  $\text{const}$  denotes a matrix independent of  $A, B, F$  (with exact value changing from instance to instance.) To see this note that

$$v - \hat{v} = -(\hat{v} - \mathbb{E}\hat{v}) + A(\hat{v} - \mathbb{E}\hat{v}) + B(\hat{y} - \mathbb{E}\hat{y}) + K(y^\dagger - \mathbb{E}\hat{y}).$$

Now, using (8.4),

$$\mathbb{E} \left( (v - \hat{v}) \otimes (v - \hat{v}) \right) = \hat{C} - \hat{C}A^\top - A\hat{C} - \hat{C}^{vy}B^\top - B(\hat{C}^{vy})^\top + C + \text{const}.$$

Noting that

$$I_W(A, B) = \frac{1}{2} \mathbb{E} \left( (v - \hat{v}) \otimes (v - \hat{v}) \right) : W,$$

and that  $D : W = D^\top : W$  for all  $D$  since  $W$  is symmetric, identity (8.8) follows from (8.6). It then also follows that minimization of  $I_W(A, B)$  subject to the constraints given by (8.5), (8.6) is equivalent to minimization of  $J_W(F)$  subject to the constraint (8.5).

To effect this latter minimization we introduce the Lagrange multiplier  $L \in \mathbb{R}^{d_v \times d_v}$ , symmetric because the constraint is symmetric, and define

$$\tilde{J}_W(F, B, L) = -F : W + L : (F\hat{C}^{-1}F^\top + B\tilde{C}B^\top - C).$$

Differentiating with respect to  $F, B$  and  $L$  respectively gives

$$(8.9a) \quad -W + 2LF\hat{C}^{-1} = 0,$$

$$(8.9b) \quad 2LB\tilde{C} = 0,$$

$$(8.9c) \quad F\hat{C}^{-1}F^\top + B\tilde{C}B^\top = C.$$

Since  $F$ ,  $W$ , and  $\hat{C}$  in (8.9a) are all invertible, the Lagrange multiplier  $L$  is necessarily invertible. Furthermore, since  $\tilde{C}$  is invertible because  $\Sigma$  is, it follows from (8.9b) that  $B = 0$  as required. ■

**Example 8.7.** Define matrix  $S$ , and from it  $A$ , by

$$S = \left( C^{\frac{1}{2}} \hat{C} C^{\frac{1}{2}} \right)^{-\frac{1}{2}}, \quad A = C^{\frac{1}{2}} S C^{\frac{1}{2}}.$$

We notice that if  $B = 0$ , as required for an optimal transport solution, then equation (8.9c) has as a solution  $F = A\hat{C}$  and then (8.9a) delivers the Lagrange multiplier  $L$ . Note further that the solution is independent of the specific choice of positive-definite  $W$ . ■

**8.2. Mean Field Maps – No Simulated Data.** Let  $\hat{v} \sim \hat{\mu}$  and assume that  $\hat{y} = h(\hat{v}) + \eta$  where  $\eta \sim \mathcal{N}(0, \Gamma)$  is independent of  $\hat{v}$ . Implicitly we have defined the joint distribution  $\nu$  of  $(\hat{v}, \hat{y})$ . We note that then, expressed in terms of  $\hat{h} := h(\hat{v})$  and quantities defined in (8.1),

$$\begin{aligned} \hat{C}^{vh} &:= \mathbb{E}(\hat{v} - \mathbb{E}\hat{v}) \otimes (\hat{h} - \mathbb{E}\hat{h}) = \hat{C}^{vy}, \\ \hat{C}^{hh} &:= \mathbb{E}(\hat{h} - \mathbb{E}\hat{h}) \otimes (\hat{h} - \mathbb{E}\hat{h}) = \hat{C}^{yy} - \Gamma. \end{aligned}$$

Thus we may rewrite (8.1) as

$$\begin{aligned} (8.10a) \quad m &= \hat{m} + \hat{C}^{vh}(\hat{C}^{hh} + \Gamma)^{-1}(y^\dagger - \mathbb{E}\hat{h}), \\ (8.10b) \quad C &= \hat{C} - \hat{C}^{vh}(\hat{C}^{hh} + \Gamma)^{-1}(\hat{C}^{vh})^\top, \end{aligned}$$

We have now eliminated reference to  $\hat{y}$  and our goal is to identify maps of the form

$$(8.11) \quad v = R\hat{v} + S\hat{h} + r$$

so that, if  $\hat{v} \sim \hat{\mu}$ , then  $v$  has mean  $m$  and covariance  $C$  given by (8.10). We make the following assumptions on the covariance under  $G\nu$  and on the matrices  $R, S$  and vector  $r$ :

**Assumptions 8.8.** The covariance under  $G\nu$  is invertible. The matrices  $R, S$  and vector  $r$  may depend on  $y^\dagger$  and measure  $\hat{\mu}$  but not on the random variable  $(\hat{v}, \hat{h})$ . ■

With these assumptions the pushforward under map (8.2), when constrained to match the desired first and second order statistics, defines a nonlinear map on the space of measures, and in particular on measure  $\hat{\mu}$ . In what follows all expectations are computed under  $\hat{\mu}$ . We note that matrix  $\hat{C}$  is invertible and that  $K$  in (8.1) may be rewritten as

$$(8.12) \quad K = \hat{C}^{vh}(\hat{C}^{hh} + \Gamma)^{-1}.$$

From equations (8.10a) and (8.11) the following is immediate:

**Lemma 8.9.** *Let Assumptions 8.8 hold and let  $\hat{v} \sim \hat{\mu}$ . If  $v$  given by (8.11) has mean given by (8.10a) then*

$$r = (I - R)\mathbb{E}\hat{v} + Ky^\dagger - (S + K)\mathbb{E}\hat{h}.$$

As a consequence it follows that

$$(8.13) \quad v = \mathbb{E}\hat{v} + R(\hat{v} - \mathbb{E}\hat{v}) + S(\hat{h} - \mathbb{E}\hat{h}) + K(y^\dagger - \mathbb{E}\hat{h}).$$

and that

$$(8.14) \quad \mathbb{E}\left((v - \mathbb{E}v) \otimes (v - \mathbb{E}v)\right) = R\hat{C}R^\top + S\hat{C}^{hh}S^\top + R\hat{C}^{vh}S^\top + S(\hat{C}^{vh})^\top R.$$

Thus, to match the covariance of the conditioned random variable, we obtain

$$(8.15) \quad C = R\hat{C}R^\top + S\hat{C}^{hh}S^\top + R\hat{C}^{vh}S^\top + S(\hat{C}^{vh})^\top R.$$

Define

$$\check{C} = \hat{C}^{hh} - (\hat{C}^{vh})^\top (\hat{C})^{-1} \hat{C}^{vh}.$$

**Theorem 8.10.** *Let Assumptions 8.8 hold and let  $\hat{v} \sim \hat{\mu}$ . If  $s$  is given by Lemma 8.9 then  $v$  defined by (8.11) has covariance (8.10b) if and only if real-valued matrices  $R$  and  $S$  are related by the identity*

$$E\hat{C}^{-1}E^\top = C - S\check{C}S^\top,$$

where

$$E = R\hat{C} + S(\hat{C}^{vh})^\top.$$

*Proof.* We complete the square on the right hand side of (8.15) to obtain

$$(R\hat{C} + S(\hat{C}^{vh})^\top)\hat{C}^{-1}(R\hat{C} + S(\hat{C}^{vh})^\top)^\top + S\check{C}S^\top = C.$$

Rearranging gives the desired result. ■

Define

$$\mathcal{S} = \{S \in \mathbb{R}^{d_v \times d_y} : C - S\check{C}S^\top \succ 0\}$$

and, for  $S \in \mathcal{S}$  consider the eigenvalue problem

$$\begin{aligned} (C - S\check{C}S^\top)\psi^{(i)} &= (o^{(i)})^2\psi^{(i)}, \\ \langle \psi^{(i)}, \psi^{(j)} \rangle &= \delta_{ij}. \end{aligned}$$

noting that this has  $d_v$  real solutions, upto sign changes in the eigenvectors and assuming the  $o^{(i)}$  to be non-negative. We now seek to express  $E$  in terms of  $S \in \mathcal{S}$ . Writing the SVD  $E\hat{C}^{-\frac{1}{2}} = W\Omega Z^\top$ , where  $W, Z \in \mathbb{R}^{d_v \times d_v}$  are orthogonal matrices and  $\Omega \in \mathbb{R}^{d_v \times d_v}$  is a diagonal matrix, we see from (8.5) that

$$W\Omega^2W^\top = C - S\check{C}S^\top$$

so that  $W$  has columns given by the  $\{\psi^{(i)}\}_{i=1}^{d_v}$  and corresponding diagonal entries of  $\Omega$ ,  $\pm o^{(i)}$ . We define

$$(8.17) \quad W = (\psi^{(1)}, \dots, \psi^{(d_v)}), \quad \Omega = \text{diag}(\pm o^{(1)}, \dots, \pm o^{(d_v)}).$$

**Corollary 8.11.** *For every  $S \in \mathcal{S}$  the choices of  $R$  such that the pair  $(R, S)$  satisfies the criterion of Theorem 8.10 are defined as follows. For  $W, \Omega$  as given in (8.17), set*

$$E = W\Omega Z^\top \widehat{C}^{\frac{1}{2}}$$

where  $Z$  is an arbitrary orthogonal matrix in  $\mathbb{R}^{d_v \times d_v}$ . Then

$$R = \left( E - S(\widehat{C}^{vh})^\top \right) \widehat{C}^{-1}.$$

**Example 8.12.** As in Example 8.5 we highlight two examples, here corresponding to  $S = 0$  and to  $R = I$ . The first, with  $S = 0$ , allows the choice  $E = C^{\frac{1}{2}} \widehat{C}^{\frac{1}{2}}$  and hence  $R = C^{\frac{1}{2}} \widehat{C}^{-\frac{1}{2}}$ . We thus obtain (8.5) again.

The second comes from setting  $R = I$ . This leads from (8.14) to the following equation for  $S$ :

$$S\widehat{C}^{hh}S^\top + \widehat{C}^{vh}S^\top + S(\widehat{C}^{vh})^\top = -\widehat{C}^{vh}(\widehat{C}^{hh} + \Gamma)^{-1}(\widehat{C}^{vh})^\top.$$

We seek a solution for  $S$  in the form

$$S = -\widehat{C}^{vh}Y^{-1}$$

and determine  $Y$ . We obtain the equation

$$Y^{-1}\widehat{C}^{hh}Y^{-T} - Y^{-T} - Y^{-1} = -(\widehat{C}^{hh} + \Gamma)^{-1}.$$

Thus, premultiplying by  $Y$  and post multiplying by  $Y^\top$ , we obtain

$$Y(\widehat{C}^{hh} + \Gamma)^{-1}Y^\top - Y - Y^\top + \widehat{C}^{hh} = 0$$

which factorizes to give

$$\left( Y(\widehat{C}^{hh} + \Gamma)^{-1} - I \right) (\widehat{C}^{hh} + \Gamma) \left( Y(\widehat{C}^{hh} + \Gamma)^{-1} - I \right)^\top = \Gamma.$$

Thus, taking the symmetric square root, we have

$$\left( Y(\widehat{C}^{hh} + \Gamma)^{-1} - I \right) (\widehat{C}^{hh} + \Gamma)^{\frac{1}{2}} = \Gamma^{\frac{1}{2}}.$$

Hence

$$\left( Y(\widehat{C}^{hh} + \Gamma)^{-1} - I \right) = \Gamma^{\frac{1}{2}} (\widehat{C}^{hh} + \Gamma)^{-\frac{1}{2}}.$$

Rearranging gives

$$Y(\widehat{C}^{hh} + \Gamma)^{-1} = \Gamma^{\frac{1}{2}} (\widehat{C}^{hh} + \Gamma)^{-\frac{1}{2}} + (\widehat{C}^{hh} + \Gamma)^{\frac{1}{2}} (\widehat{C}^{hh} + \Gamma)^{-\frac{1}{2}}.$$

Thus

$$Y = \left( \Gamma^{\frac{1}{2}} + (\widehat{C}^{hh} + \Gamma)^{\frac{1}{2}} \right) (\widehat{C}^{hh} + \Gamma)^{\frac{1}{2}}.$$

We obtain  $S = -\widetilde{K}$  where

$$\widetilde{K} = \widehat{C}^{vh} \left( (\widehat{C}^{hh} + \Gamma) + \Gamma^{1/2} (\widehat{C}^{hh} + \Gamma)^{1/2} \right)^{-1}.$$

The map (8.13) becomes

$$\begin{aligned} v &= \hat{v} - \tilde{K}(\hat{h} - \mathbb{E}\hat{h}) + \hat{C}^{vh}(\hat{C}^{hh} + \Gamma)^{-1}(y^\dagger - \mathbb{E}\hat{h}), \\ &= \hat{v} - \tilde{K}(\hat{h} - \mathbb{E}\hat{h}) + K(y^\dagger - \mathbb{E}\hat{h}), \\ &= m + (\hat{v} - \hat{m}) - \tilde{K}(\hat{h} - \mathbb{E}\hat{h}). \end{aligned}$$

**8.3. Minimum Variance Approximation.** In the two preceding subsections we have identified an uncountable set of transport maps that match the second order statistics of true transport. Among all these, the *Kalman transport* (2.46) has a particular appeal because it is constructed around the *Kalman gain* familiar from filtering in the linear Gaussian setting. In this subsection we show how the principle of minimizing the variance within a class of *linear* estimators of the state, given observation, leads to this choice of transport map. We believe that the second order transport approach, which we highlight in the main text, provides a more fundamental viewpoint on the mean-field models which underpin ensemble Kalman methods; however the minimum variance perspective is widely adopted in the statistics and geophysics communities (see Subsection 2.7) and hence has an important place in the subject of ensemble Kalman methods.

Recall that the Kalman transport approach leads back to the map (2.14c), motivated by control theoretic considerations, and identifies a specific choice of Kalman gain  $K_n$ , a choice which depends on the law of the predicted state and data. In the Gaussian case the Kalman transport map exactly generates the desired transport, a fact which we establish in Theorem 2.9. The general form of approximate stochastic second order transport maps which we study using the second order transport approach in the main text is (2.42). Our goal here is to motivate a specific choice of  $T^S$  in (2.42c). In this subsection we achieve this by first defining, and identifying, the *best linear unbiased estimator*, BLUE for short. From this we will derive Kalman transport.

**Lemma 8.13.** *Assume that  $\Gamma \succ 0$ . Let all expectations be computed under  $\text{Law}(\hat{v}_{n+1}, \hat{y}_{n+1})$  and consider  $m_{n+1}^{\text{BL}}$  in the form*

$$m_{n+1}^{\text{BL}} = a' + B\hat{y}_{n+1}.$$

Define  $\hat{C}_{n+1}$ ,  $\hat{C}_{n+1}^{vy}$  and  $\hat{C}_{n+1}^{yy}$  by (2.23), (2.24) and

$$l(a', B) := \mathbb{E}|\hat{v}_{n+1} - m_{n+1}^{\text{BL}}|^2.$$

Then  $m_{n+1}^{\text{BL}}$  is said to be the BLUE of  $\hat{v}_{n+1}$  given  $\hat{y}_{n+1}$ , if vector  $a'$  and matrix  $B$  are independent of  $(\hat{v}_{n+1}, \hat{y}_{n+1})$ , but may depend on  $\text{Law}(\hat{v}_{n+1}, \hat{y}_{n+1})$ , and are chosen to minimize  $l(a', B)$ . Then

$$(8.18) \quad m_{n+1}^{\text{BL}} = \mathbb{E}\hat{v}_{n+1} + \hat{C}_{n+1}^{vy}(\hat{C}_{n+1}^{yy})^{-1}(\hat{y}_{n+1} - \mathbb{E}\hat{y}_{n+1}).$$

Furthermore, the estimator (8.18) is unbiased, that is,

$$\mathbb{E}(\hat{v}_{n+1} - m_{n+1}^{\text{BL}}) = 0,$$

and its covariance with respect to  $\text{Law}(\hat{v}_{n+1}, \hat{y}_{n+1})$ ,

$$C_{n+1}^{\text{BL}} := \mathbb{E}((\hat{v}_{n+1} - m_{n+1}^{\text{BL}})(\hat{v}_{n+1} - m_{n+1}^{\text{BL}})^\top),$$

is given by

$$(8.19) \quad C_{n+1}^{\text{BL}} = \hat{C}_{n+1} - \hat{C}_{n+1}^{vy}(\hat{C}_{n+1}^{yy})^{-1}(\hat{C}_{n+1}^{vy})^\top.$$

*Proof.* Noting that we may, without loss of generality, reparametrize the proposed form of  $m_{n+1}^{\text{BL}}$  as

$$m_{n+1}^{\text{BL}} = \mathbb{E}\hat{v}_{n+1} + a + B(\hat{y}_{n+1} - \mathbb{E}\hat{y}_{n+1}),$$

we see that the desired objective to be minimized over vector-matrix pair  $(a, B)$  is

$$\begin{aligned} J(a, B) &:= \frac{1}{2} \mathbb{E}|\hat{v}_{n+1} - \mathbb{E}\hat{v}_{n+1} - a - B(\hat{y}_{n+1} - \mathbb{E}\hat{y}_{n+1})|^2 \\ &= \frac{1}{2} \mathbb{E}|\hat{v}_{n+1} - \mathbb{E}\hat{v}_{n+1}|^2 + \frac{1}{2} |a|^2 \\ &\quad + \frac{1}{2} \mathbb{E}|B(\hat{y}_{n+1} - \mathbb{E}\hat{y}_{n+1})|^2 - \mathbb{E}\langle \hat{v}_{n+1} - \mathbb{E}\hat{v}_{n+1}, B(\hat{y}_{n+1} - \mathbb{E}\hat{y}_{n+1}) \rangle \\ &= \frac{1}{2} \mathbb{E}|\hat{v}_{n+1} - \mathbb{E}\hat{v}_{n+1}|^2 + \frac{1}{2} |a|^2 + \frac{1}{2} (BB^\top) : \hat{C}_{n+1}^{yy} - B : \hat{C}_{n+1}^{vy}. \end{aligned}$$

Clearly the minimizer with respect to  $a$  is achieved by setting  $a = 0$ . Differentiating with respect to  $B$ , noting that  $\hat{C}_{n+1}^{yy}$  is symmetric, shows that  $B = K_n$  given by (2.25). That the resulting pair is indeed a minimizer, and not another critical point, follows from the fact that  $\hat{C}_{n+1}^{yy}$  is positive-definite; this is implied by the assumption  $\Gamma \succ 0$ . Thus we obtain the estimator (8.18). A straightforward calculation shows that the estimator is unbiased and that its covariance is given by (8.19).  $\blacksquare$

We now connect the BLUE to an approximate (second order) transport map. To this end, note that (8.18) may be viewed as mapping  $\hat{y}_{n+1}$  into  $m_{n+1}^{\text{BL}} = m^{\text{BL}}(\hat{y}_{n+1})$ . With this notation we define  $m_{n+1}^\dagger$  by

$$(8.20a) \quad m_{n+1}^\dagger = m^{\text{BL}}(y_{n+1}^\dagger)$$

$$(8.20b) \quad = \mathbb{E}\hat{v}_{n+1} + \hat{C}_{n+1}^{vy}(\hat{C}_{n+1}^{yy})^{-1}(y_{n+1}^\dagger - \mathbb{E}\hat{y}_{n+1}).$$

We may now make the following connection between BLUE and Kalman transport:

**Theorem 8.14.** *Let  $(\hat{v}_{n+1}, \hat{y}_{n+1})$  be distributed according to measure  $\nu_{n+1}$ . Then the transport map (2.46c) has the properties:*

$$\begin{aligned} \mathbb{E}v_{n+1} &= m_{n+1}^\dagger \\ \mathbb{E}((v_{n+1} - m_{n+1}^\dagger)(v_{n+1} - m_{n+1}^\dagger)^\top) &= C_{n+1}^{\text{BL}}, \end{aligned}$$

where  $m_{n+1}^\dagger$  and  $C_{n+1}^{\text{BL}}$  are given by (8.20) and (8.19) respectively.

*Proof.* Note that the transport map (2.5.3) can now be reformulated as

$$v_{n+1} = \widehat{v}_{n+1} + (m_{n+1}^\dagger - m_{n+1}^{\text{BL}}).$$

Thus

$$v_{n+1} = m_{n+1}^\dagger + \widehat{v}_{n+1} - m_{n+1}^{\text{BL}}.$$

The desired properties of the mean and covariance follow from Lemma 8.13.  $\blacksquare$

**Remark 8.15.** We now have two derivations of the Kalman gain, the approximate transport derivation from Subsection 2.5.3, and the minimum variance derivation given here. We include a third, dimensional, argument that motivates its form. Let **state** denote the physical units associated with the state variable and **data** those associated with the observation. Then the physical units of the gain matrix  $K$  should equal **state/data**. We note that  $\widehat{C}^{yy}$  has units of **data** squared whilst the units of  $\widehat{C}^{vy}$  are the product of **state** and **data**. If we then constrain the gain to be determined by covariance matrices involving the state and the data it is natural to choose it to be formed as  $\widehat{C}^{vy}(\widehat{C}^{yy})^{-1}$  where  $\widehat{C}^{yy}$  is an estimate of covariance in the data, and  $\widehat{C}^{vy}$  an estimate of covariance between state and data. Making a choice of this type leads to the right units for the gain, since the innovation has units **data**, and relies only on use of first and second order statistics. This dimensional argument motivates the form (2.25) as derived in both Subsections 8.3 and 2.4.  $\blacksquare$

## 9. Appendix D (Stochastic Calculus Considerations).

**9.1. Derivation of the Kushner-Stratonovich Equation.** In Section 3, where we derived continuous time limits from discrete models, we used the two small parameters  $\delta$  and  $\Delta t$ . The first characterized the data frequency and the second a time-increment. In this appendix we make the choice  $\delta = \Delta t$  and study the limit  $\Delta t \rightarrow 0$  to derive continuum models. Studying this limit enables us to convert between different modes of stochastic integration in an explicit fashion; this may be helpful to some readers as it avoids the need to invoke abstract results on covariation.

**Lemma 9.1.** *The Itô and Stratonovich interpretations of the nonlocal nonlinear stochastic evolution equation for density  $r(v, t)$  in (3.16) are related through*

$$(9.1a) \quad dr = r \left\langle \mathbf{h} - \mathbb{E}\mathbf{h}, \circ d\mathbf{z}^\dagger \right\rangle_\Gamma - \frac{r}{2} \left\{ |\mathbf{h}|_\Gamma^2 - \mathbb{E} |\mathbf{h}|_\Gamma^2 \right\} dt$$

$$(9.1b) \quad = r \left\langle \mathbf{h} - \mathbb{E}\mathbf{h}, d\mathbf{z}^\dagger - \mathbb{E}\mathbf{h}dt \right\rangle_\Gamma$$

*Proof.* Consider (9.1a) and the term  $r \langle \mathbf{h} - \mathbb{E}\mathbf{h}, \circ d\mathbf{z}^\dagger \rangle_\Gamma$  in particular. Define the corresponding Itô and Stratonovich integrals

$$I := \int_0^T r \langle \mathbf{h} - \mathbb{E}\mathbf{h}, d\mathbf{z}^\dagger \rangle_\Gamma, \quad S := \int_0^T r \langle \mathbf{h} - \mathbb{E}\mathbf{h}, \circ d\mathbf{z}^\dagger \rangle_\Gamma.$$

We aim to write  $S$  as the sum of  $I$  and an added correction. Consider the space

$$\mathcal{X} := \{\varrho \in L^1(\mathbb{R}^{d_v}; \mathbb{R}^+) : \|\varrho\|_{L^1} = 1\}$$

of probability density functions. We first choose an increasing sequence  $(t_j)_{j=1,\dots,N}$  with  $\Delta t := t_{j+1} - t_j$  such that  $N\Delta t = T$ . We next define

$$\Delta r_{t_j} := r_{t_{j+1}} - r_{t_j} \quad \Delta h_{t_j} := h_{t_{j+1}} - h_{t_j} \quad \Delta z_{t_j}^\dagger := z_{t_{j+1}}^\dagger - z_{t_j}^\dagger.$$

We recall the driving evolution equation for  $z^\dagger$

$$dz^\dagger = h(v^\dagger)dt + \sqrt{\Gamma}dW,$$

from which, recalling the properties of Brownian motion  $W$ , we deduce the discretization

$$(9.2) \quad \Delta z_{t_j}^\dagger = h(v_{t_j}^\dagger)\Delta t + \sqrt{\Gamma\Delta t}\xi_{t_j} + \mathcal{O}(\Delta t^{3/2}),$$

where  $\xi_{t_j}$  are independent mean-zero normal random variables with variance  $I_{dy}$  for each  $j$ . The fact that this discretization is accurate up to terms of  $\mathcal{O}(\Delta t^{3/2})$  follows from Itô-Taylor expansion [Kloeden & Platen \(1991\)](#). Recalling the definition of the Stratonovich stochastic integral as a limit, we consider the following finite sum approximation of  $S$ :

$$(9.3) \quad S_{\Delta t} := \sum_{j=1}^N \frac{r_{t_{j+1}} + r_{t_j}}{2} \left\langle h - \int \frac{r_{t_{j+1}} + r_{t_j}}{2} h dv, \Delta z_{t_j}^\dagger \right\rangle_\Gamma;$$

this converges in the  $L^2_{\mathbb{P}}(\Omega; \mathcal{C}([0, T]; \mathcal{X}))$  sense to  $S$  as  $\Delta t \rightarrow 0$  (and thus as  $N \rightarrow \infty$ ). Expanding now the sum in (9.3), we obtain

$$(9.4a) \quad S_{\Delta t} = \sum_{j=1}^N \left( r_{t_j} + \frac{\Delta r_{t_j}}{2} \right) \left\langle h - \int \left( r_{t_j} + \frac{\Delta r_{t_j}}{2} \right) h dv, \Delta z_{t_j}^\dagger \right\rangle_\Gamma$$

$$(9.4b) \quad = \sum_{j=1}^N r_{t_j} \left\langle h - \int r_{t_j} h dv, \Delta z_{t_j}^\dagger \right\rangle_\Gamma + \frac{1}{2} \sum_{j=1}^N \Delta r_{t_j} \left\langle h - \int r_{t_j} h dv, \Delta z_{t_j}^\dagger \right\rangle_\Gamma$$

$$(9.4c) \quad - \frac{1}{2} \sum_{j=1}^N r_{t_j} \left\langle \int \Delta r_{t_j} h dv, \Delta z_{t_j}^\dagger \right\rangle_\Gamma - \frac{1}{4} \sum_{j=1}^N \Delta r_{t_j} \left\langle \int \Delta r_{t_j} h dv, \Delta z_{t_j}^\dagger \right\rangle_\Gamma.$$

Now, we note that by discretizing (9.1a) we can write

$$\Delta r_{t_j} = r_{t_j} \left\langle h - \int r_{t_j} h dv, \Delta z_{t_j}^\dagger \right\rangle_\Gamma + \mathcal{O}(\Delta t).$$

By substituting this expression in the expanded sum in (9.4b) we notice that the last term in (9.4c) will be of order  $\mathcal{O}(N\Delta t^{3/2})$ . We can thus write (9.4) as

$$(9.5) \quad S_{\Delta t} = I_{\Delta t} + J_{1,\Delta t} + J_{2,\Delta t} + \mathcal{O}(N\Delta t^{3/2}),$$

where we have defined

$$I_{\Delta t} := \sum_{j=1}^N r_{t_j} \left\langle h - \int r_{t_j} h dv, \Delta z_{t_j}^\dagger \right\rangle_\Gamma, \quad J_{1,\Delta t} := \frac{1}{2} \sum_{j=1}^N r_{t_j} \left| \left\langle h - \int r_{t_j} h dv, \Delta z_{t_j}^\dagger \right\rangle_\Gamma \right|^2,$$

$$J_{2,\Delta t} := -\frac{1}{2} \sum_{j=1}^N r_{t_j} \left\langle \int r_{t_j} \left\langle h - \int r_{t_j} h dv, \Delta z_{t_j}^\dagger \right\rangle_\Gamma h dv, \Delta z_{t_j}^\dagger \right\rangle_\Gamma.$$



The first term in the sum (9.5),  $I_{\Delta t}$ , converges in the  $L^2_{\mathbb{P}}$  sense to  $I$  as  $\Delta t \rightarrow 0$ . Considering now the term  $J_{1,\Delta t}$  and using the discretization (9.2) we have that

$$\begin{aligned} J_{1,\Delta t} &= \frac{1}{2} \sum_{j=1}^N r_{t_j} \left| \left\langle \mathbf{h} - \int r_{t_j} \mathbf{h} dv, \Delta z_{t_j}^\dagger \right\rangle_{\Gamma} \right|^2 \\ &= \frac{1}{2} \sum_{j=1}^N r_{t_j} \Delta t \left( \mathbf{h} - \int r_{t_j} \mathbf{h} dv \right)^\top \Gamma^{-1/2} \xi_{t_j} \xi_{t_j}^\top \Gamma^{-1/2} \left( \mathbf{h} - \int r_{t_j} \mathbf{h} dv \right) + \sum_{j=1}^N \mathcal{O}(\Delta t^{3/2}). \end{aligned}$$

Since  $\sum_{j=1}^N \mathcal{O}(\Delta t^{3/2}) = \mathcal{O}(\Delta t^{1/2})$ , taking the  $\Delta t \rightarrow 0$  limit and using the independence of the  $\xi_{t_j}$  for each  $j$ , we see that

$$J_{1,\Delta t} \rightarrow \frac{1}{2} \int_0^T \left[ r (\mathbf{h} - \mathbb{E}\mathbf{h})^\top \Gamma^{-1/2} \mathbb{E} \xi \xi^\top \Gamma^{-1/2} (\mathbf{h} - \mathbb{E}\mathbf{h}) \right] dt = \int_0^T \frac{r}{2} |\mathbf{h} - \mathbb{E}\mathbf{h}|_{\Gamma}^2 dt,$$

in the  $L^2_{\mathbb{P}}$  sense. Similarly for  $J_{2,\Delta t}$  we have that,

$$\begin{aligned} J_{2,\Delta t} &= -\frac{1}{2} \sum_{j=1}^N r_{t_j} \left\langle \int r_{t_j} \left\langle \mathbf{h} - \int r_{t_j} \mathbf{h} dv, \Delta z_{t_j}^\dagger \right\rangle_{\Gamma} \mathbf{h} dv, \Delta z_{t_j}^\dagger \right\rangle_{\Gamma} \\ &= -\frac{1}{2} \sum_{j=1}^N r_{t_j} \int r_{t_j} \left\langle \left\langle \mathbf{h} - \int r_{t_j} \mathbf{h} dv, \Delta z_{t_j}^\dagger \right\rangle_{\Gamma} \mathbf{h}, \Delta z_{t_j}^\dagger \right\rangle_{\Gamma} dv \\ &= -\frac{1}{2} \sum_{j=1}^N r_{t_j} \Delta t \int r_{t_j} \mathbf{h}^\top \Gamma^{-1/2} \xi_{t_j} \xi_{t_j}^\top \Gamma^{-1/2} \left( \mathbf{h} - \int r_{t_j} \mathbf{h} dv \right) dv + \sum_{j=1}^N \mathcal{O}(\Delta t^{3/2}). \end{aligned}$$

Since  $\sum_{j=1}^N \mathcal{O}(\Delta t^{3/2}) = \mathcal{O}(\Delta t^{1/2})$ , taking the  $\Delta t \rightarrow 0$  limit and using the independence of the  $\xi_{t_j}$  for each  $j$ , we see that, in the  $L^2_{\mathbb{P}}$  sense,

$$J_{2,\Delta t} \rightarrow -\frac{1}{2} \int_0^T r \int r \mathbf{h}^\top \Gamma^{-1/2} \mathbb{E} (\xi \xi^\top) \Gamma^{-1/2} (\mathbf{h} - \mathbb{E}\mathbf{h}) dv dt = -\int_0^T \frac{r}{2} \mathbb{E} |\mathbf{h} - \mathbb{E}\mathbf{h}|_{\Gamma}^2 dt.$$

Finally, by taking the  $\Delta t \rightarrow 0$  limit on both sides of (9.5), we conclude

$$S = I + \int_0^T \frac{r}{2} |\mathbf{h} - \mathbb{E}\mathbf{h}|_{\Gamma}^2 dt - \int_0^T \frac{r}{2} \mathbb{E} |\mathbf{h} - \mathbb{E}\mathbf{h}|_{\Gamma}^2 dt,$$

in the  $L^2_{\mathbb{P}}$  sense. Hence by using the above Stratonovich-to-Itô correction in (9.1a), we obtain

$$\begin{aligned} dr &= r \left\langle \mathbf{h} - \mathbb{E}\mathbf{h}, \odot dz^\dagger \right\rangle_{\Gamma} - \frac{r}{2} \left\{ |\mathbf{h}|_{\Gamma}^2 - \mathbb{E} |\mathbf{h}|_{\Gamma}^2 \right\} dt \\ &= r \left\langle \mathbf{h} - \mathbb{E}\mathbf{h}, dz^\dagger \right\rangle_{\Gamma} + \frac{r}{2} |\mathbf{h} - \mathbb{E}\mathbf{h}|_{\Gamma}^2 dt - \frac{r}{2} \mathbb{E} |\mathbf{h} - \mathbb{E}\mathbf{h}|_{\Gamma}^2 dt - \frac{r}{2} \left\{ |\mathbf{h}|_{\Gamma}^2 - \mathbb{E} |\mathbf{h}|_{\Gamma}^2 \right\} dt \\ &= r \left\langle \mathbf{h} - \mathbb{E}\mathbf{h}, dz^\dagger - \mathbb{E}\mathbf{h} dt \right\rangle_{\Gamma}. \end{aligned}$$

■

**Lemma 9.2.** *The probability density for the solution  $v$  of (3.29), with respect to randomness induced by the law of  $\widehat{z}$  and the initial condition  $v(0)$ , with  $z^\dagger$  a fixed data sample path, is given by (3.30).*

*Proof.* Recall that in equation (3.29) the evolution of  $z^\dagger$  is given by (3.8), with  $B^\dagger$  and  $B$  independent draws from unit Brownian motion in  $\mathbb{R}^{d_v}$ . Thus

$$dv = a(v; \rho)dt + K(v; \rho) \left( (h(v^\dagger) - h(v))dt + \sqrt{\Gamma}dB^\dagger - \sqrt{\Gamma}dB \right).$$

We wish to find the probability density function  $\rho(v, t)$  for  $v$ , with respect to randomness induced by the law of  $B$  and the initial condition  $v(0)$ , but with  $v^\dagger, B^\dagger$  fixed signal and observational noise sample paths. Let  $\phi : \mathbb{R}^{d_v} \rightarrow \mathbb{R}$  be smooth and note that the Itô formula shows that

$$d\phi(v(t)) = (\mathcal{L}\phi)(v(t))dt + \langle K(v(t); \rho(\cdot, t))\sqrt{\Gamma}(dB^\dagger - dB), \nabla\phi(v(t)) \rangle,$$

where

$$\mathcal{L}\psi(v) = \left\langle \left( a(v; \rho) + K(v; \rho)(h(v^\dagger) - h(v)) \right), \nabla\psi \right\rangle + K(v; \rho)\Gamma K(v; \rho)^\top : \nabla\nabla\psi,$$

and the integrals are to be interpreted in the Itô sense. Note the factor 1 in the second order term, arising because of the independent quadratic variation contributions from both  $B$  and  $B^\dagger$ . Taking expectation  $\mathbb{E}$  with respect to  $B$  and initial condition  $v(0)$ , with  $B^\dagger$  fixed, for  $a$  and  $K$  functions of  $v$  and  $\rho$ , yields, using again that  $z^\dagger$  is given by (3.8),

$$\begin{aligned} d\mathbb{E}\phi(v) &= \mathbb{E} \left\langle \left( a + K(h(v^\dagger) - h) \right), \nabla\phi \right\rangle dt + \mathbb{E} \langle K\sqrt{\Gamma}dB^\dagger, \nabla\phi \rangle + \mathbb{E} K\Gamma K^\top : \nabla\nabla\phi dt \\ &= \mathbb{E} \langle (a - Kh), \nabla\phi \rangle dt + \mathbb{E} \langle Kdz^\dagger, \nabla\phi \rangle + \mathbb{E} K\Gamma K^\top : \nabla\nabla\phi dt. \end{aligned}$$

Noting that the expectation operation corresponds to multiplication by  $\rho(v, t)$  and integration over  $v \in \mathbb{R}^{d_v}$ , integrating by parts shows that  $\rho$  satisfies the desired equation (3.30), in a weak sense. ■

**9.2. Diamond Integration.** In this section we use notation analogous to that established in the proof of Lemma 9.1. Consider the equation (3.28), and in particular the contribution  $K(dz^\dagger - d\widehat{z})$ . We first choose an increasing sequence  $(t_j)_{j=0, \dots, N-1}$  with  $\Delta t := t_{j+1} - t_j$  such that  $N\Delta t = T$ . The Itô integral interpretation of this contribution, on time interval  $(0, T)$ , is as the  $L^2_{\mathbb{P}}$  limit of

$$I_{\Delta t} := \sum_{j=0}^{N-1} K(v_{t_j}; \rho_{t_j})(\Delta z^\dagger_{t_j} - \Delta \widehat{z}_{t_j})$$

We define the Stratonovich integral interpretation as the  $L^2_{\mathbb{P}}$  limit of

$$S_{\Delta t} := \sum_{j=0}^{N-1} K \left( \frac{v_{t_{j+1}} + v_{t_j}}{2}, \frac{\rho_{t_{j+1}} + \rho_{t_j}}{2} \right) (\Delta z^\dagger_{t_j} - \Delta \widehat{z}_{t_j});$$

as is standard, we use  $\circ$  to denote Stratonovich stochastic integration. Finally we define the diamond integral interpretation as the  $L^2_{\mathbb{P}}$  limit of

$$R_{\Delta t} := \sum_{j=0}^{N-1} K \left( \frac{v_{t_{j+1}} + v_{t_j}}{2}; \rho_{t_j} \right) (\Delta z_{t_j}^\dagger - \Delta \hat{z}_{t_j}).$$

Note that this is akin to a Stratonovich integral, but only with respect variation of  $K$  with respect to  $v$ , not  $\rho$ . We use  $\diamond$  to denote this unusual form of stochastic integration.

Throughout this subsection we inter-convert between these three forms of stochastic integration. To shorten the presentation we will sometimes use the  $=$  symbol when in fact we mean equality up to an additive constant which disappears in the  $\Delta t \rightarrow 0$  limit. Note that the evolution equation (3.28) for  $v$  is driven by  $z^\dagger$  and  $\hat{z}$ , whereas the Kushner-Stratonovich equation (3.18) for  $\rho$  driven only by  $z^\dagger$ . This difference will have implications for the calculations that follow, in which we compute inter-conversions between the different stochastic integrals. The first result highlights an interesting interpretation of the contribution

$$a = \nabla \cdot (K \Gamma K^\top) - K \Gamma \nabla \cdot K^\top;$$

to the drift in (3.28), namely that it is simply the Itô-to-diamond correction, giving a compact re-interpretation of the mean-field model:

**Lemma 9.3.** *Let  $\rho$  solve the Kushner-Stratonovich equation (3.18) and let  $z^\dagger$  be given by (3.8). The Itô interpretation of equation (3.28) and its interpretation with respect to the  $\diamond$  form of stochastic integration are related through the following equivalence. The system*

$$\begin{aligned} dv &= f(v)dt + \sqrt{\Sigma}dW + \nabla \cdot (K \Gamma K^\top)dt - K \Gamma \nabla \cdot K^\top dt + K(dz^\dagger - d\hat{z}), \\ d\hat{z} &= h(v)dt + \sqrt{\Gamma}dB, \end{aligned}$$

where  $K = K(v, \rho)$ , is equivalent to

$$\begin{aligned} dv &= f(v)dt + \sqrt{\Sigma}dW + K \diamond (dz^\dagger - d\hat{z}) \\ d\hat{z} &= h(v)dt + \sqrt{\Gamma}dB. \end{aligned}$$

*Proof.* We first recall the evolution equations for  $z^\dagger$  and  $\hat{z}$ :

$$\begin{aligned} dz^\dagger &= h(v^\dagger)dt + \sqrt{\Gamma}dB^\dagger, \\ d\hat{z} &= h(v)dt + \sqrt{\Gamma}dB. \end{aligned}$$

Noting that  $v$  is driven by  $(z^\dagger - \hat{z})$  and that we are interconverting between Itô and diamond integration, so that the noisy driving of the  $\rho$  equation does not play a role, we see that it suffices to consider the  $L^2_{\mathbb{P}}$  limits of the two quantities

$$\begin{aligned} I_{\Delta t} &= \sum_{j=0}^{N-1} K(v_{t_j}; \rho_{t_j}) \sqrt{2\Gamma \Delta t} \xi_{t_j}, \\ R_{\Delta t} &= \sum_{j=0}^{N-1} K \left( \frac{v_{t_{j+1}} + v_{t_j}}{2}; \rho_{t_j} \right) \sqrt{2\Gamma \Delta t} \xi_{t_j}, \end{aligned}$$

where the  $\xi_{t_j}$  are i.i.d. draws from a unit Gaussian. By adding and subtracting the Itô contribution, we obtain

$$\begin{aligned} R_{\Delta t} &= \sum_{j=0}^{N-1} K\left(\frac{v_{t_{j+1}} + v_{t_j}}{2}; \rho_{t_j}\right) \sqrt{2\Gamma\Delta t} \xi_{t_j} \\ &= \sum_{j=0}^{N-1} K(v_{t_j}; \rho_{t_j}) \sqrt{2\Gamma\Delta t} \xi_{t_j} + \sum_{j=0}^{N-1} \left( K\left(\frac{v_{t_{j+1}} + v_{t_j}}{2}; \rho_{t_j}\right) - K(v_{t_j}; \rho_{t_j}) \right) \sqrt{2\Gamma\Delta t} \xi_{t_j} \\ &= I_{\Delta t} + \sum_{j=0}^{N-1} \left( \frac{1}{2} D_v K(v_{t_j}; \rho_{t_j}) (v_{t_{j+1}} - v_{t_j}) + \mathcal{O}(|v_{t_{j+1}} - v_{t_j}|^2) \right) \sqrt{2\Gamma\Delta t} \xi_{t_j}, \end{aligned}$$

where the last line follows from a first order Taylor expansion. Using a discretization of the evolution for  $v$ , and neglecting the terms that do not contribute to the quadratic variation when computing the  $L^2_{\mathbb{P}}$  limit, we substitute for  $v_{t_{j+1}} - v_{t_j}$  to obtain

$$(9.6) \quad I_{\Delta t} + \sum_{j=0}^{N-1} \frac{1}{2} D_v K(v_{t_j}; \rho_{t_j}) \left( K(v_{t_j}; \rho_{t_j}) \sqrt{2\Gamma\Delta t} \xi_{t_j} \right) \sqrt{2\Gamma\Delta t} \xi_{t_j}.$$

We now consider the correction term resulting from (9.6), which is determined by expectation of the summand with respect to the random increments  $\xi$ , scaled by  $\Delta t^{-1}$ . Dropping the  $v$  and  $\rho$  dependence of  $K$  and the  $t_j$  dependence for notational convenience, its  $k$ 'th component is given by<sup>22</sup>

$$\begin{aligned} \left[ \mathbb{E} (D_v K) \left( K \Gamma^{1/2} \xi \right) \Gamma^{1/2} \xi \right]_k &= \left[ \mathbb{E} (\partial_{v_i} K) \left[ K \Gamma^{1/2} \xi \right]_i \Gamma^{1/2} \xi \right]_k \\ &= \left[ \mathbb{E} (\partial_{v_i} K) \left( K_{il} (\Gamma^{1/2})_{lj} \xi_j \right) \Gamma^{1/2} \xi \right]_k \\ &= \mathbb{E} \left( K_{il} (\Gamma^{1/2})_{lj} \xi_j \right) (\partial_{v_i} K)_{kn} (\Gamma^{1/2})_{nm} \xi_m \\ &= (\partial_{v_i} K_{kn}) \Gamma_{ln} K_{il}. \end{aligned}$$

But,

$$\begin{aligned} (\partial_{v_i} K_{kn}) \Gamma_{ln} K_{il} &= \partial_{v_i} (K_{kn} \Gamma_{ln} K_{il}) - K_{kn} \Gamma_{ln} (\partial_{v_i} K_{il}) \\ &= \left[ \nabla \cdot (K \Gamma K^\top) \right]_k - \left[ K \Gamma \nabla \cdot (K^\top) \right]_k, \end{aligned}$$

Recalling that the only contributions in  $R_{\Delta t}$  which do not vanish under the  $\Delta t \rightarrow 0$  limit are the ones given by (9.6), taking the  $\Delta t \rightarrow 0$  limit of  $R_{\Delta t}$  yields

$$R = I + \int_0^T \left( \nabla \cdot (K \Gamma K^\top) - K \Gamma \nabla \cdot (K^\top) \right) dt,$$

where the convergence is in the  $L^2_{\mathbb{P}}(\Omega; \mathcal{C}([0, T]; \mathbb{R}^{d_v}))$  sense; this concludes the proof. ■

<sup>22</sup>Using Einstein summation convention, as described for example in [Gonzalez & Stuart \(2008\)](#), so that index repeated twice is summed over.

**Lemma 9.4.** *Let  $\rho$  solve the Kushner-Stratonovich equation (3.18) and let  $z^\dagger$  be given by (3.8). The interpretation with respect to the  $\diamond$  form of stochastic integration of equation (3.28) and its Stratonovich interpretation are related through the following equivalence. The system*

$$\begin{aligned} dv &= f(v)dt + \sqrt{\Sigma}dW + K \diamond (dz^\dagger - d\hat{z}) \\ d\hat{z} &= h(v)dt + \sqrt{\Gamma}dB, \end{aligned}$$

where  $K = K(v, \rho)$ , is equivalent to

$$\begin{aligned} dv &= f(v)dt + bdt + \sqrt{\Sigma}dW + K \circ (dz^\dagger - d\hat{z}) \\ d\hat{z} &= h(v)dt + \sqrt{\Gamma}dB, \end{aligned}$$

where the term  $b = b(v, \rho)$  satisfies

$$b(v, \rho) = \frac{\rho}{2} D_\rho K (h - \mathbb{E}h).$$

*Proof.* To make the interconversion between diamond and Stratonovich integration we need only consider the quadratic variation contribution induced by  $z^\dagger$  since the equation for  $\rho$  is driven only by  $z^\dagger$  and not by  $\hat{z}$ . Thus it suffices to compare the  $L^2_{\mathbb{P}}$  limits of

$$\begin{aligned} R_{\Delta t} &= \sum_{j=0}^{N-1} K \left( \frac{v_{t_{j+1}} + v_{t_j}}{2}; \rho_{t_j} \right) \sqrt{\Gamma \Delta t} \xi_{t_j}^\dagger, \\ S_{\Delta t} &= \sum_{j=0}^{N-1} K \left( \frac{v_{t_{j+1}} + v_{t_j}}{2}; \frac{\rho_{t_{j+1}} + \rho_{t_j}}{2} \right) \sqrt{\Gamma \Delta t} \xi_{t_j}^\dagger; \end{aligned}$$

Here  $\xi_{t_j}^\dagger$  are i.i.d. draws from a unit Gaussian. By adding and subtracting the diamond contribution, we obtain

$$\begin{aligned} S_{\Delta t} &= \sum_{j=0}^{N-1} K \left( \frac{v_{t_{j+1}} + v_{t_j}}{2}; \frac{\rho_{t_{j+1}} + \rho_{t_j}}{2} \right) \sqrt{\Gamma \Delta t} \xi_{t_j}^\dagger \\ &= R_{\Delta t} + \sum_{j=0}^{N-1} \left( K \left( \frac{v_{t_{j+1}} + v_{t_j}}{2}; \frac{\rho_{t_{j+1}} + \rho_{t_j}}{2} \right) - K \left( \frac{v_{t_{j+1}} + v_{t_j}}{2}; \rho_{t_j} \right) \right) \sqrt{\Gamma \Delta t} \xi_{t_j}^\dagger \\ &= R_{\Delta t} + \sum_{j=0}^{N-1} \left( \frac{1}{2} D_\rho K \left( \frac{v_{t_{j+1}} + v_{t_j}}{2}; \rho_{t_j} \right) (\rho_{t_{j+1}} - \rho_{t_j}) + \mathcal{O}(|\rho_{t_{j+1}} - \rho_{t_j}|^2) \right) \sqrt{\Gamma \Delta t} \xi_{t_j}^\dagger, \end{aligned}$$

where the last line follows from a first order Taylor expansion in  $\rho$ . Using a discretization of the Kushner-Stratonovich equation given in Theorem 3.3, and neglecting the terms that do not contribute to the quadratic variation in the  $L^2_{\mathbb{P}}$  limit, we substitute for  $\rho_{t_{j+1}} - \rho_{t_j}$  to obtain

$$S_{\Delta t} = R_{\Delta t} + \sum_{j=0}^{N-1} \left( \frac{1}{2} D_\rho K \left( \frac{v_{t_{j+1}} + v_{t_j}}{2}; \rho_{t_j} \right) \langle \rho_{t_j} \Gamma^{-1} (h_{t_j} - \mathbb{E}h_{t_j}), \sqrt{\Gamma \Delta t} \xi_{t_j}^\dagger \rangle + \mathcal{O}(\Delta t) \right) \sqrt{\Gamma \Delta t} \xi_{t_j}^\dagger.$$

We now perform a first order Taylor expansion in  $v$  of  $D_\rho K$ . Disregarding  $\mathcal{O}(\Delta t^{3/2})$  terms which will vanish in the  $\Delta t \rightarrow 0$  limit, we obtain

$$(9.7) \quad S_{\Delta t} = R_{\Delta t} + \sum_{j=0}^{N-1} \frac{1}{2} D_\rho K(v_{t_j}; \rho_{t_j}) \langle \rho_{t_j} \Gamma^{-1}(\mathbf{h}_{t_j} - \mathbb{E}\mathbf{h}_{t_j}), \sqrt{\Gamma \Delta t} \xi_{t_j}^\dagger \rangle \sqrt{\Gamma \Delta t} \xi_{t_j}^\dagger.$$

We now consider the correction term resulting from (9.7), which is determined by expectation of the summand with respect to the random increments  $\xi^\dagger$ , scaled by  $\Delta t^{-1}$ . Indeed, dropping the  $v$  and  $\rho$  dependence of  $K$ , for each  $j = 0, \dots, N-1$ , its  $l$ 'th component is given by <sup>23</sup>

$$\begin{aligned} \mathbb{E} \left[ \frac{1}{2} D_\rho K(v_{t_j}; \rho_{t_j}) \langle \rho_{t_j} \Gamma^{-1}(\mathbf{h}_{t_j} - \mathbb{E}\mathbf{h}_{t_j}), \sqrt{\Gamma} \xi_{t_j}^\dagger \rangle \sqrt{\Gamma} \xi_{t_j}^\dagger \right]_l &= \\ &= \frac{1}{2} \rho_{t_j} \mathbb{E} \left( \left[ \Gamma^{-1/2}(\mathbf{h}_{t_j} - \mathbb{E}\mathbf{h}_{t_j}) \right]_k \left[ \xi_{t_j}^\dagger \right]_k [D_\rho K]_{lm} \left[ \Gamma^{1/2} \right]_{mn} \left[ \xi_{t_j}^\dagger \right]_n \right) \\ &= \frac{1}{2} \rho_{t_j} [D_\rho K]_{lm} [\mathbf{h}_{t_j} - \mathbb{E}\mathbf{h}_{t_j}]_m. \end{aligned}$$

Thus taking the  $\Delta t \rightarrow 0$  limit of  $S_{\Delta t}$  yields

$$S = R + \int_0^T \frac{1}{2} \rho D_\rho K(v; \rho)(\mathbf{h} - \mathbb{E}\mathbf{h}) dt,$$

where the convergence is in the  $L_{\mathbb{P}}^2(\Omega; \mathcal{C}([0, T]; \mathbb{R}^{d_v}))$  sense; this concludes the proof. ■

---

<sup>23</sup>Again using Einstein summation convention, but not with respect to index  $j$  which simply denotes a fixed time.